University of Tennessee, Knoxville
TRACE: Tennessee Research and Creative Exchange

Doctoral Dissertations | Graduate School

12-2013

Syntheses and Reactions of Early Transition Metal Amidinate Compounds

Adam Christopher Lamb
University of Tennessee - Knoxville, alamb3@utk.edu

Follow this and additional works at: https://trace.tennessee.edu/utk_graddiss

 Part of the Inorganic Chemistry Commons

Recommended Citation

Lamb, Adam Christopher, "Syntheses and Reactions of Early Transition Metal Amidinate Compounds. " PhD diss., University of Tennessee, 2013.
https://trace.tennessee.edu/utk_graddiss/2587

This Dissertation is brought to you for free and open access by the Graduate School at TRACE: Tennessee Research and Creative Exchange. It has been accepted for inclusion in Doctoral Dissertations by an authorized administrator of TRACE: Tennessee Research and Creative Exchange. For more information, please contact trace@utk.edu.

To the Graduate Council:

I am submitting herewith a dissertation written by Adam Christopher Lamb entitled "Syntheses and Reactions of Early Transition Metal Amidinate Compounds." I have examined the final electronic copy of this dissertation for form and content and recommend that it be accepted in partial fulfillment of the requirements for the degree of Doctor of Philosophy, with a major in Chemistry.

Ziling Xue, Major Professor

We have read this dissertation and recommend its acceptance:

David J. Jenkins, Robert N. Compton, David C. Joy

Accepted for the Council:

Carolyn R. Hodges

Vice Provost and Dean of the Graduate School

(Original signatures are on file with official student records.)

Syntheses and Reactions of Early Transition Metal Amidinate Compounds

A Dissertation

Presented for the

Doctor of Philosophy Degree

The University of Tennessee, Knoxville

Adam Christopher Lamb

December 2013

Dedication

This dissertation is dedicated to my parents, Barbara and Eddie Lamb for their continuous love and support and for being with me every step of the way. I would also like to dedicate this to my brother, Corey Lamb; sister-in-law, Lorie; niece, Keirstan; and nephew, Braeden for their love and supporting my career choice.

Acknowledgement

I would first and foremost like to thank my advisor, Dr. Ziling (Ben) Xue for his guidance and knowledge in teaching me to be a better scientist during my time here at UTK. I would also like to acknowledge my committee members: Dr. Bob Compton, Dr. David Jenkins and Dr. David Joy for their time and consideration of my dissertation. I would like to extend a special thanks to Dr. Carlos Steren for his help with all the different NMRs and setting up experiments especially last minute ones. Also, thank you for your willingness to help me understand my results. I would like to thank Dr. Liguo Song, Stephen Gibson, and Allen Zhu for their patience and guidance in running mass spectroscopies. Matt Dembo helped obtain a solid-state NMR spectrum.

I would like to thank my past and present group members for all their help in achieving this accomplishment. I want to extend a special thanks to Julia Abbott, Shujian (Jim) Chen, and Brenda Dougan for teaching me lab skills, how to use instruments, and how to get through the program. I would like to acknowledge other group members Stefanie Bragg, Tabitha Callaway, Thomas Carpenter, Royce Dansby-Sparks, Jonathan Fong, Seth Hunter, Sam Rosolina, Bhavna Sharma, and Clarissa Tatum.

I would like to thank the National Science Foundation for supporting my graduate research.

Abstract

Homoleptic Groups 4 and 5 metal amide compounds have been used as precursors in CVD/ALD processes to make microelectronic metal oxide thin films. These compounds are often very air sensitive. Ancillary ligands such as amidinates have been used to reduce their air sensitivity and to make their handling easier. Reactions of amidinates with dioxygen and water have thus been used to make metal oxide thin films. Studies of these reactions are important in order to make better precursors and purer thin films. This dissertation focuses on the following areas: (a) Syntheses of zirconium and Group 5 amidinate amides; (b) Studies of the reactions of zirconium amidinate amides with dioxygen or water; (c) Probing the pathway in the formation of an archetypical tungsten alkylidyne complex. $Zr[MeC(N^{i}Pr)_2]_2(NMe_2)_2$ [zirconium amidinate amide] has been prepared through three different routes: two salt metathesis reactions and one aminolysis. The aminolysis of $M(NR_2)_n$ [metal amide] with $^{i}PrN(H)C(Me)=N^{i}Pr$ [diisopropylamidine] gives cleaner products in better yields and this route has been chosen to make amidinates in this dissertation. Reactions of zirconium amidinate amide complexes with dioxygen, water or hydrogen peroxide have been studied. Metal-containing products were $\{(\mu\text{-}O)Zr[MeC(N^{i}Pr)_2]_2\}_2$ [zirconium amidinate oxo dimer] and $\{(\mu\text{-}O)Zr[MeC(N^{i}Pr)_2]_2\}_n$ [zirconium amidinate oxo polymer] based on NMR, IR, MS

and elemental analysis. Also, the reaction of $Zr[MeC(N^iPr)_2]_2(NMe_2)_2$ with dioxygen yields $\{(\mu\text{-}\eta^2\text{:}\eta^2\text{-}O_2)Zr[MeC(N^iPr)_2]_2\}_3$ [zirconium peroxo amidinate trimer] and its crystal structure is reported. $Ta[MeC(N^iPr)_2](NMe_2)_4$ [tantalum amidinate amide] and carbon tetrachloride undergo an amide-chloride exchange, giving $Ta[MeC(N^iPr)_2](NMe_2)_3Cl$ [tantalum amidinate amide chloride]. $Ta[MeC(N^iPr)_2](NMe_2)_3Cl$ has also been synthesized through the aminolysis of $Ta(NMe_2)_4Cl$ [tantalum amide chloride] with a diisopropyl amidine. $W(CH_2{}^tBu)_3(\equiv C{}^tBu)$ [tungsten neopentyl neopentylidyne] has been prepared through the reaction of $W(OMe)_3Cl_3$ [tungsten chloride methoxide] and $Zn(CH_2{}^tBu)_2$ [dineopentyl zinc]. Also, a side product which has been characterized through NMR spectroscopies to be $W(OMe)_2Cl(CH_2{}^tBu)_3$ [tungsten neopentyl chloride methoxide].

Table of Contents

List of Tables

List of Figures

List of Schemes

Numbering Scheme for the Compounds in the Text

1 $Zr(NMe_2)_4$

2 $CyN(H)C(NMe_2)=NCy$

3 $Zr[NMe_2C(NCy)_2](NMe_2)_3$

4 $Zr[NMe_2C(NCy)_2]_2(NMe_2)_2$

5 $^{i}PrN=C=N^{i}Pr$

6 $Li[MeC(N^{i}Pr)_2]$

7 $^{i}PrN(H)C(Me)=N^{i}Pr$

8 $Zr[MeC(N^{i}Pr)_2]_2Cl_2$

9 $Zr[MeC(N^{i}Pr)_2](NMe_2)_3$

10 $Zr[MeC(N^{i}Pr)_2]_2(NMe_2)_2$

11 $Zr[MeC(N^{i}Pr)_2](NEt_2)_3$

12 $Zr[MeC(N^{i}Pr)_2]_2(NEt_2)_2$

13 $(O=)Zr[MeC(N^{i}Pr)_2]_2$

14 $\{(\mu\text{-}O)Zr[MeC(N^{i}Pr)_2]_2\}_2$

15 $\{(\mu\text{-}O)Zr[MeC(N^{i}Pr)_2]_2\}_3$

16 $\{(\mu\text{-}O)Zr[MeC(N^{i}Pr)_2]_2\}_4$

17 $\{(\mu\text{-}O)Zr[MeC(N^{i}Pr)_2]_2\}_n$

18 $Zr(OH)_2[MeC(N^{i}Pr)_2]_2$

19 $CH_2(NMe_2)_2$

20 $\{(\mu\text{-}\eta^2\text{:}\eta^2\text{-}O_2)Zr[MeC(N^iPr)_2]_2\}_3$

21 $\{(\mu\text{-}O_2)Zr[MeC(N^iPr)_2]_2\}_2$

22 $(\eta^2\text{-}O_2)_2Zr(diimine)_2$

23 $[Zr_2(O_2)_2(SiW_{11}O_{39})_2]^{12-}$

24 $[Zr_2(O_2)_2(GeW_{11}O_{39})_2]^{12-}$

25 $[Zr\{N(^iPr_2PO)_2\}_2]_2(\mu\text{-}\eta^2\text{:}\eta^2\text{-}O_2)_2$

26 $Nb[MeC(N^iPr)_2](NMe_2)_4$

27 $Ta[MeC(N^iPr)_2](NMe_2)_4$

28 $Ta[MeC(N^iPr)_2](NMe_2)_3Cl$

29 $W(OMe)_3Cl_3$

30 $W(CH_2{}^tBu)_3(\equiv C{}^tBu)$

31 $W(OMe)_2Cl(CH_2{}^tBu)_3$

Part 1

Introduction

1.1. Foreword

Reactions of metal complexes with O_2 or water are of intense current interest.[1-10] In particular, the activation of O_2 by metal complexes and applications in biochemistry, catalysis and materials science have been actively studied. The focus has been on the reactions of O_2 with late transition meal complexes containing valance *d* electrons (d^n).[6] Reactivities of d^0 early transition metal complexes toward O_2 are much less known.[1-5]

Early transition metals are usually oxophilic, and the reactions of their complexes with O_2 to give metal oxides (MO_n) have been used to make microelectronic devices.[9] Reactions of d^0 early transition metal complexes with H_2O have also been used to make oxides.[10] This has led to recent interest in the nature of the reactions between d^0 early transition metal complexes and O_2 or H_2O.

The microelectronic industry has a high demand for faster, more powerful devices with an extended battery life. There is a continuous demand for new materials in microelectronic industry as devices are shrinking in size or becoming lighter in weight. One focus in inorganic chemistry is the preparation of metal oxides as the insulating layer in microelectronic devices. A transistor in a microprocessor is depicted in Scheme 1.1.

Currently, SiO_2 is the most abundant material used for the insulating layer in transistors because it is easily prepared from silicon wafers. As electronic devices become smaller, the transistors need to become smaller as well. The problem arises when the insulating oxide layer becomes too thin and can no

longer insulate well.[7] SiO_2 has a low dielectric constant (k = 3.9), and its ability to insulate is limited. When the insulating layer is less than 2 nm thick, the use of SiO_2 leads to a large current leakage through the insulating layer, making SiO_2 inadequate as a gate material.

One solution is replacing the SiO_2 thin film by a metal oxide film with a dielectric constant higher than k = 10.[7] Metal oxides such as HfO_2 (k = 25) and Ta_2O_5 (k = 26) are of intense interest. Several companies, such as Apple, Intel, and Samsung, have started replacing SiO_2 by HfO_2. In 2007, the current size of the transistor was 45 nm and the transistor shrunk by 40 percent in 2009 by this switch. The recent use of thinner and better insulating MO_n allows the number of transistors on integrated circuits to increase, doubling approximately every two years as observed by the Moore's law.[7] Chips using the MO_n-based insulators are faster, smaller, and last longer. In addition, batteries in, e.g., new tablet computers last much longer after charging.

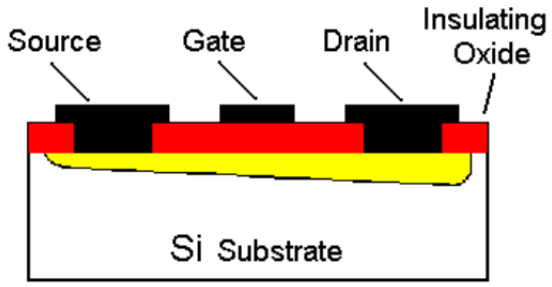

Scheme 1.1. Transistor in a microelectronic device.

Reactions of d^0 early transition metal complexes with oxygen or water have been employed to make microelectronic metal oxide (MO_n) through chemical vapor deposition (CVD) or atomic layer deposition (ALD) processes (Scheme 1.2).[7-10] Groups 4 and 5 homoleptic amide[9a-o,10b,e,f] and amide imide[9q,r] complexes are attractive for CVD and ALD processes because of their chemical and physical properties such as volatility, stability and decomposition characteristics.[10,11] However, these compounds are very air sensitive, making them difficult to handle. Ancillary ligands such as amdinate, β-diketonate, cyclopentadienyl, and guanidinate ligands have been used in precursors to make the compounds less sensitive to air and easier to handle.

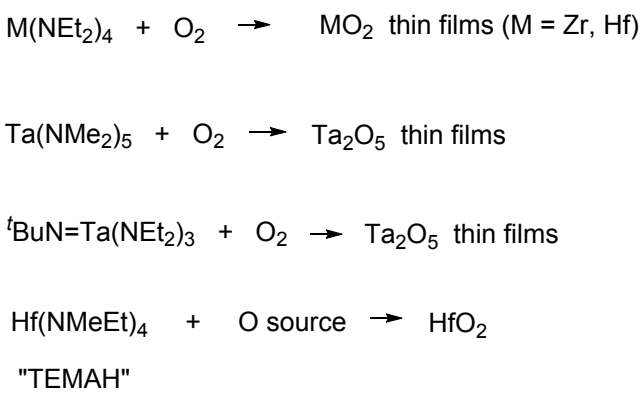

Scheme 1.2. Synthesis of metal-oxide thin films.

Reactions of d^n middle and late transition metal complexes with O_2 often involve metal oxidation. For example, Theopold and coworkers have studied the reaction of a chromium "nacnac" (i.e., β-diketiminate) complex with O_2.[6g] Magnesium reduction of $[(^i Pr_2Ph)_2nacnacCr(\mu\text{-}I)]_2$ resulted in the formation of $[(^i Pr_2Ph)_2nacnacCr]_2(\mu\text{-}N_2)$. The Cr-dinitrogen complex reacted with O_2 to yield $[(^i Pr_2Ph)_2nacnacCr](O)_2$ (Scheme 1.3). This is a rare example of a four-electron oxidative addition of O_2 to a single metal center and, in this case, the formation of a mononuclear, d^1 Cr(V) dioxo complex.

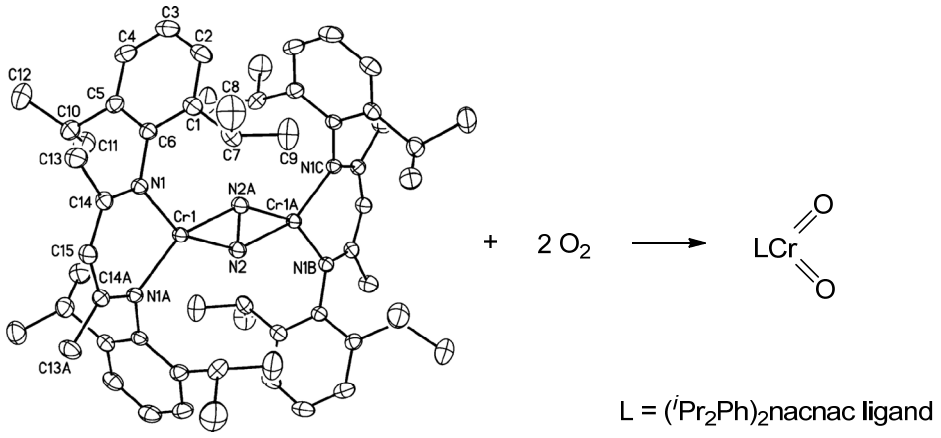

Scheme 1.3. Reaction of a Cr β-diketiminate complex with O_2.[6g]

Another example of metal oxidation by O_2 was studied by Prokop and Goldberg. They observed a direct conversion of a Mn^{III} complex $(TBP_8Cz)Mn^{III}$ [TBP_8Cz = octakis(*p*-tert-butylphenyl)corrolazinato^{3-}] to a Mn^V-oxo complex

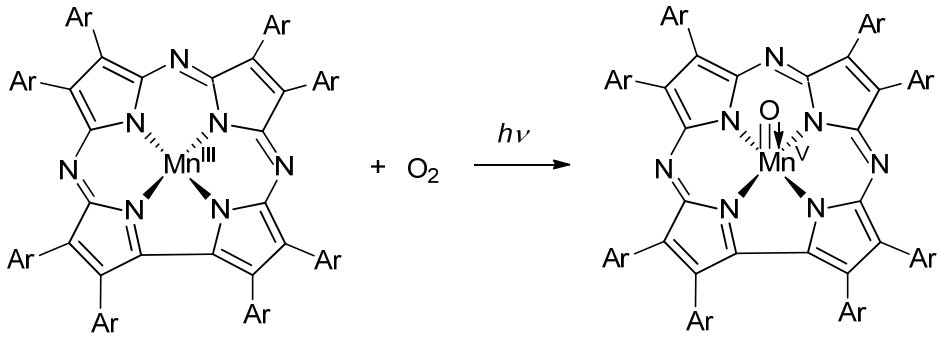

Scheme 1.4. Reaction of a Mn^{III} complex with O_2.[6j]

$(TBP_8Cz)Mn^{V}(O)$ with O_2 under visible light (Scheme 1.4).[6j] There are few examples of reactions that show a smooth conversion to well-defined high-valent terminal oxo complexes with treatment of O_2.

Complexes with no *d* electrons (d^0) are expected to follow different pathways in their reactions with O_2 and these pathways are not well defined (Scheme 1.5).[9,10] Tilley has reported the reaction of O_2 with $(\eta^5\text{-}C_5H_5)_2Zr(SiMe_3)Cl$ and the formation of the siloxide $(\eta^5\text{-}C_5H_5)_2Zr(OSiMe_3)Cl$.[1a] Schwartz and coworkers have reported that under mild conditions, $(\eta^5\text{-}C_5H_5)_2Zr(R)Cl$ (R = alkyl) complexes react with O_2 (Scheme 1.5).[1b]

Our group has reported that the reactions of d^0 amides $M(NMe_2)_4$ (M = Zr, Hf) with O_2 yield unusual trinuclear oxo aminoxide complexes $M_3(NMe_2)_6(\mu\text{-}NMe_2)_3(\mu_3\text{-}O)(\mu_3\text{-}ONMe_2)$ (M = Zr, Hf) (Scheme 1.6).[11a] Density functional theory calculations revealed the mechanistic pathways in the reactions of model complexes $Zr(NR_2)_4$ (R = H, Me) and $[Zr(NR_2)_4]_2$ (R = H, Me) with triplet O_2. Monomeric and dimeric reaction pathways were proposed.[11]

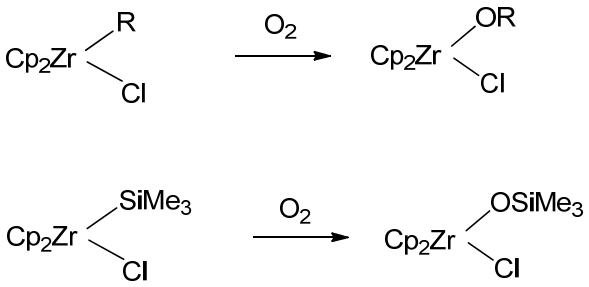

Scheme 1.5. Examples of the reactions between early transition metal complexes and O_2.[1a,b]

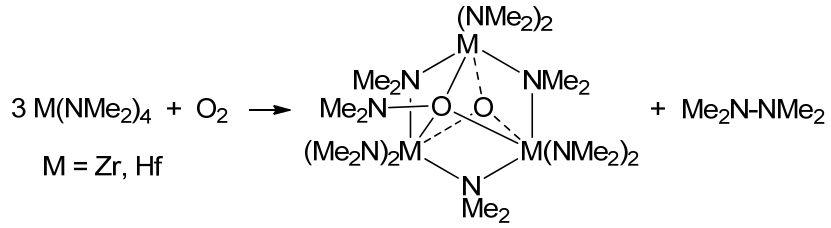

Scheme 1.6. Reactions of Zr and Hf amides with O_2.[11a]

Our group has also studied reactions of Group 5 amides with O_2 (Scheme 1.7).[11] The reaction of $Nb(NMe_2)_5$ with O_2 gives three complexes: monomeric $(Me_2N)_nNb(\eta^2\text{-}ONMe_2)_{5-n}$ (n = 3, 4) and dimeric $(Me_2N)_4Nb_2[\eta^2\text{-}N(Me)CH_2NMe_2]_2(\mu\text{-}O)_2$.[11e] Anionic amide ligands undergo oxidation, yielding $ONMe_2$ and oxo ligands.[11]

Transistion-metal amidinate complexes have been actively studied in recent years. Amidinates are versatile ligands and have been used in catalysis,[12a] N_2 activation,[12b] Si-H/Si-Cl bond actication,[12c] and chemical vapor deposition (CVD).[12d] They bond to a metal ion in a bidentate fashion through a conjugated system. The amidinate ligand is considered sterically equivalent to η^5-cyclopentadienyl but isoelectronic with π-allyl ligands. Parts 2-4 of this dissertation focus on Groups 4 and 5 amidinate amide complexes and their reactivities towards H_2O, H_2O_2, and O_2.

Another actively studied area is d^0 transition metal carbyne complexes. A carbyne complex contains at least one M≡C triple bond. The first carbyne complex, containing a d^n metal, was synthesized by E. O. Fischer in 1973.[13] After Fischer's discovery, R. R. Schrock and others have prepared carbyne complexes containing d^0 metals that have been called Schrock carbynes or alkylidyne compounds.[14] Alkylidyne complexes are typically those of early transition metals at high oxidation state (d^0). Part 5 of this dissertation is focused on mechanistic studies to help understand the formation of an archetypical W(VI) alkylidyne complex. It is not understood when the triple bond forms in the reaction to give

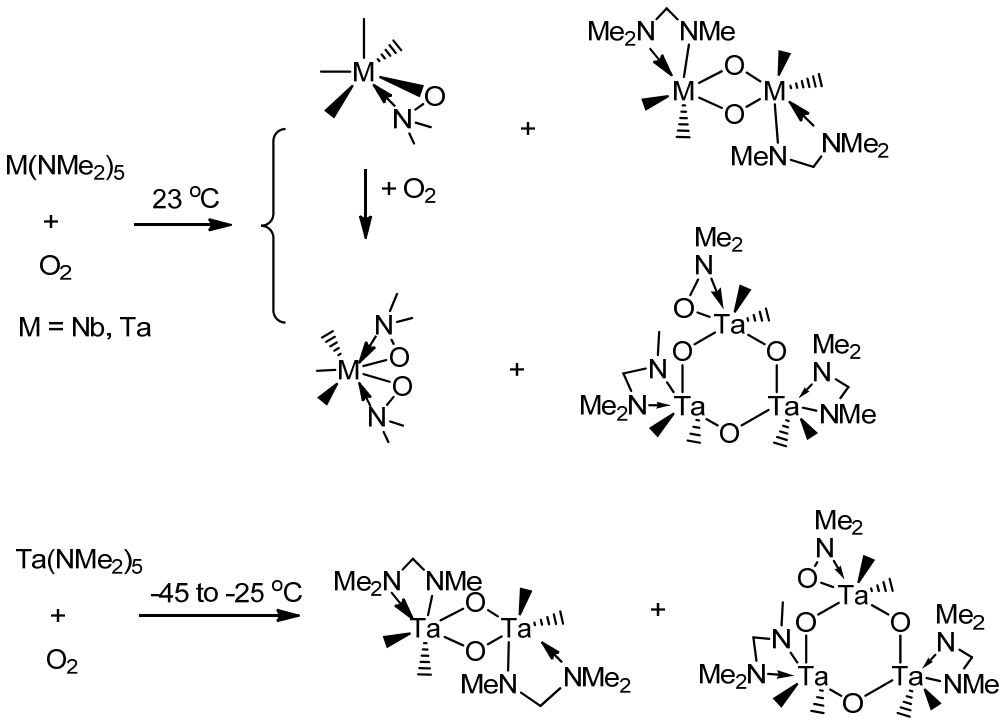

Scheme 1.7. Reactions of $M(NMe_2)_5$ (M = Nb, Ta) with O_2.[11b,e]

the carbyne complex. A typical reaction to give a Schrock carbyne is given in Scheme 1.8.[14b]

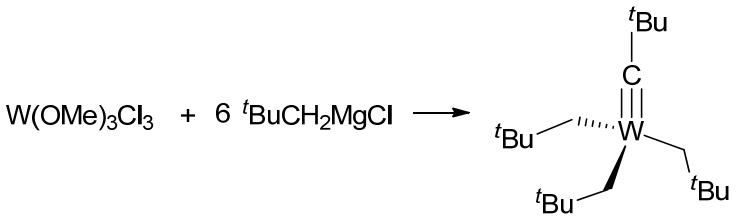

Scheme 1.8. Formation of a Schrock-type carbyne.[14b]

1.2. Current Dissertation

1.2.1. Part 2

$Zr[MeC(N^iPr)_2]_2(NMe_2)_2$ (**10**) has been prepared by three different routes. Two are salt metathesis based on the reactions of $Zr(NMe_2)_2Cl_2$ with lithium amidinate $Li[MeC(N^iPr)_2]$ (**6**) and $Zr[MeC(N^iPr)_2]_2Cl_2$ (**8**) with $LiNMe_2$, respectively. The third route is aminolysis in which $Zr(NR_2)_4$ (R = Me, Et) reacts with amidine $^iPrN(H)C(Me)=N^iPr$ (**7**) to form $Zr[MeC(N^iPr)_2]_2(NR_2)_2$ (R = Me, **10**; Et, **12**). The aminolysis gives cleaner products, higher yields and is easier to operate. The aminolysis route is thus chosen throughout this dissertation. $Zr[MeC(N^iPr)_2]_2Cl_2$ (**8**) and mono amidinates $Zr[MeC(N^iPr)_2](NMe_2)_3$ (**9**) and $Zr[MeC(N^iPr)_2](NEt_2)_3$ (**11**) have also been prepared and characterized.

1.2.2. Part 3

The reactions of Zr amidinate amides $Zr[MeC(N^iPr)_2]_2(NR_2)_2$ (R = Me, **10**; Et, **12**) with water or O_2 have been studied. Two major reaction products are a soluble oxo-bridged dimer $\{(\mu\text{-}O)Zr[MeC(N^iPr)_2]_2\}_2$ (**14**) and an insoluble polymer $\{(\mu\text{-}O)Zr[MeC(N^iPr)_2]_2\}_n$ (**17**). Another product in the reaction of **10** with O_2 at -30 °C is the peroxo-bridged trimer $\{(\mu\text{-}\eta^2\text{:}\eta^2\text{-}O_2)Zr[MeC(N^iPr)_2]_2\}_3$ (**20**). Its crystal structure is reported here. Peroxo dimer $\{(\mu\text{-}O_2)Zr[MeC(N^iPr)_2]_2\}_2$ (**21**) was observed in MS studies of the crystals of **20**. **20** was also prepared from the reaction of $Zr[MeC(N^iPr)_2]_2Cl_2$ (**8**) with Na_2O_2. **20** reacts with $Zr[MeC(N^iPr)_2]_2(NMe_2)_2$ (**10**) to give the oxo-bridged dimer $\{(\mu\text{-}O)Zr[MeC(N^iPr)_2]_2\}_2$ (**14**), polymer $\{(\mu\text{-}O)Zr[MeC(N^iPr)_2]_2\}_n$ (**17**), $HNMe_2$, and $CH_2(NMe_2)_2$ (**19**).

1.2.3. Part 4

Group 5 amidinate amide complexes $M[MeC(N^iPr)_2](NMe_2)_4$ (M = Nb, **22**; Ta, **23**) have been prepared by the aminolysis of $M(NMe_2)_5$ (M = Nb, Ta) with amidine ^{i}PrN(H)C(Me)=N^{i}Pr (**7**). **22** and **23** have been characterized by ^{1}H and ^{13}C NMR spectroscopies and elemental analysis. Reaction between CCl_4 and **23** yields $Ta[MeC(N^iPr)_2](NMe_2)_3Cl$ (**24**) which has been characterized by NMR spectroscopies and MS.

1.2.4. Part 5

Reaction between $W(OMe)_3Cl_3$ (**29**) and $Zn(CH_2{}^tBu)_2$ gives the previously reported alkylidyne complex $W(CH_2{}^tBu)_3(\equiv C{}^tBu)$ (**30**). The study, using the alkyl zinc reagent, which is a weaker nucleophilic reagent than $LiCH_2{}^tBu$ and $Mg(CH_2{}^tBu)_2$, is an attempt to identify an intermediate in the formation of $W(CH_2{}^tBu)_3(\equiv C{}^tBu)$ (**30**). The reaction between $W(OMe)_3Cl_3$ and $Zn(CH_2{}^tBu)_2$ also yields another product identified to be $W(OMe)_2Cl(CH_2{}^tBu)_3$ (**31**) based on ^1H, $^{13}C\{^1H\}$, HSQC, DEPT, and 1-D and 2-D NOESY NMR spectroscopies.

1.2.5. Part 6

A summary of the research in this dissertation is presented. Important findings in each part in the dissertation are given. Research in the future is proposed.

References

1. (a) Tilley, T. D. *Organometallics* **1985**, *4*, 1452. (b) Blackburn, T. F.; Labinger, J. A.; Schwartz, J. *Tetrahedron Lett.* **1975**, *16*, 3041. (c) Labinger, J. A.; Hart, D. W.; Seibert, W. E.; Schwartz, J. *J. Am. Chem. Soc.* **1975**, *97*, 3851. (d) Lubben, T. V.; Wolczanski, P. T. *J. Am. Chem. Soc.* **1987**, *109*, 424. (e) Lubben, T. V.; Wolczanski, P. T. *J. Am. Chem. Soc.* **1985**, *107*, 701. (f) Wang, R.; Folting, K.; Huffman, J. C.; Chamberlain, L. R.; Rothwell, I. P. *Inorg. Chim. Acta* **1986**, *120*, 81. (g) Gibson, V. C.; Redshaw, C.; Walker, G. L. P.; Howard, J. A. K.; Hoy, V. J.; Cole, J. M.; Kuzmina, L. G.; De Silva, D. S. *J. Chem. Soc., Dalton Trans.* **1999**, 161. (h) Schaverien, C. J.; Orpen, A. G. *Inorg. Chem.* **1991**, *30*, 4968. (i) Liu, X.; Cui, D. *Dalton Trans.* **2008**, 3747. (j) Van Asselt, A.; Santarsiero, B. D.; Bercaw, J. E. *J. Am. Chem. Soc.* **1986**, *108*, 8291. (k) Brindley, P. B.; Hodgson, J. C. *J. Organomet. Chem.* **1974**, *65*, 57. (l) Kim, S. J.; Choi, D. W.; Lee, Y. J.; Chae, B. H.; Ko, J. J.; Kang, S. O. *Organometallics* **2004**, *23*, 559. (m) Morris, A. M.; Pierpont, C. G.; Finke, R. G. *Inorg. Chem.* **2009**, *48*, 3496. (n) Adam, W.; Putterlik, J.; Schuhmann, R. M.; Sundermeyer, J. *Organometallics* **1996**, *15*, 4586. (o) Vetter, W. M.; Sen, A. *Organometallics* **1991**, *10*, 244. (p) Van Asselt, A.; Trimmer, M. S.; Henling, L. M.; Bercaw, J. E. *J. Am. Chem. Soc.* **1988**, *110*, 8254. (q) Boro, B. J.; Lansing, R.; Goldberg, K. I.; Kemp, R. A. *Inorg. Chem. Comm.* **2011**, *14*, 531.
2. Stanciu, C.; Jones, M. E.; Fanwick, P. E.; Abu-Omar, M. M. *J. Am. Chem. Soc.* **2007**, *129*, 12400.

3. Lu, F.; Zarkesh, R. A.; Heyduk, A. F. *Eur. J. Inorg. Chem.* **2012**, 467.
4. Chisholm, M. H.; Hammond, C. E.; Huffman, J. C. *J. Chem. Soc., Chem. Commun.* **1987**, 1423.
5. Brindley, P. B.; Hodgson, J. C. *J. Organomet. Chem.* **1974**, *65*, 57.
6. For studies of the reactions between O_2 and late transition metal complexes, see, for example, (a) Campbell, A. N.; Stahl, S. S. *Acc. Chem. Res.* **2012**, *45*, 851. (b) Theopold, K. H.; Reinaud, O. M.; Blanchard, S.; Leelasubeharoen, S.; Hess, A.; Thyagarajan, S. *ACS Symp. Ser.* **2002**, *823*, 75. (c) Que, L.; Tolman, W. B. *Nature* **2008**, *455*, 333. (d) Himes, R. A.; Karlin, K. D. *Curr. Top. Chem. Biol.* **2009**, *13*, 119. (e) Shook, R. L.; Borovik, A. S. *Chem. Comm.* **2008**, 6095. (f) Sheldon, R. A. in *Biomimetic Oxidations Catalyzed by Transition Metal Complexes*, Meunier, B. ed., Imperial College Press, 2000, pp. 613-662. (g) Monillas, W. H.; Yap, G. P. A.; MacAdams, L. A.; Theopold, K. H. *J. Am. Chem. Soc.* **2007**, *129*, 8090. (h) McQuilken, A. C.; Jiang, Y.; Siegler, M. A.; Goldberg, D. P. *J. Am. Chem. Soc.* **2012**, *134*, 8758. (i) Scheuermann, M. L.; Fekl, U.; Kaminsky, W.; Goldberg, K. I. *Organometallics* **2010**, *29*, 4749. (j) Boisvert, L.; Denney, M. C.; Kloek Hanson, S.; Goldberg, K. I. *J. Am. Chem. Soc.* **2009**, *131*, 15802. (k) Khusnutdinova, J. R.; Rath, N. P.; Mirica, L. M. *J. Am. Chem. Soc.* **2012**, *134*, 2414. (l) Nguyen, K. T.; Rath, S. P.; Latos-Grazynski, L.; Olmstead, M. M.; Balch, A. L. *J. Am. Chem. Soc.* **2004**, *126*, 6210. (m) Maury, J.; Feray, L.; Bazin, S.; Clement, J.-L.; Marque, S. R. A.; Siri, D.; Bertrand, M. P. *Chem. Eur. J.* **2011**, *17*, 1586. (n) Lewinski, J.; Koscielski, M.; Suwala, K.; Justyniak,

I. *Angew. Chem. Int. Ed.* **2009**, *48*, 7017. (o) Mukherjee, D.; Ellern, A.; Sadow, A. D. *J. Am. Chem. Soc.* **2012**, *134*, 13018. (p) Jana, S.; Berger, R. J. F.; Fröhlich, R.; Pape, T.; Mitzel, N. W. *Inorg. Chem.* **2007**, *46*, 4293. (q) Lee, C.-M.; Chuo, C.-H.; Chen, C.-H.; Hu, C.-C.; Chiang, M.-H.; Tseng, Y.-J.; Hu, C.-H.; Lee, G.-H. *Angew. Chem. Int. Ed.* **2012**, *51*, 5427. (r) Kelley, M. R.; Rohde, J.-U. *Chem. Comm.* **2012**, *48*, 2876. (s) Brown, S. N.; Mayer, J. M. *Inorg. Chem.* **1992**, *31*, 4091.

7. (a) Robertson, J. *Rep. Prog. Phys.* **2006**, *69*, 327. (b) Jones, A. C.; Aspinall, H. C.; Chalker, P. R.; Potter, R. J.; Kukli, K.; Rahtu, A.; Ritala, M.; Leskelae, M. *J. Mater. Chem.* **2004**, *14*, 3101. (c) Arghavani, R.; Miner, G.; Agustin, M. *Semicond. Internal.* **2007**, *30*, 32-34, 36, 38.

8. (a) Miller, J. B.; Schwartz, J.; Bernasek, S. L., *J. Am. Chem. Soc.* **1984**, *115*, 8239. (b) Feinstein-Jaffe, I.; Gibson, D.; Lippard, S. J.; Schrock, R. R.; Spool, A. *J. Am. Chem. Soc.* **1984**, *106*, 6305. (c) Schoettel, G.; Kress, J.; Fischer, J.; Osborn, J. A., *J. Chem. Soc. Chem. Comm*. **1988**, 914. (d) Legzdins P.; Phillips, E. C.; Rettig, S. J.; Sanchez, L.; Trotter, J.; Yee, V. C. *Organometallics*, **1988**, *7*, 1877. (e) Gamble, A. S.; Boncella, J. M., *Organometallics* **1993**, *12*, 2814. (f) Guzyr, O. I.; Prust, J.; Roesky, H. W.; Lehmann, C.; Teichert, M.; Cimpoesu, F. *Organometallics* **2000**, *19*, 1549. (g) Yoon, M.; Tyler, D. R., *Chem. Comm.* **1997**, 639. (h) Chen, S.-J.; Abbott, J. K. C.; Steren, C. A.; Xue, Z.-L. *J. Clust. Sci.* **2010**, *21*, 325. (i) Chen, S.-J.; Cai, H.; Xue, Z.-L. *Organometallics* **2009**, *28*, 167.

9. For CVD of metal oxides using O_2, see, for example, (a) Son, K.-A.; Mao, A.

Y.; Sun, Y.-M.; Kim, B. Y.; Liu, F.; Kamath, A.; White, J. M.; Kwong, D. L.; Roberts, D. A.; Vrtis, R. N. *Appl. Phys. Lett.* **1998**, *72*, 1187. (b) Niimi, H.; Johnson, R. S.; Lucovsky, G.; Massoud, H. Z. *Proc. Electrochem. Soc.* **2000**, *2000-2*, 487. (c) Eichler, J. F.; Just, O.; Rees, W. S., Jr. *J. Mater. Chem.* **2004**, *14*, 3139. (d) Takahashi, K.; Funakubo, H.; Hino, S.; Nakayama, M.; Ohashi, N.; Kiguchi, T.; Tokumitsu, E. *J. Mater. Res.* **2004**, *19*, 584. (e) Ogura, A.; Ito, K.; Ohshita, Y.; Ishikawa, M.; Machida, H. *Thin Solid Films* **2003**, *441*, 161. (f) Rodriguez-Reyes, J. C. F.; Teplyakov, A. V. *J. Appl. Phys.* **2008**, *104*, 084907. (g) Ohshita, Y.; Ogura, A.; Ishikawa, M.; Kada, T.; Machida, H. *Jpn. J. Appl. Phys. 2.* **2003**, *42*, L578. (h) Matero, R.; Ritala, M.; Leskelae, M.; Sajavaara, T.; Jones, A. C.; Roberts, J. L. *Chem. Mater.* **2004**, *16,* 5630. (i) Kan, B.-C.; Boo, J.-H.; Lee, I.; Zaera, F. *J. Phys. Chem. A* **2009**, *113*, 3946. (j) Hausmann, D. M.; de Rouffignac, P.; Smith, A.; Gordon, R.; Monsma, D. *Thin Solid Films* **2003**, *443*, 1. (k) Meiere, S. H.; Peck, J.; Litwin, M. *ECS Trans.* **2006**, *1*, 103. (l) Chen, T.; Cameron, T. M.; Nguyen, S. D.; Stauf, G. T.; Peters, D. W.; Maylott, L.; Li, W.; Xu, C.; Roeder, J. F.; Hendrix, B. C.; Hilgarth, M.; Niinisto, J.; Kukli, K.; Ritala, M.; Leskela, M. *ECS Trans.* **2008**, *16*, 87. (m) Lee, S.; Kim, W.-G.; Rhee, S.-W.; Yong, K. *J. Electrochem. Soc.* **2008**, *155*, H92. (n) Schaeffer, J.; Edwards, N. V.; Liu, R.; Roan, D.; Hradsky, B.; Gregory, R.; Kulik, J.; Duda, E.; Contreras, L.; Christiansen, J.; Zollner, S.; Tobin, P.; Nguyen, B.-Y.; Nieh, R.; Ramon, M.; Rao, R.; Hegde, R.; Rai, R.; Baker, J.; Voight, S. *J. Electrochem. Soc.* **2003**, *150*, F67. (o) Woods, J. B.; Beach, D. B.; Nygren, C. L.; Xue, Z.-L.

Chem. Vap. Deposition **2005**, *11*, 289. (p) Lehn, J.-S.; Javed, S.; Hoffman, D. M. *Chem. Vap. Deposition* **2006**, *12*, 280. (q) Chiu, H.-T.; Wang, C.-N.; Chuang, S.-H.; *Chem. Vap. Deposition* **2000**, *6*, 223. (r) Wiedmann, M. K.; Heeg, M. J.; Winter, C. H. *Inorg. Chem.* **2009**, *48*, 5382.

10. For CVD of metal oxides using water, see, for example, (a) Dezelah, C. L., IV; Niinisto, J.; Kukli, K.; Munnik, F.; Lu, J.; Ritala, M.; Leskela, M.; Niinisto, L. *Chem. Vap. Deposition* **2008**, *14*, 358. (b) Dezelah, C. L., IV; El-Kadri, O. M.; Szilagyi, I. M.; Campbell, J. M.; Arstila, K.; Niinistoe, L.; Winter, C. H. *J. Am. Chem. Soc.* **2006**, *128*, 9638. (c) Majumder, P.; Jursich, G.; Takoudis, C. *J. Appl. Phys.* **2009**, *105*, 104106/1. (d) Consiglio, S.; Clark, R. D.; Nakamura, G.; Wajda, C. S.; Leusink, G. J. *J. Vacuum Sci. Technol. A* **2012**, *30*, 01A119/1. (e) Tao, Q.; Kueltzo, A.; Singh, M.; Jursich, G.; Takoudis, C. G. *J. Electrochem. Soc.* **2011**, *158*, G27. (f) Shi, X.; Tielens, H.; Takeoka, S.; Nakabayashi, T.; Nyns, L.; Adelmann, C.; Delabie, A.; Schram, T.; Ragnarsson, L.; Schaekers, M.; Date, L.; Schreutelkamp, R.; Van Elshocht, S. *J. Electrochem. Soc.* **2011**, *158*, H69.

11. (a) Wang, R.; Zhang, X.; Chen, S.-J.; Yu, X.; Wang, C.; Beach, D. B.; Wu, Y.; Xue, Z. *J. Am. Chem. Soc.* **2005**, *127*, 5204. (b) Chen, S.-J.; Zhang, X.; Yu, X.; Qiu, H.; Yap, G. P. A.; Guzei, I. A.; Lin, Z.; Wu, Y.; Xue, Z. *J. Am. Chem. Soc.* **2007**, *129*, 14408. (c) Chen, S.-J.; Zhang, X.-H.; Lin, Z.; Wu, Y.-D.; Xue, Z.-L. *Sci. China Chem. **2009**, 52*, 1723. (d) Chen, S.-J.; Yap, G. P. A.; Xue, Z.-L. *Sci. China Chem. **2009**, 52, 1583.* (e) Chen, S.-J.; Zhang, J.; Yu, X.; Bu, X.; Chen, X.; Xue, Z. *Inorg. Chem.* **2010**, *49*, 4017. (f) Chen, T.-N.; Zhang, X.-

H.; Wang, C.-S.; Chen, S.-J.; Wu, Z.-Z.; Li, L.-T.; Sorasaenee, K. R.; Diminnie, J. B.; Pan, H.-J.; Guzei, I. A.; Rheingold, A. L.; Wu, Y.-D.; Xue, Z.-L. *Organometallics* **2005**, *24*, 1214. (g) Qiu, H.; Chen, S.-J.; Wang, C.-S.; Wu, Y.-D.; Guzei, I. A.; Chen, X.-T.; Xue, Z.-L. *Inorg. Chem.* **2009**, *48*, 3073. (h) Yu, X.; Chen, X.-T.; Xue, Z.-L. *Organometallics* **2009**, *28*, 6642. (i) Chen, S.-J.; Xue, Z.-L. *Organometallics* **2010**, *29*, 5579. (j) Wu, Z.; Cai, H.; Yu, X.-H.; Blanton, J. R.; Diminnie, J. B.; Pan, H.-J. ; Xue, Z.-L. *Organometallics* **2002**, *21*, 3973.

12. For the use of amidinate ligands, see, for example, (a) Cao, Y.; Du, Z.; Li, J.; Zhang, Y.; Zu, F.; Shen, Q. *Inorg. Chem.* **2011**, 50, 3729. (b) Fontaine, P. P.; Yonke, B. L.; Zavalij, P. Y.; Sita, L. R. *J. Am. Chem. Soc.* **2010**, *132*, 12273. (c) Tiong, P. J.; Nova, A.; Clot, E.; Mountford, P. *Chem. Commum.* **2001**, *47*, 3147. (d) Krisyuk, V.; Aloui, L.; Prud'homme, N.; Sysoev, S.; Senocq, F.; Samelor, D.; Vahlas, C. *Electrochemical and Solid-State Letters* **2011**, *14*, D26.
13. Fischer, E. O.; Kreis, G.; Kreiter, C. G.; Mülle, J.; Hunter, G.; Lorenz, H. *Agnew. Chem.* **1973**, 85, 618.
14. (a) Clark, D. N.; Schrock, R. R. *J. Am. Chem. Soc.* **1978**, 100, 6774. (b) Schrock, R. R.; Clark, D. N.; Sancho, J.; Wengrovius, J. H.; Rocklage, S. M.; Pedersen, S. F. *Organometallics* **1982**, *1*, 1645.

Part 2

Syntheses and Characterization of Zirconium Amidinate Amides

Abstract

$Zr[MeC(N^iPr)_2]_2(NMe_2)_2$ (**10**) has been prepared by three different routes: two salt metathesis reactions and one aminolysis. When the reaction was carried out by aminolysis, the yield of the final product **10** was the highest. The amidine $^iPrN(H)C(Me)=N^iPr$ (**7**) has an active proton which reacts with $Zr(NMe_2)_4$ (**1**) and releases $HNMe_2$. After perfecting the reaction conditions for the preparation of **10**, similar conditions were used to prepare $Zr[MeC(N^iPr)_2](NMe_2)_3$ (**9**), $Zr[MeC(N^iPr)_2](NEt_2)_3$ (**11**), and $Zr[MeC(N^iPr)_2]_2(NEt_2)_2$ (**12**). $Zr[MeC(N^iPr)_2]_2Cl_2$ (**8**) has been prepared from the reaction of $ZrCl_4$ with 2 equiv of $Li[MeC(N^iPr)_2]$ (**6**) through a salt metathesis reaction.

Compound **12** revealed an interesting dynamic NMR behavior. Variable-temperature NMR spectroscopy has been used to study the Bailar twist process. The activation parameters determined are $\Delta H^{\ddagger}$ = 10.9(1.1) kcal mol^{-1}, $\Delta S^{\ddagger}$ = -11(4) eu and $\Delta G^{\ddagger}_{303\,K}$ = 14(2) kcal mol^{-1}.

2.1. Introduction

Reactions of early transition metal complexes with O_2[1-5] are different from late transition metal complexes.[6] This is mainly due to the fact that early transition metal complexes are usually in their highest oxidation states and have no valence *d* elections (d^0). When late transition metal complexes react with O_2, the metal is often oxidized and its oxidation state is increased.

Metal oxide (MO_n) thin films are important microelectronic materials and they have been prepared through chemical vapor deposition (CVD) and atomic layer deposition (ALD) processes.[7-9] d^0 Amide[8a-o,9b,e,f] complexes, which were originally prepared by Bradley and Thomas,[10] are widely used as precursors to make metal oxide thin films through the reactions of metal amides with O_2 or water. d^0 Amides, especially homoleptic Groups 4 and 5 amide complexes $M(NR_2)_n$, are very reactive towards oxygen sources (O-sources such as H_2O, H_2O_2, NO, O_2, and O_3) and they are thus usually handled in an inert atmosphere.[1-6] In this dissertation the O-sources are H_2O, H_2O_2, and O_2.

Previous studies of the reactions between d^0 early transition metal complexes and O_2[1] focused on O insertion into the Zr-Si bond in $Cp_2Zr(SiMe_3)Cl$,[1a] and M-C bonds in Cp_2ZrRCl/Cp_2ZrR_2 (R = alkyl),[1b] $(RO)_2TiMe_2$,[1c] $(ArO)_2TaMe_3$,[1d] and $(ArN=)_2MoMe_2$.[1e] Also, a Zr(IV) bisperoxo complex was obtained as a product from the reaction of O_2 with a Zr(IV) complex that contains redox-active diimine ligands.[2] Complexes with no valence *d* electrons (d^0) have also been prepared using O_2 as a reactant. For example, $Mo(NMe_2)_6$, a d^0 complex was prepared from $Mo(NMe_2)_4$, a d^2 complex, and

adventitious O_2.[4a] Rapid autoxidation of $M(CH_2R)_4$ by O_2 has been studied.[4b] Our group has revealed unusual reactivities of d^0 Groups 4 and 5 complexes toward O_2.[11a,b,e] The reactions between $M(NMe_2)_4$ (M = Zr, Hf) and O_2 were found to give oxo aminoxides $M_3(NMe_2)_6(\mu\text{-}NMe_2)_3(\mu_3\text{-}O)(\mu_3\text{-}ONMe_2)$ and Me_2NNMe_2 (Scheme 2.1).[11a] These reactions provide an insight in the formation of metal oxides and the incorporation of O atoms into early transition metal complexes. Density functional theory (DFT) studies reveal that the O_2 reactions are radical in nature. These studies were started after TiO_2 thin films were prepared from $Ti(NMe_2)_4$ and O_2 through a CVD process.[9o] Our group has also studied the reactions of $M(NMe_2)_5$ (M = Nb, Ta) with O_2 and several products were isolated.[11b,e] Three products from the reaction of $Nb(NMe_2)_5$ with O_2 are given in Scheme 2.2. DFT calculations reveal that O_2 insertion into a M-N bond in $M(NMe_2)_5$ to give a peroxide intermediate is a key step in the formation of the products.

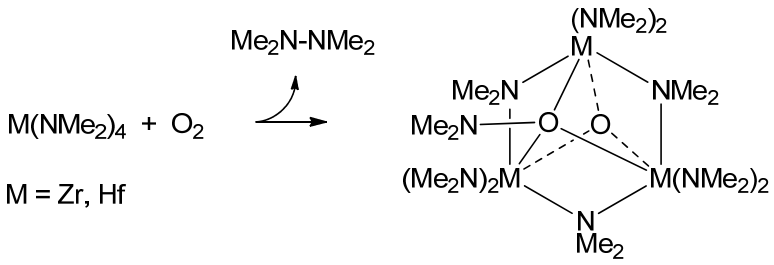

Scheme 2.1. Reactions of $M(NMe_2)_4$ M = Zr, Hf with O_2.[11a]

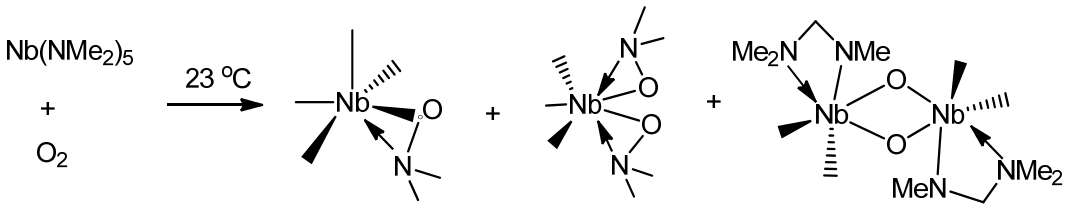

Scheme 2.2. Reaction of $Nb(NMe_2)_5$ with O_2.[11b]

Homoleptic metal amide compounds $M(NR_2)_n$ are often too sensitive to air and difficult to handle. For example, $Ta(NMe_2)_5$ reacts with O_2 at -25 °C,[11e] and with H_2O at -40 ºC.[5] Bidentate ligands such as amidinate, β-diketiminate, and guanidinate (Figure 2.1) have been introduced as ancillary ligands in order to make complexes more stable or less reactive towards an O-source.

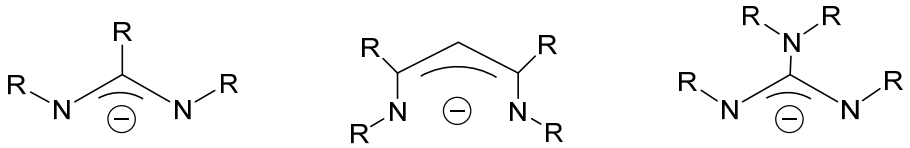

Figure 2.1. Bidentate nitrogen donor ancillary ligands.

Amidinates are versatile ligands and have been used in catalysis,[12] N_2 activation,[13] Si-H/Si-Cl bond activation,[14] and chemical vapor deposition (CVD).[15]

They bond to a metal ion in a bidentate fashion through conjugation. Although one bond is covalent while the other bond is a dative bond, the conjugation and resonance make the two bonds equivalent. The amidinate ligand $[RC(NR')_2]^-$ is considered sterically equivalent to η^5-cyclopentadienyl but isoelectronic with π-allyl ligands.[31] Devi et al. have used a hafnium amidinate complex in CVD to give a HfO_2 thin film (Scheme 2.3).[15f]

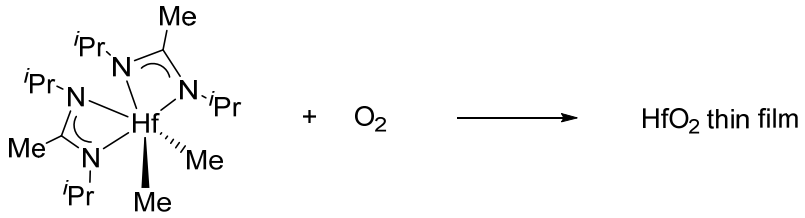

Scheme 2.3. Hafnium amidinate complex used as a CVD precursor.[15f]

Our group has also prepared several Group 4 amidinate amide complexes from MCl_4 (M = Ti, Zr, or Hf). Reactions between $TiCl_4$ and 2 equiv of $LiNMe_2$, followed by 2 equiv of the lithium amidinate salt $Li[MeC(NCy)_2]_2$, gave, e.g., $Ti[MeC(NCy)_2]_2(NMe_2)_2$ (Scheme 2.4). For Zr and Hf complexes, the reactions proceeded in the reverse order. Two equiv of the lithium amidinate salt were added to MCl_4 (M = Zr and Hf) followed by 2 equiv of lithium amide to yield

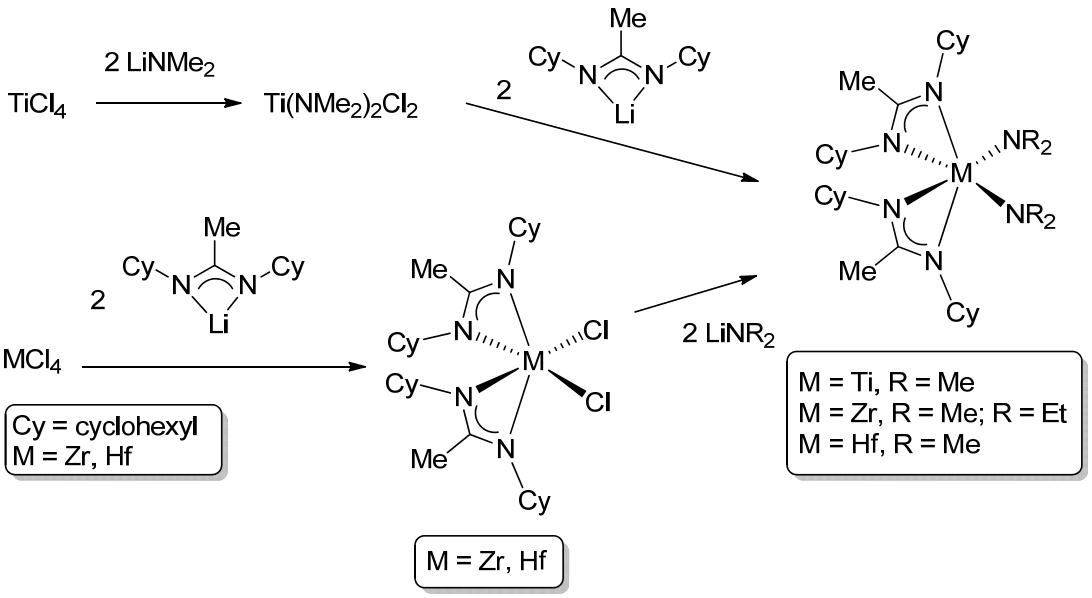

Scheme 2.4. Salt metathesis for Group 4 bisamidinate bisamide complexes.[16]

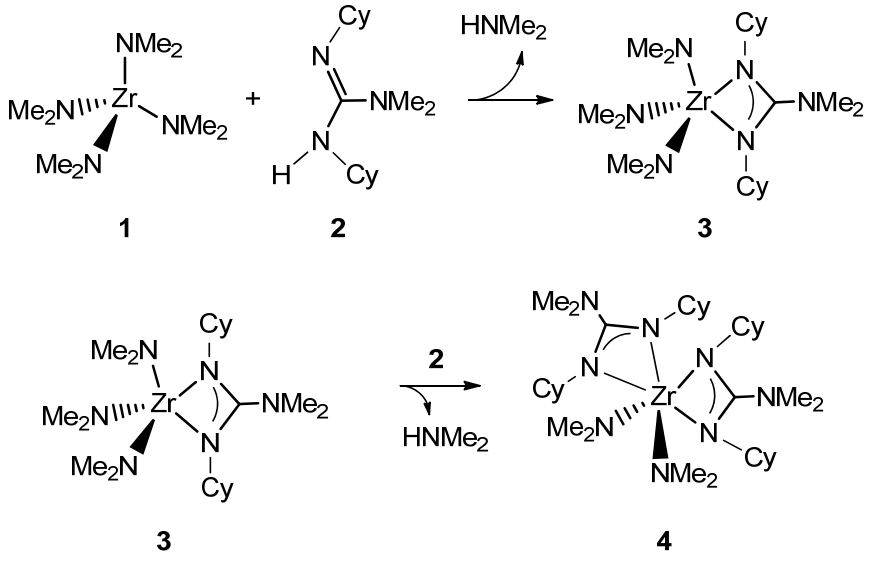

Scheme 2.5. Preparation of **3** and **4** through aminolysis.[17]

$M[MeC(NCy)_2]_2(NR_2)_2$ (M = Zr, R = Me, Et; M = Hf, R = Me) (Scheme 2.4).[16] We have also reported several Group 4 guanidinate amide complexes through the aminolysis of $Zr(NMe_2)_4$ (**1**) with 1 and 2 equiv of the guanidine **2** (Scheme 2.5).[17] It was found difficult to control the aminolysis with 1 equiv of guanidine.

In the current work, several zirconium amidinate amide complexes have been prepared through aminolysis in order to study their reactions with H_2O, H_2O_2 and O_2 in Part 3. Our syntheses and characterization of these complexes are reported here.

2.2. Results and Discussion

2.2.1. Synthesis of ^{i}PrN(H)C(Me)=N^{i}Pr (7)

Amidines are usually prepared by the reaction of an amine and nitrile in the presence of, e.g., a lanthanide catalyst.[18] In the current work, **7** is prepared by reacting 1 equiv of MeLi with a carbodiimide ^{i}Pr-N=C=N-^{i}Pr (**5**) to give its salt, $Li[MeC(N^{i}Pr)_2]$ (**6**). **6** is then acidified with H_2O to give **7** (Scheme 2.6) which is a liquid and purified by distillation at 115 °C and ~0.1 mmHg.

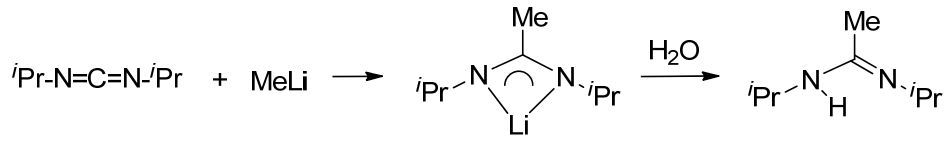

5 **6** **7**

Scheme 2.6. Preparation of **6** and **7**.

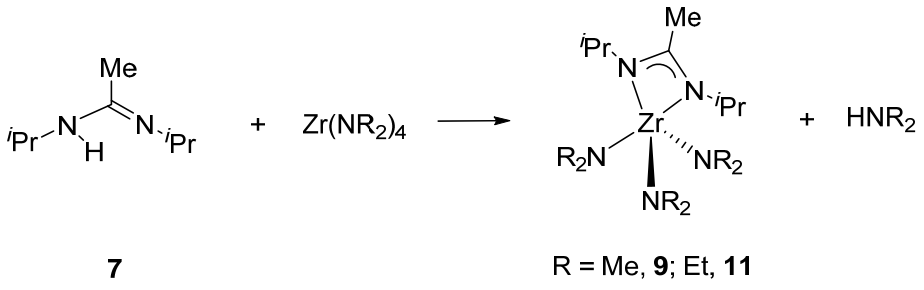

7

R = Me, **9**; Et, **11**

Scheme 2.7. Preparation of **9** and **11**.

^{1}H NMR spectra of **7** in $CDCl_3$[18c] and CD_3CN[18a] have been reported. We have found that at room temperature the ^{1}H NMR spectrum in toluene-d_8 showed a dynamic exchange as the peaks were broad. At 208 K, the ^{1}H NMR spectrum (Figure 2.2) of **7** in toluene-d_8 showed the –CH*Me*$_2$ groups appear at 1.11 and 1.22 ppm. The methyl on the quaternary carbon, -N(H)C(*Me*)=N-, was observed at 1.60 ppm. Two peaks at 3.47 and 4.28 ppm were assigned to the C*H* protons. The N*H* proton was observed at 4.71 ppm.

The ^{13}C{^{1}H} NMR spectrum of **7** (Figure 2.3) at 208 K showed the –CH*Me*$_2$ groups appear at 22.54 and 25.59 ppm. The methyl on the amidinate ligand was observed at 15.79 ppm. The *C*HMe$_2$ carbon atoms were observed at 41.10 and 49.04 ppm. The quaternary carbon atom appears at 152.11 ppm. Compound **7** was also characterized by mass spectrometry with *m*/z = 143.15488 [**7**+H$^+$], Calculated m/z = 143.15482 [**7**+H$^+$].

At room temperature, there were broad peaks and a variable temperature NMR experiment was performed. A ^{1}H and ^{13}C{^{1}H} NMR spectrum was collected

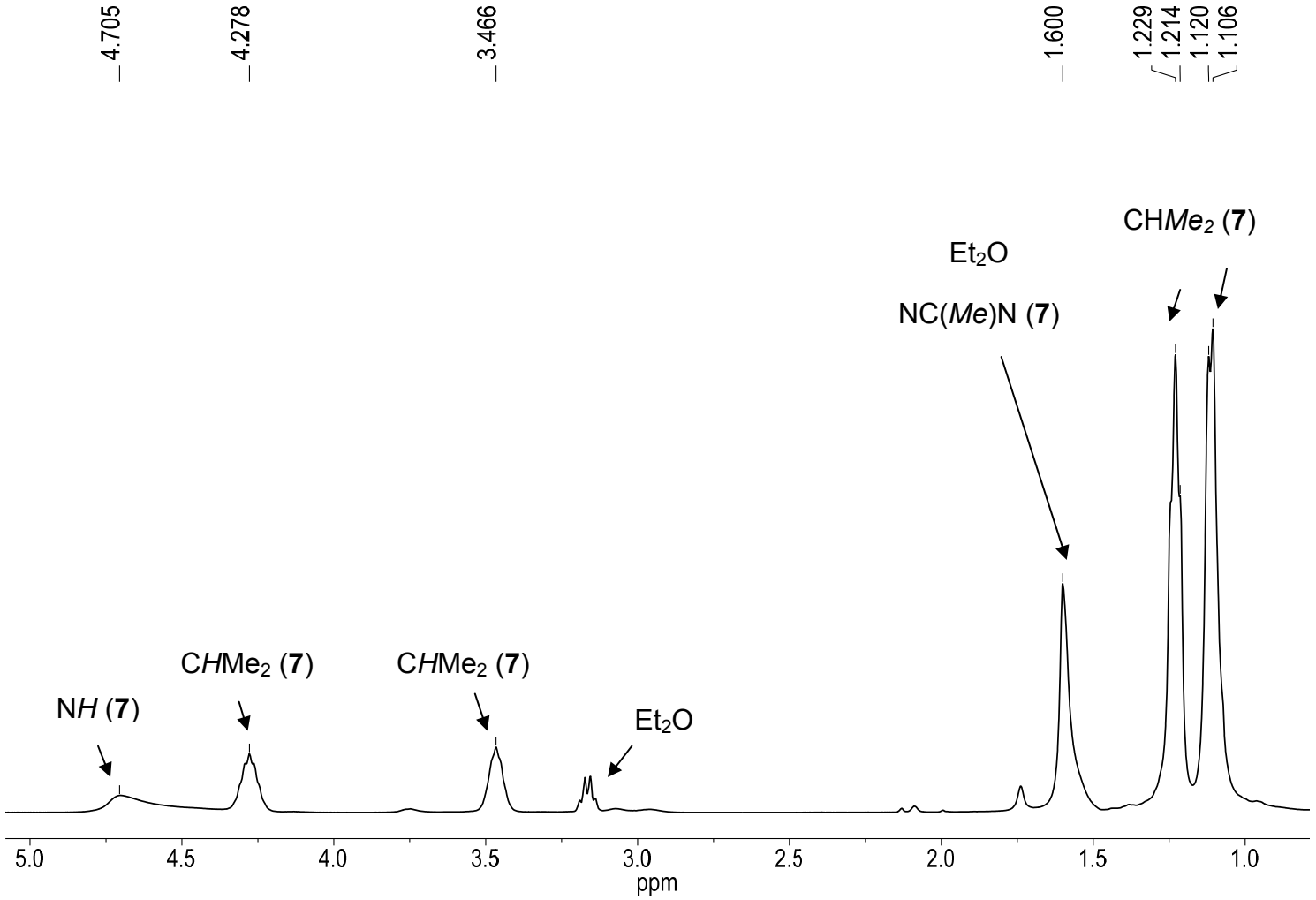

Figure 2.2. ^{1}H NMR spectrum of **7** in toluene-d_8 at 208 K.

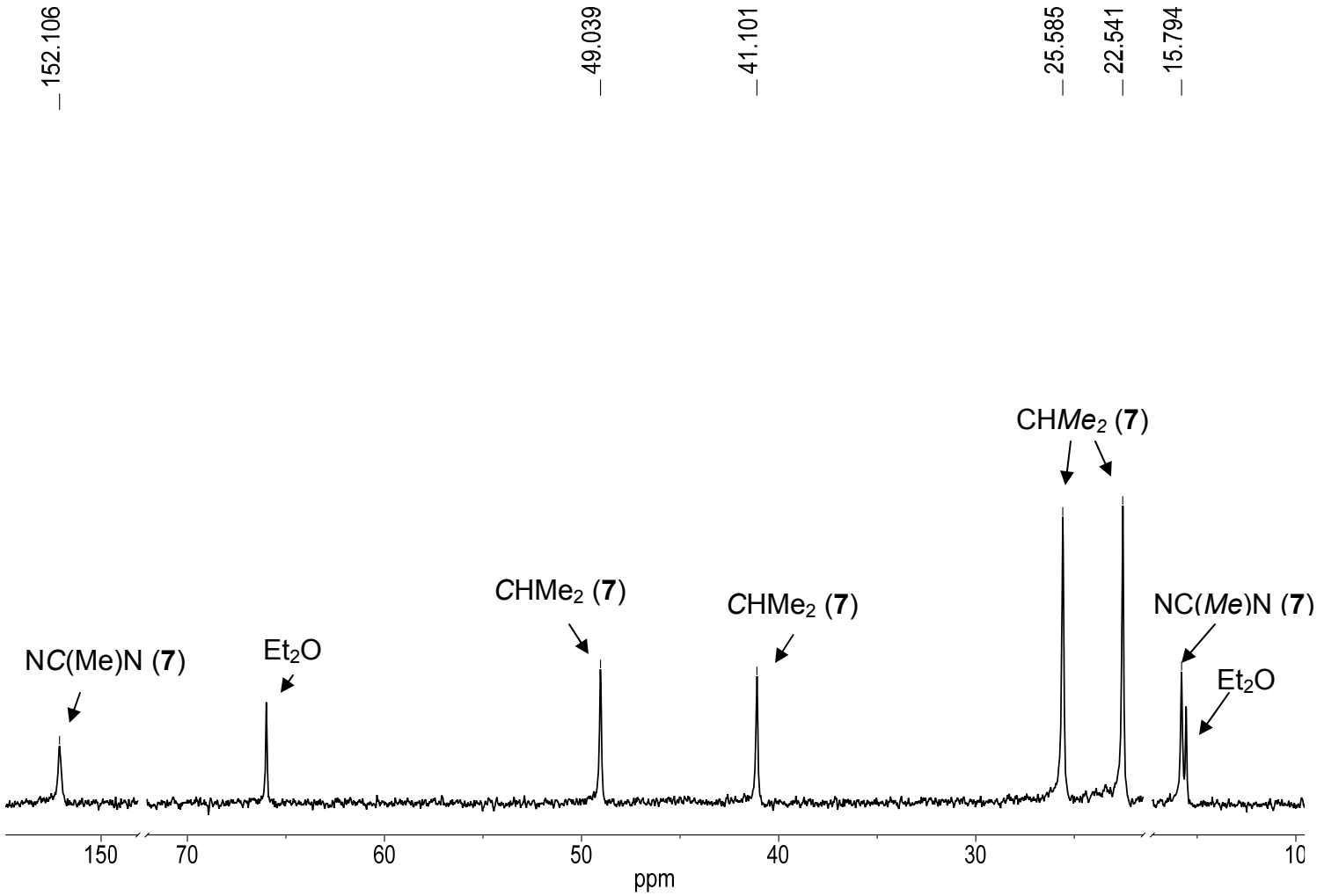

Figure 2.3. $^{13}C\{^{1}H\}$ NMR spectrum of **7** in toluene-d_8 at 208 K.

from 203 K to 298 K in 5 K intervals. We had hoped to obtain its rate of exchange and calculate its activation parameters. However, due to peak overlap in the ^{1}H NMR these efforts were not successful.

2.2.2. Synthesis and Mass Spectrum of Zr[MeC(N^{i}Pr)$_2$]$_2$Cl$_2$ (8)

Zr[MeC(N^{i}Pr)$_2$]$_2$Cl$_2$ (**8**) was prepared by adding 2 equiv of Li[MeC(N^{i}Pr)$_2$] (**6**) to freshly sublimed $ZrCl_4$ in a hexanes solution at -30 °C. After the mixture was warmed to 23 °C, it was refluxed at 70 °C for 6 h. Filtration and removal of volatiles gave the raw product as a neon green solid.

The ^{1}H NMR spectrum of **8** in benzene-d_6 (Figure 2.4) showed a doublet at 1.30 ppm for the CH*Me*$_2$ groups. A multiplet for the C*H* groups on the isopropyl groups appeared at 3.34 ppm. A singlet was observed for the methyl group on the amidinate ligand at 1.39 ppm. In the ^{13}C{^{1}H} NMR spectrum of **8** in benzene-d_6 (Figure 2.5), CH*Me*$_2$ groups appear at 24.51 ppm. The *C*H atom on the isopropyl groups at 48.63 ppm. The methyl group on the amidinate appeared at 10.52 ppm. The quaternary carbon atom was observed at 178.27 ppm. Devi and coworkers have prepared the Hf analog of **8** and the ^{1}H and ^{13}C{^{1}H} NMR spectra of **8** are consistent with those of the Hf analog.[15f]

Compound **8** was also characterized by mass spectrometry with a *m*/z = 443.09 [**8**+H^{+}]. Zirconium has five stable isotopes (^{90}Zr, ^{91}Zr, ^{92}Zr, ^{94}Zr, and ^{96}Zr; Table 2.1). In a mass spectrum, it is easy to see the isotopic pattern of a monomer Zr center. In addition, chlorine has two isotopes (^{35}Cl, ^{37}Cl; Table 2.2). Thus MS of **8** is expected to show a unique pattern. Solid powders of **8** were

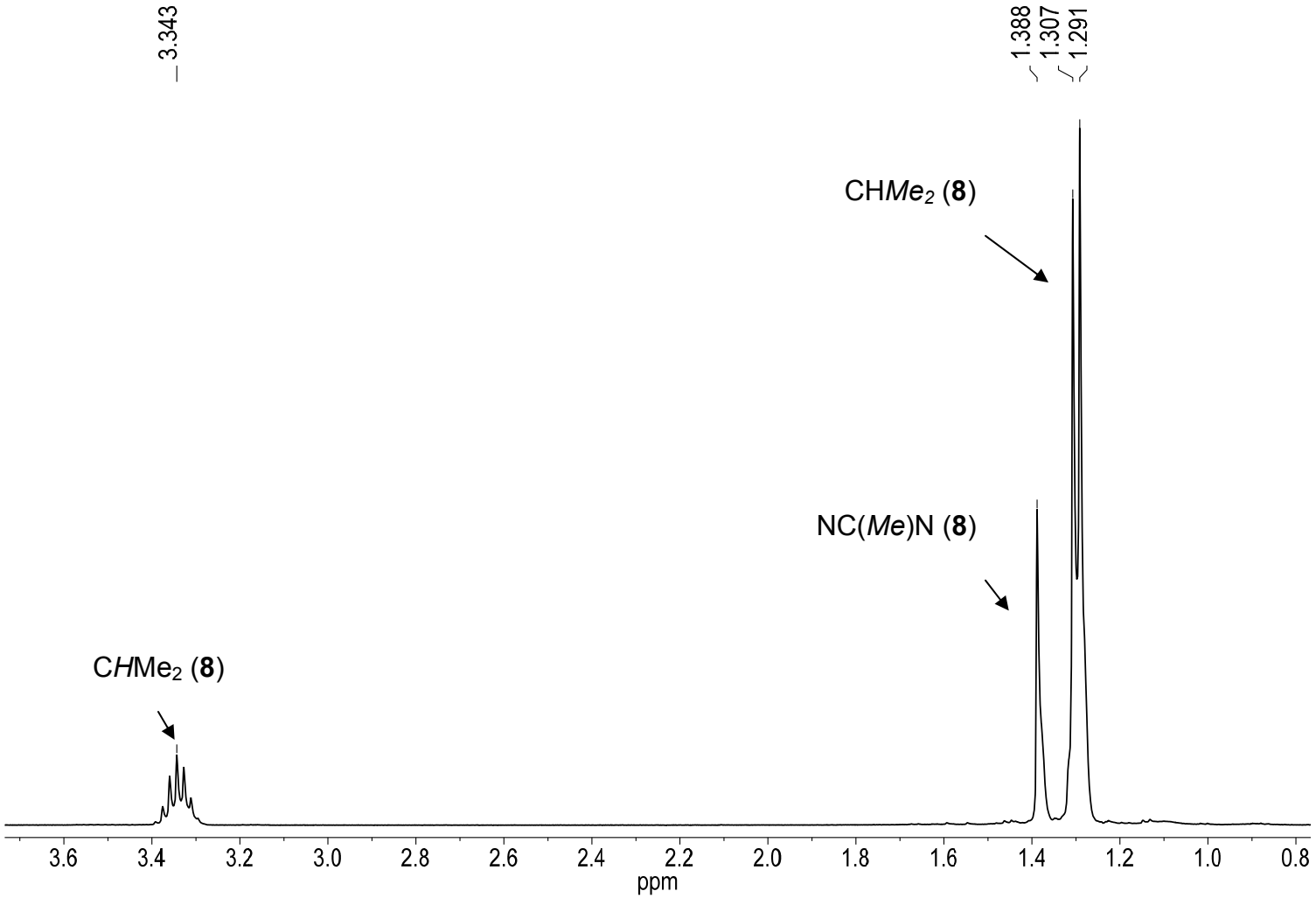

Figure 2.4. ^{1}H NMR spectrum of **8** in benzene-d_6.

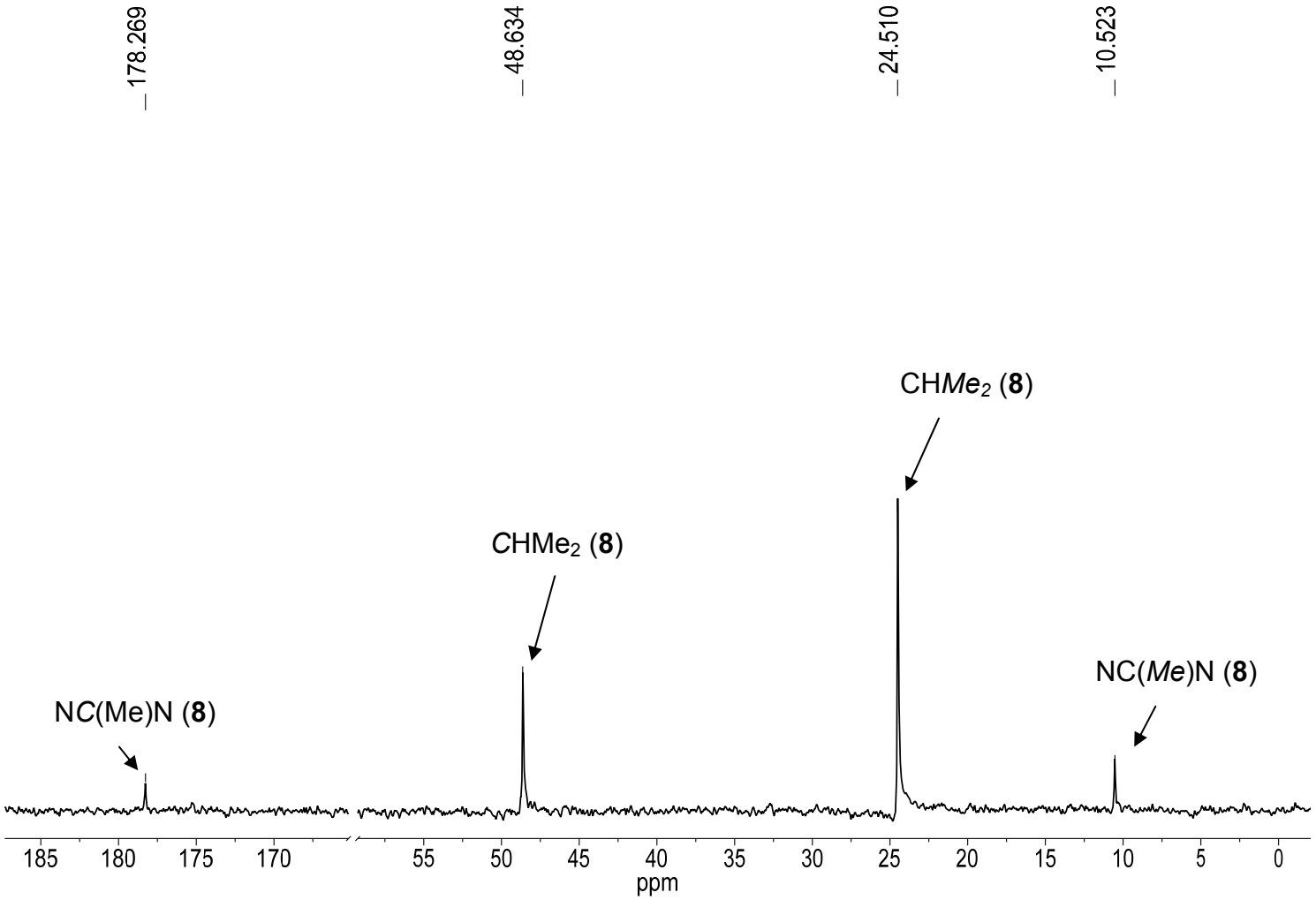

Figure 2.5. $^{13}C\{^{1}H\}$ NMR spectrum of **8** in benzene-d_6.

placed in a heated (200 °C) He stream by the sealed end of a capillary tube. The MS spectrum is given in Figure 2.6 along with the predicted spectrum. It confirmed the identity of **8**.

2.2.3. Synthesis and Characterization of the Monoamidinate $Zr[MeC(N^iPr)_2](NMe_2)_3$ (9)

$Zr[MeC(N^iPr)_2](NMe_2)_3$ (**9**) was prepared by adding 1 equiv of $^iPrN(H)C(Me)=N^iPr$ (**7**) in pentane to $Zr(NMe_2)_4$ (**1**) at -50 °C with the release of $HNMe_2$. The addition should be very slow to avoid the formation of the bisamidinate $Zr[MeC(N^iPr)_2]_2(NMe_2)_2$ (**10**). The yield of the raw product was 53%.

The ^1H NMR spectrum of **9** in benzene-d_6 (Figure 2.7) showed a doublet at 1.04 ppm for the CHMe_2 groups. Two singlets at 1.52 and 3.09 ppm were assigned to -C(*Me*) group on the amidinate and amide (NMe_2) ligands, respectively. A mulitiplet for the C*H*Me_2 groups appears at 3.34 ppm.

In the $^{13}C\{^1H\}$ NMR spectrum (Figure 2.8), peaks at 10.48 and 175.42 ppm were assigned to -C(*Me*) and -*C*(Me)- groups on the amidinate, respectively. The peak at 25.02 ppm accounts for the CHMe_2 groups. The NMe_2 ligands appear at 42.62 ppm.

Table 2.1. Stable isotopes of zirconium

Isotope	Accurate Mass	% Natural Abundance
^{90}Zr	89.9047026(26)	51.45(2)
^{91}Zr	90.9056439(26)	11.22(2)
^{92}Zr	91.9050386(26)	17.15(1)
^{94}Zr	93.9063148(28)	17.38(2)
^{96}Zr	95.908275(4)	2.80(1)

Table 2.2. Stable isotopes of chlorine

Isotope	Accurate Mass	% Natural Abundance
^{35}Cl	34.968852721(69)	75.78(4)
^{37}Cl	36.96590262(11)	24.22(4)

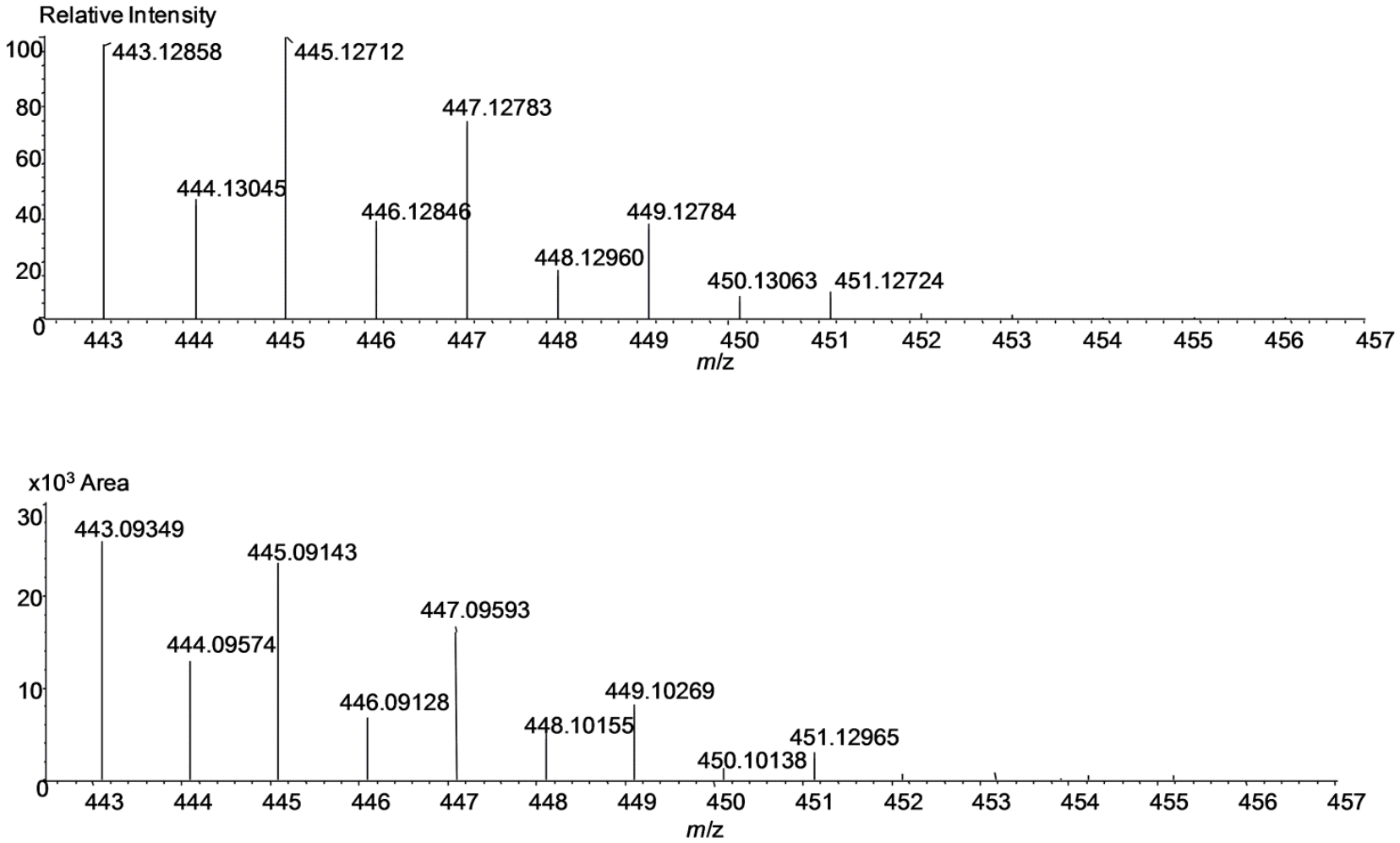

Figure 2.6. (Top) Calculated and (Bottom) Observed MS of [**8**+H^+].

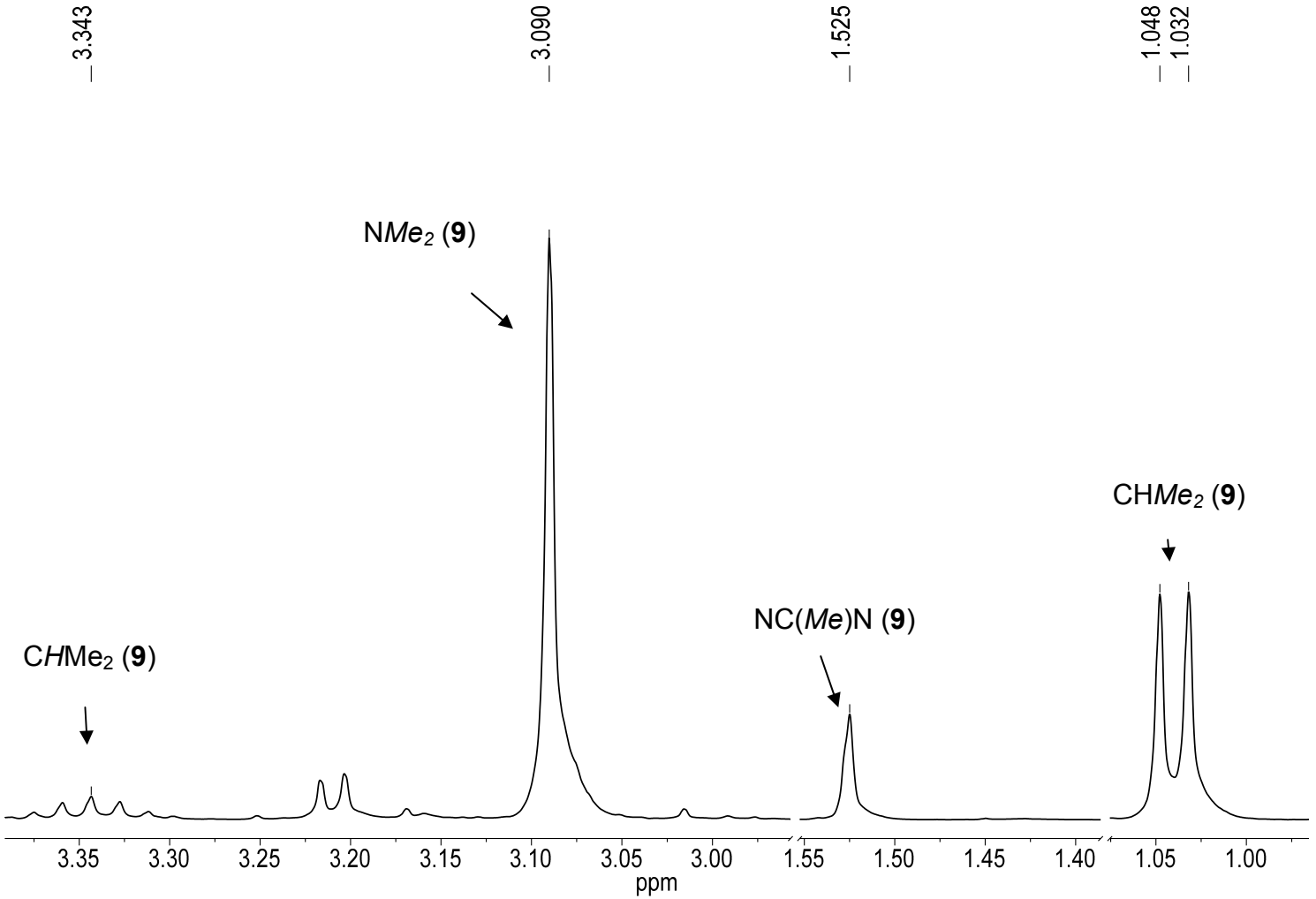

Figure 2.7. ^{1}H NMR spectrum of **9** in benzene-d_6.

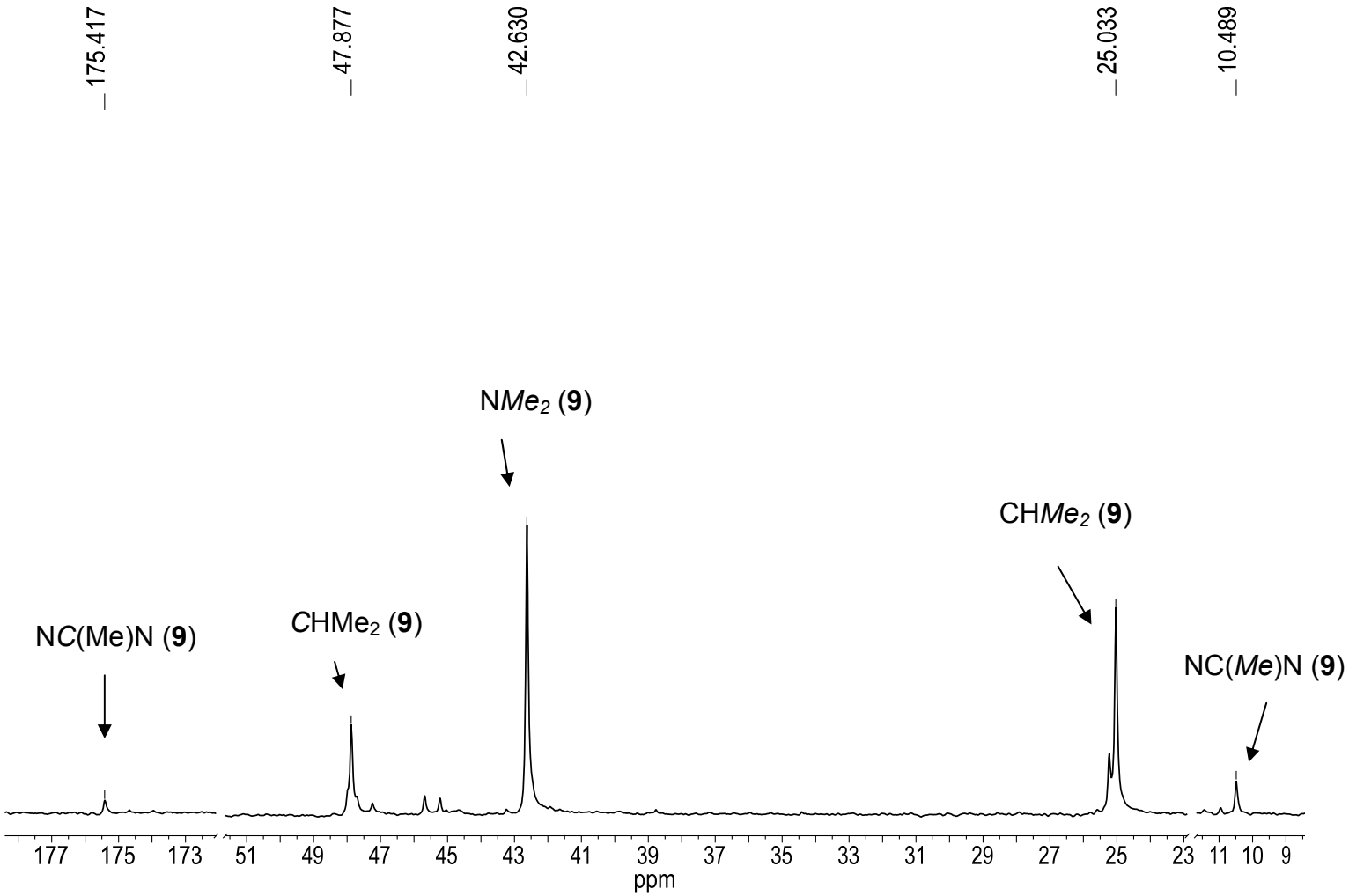

Figure 2.8. $^{13}C\{^{1}H\}$ NMR spectrum of **9** in benzene-d_6.

2.2.4. Synthesis of $Zr[MeC(N^iPr)_2]_2(NMe_2)_2$ (10)

$Zr[MeC(N^iPr)_2]_2(NMe_2)_2$ (**10**) has been prepared by three different routes with different yields. In Route 1, **10** was synthesized by first reacting $ZrCl_4$ with 2 equiv of $LiNMe_2$ to give $Zr(NMe_2)_2Cl_2$, followed by replacement of the two remaining chloride ligands by 2 equiv of $Li[MeC(N^iPr)_2]$ (**6**, Scheme 2.8). This method does not give pure product. Instead a messy mixture of products was obtained. The yield of **10** was less than 5% according to a ^1H NMR spectrum.

In Route 2, the order of the reactants was switched. First, 2 equiv of **6** was added to $ZrCl_4$ to make the intermediate compound $Zr[MeC(N^iPr)_2]_2Cl_2$ (**8**). **8** then reacted with 2 equiv of $LiNMe_2$ to give **10** in 22% yield (Scheme 2.9).

In Route 3, $Zr(NMe_2)_4$ (**1**) was first prepared from $LiNMe_2$ and freshly sublimed $ZrCl_4$.[7] Two equiv of $^iPrN(H)C(Me)=N^iPr$ (**7**) was added to **1** to give **10** and 2 equiv of $HNMe_2$ (Scheme 2.10). Removal of volatiles gave analytically pure **10** in 95% yield. This is the route chosen to make **10** throughout this dissertation.

The ^1H NMR spectrum of **10** in benzene-d_6 (Figure 2.9) shows a doublet at 1.18 ppm for the CHMe_2 groups. Two singlets at 1.58 and 3.23 ppm were assigned to -C(*Me*) group on the amidinate and amide (NMe_2) ligands, respectively. A mulitiplet for the C*H*Me_2 groups appears at 3.45 ppm.

These observations suggest that **10** undergoes a rapid exchange at room temperature by the Bailar twist mechanism.[19] The Bailar twist mechanism occurs when two enantiomers exchange through a trigonal-prismatic intermediate (Scheme 2.11). In this case the exchange makes all four isopropyl groups equivalent. Our group has studied this twisting mechanism with a similar Zr(IV)

bisamidinate bisamide, $Zr[MeC(NCy)_2]_2(NMe_2)_2$, by variable-temperature NMR spectroscopy.[16] The exchange in **10** was thus not studied further.

In the $^{13}C\{^1H\}$ NMR spectrum of **10** (Figure 2.10), peaks at 11.31 and 175.07 ppm were assigned to -C(*Me*) and -*C*(Me)- groups on the amidinate, respectively. The CH*Me*$_2$ groups appear at 25.61 ppm. The N*Me*$_2$ ligands appear at 46.10 ppm. The *C*H carbon atom on the isopropyl groups appear at 48.34 ppm.

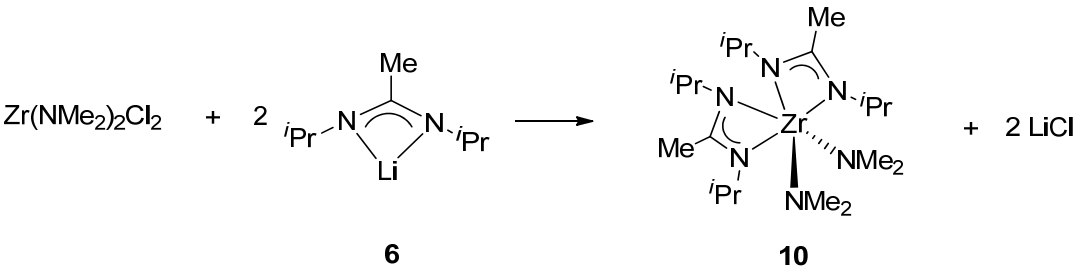

Scheme 2.8. Route 1 to prepare **10**.

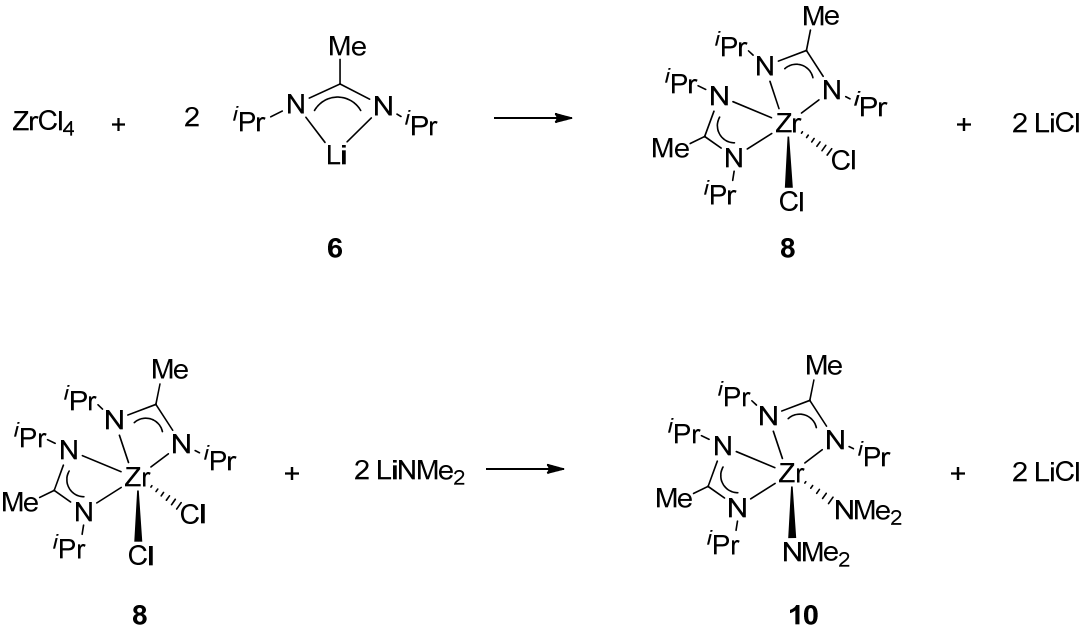

Scheme 2.9. Route 2 to prepare **10**.

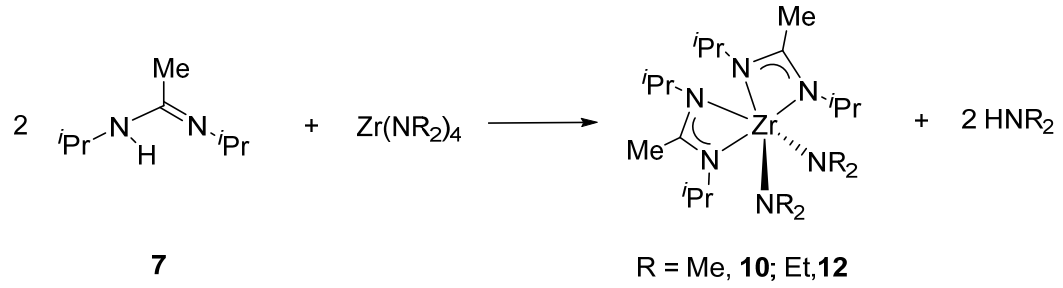

Scheme 2.10. Route 3 to prepare **10** and **12**.

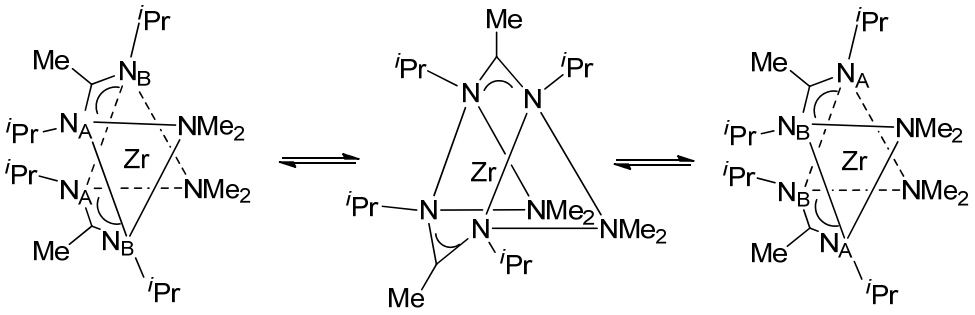

Scheme 2.11. Bailar twist mechanism for the exchange in **10**.[19]

2.2.5. Synthesis of Zr[MeC(N^{i}Pr)$_2$](NEt$_2$)$_3$ (11)

Zr[MeC(N^{i}Pr)$_2$](NEt$_2$)$_3$ (**11**) was made by reacting 1 equiv of **7** with Zr(NEt$_2$)$_4$ (Scheme 2.7). Unlike its NMe$_2$ analog **9**, this reaction was carried out at room temperature to give a crude product as a yellow solid with 91% yield.

The ^{1}H NMR spectrum of **11** in benzene-d_6 (Figure 2.11) showed a doublet at 1.12 ppm for the CH*Me$_2$* groups. A triplet for the N(CH$_2$C*H$_3$*)$_2$ groups appear at 1.20 ppm. A singlet at 1.53 ppm was assigned for the methyl on the amidinate. A multiplet for the C*H*Me$_2$ groups at 3.37 ppm. A quintet for the N(C*H$_2$*CH$_3$)$_2$ groups at 3.46 ppm.

The ^{13}C{^{1}H} NMR spectrum (Figure 2.12), peaks at 10.89 and 175.08 ppm were assigned to -C(*Me*) and -*C*(Me)- groups on the amidinate, respectively. The peak at 15.90 ppm was assigned to the N(CH$_2$*C*H$_3$)$_2$ groups. The peak at 25.22 ppm accounts for the CH*Me$_2$* groups. The peak at 44.49 accounts for the N(*C*H$_2$CH$_3$)$_2$. The *C*H carbon atoms of the *C*HMe$_2$ groups appear at 47.82 ppm.

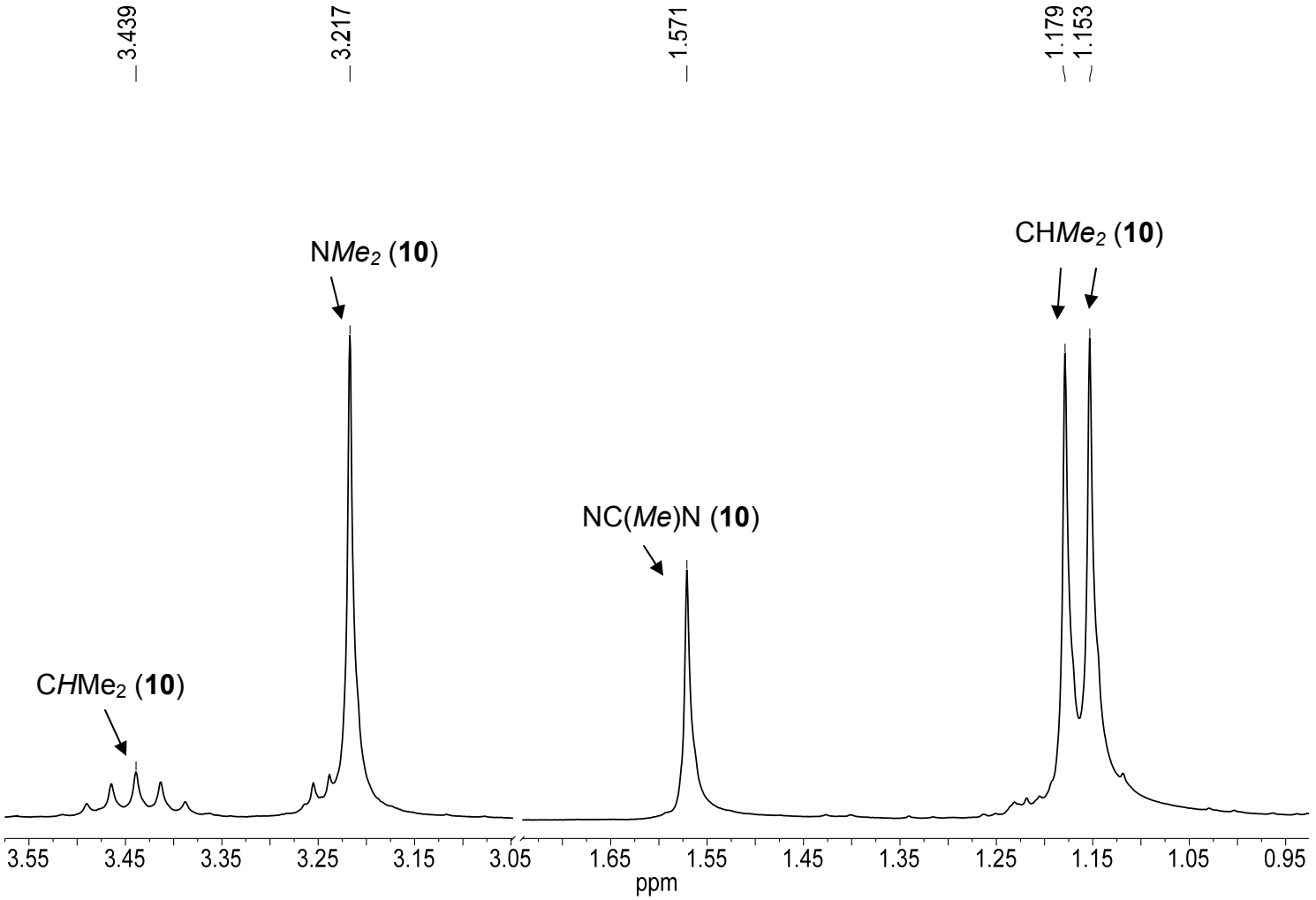

Figure 2.9. ^{1}H NMR spectrum of **10** in benzene-d_6.

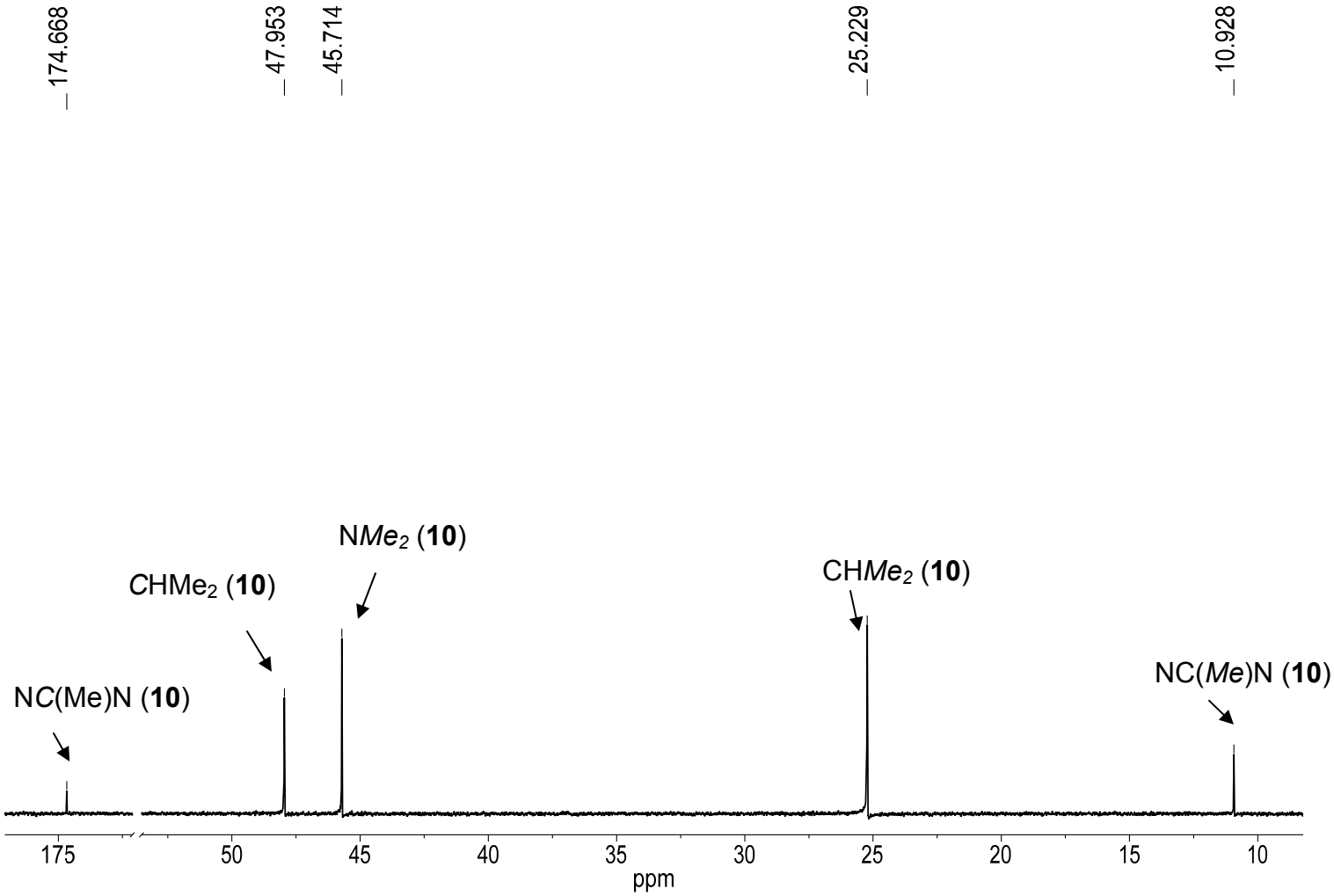

Figure 2.10. $^{13}C\{^{1}H\}$ NMR spectrum of **10** in benezene-d_6.

2.2.6. Synthesis of $Zr[MeC(N^iPr)_2]_2(NEt_2)_2$ (12)

$Zr[MeC(N^iPr)_2]_2(NEt_2)_2$ (**12**) was prepared from **7** and $Zr(NEt_2)_4$ (Scheme 2.10). Removing volatiles gave analytically pure **12** in 92% yield. At room temperature, the ^1H NMR spectrum of **12** in benzene-d_6 showed broad peaks for the $N(CH_2CH_3)_2$, $CHMe_2$, and $CHMe_2$ groups. In the $^{13}C\{^1H\}$ NMR spectrum there are two broad peaks for $CHMe_2$ and $CHMe_2$ groups. Variable-Temperature NMR studies of **12** are discussed in Section 2.2.7. Mass spectrometry was also used to characterize **12** and a *m*/z = 444.26 [**12**-NEt_2^+] was observed (Figure 2.13). Here **12** was ionized and lost a diethylamide ligand.

2.2.7. Variable-Temperature NMR Studies of $Zr[MeC(N^iPr)_2]_2(NEt_2)_2$ (12)

Since at room temperature some ^1H NMR peaks of **12** were broad, we have studied its dynamic behavior by variable-temperature NMR (VT-NMR) and obtained the activation parameters for the process.

One contributing factor to the fluxionality is the bulky NEt_2 groups which slow down the exchanges in comparison to its NMe_2 analog **10**. As the temperature was lowered to 213 K, de-coalescence of all peaks occurred. At 213 K, four doublets appear for the isopropyl ($CHMe_2$) groups at 25.93, 25.91, 25.52, and 23.52 ppm. Two peaks for $CHMe_2$ appear at 3.47 and 3.32 ppm. Two peaks for NCH_2CH_3 were observed at 3.96 and 3.64 ppm.

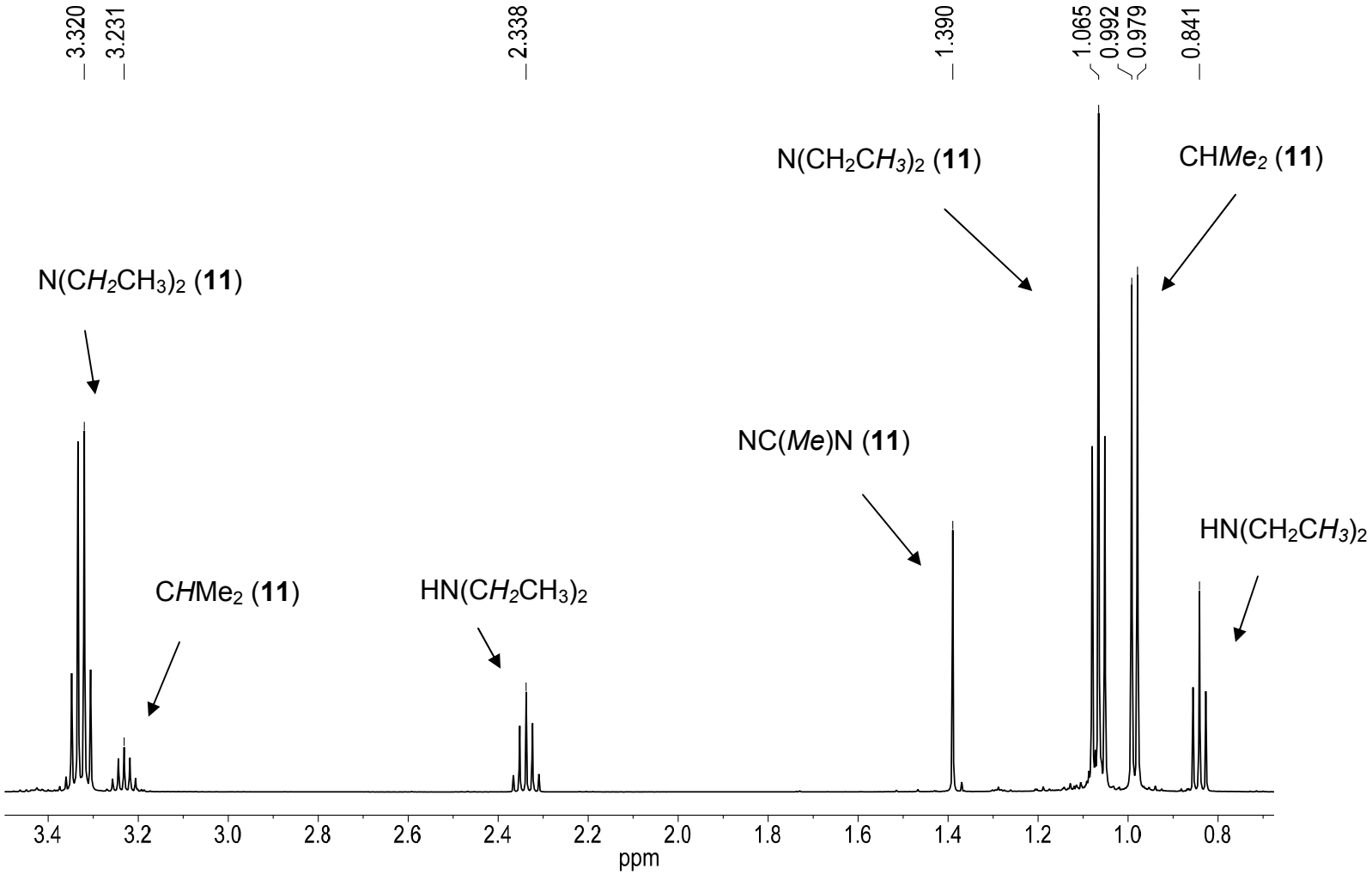

Figure 2.11. ^{1}H NMR spectrum of **11** in benzene-d_6.

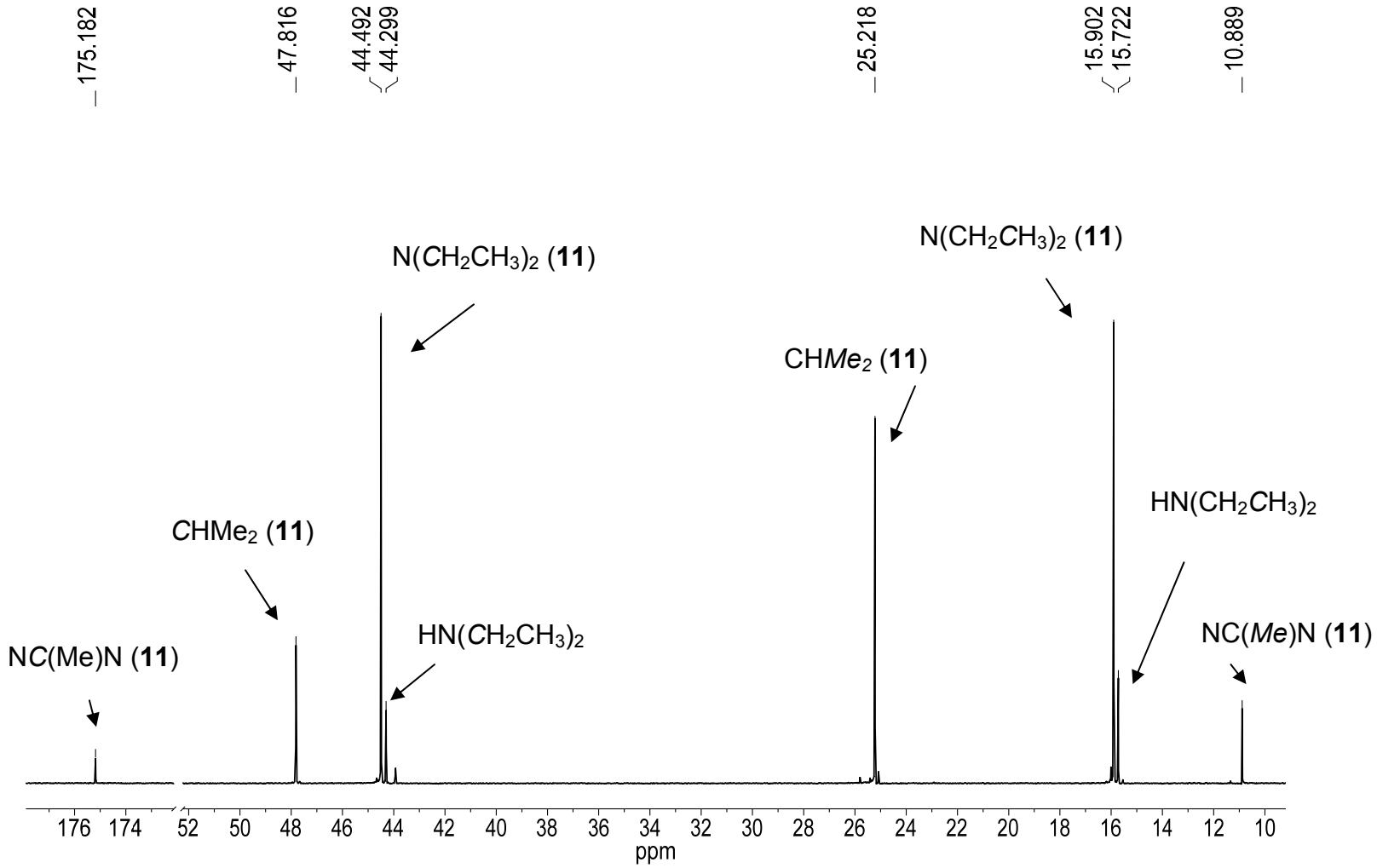

Figure 2.12. $^{13}C\{^{1}H\}$ NMR spectrum of **11** in benzene-d_6.

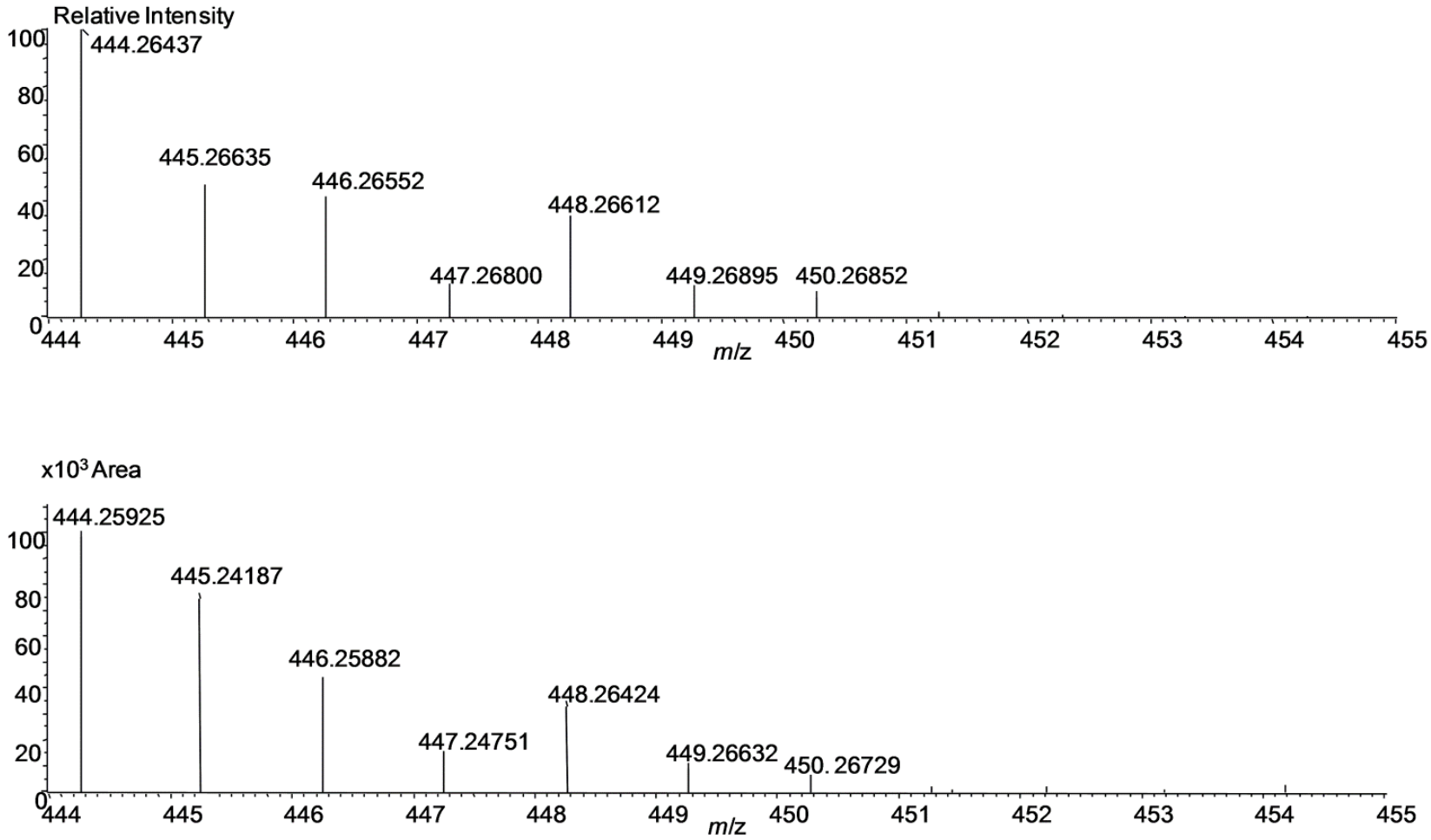

Figure 2.13. (Top) Calculated and (Bottom) Observed MS for [**12**-NEt_2^+].

To our surprise, the methyls on CH*Me*$_2$ separated out into four doublets and two of them were overlapping with N(CH$_2$C*H*$_3$)$_2$. This was also confirmed by the $^{13}C\{^1H\}$ NMR spectrum in which four peaks for CH*Me*$_2$ were observed. Low temperature 2-D NMR (HMBC, HSQC) experiments confirmed the assignments, as discussed in Section 2.2.8.

Partial VT ^{1}H NMR spectra for the C*H*Me$_2$ and N(C*H*$_2$CH$_3$)$_2$ region are given in Figure 2.14. As the temperature increases, the exchange based on the Bailar twist process speeds up,[19] eventually reaching the coalescence at 303 K.[20] The rate constants of this interconversion at various temperatures were calculated from Eq. 2.1:

$$k = \pi\sqrt{2(\Delta\nu_0^{\,2} - \Delta\nu^2)} \qquad \text{(Eq. 2.1)}$$

where $\Delta\nu_0$ and $\Delta\nu$ are frequency differences (Hz) between the site of the slow exchange limit and the exchange-broadened sites at temperature T, respectively.[21-24]

The rate constants are given in Table 2.3. The frequency differences (Hz) were taken from the two C*H*Me$_2$ on the isopropyl group and used in Eq 2.1. The activation parameters of the exchange were determined from an Erying plot (Figure 2.15) to give: $\Delta H^{\ddagger}$ = 10.9(1.1) kcal mol^{-1}, $\Delta S^{\ddagger}$ = -11(4) eu. A $\Delta G^{\ddagger}_{303\ K}$ value was calculated to be $\Delta G^{\ddagger}_{303\ K}$ = 14(2) kcal mol^{-1} which is close to those in

an analog complex Zr(IV) complex $Zr[NMe_2C(NCy)_2]_2(NEt_2)_2$ containing two bis(cyclohexyl)amidinate and two NEt_2 ligands.[16]

At 23 °C, the $^{13}C\{^1H\}$ NMR spectrum of **12** in toluene-d_8 also show a dynamic feature in which the *C*H and *C*HMe_2 resonances are broad at 48.27 and 25.67 ppm, respectively where as at 213 K two sharp *C*H peaks at 48.14 and 47.55 ppm and four sharp CH*Me*$_2$ appear at 25.93, 25.91, 25.52, and 23.52 ppm.

2.2.8. 2-D NMR Studies of $Zr[MeC(N^iPr)_2]_2(NEt_2)_2$ (12)

The integration of the CH(C*H*$_3$)$_2$ and N(CH_2C*H*$_3$)$_2$ peaks in the ^1H NMR spectrum of **12** at 213 K did not match what were expected (Figure 2.16). Also, in the $^{13}C\{^1H\}$ NMR spectrum four CH*Me*$_2$ peaks appear, suggesting a peak overlap. In a similar Zr(IV) guanidinate complex, $(Et_2N)_2Zr[^iPrNC(NEt_2)N^iPr]_2$,[28] the ^1H NMR spectrum at room temperature shows four doublets for the CH*Me*$_2$ groups. With this knowledge, HMBC and HSQC NMR experiments were conducted at 213 K. In the HSQC, the four isopropyl groups in the $^{13}C\{^1H\}$ NMR spectrum relates to their corresponding protons in the ^1H NMR (Figure 2.18). In the HMBC, two different methyl groups on the isopropyl groups are connected to its respective C*H* of the isopropyl group.

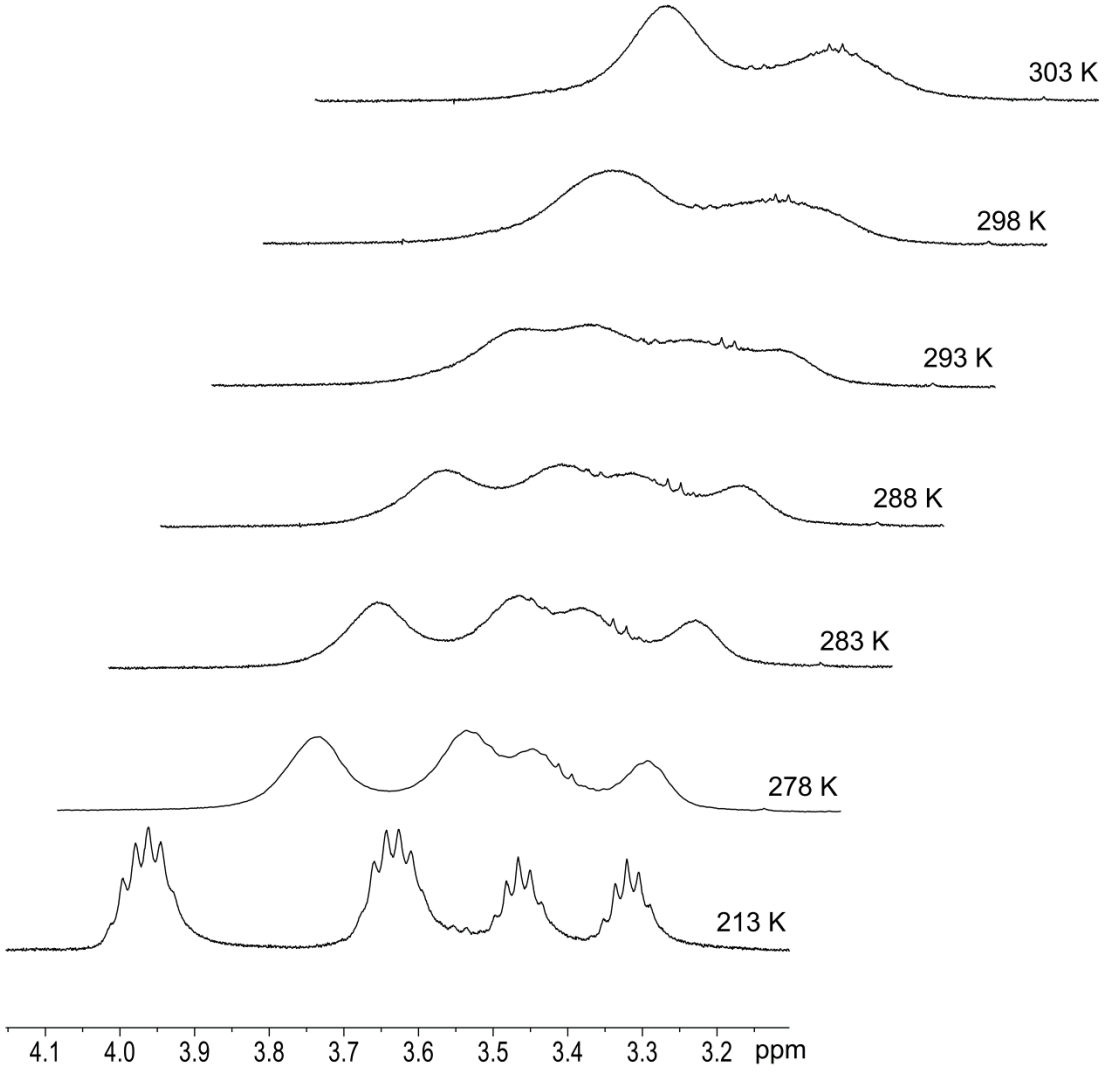

Figure 2.14. Partial VT ^{1}H NMR spectra of **12** in toluene-d_8.

Table 2.3. Rate constants of interconversions in **12**

Temperature (K)	$\Delta\nu$ (Hz)	Rate Constant k (s^{-1})
303	0	280(3)
298	33.8	237(2)
293	50.7	166(8)
288	57.8	112(7)
283	60.4	80(6)
278	62.2	45.0(0.2)

The total uncertainty $\delta k'/k'$ of 0.092 was calculated from $\delta k'_{ran}/k' = 0.077$ and $\Delta k'_{sys}/k' = 0.05$.[26,27]

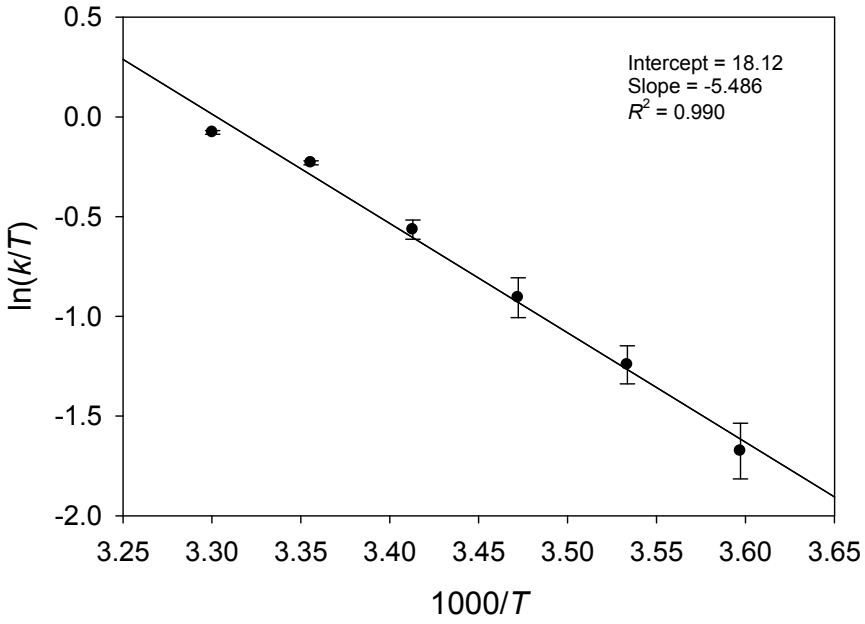

Figure 2.15. Eyring plot of the exchange in **12**, yielding activation parameters of the exchange.

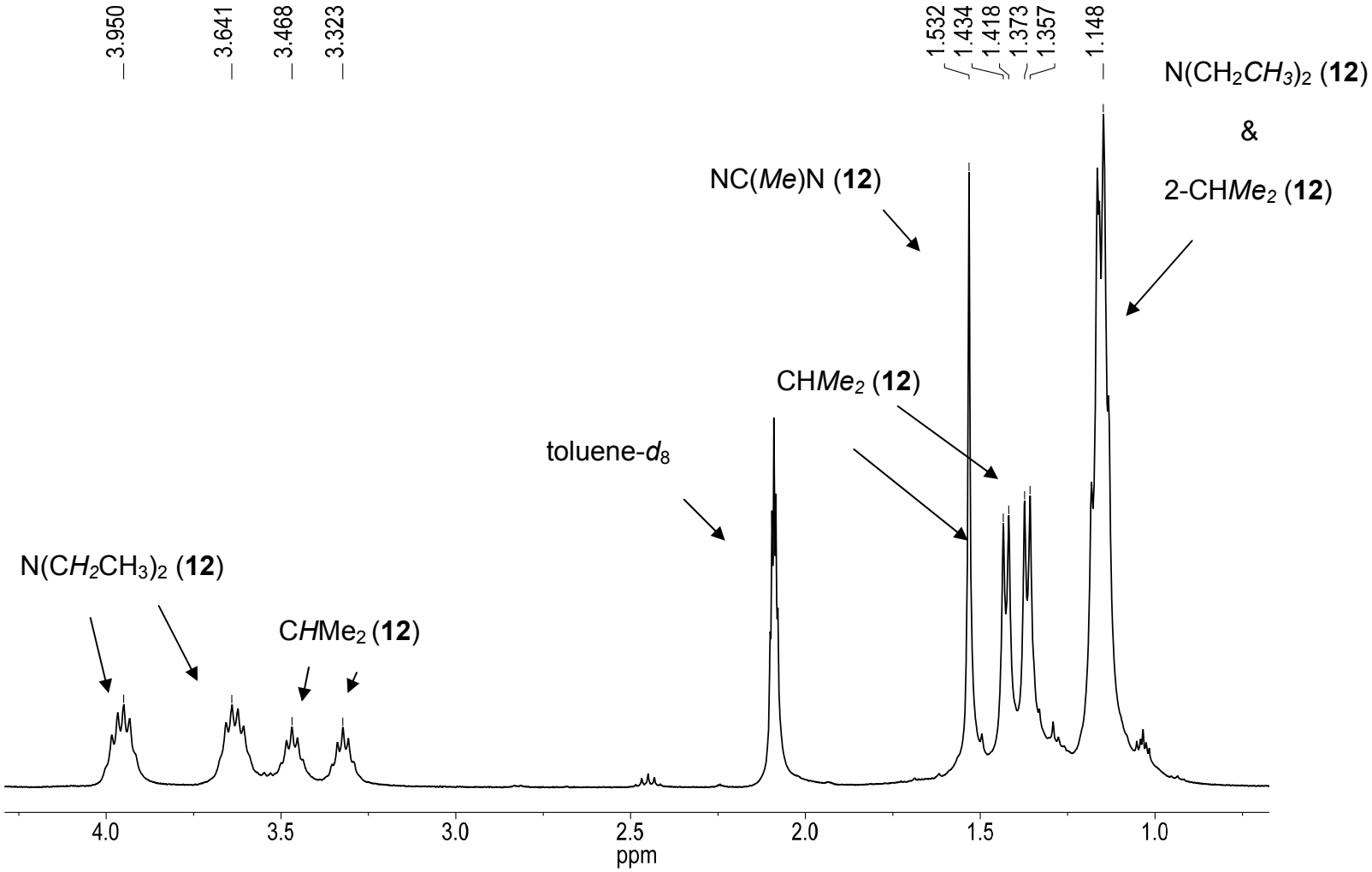

Figure 2.16. ^{1}H NMR spectrum of **12** in toluene-d_8 at 213 K.

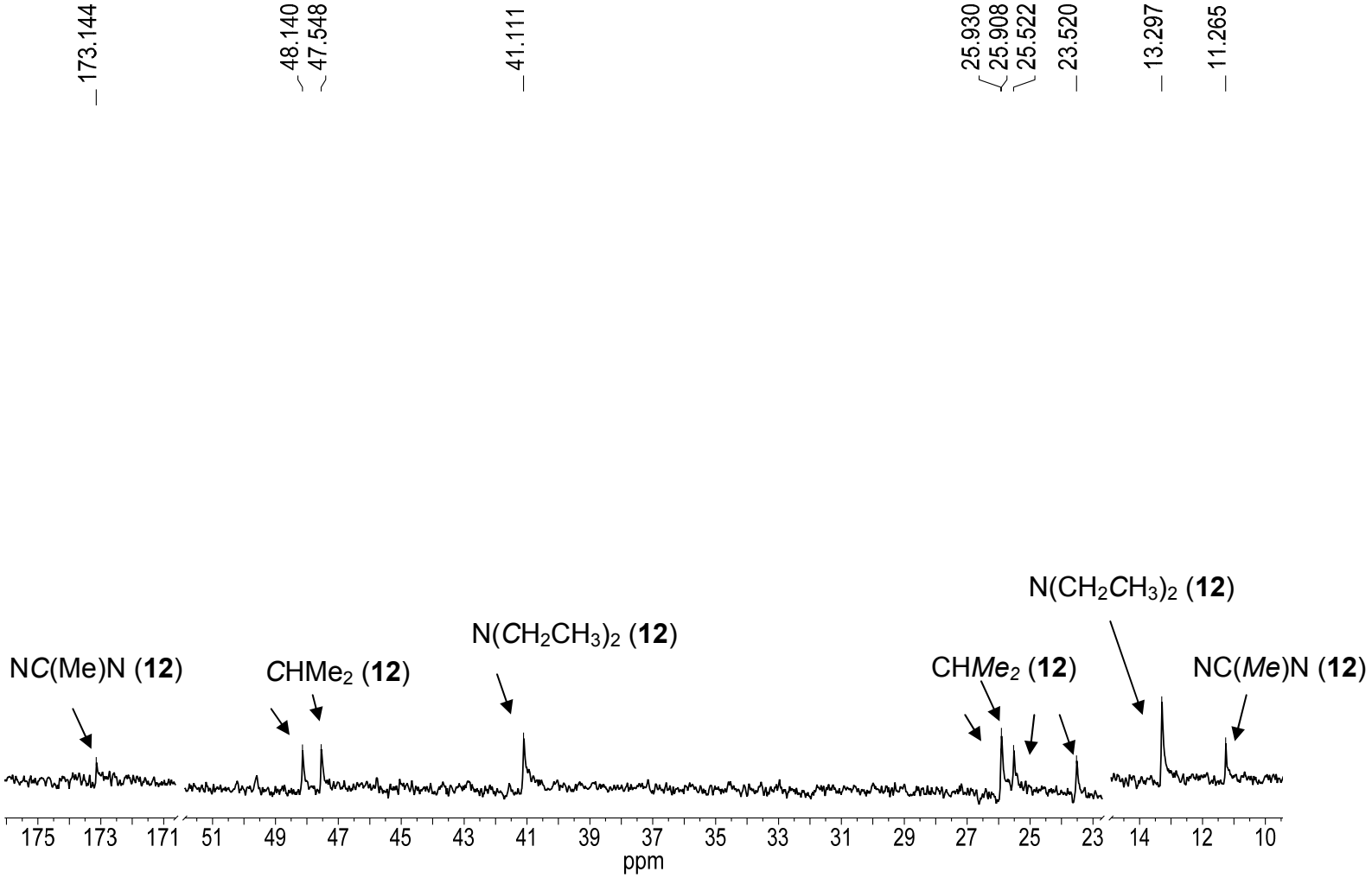

Figure 2.17. $^{13}C\{^{1}H\}$ NMR spectrum of **12** in toluene-d_8 at 213 K.

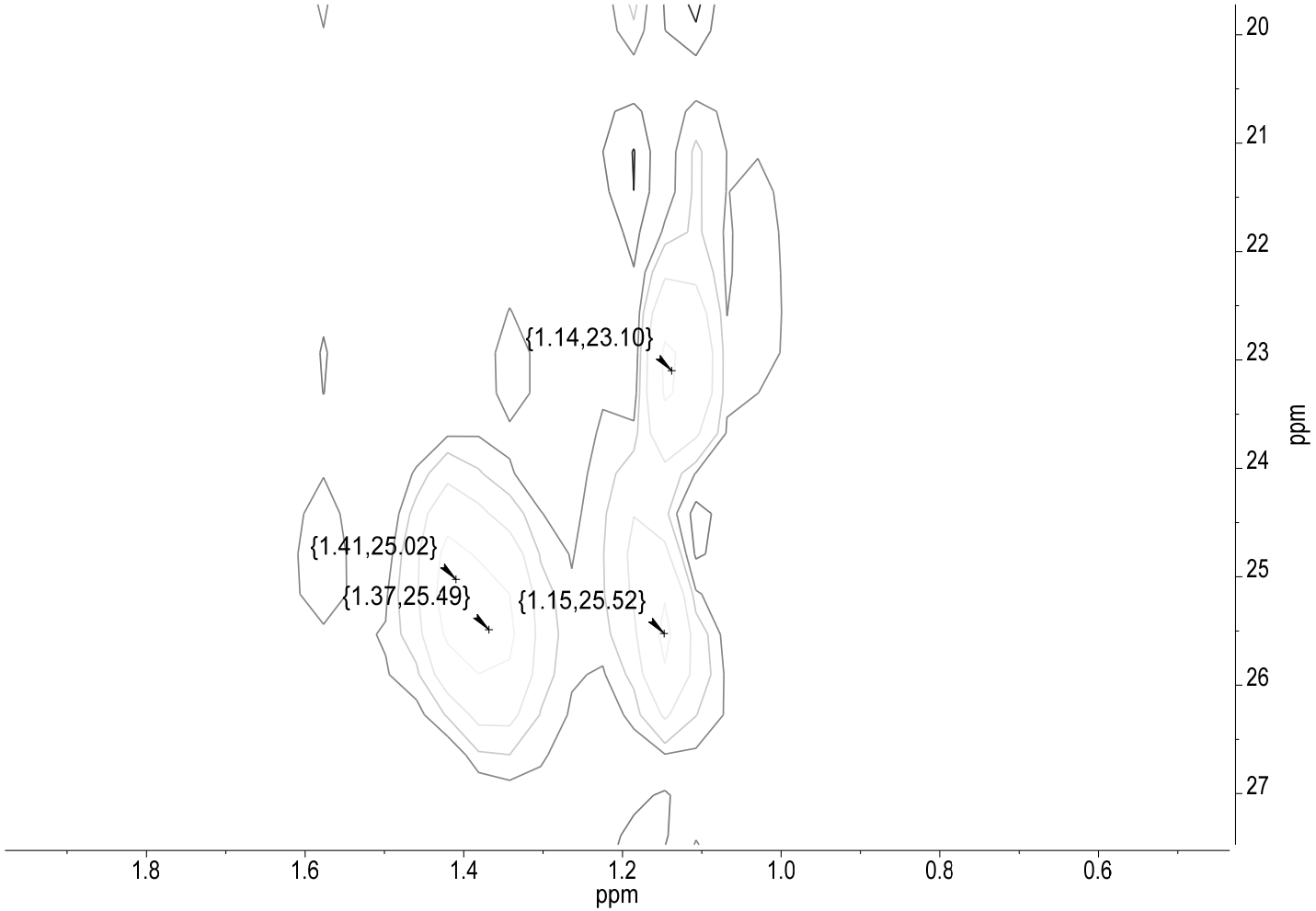

Figure 2.18. HSQC of **12** in toluene-d_8 at 213 K, correlating H atoms to their respective C atoms for the methyl groups on the ^{i}Pr groups.

2.3. Concluding Remarks

Several Group 4 amidinate amide complexes have been prepared and characterized. $Zr[MeC(N^iPr)_2]_2(NMe_2)_2$ (**10**) has been synthesized by three different routes. The route that gave the highest yield was through the aminolysis of an amidine and a metal amide. This route was used to make all other zirconium and Group 5 amidinate amide complexes in this dissertation. It would be interesting to study the reactivities of these compounds towards O_2 and potentially see if any unusual products form. Reactions of compound **10** with H_2O, H_2O_2, and O_2 will be discussed in Part 3. The reactivities of **12** towards H_2O and O_2 will also be discussed in Part 3.

Also, compound **12** revealed an interesting dynamic NMR behavior. A variable temperature NMR experiment was conducted and the activation parameters for the Bailar twist process were determined: $\Delta H^{\ddagger}$ = 10.9(1.1) kcal mol^{-1}, $\Delta S^{\ddagger}$ = -11(4) eu and $\Delta G^{\ddagger}_{303\,K}$ = 14(2) kcal mol^{-1}.

2.4. Experimental Section

All manipulations were carried out under a dry nitrogen atmosphere with the use of either a glovebox or standard Schlenk techniques. N,N'-Diisopropylcarbodiimide (**5**), $LiNMe_2$ and MeLi (1.6 M in Et_2O) were purchased from Acros and used without further purification. Solvents were purified by distillation from a potassium benzophenone ketyl. NMR solvents were dried and stored over 5 Å molecular sieves. $ZrCl_4$ was purchased from Strem and sublimed at 170 °C before use. $Zr(NMe_2)_4$ (**1**) and $Zr(NEt_2)_4$ were prepared according to

literature.[7,29] Deionized H_2O was degassed and stored in a Schlenk flask. ^1H and $^{13}C\{^1H\}$ NMR spectra were recorded on an AMX-400 FT or Varian VNMRS-500 spectrometer. Elemental analyses were conducted by Complete Analysis Laboritories, Inc., Parsippany, NJ. Mass spectra were recorded on a JEOL AccuTOF™ DART Mass Spectrometer.

2.4.1. Calculating Errors in Variable-Temperature NMR Studies

The activation parameters determined from the Eyring plot, were obtained by using the average rate constants which were obtained through two separate experiments at a given temperarute and their averages are listed in Table 2.3. The maximum random uncertainty in the rate constants was combined with the estimated systematic uncertainty of 5%. The total uncertainties in the rate constants k were used in the $\ln(k_{eq}/T)$ vs. $1000/T$ plot in Figure 2.15 and error calculations. The NMR probe temperature measurements contribute to an estimated uncertainty of 1 K. The uncertainties in $\Delta H^{‡}$ and $\Delta S^{‡}$ were calculated from the following error formulas derived from $R\ln(kh/k_bT) = -\Delta H^{‡}/T + \Delta S^{‡}$.[30]

$$(\sigma\Delta H^{\neq})^2 = \frac{R^2 T_{max}^2 T_{min}^2}{\Delta T^2}\left\{\left(\frac{\sigma T}{T}\right)^2\left[\left(1+T_{min}\frac{\Delta L}{\Delta T}\right)^2+\left(1+T_{max}\frac{\Delta L}{\Delta T}\right)^2\right]+2\left(\frac{\sigma \mathrm{k}}{k}\right)^2\right\}$$

$$(\sigma\Delta S^{\neq})^2 = \frac{R^2}{\Delta T^2}\left\{\left(\frac{\sigma T}{T}\right)^2\left[T_{max}^2\left(1+T_{min}\frac{\Delta L}{\Delta T}\right)^2+T_{min}^2\left(1+T_{max}\frac{\Delta L}{\Delta T}\right)^2\right]+\left(\frac{\sigma k}{k}\right)^2\left(T_{max}^2+T_{min}^2\right)\right\}$$

where $\Delta L = [\ln(k_{max}/T_{max}) - \ln(k_{min}/T_{min})]$ and $\Delta T = (T_{max} - T_{min})$.

2.4.2. Synthesis of Li[MeC(N^{i}Pr)$_2$] (6)

Compound **5** was prepared by the addition of MeLi (33.5 mL, 1.6 M in Et_2O, 53.7 mmol) to ^{i}PrN=C=N^{i}Pr (**5**, 6.765 g, 53.61 mmol) and in Et_2O (40 mL) at 0 °C. The solution was allowed to stir overnight and the volatiles were removed in vacuo affording a white solid. The solid was washed with pentane and volatiles were removed in vacuo to afford Li[MeC(N^{i}Pr)$_2$] (**6**) (5.894 g, 39.78 mmol, 74.2% yield). Compound **6** is not soluble in benzene-d_6. ^{1}H NMR (tetrahydrofuran-d_8, 499.73 MHz, 23 °C): δ 3.45 (m, 2H, C*H*Me$_2$), 1.75 (s, 3H, NC(*Me*)N), 0.95 (d, 12H, CH*Me$_2$*); ^{13}C{^{1}H} NMR (tetrahydrofuran-d_8, 125.67 MHz, 23 °C) δ 168.97 (N*C*(Me)N), 47.96 (*C*HMe$_2$), 27.63 (CH*Me$_2$*), 10.79 (NC(*Me*)N). ^{1}H and ^{13}C{^{1}H} NMR assignments were confirmed by DEPT and HSQC experiments. ^{1}H and ^{13}C{^{1}H} NMR spectra are given in Figures 2.19 and 2.20, respectively.

2.4.3. Synthesis of ^{i}PrN(H)C(Me)=N^{i}Pr (7)

Li[MeC(N^{i}Pr)$_2$] (**5**) (5.893 g, 39.77 mmol) was dissolved in THF (50 mL) and H_2O (0.80 mL, 0.80 g, 44.42 mmol) was added via syringe. The solution was allowed to stir for 20 min and Et_2O (100 mL) was added. Na_2SO_4, a drying agent, was added to the solution and stirred for 12 h, followed by filtration. Et_2O in the filtrate was removed at 23 °C. The liquid product **7** was distilled from the liquid residue at 115 °C and ~0.1 Torr. ^{1}H NMR (benzene-d_6, 400.17 MHz, 23 °C): δ 3.85 (br, 2H, C*H*Me$_2$), 3.01 (br, 1H, N*H*), 1.36 (s, 3H, NC(*Me*)N), 1.13 (d, 12H, CH*Me$_2$*); ^{13}C{^{1}H} NMR (benzene-d_6, 100.62 MHz, 23 °C) δ 151.58 (N*C(*Me)N),

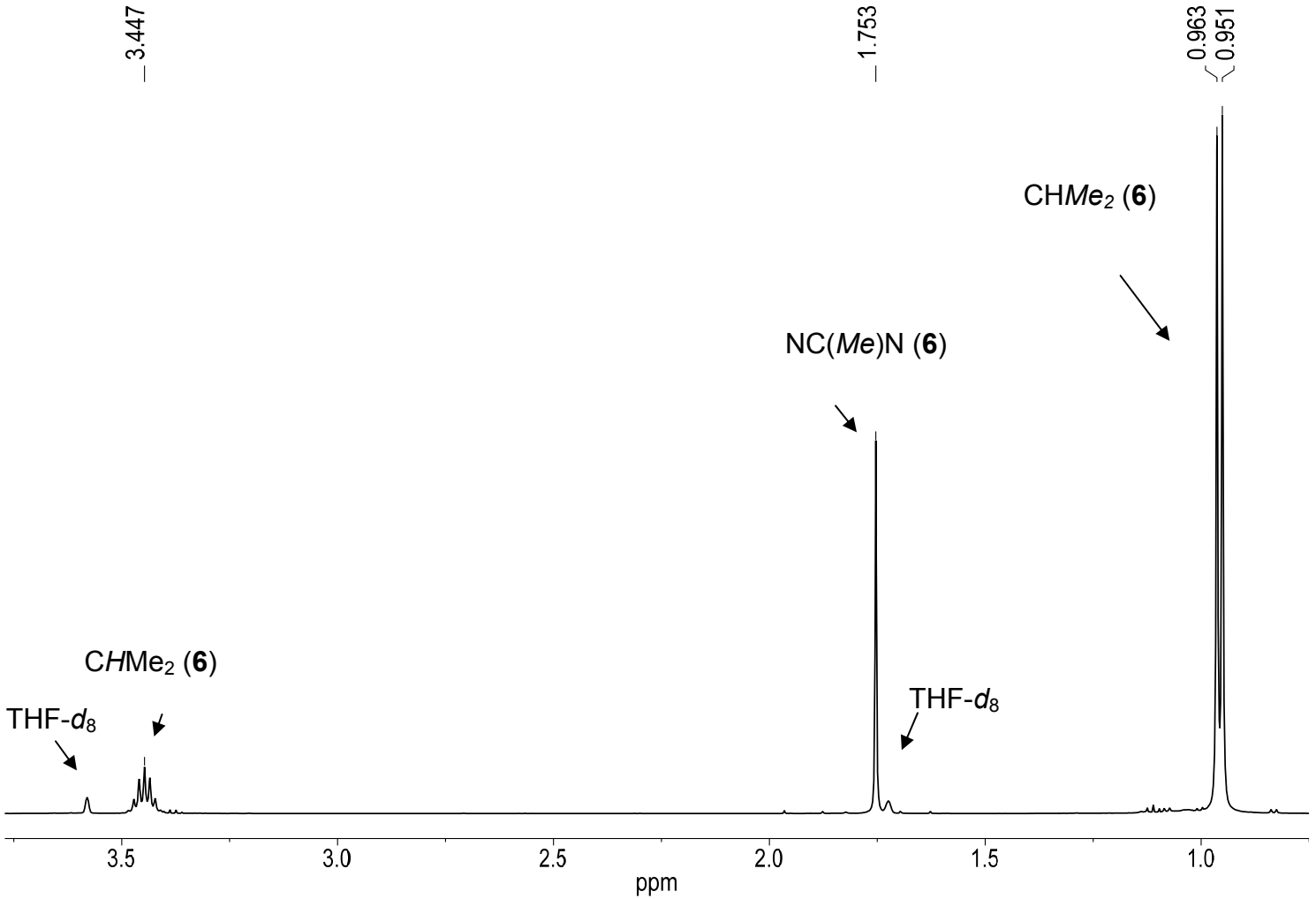

Figure 2.19. ^{1}H NMR spectrum of **6** in THF-d_8.

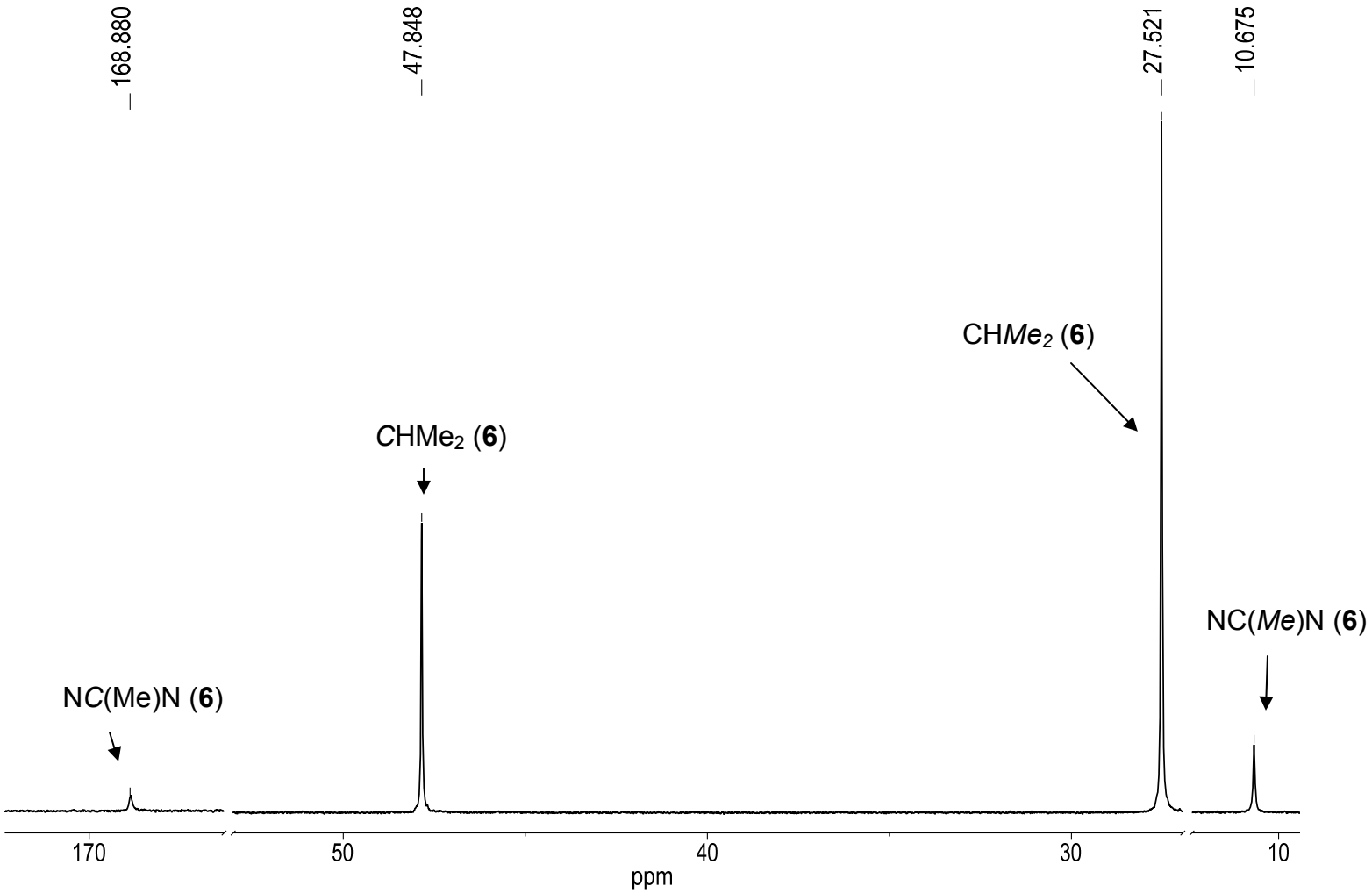

Figure 2.20. $^{13}C\{1H\}$ NMR spectrum of **6** in THF-d_8.

45.29 (br, *C*HMe$_2$), 24.22 (CH*Me$_2$*), 15.71 (NC(*Me*)N). ^{1}H NMR (toluene-d_8, 400.17 MHz, 23 °C): δ 3.74 (br, 1H, N*H*), 3.33 (br, 2H, C*H*Me$_2$), 1.43 (s, 3H, NC(*Me*)N), 1.04 (d, 12H, CH*Me$_2$*); ^{13}C{^{1}H} NMR (toluene-d_8, 100.62 MHz, 23 °C): δ 151.55 (N*C(*Me)N), 45.18 (br, *C*HMe$_2$), 24.18 (CH*Me$_2$*), 15.47 (NC(*Me*)N). ^{1}H NMR (toluene-d_8, 400.17 MHz, -65 °C): δ 4.71 (br, 1H, N*H*), 4.28 (m, 1H, C*H*Me$_2$), 3.47 (m, 1H, C*H*Me$_2$), 1.60 (s, 3H, NC(*Me*)N), 1.22 (d, 6H, CH*Me$_2$*), 1.11 (d, 6H, CH*Me$_2$*); ^{13}C{^{1}H} NMR (toluene-d_8, 100.62 MHz, -65 °C): δ 152.11 (N*C(*Me)N), 49.04 (*C*HMe$_2$), 41.10 (*C*HMe$_2$), 25.58 (CH*Me$_2$*), 22.54 (CH*Me$_2$*), 15.79 (NC(*Me*)N). DART-MS: Calculated *m*/z = 143.15482 [**7**+H$^+$], Found *m*/z = 143.15488 [**7**+H$^+$]; 0.419 ppm difference.

2.4.4. Synthesis of Zr[MeC(N^{i}Pr)$_2$]$_2$Cl$_2$ (8)

Freshly sublimed $ZrCl_4$ (3.436 g, 14.74 mmol) was stirred in hexanes to form a slurry. The slurry was cooled to -35 °C. Li[MeC(N^{i}Pr)$_2$] (**6**, 4.226 g, 28.52 mmol) was dissolved in hexanes and added dropwise to the hexanes slurry of $ZrCl_4$. The solution was refluxed for 6 h and then filtered. Volatiles were removed in vacuo affording a bright green solid (4.490 g, 10.10 mmol, 68.5% yield). ^{1}H NMR (benzene-d_6, 400.17 MHz, 23 °C): δ 3.34 (m, 4H, C*H*Me$_2$), 1.39 (s, 6H, NC(*Me*)N), 1.30 (d, 24H, CH*Me$_2$*); ^{13}C{^{1}H} NMR (benzene-d_6, 100.63 MHz, 23 °C): δ 178.06 (N*C(*Me)N), 48.42 (*C*HMe$_2$), 24.29 (CH*Me$_2$*), 10.33 (NC(*Me*)N). ^{1}H and ^{13}C{^{1}H} NMR assignments were confirmed by HSQC experiments. DART-MS: *m*/z = 443.09 [**8**+H$^+$].

2.4.5. Synthesis of $Zr[MeC(N^iPr)_2](NMe_2)_3$ (9)

$Zr(NMe_2)_4$ (**1**, 1.104 g, 4.128 mmol) was dissolved in pentane (50 mL) and cooled to -50 °C. Compound **7** (0.5847 g, 4.111 mmol) was dissolved in pentane (50 mL) and added dropwise to the pentane solution of $Zr(NMe_2)_4$ (**1**) and kept cooled for 4 h. The solution was warmed to room temperature and stirred for an additional 12 h and volatiles removed in vacuo affording a yellow solid (0.8047 g, 2.207 mmol, 53.5% yield). ^{1}H NMR (benzene-d_6, 399.17 MHz, 23 °C): δ 3.34 (m, 2H, C*H*Me_2), 3.09 (s, 18H, N*Me*$_2$), 1.52 (s, 3H, NC(*Me*)N), 1.04 (d, 12H, CH*Me*$_2$); ^{13}C{^{1}H} NMR (benzene-d_6, 100.63 MHz, 23 °C): δ 175.42 (N*C*(Me)N), 47.87 (*C*HMe_2), 42.62 (N*Me*$_2$), 25.02 (CH*Me*$_2$), 10.48 (NC(*Me*)N). ^{1}H and ^{13}C{^{1}H} NMR assignments were confirmed by DEPT experiments. **9** is an intermediate in the formation of **10** below, and was not characterized further.

2.4.6. Synthesis of $Zr[MeC(N^iPr)_2]_2(NMe_2)_2$ (10)

$Zr(NMe_2)_4$ (**1**) (1.601 g, 5.984 mmol) was dissolved in pentane (50 mL) and cooled to -30 °C. **7** (1.758 g, 12.36 mmol) was dissolved in pentane (50 mL) and added dropwise to the solution of **1**. The solution was stirred for 12 h and volatiles were removed in vacuo affording a yellow solid (2.7640 g, 5.985 mmol, 95.6% yield). ^{1}H NMR (benzene-d_6, 399.17 MHz, 23 °C): δ 3.45 (m, 4H, C*H*Me_2), 3.23 (s, 12H, N*Me*$_2$), 1.58 (s, 6H, NC(*Me*)N), 1.18 (d, 24H, CH*Me*$_2$); ^{13}C{^{1}H} NMR (benzene-d_6, 100.63 MHz, 23 °C): δ 175.07 (N*C*(Me)N), 48.34 (*C*HMe_2), 46.10 (N*Me*$_2$), 25.61 (CH*Me*$_2$), 11.31 (NC(*Me*)N). ^{1}H and ^{13}C{^{1}H} NMR assignments

were confirmed by DEPT, HMBC and HSQC experiments. Anal. Calcd: C, 52.01; H, 10.04. Found: C, 51.86; H, 9.98.

2.4.7. Synthesis of $Zr[MeC(N^iPr)_2](NEt_2)_3$ (11)

This reaction was conducted in a J. Young's tube and reagents were mixed in a glovebox. $Zr(NEt_2)_4$ (0.0280 g, 0.0737 mmol) was dissolved in benzene-d_6 (1 mL). Compound **7** (0.0102 g, 0.0717 mmol) was added to a vial and dissolved in benzene-d_6 (1 mL) and added dropwise via pipette to the solution of $Zr(NEt_2)_4$. The solution was allowed to be mixed and volatiles removed in vacuo affording a yellow solid (0.0302 g, 0.0673 mmol, 91.3% yield). ^{1}H NMR (benzene-d_6, 499.73 MHz, 23 °C): δ 3.46 (q, 12H, N(C*H*$_2$CH$_3$)$_2$), 3.37 (m, 2H, C*H*Me$_2$), 1.53 (s, 3H, NC(*Me*)N), 1.20 (t, 18H, N(CH$_2$*CH*$_3$)$_2$), 1.12 (d, 12H, CH*Me*$_2$); ^{13}C{^{1}H} NMR (benzene-d_6, 125.67 MHz, 23 °C): δ 175.08 (N*C*(Me)N), 47.82 (C*H*Me$_2$), 44.49 (N(*CH*$_2$CH$_3$)$_2$), 25.22 (CH*Me*$_2$), 15.90 (N(CH$_2$*C*H$_3$)$_2$), 10.89 (NC(*Me*)N). ^{1}H and ^{13}C{^{1}H} NMR assignments were confirmed by a HSQC experiment. **11** is an intermediate in the formation of **12** below, and was not characterized further.

2.4.8. Synthesis of $Zr[MeC(N^iPr)_2]_2(NEt_2)_2$ (12)

$Zr(NEt_2)_4$ (2.344 g, 6.171 mmol) was dissolved in pentane (50 mL) and cooled to -30 °C. Compound **7** (1.761 g, 12.38 mmol) was dissolved in pentane (50 mL) and added dropwise to the pentane solution of $Zr(NEt_2)_4$. The solution was stirred for 12 h and volatiles removed in vacuo affording a yellow solid

(2.954 g, 5.702 mmol, 92.4% yield). ^{1}H NMR (benzene-d_6, 400.17 MHz, 23 °C): δ 3.71 (br, 8H, N(CH_2CH$_3$)$_2$), 3.46 (br, 4H, CHMe$_2$), 1.59 (s, 6H, NC(*Me*)N), 1.20 (br, 24H, CH*Me$_2$*), 1.10 (t, 12H, N(CH$_2$C*H$_3$*)$_2$); ^{13}C{^{1}H} NMR (benzene-d_6, 100.62 MHz, 23 °C): δ 173.35 (N*C(*Me)N), 48.04 (*C*HMe$_2$), 41.67 (N(*C*H$_2$CH$_3$)$_2$), 25.62 (CH*Me$_2$*), 13.69 (N(CH$_2$*C*H$_3$)$_2$), 11.90 (NC(*Me*)N). ^{1}H NMR (toluene-d_8, 400.08 MHz, 23 °C): δ 3.68 (br, 8H, N(CH_2CH$_3$)$_2$), 3.46 (br, 4H, CHMe$_2$), 1.61 (s, 6H, NC(*Me*)N), 1.26 (br, 24H, CH*Me$_2$*), 1.09 (t, 12H, N(CH$_2$C*H$_3$*)$_2$); ^{13}C{^{1}H} NMR (toluene-d_8, 100.60 MHz, 23 °C): δ 172.64 (N*C(*Me)N), 48.27 (br, *C*HMe$_2$), 41.65 (N(*C*H$_2$CH$_3$)$_2$), 25.67 (br, CH*Me$_2$*), 13.68 (N(CH$_2$*C*H$_3$)$_2$), 11.81 (NC(*Me*)N). ^{1}H NMR (toluene-d_8, 400.08 MHz, -60 °C): δ 3.95 (m, 4H, N(CH_2CH$_3$)$_2$), 3.62 (m, 4H, N(CH_2CH$_3$)$_2$), 3.47 (m, 2H, CHMe$_2$), 3.32 (m, 2H, CHMe$_2$), 1.53 (s, 6H, NC(*Me*)N), 1.42 (d, 6H, CH*Me$_2$*), 1.36 (d, 6H, CH*Me$_2$*), 1.14 (d, 6H, CH*Me$_2$*), 1.13 (d, 6H, CH*Me$_2$*), 1.13 (t, 12H, N(CH$_2$C*H$_3$*)$_2$); ^{13}C{^{1}H} NMR (toluene-d_8, 100.60 MHz, -60 °C): δ 173.14 (N*C(*Me)N), 48.15 (*C*HMe$_2$), 47.55 (*C*HMe$_2$), 41.11 (N(*C*H$_2$CH$_3$)$_2$), 25.93 (CH*Me$_2$*), 25.91 (CH*Me$_2$*), 25.53 (CH*Me$_2$*), 23.52 (CH*Me$_2$*), 13.30 (N(CH$_2$*C*H$_3$)$_2$), 11.27 (NC(*Me*)N). ^{1}H and ^{13}C{^{1}H} NMR assignments were confirmed by HMBC and HSQC experiments at 213 K. Anal. Calcd: C, 55.65; H, 10.51; N, 16.23. Found: C, 55.49; H, 10.40; N, 16.17.

2.4.9. Mass Spectrometry Studies

Mass spectra were recorded on a JEOL AccuTOF™ DART Mass Spectrometer. The closed end of a capillary tube was inserted into solids of the samples to pick up the samples, and the tube was placed into a heated stream of

He (200, 300 or 400 °C) in the spectrometer. This method was used throughout this dissertation.

References

1. (a) Tilley, T. D. *Organometallics* **1985**, *4*, 1452. (b) Blackburn, T. F.; Labinger, J. A.; Schwartz, J. *Tetrahedron Lett.* **1975**, *16*, 3041. (c) Labinger, J. A.; Hart, D. W.; Seibert, W. E.; Schwartz, J. *J. Am. Chem. Soc.* **1975**, *97*, 3851. (d) Lubben, T. V.; Wolczanski, P. T. *J. Am. Chem. Soc.* **1987**, *109*, 424. (e) Lubben, T. V.; Wolczanski, P. T. *J. Am. Chem. Soc.* **1985**, *107*, 701. (f) Wang, R.; Folting, K.; Huffman, J. C.; Chamberlain, L. R.; Rothwell, I. P. *Inorg. Chim. Acta* **1986**, *120*, 81. (g) Gibson, V. C.; Redshaw, C.; Walker, G. L. P.; Howard, J. A. K.; Hoy, V. J.; Cole, J. M.; Kuzmina, L. G.; De Silva, D. S. *J. Chem. Soc., Dalton Trans.* **1999**, 161. (h) Schaverien, C. J.; Orpen, A. G. *Inorg. Chem.* **1991**, *30*, 4968. (i) Liu, X.; Cui, D. *Dalton Trans.* **2008**, 3747. (j) Van Asselt, A.; Santarsiero, B. D.; Bercaw, J. E. *J. Am. Chem. Soc.* **1986**, *108*, 8291. (k) Brindley, P. B.; Hodgson, J. C. *J. Organomet. Chem.* **1974**, *65*, 57. (l) Kim, S. J.; Choi, D. W.; Lee, Y. J.; Chae, B. H.; Ko, J. J.; Kang, S. O. *Organometallics* **2004**, *23*, 559. (m) Morris, A. M.; Pierpont, C. G.; Finke, R. G. *Inorg. Chem.* **2009**, *48*, 3496. (n) Adam, W.; Putterlik, J.; Schuhmann, R. M.; Sundermeyer, J. *Organometallics* **1996**, *15*, 4586. (o) Vetter, W. M.; Sen, A. *Organometallics* **1991**, *10*, 244. (p) Van Asselt, A.; Trimmer, M. S.; Henling, L. M.; Bercaw, J. E. *J. Am. Chem. Soc.* **1988**, *110*, 8254. (q) Boro, B. J.; Lansing, R.; Goldberg, K. I.; Kemp, R. A. *Inorg. Chem. Comm.* **2011**, *14*, 531.
2. Stanciu, C.; Jones, M. E.; Fanwick, P. E.; Abu-Omar, M. M. *J. Am. Chem. Soc.* **2007**, *129*, 12400.
3. Lu, F.; Zarkesh, R. A.; Heyduk, A. F. *Eur. J. Inorg. Chem.* **2012**, 467.

4. (a) Chisholm, M. H.; Hammond, C. E.; Huffman, J. C. *J. Chem. Soc., Chem. Commun.* **1987**, 1423. (b) Brindley, P. B.; Hodgson, J. C. *J. Organomet. Chem.* **1974**, *65*, 57.

5. Chen, S.-J.; Abbott, J. K. C.; Steren, C. A.; Xue, Z.-L. *J. Clust. Sci.* **2010**, *21*, 325.

6. For studies of the reactions between O_2 and late transition metal complexes, see, for example, (a) Campbell, A. N.; Stahl, S. S. *Acc. Chem. Res.* **2012**, *45*, 851. (b) Theopold, K. H.; Reinaud, O. M.; Blanchard, S.; Leelasubeharoen, S.; Hess, A.; Thyagarajan, S. *ACS Symp. Ser.* **2002**, *823*, 75. (c) Que, L.; Tolman, W. B. *Nature* **2008**, *455*, 333. (d) Himes, R. A.; Karlin, K. D. *Curr. Top. Chem. Biol.* **2009**, *13*, 119. (e) Shook, R. L.; Borovik, A. S. *Chem. Comm.* **2008**, 6095. (f) Sheldon, R. A. in *Biomimetic Oxidations Catalyzed by Transition Metal Complexes*, Meunier, B. ed., Imperial College Press, 2000, pp. 613-662. (g) *Metal-Dioxygen Complexes: A Perspective.* Special Issue, *Chem. Rev.* **1994**, *94*, Issue 3, 567-856. (h) Monillas, W. H.; Yap, G. P. A.; MacAdams, L. A.; Theopold, K. H. *J. Am. Chem. Soc.* **2007**, *129*, 8090. (i) McQuilken, A. C.; Jiang, Y.; Siegler, M. A.; Goldberg, D. P. *J. Am. Chem. Soc.* **2012**, *134*, 8758. (j) Prokop, K. A.; Goldberg, D. P. *J. Am. Chem. Soc.* **2012**, *134*, 8014. (k) Scheuermann, M. L.; Fekl, U.; Kaminsky, W.; Goldberg, K. I. *Organometallics* **2010**, *29*, 4749. (l) Boisvert, L.; Denney, M. C.; Kloek Hanson, S.; Goldberg, K. I. *J. Am. Chem. Soc.* **2009**, *131*, 15802. (m) Khusnutdinova, J. R.; Rath, N. P.; Mirica, L. M. *J. Am. Chem. Soc.* **2012**, *134*, 2414. (n) Nguyen, K. T.; Rath, S. P.; Latos-Grazynski, L.; Olmstead, M. M.;

Balch, A. L. *J. Am. Chem. Soc.* **2004**, *126*, 6210. (o) Maury, J.; Feray, L.; Bazin, S.; Clement, J.-L.; Marque, S. R. A.; Siri, D.; Bertrand, M. P. *Chem. Eur. J.* **2011**, *17*, 1586. (p) Lewinski, J.; Koscielski, M.; Suwala, K.; Justyniak, I. *Angew. Chem. Int. Ed.* **2009**, *48*, 7017. (q) Mukherjee, D.; Ellern, A.; Sadow, A. D. *J. Am. Chem. Soc.* **2012**, *134*, 13018. (r) Jana, S.; Berger, R. J. F.; Fröhlich, R.; Pape, T.; Mitzel, N. W. *Inorg. Chem.* **2007**, *46*, 4293. (s) Lee, C.-M.; Chuo, C.-H.; Chen, C.-H.; Hu, C.-C.; Chiang, M.-H.; Tseng, Y.-J.; Hu, C.-H.; Lee, G.-H. *Angew. Chem. Int. Ed.* **2012**, *51*, 5427. (t) Kelley, M. R.; Rohde, J.-U. *Chem. Comm.* **2012**, *48*, 2876. (u) Brown, S. N.; Mayer, J. M. *Inorg. Chem.* **1992**, *31*, 4091. (v) Parkin, G.; Bercaw, J. E. *J. Am. Chem. Soc.* **1989**, *111*, 391.

7. (a) Robertson, J. *Rep. Prog. Phys.* **2006**, *69*, 327. (b) Jones, A. C.; Aspinall, H. C.; Chalker, P. R.; Potter, R. J.; Kukli, K.; Rahtu, A.; Ritala, M.; Leskelae, M. *J. Mater. Chem.* **2004**, *14*, 3101. (c) Arghavani, R.; Miner, G.; Agustin, M. *Semicond. Internal.* **2007**, *30*, 32-34, 36, 38.

8. For CVD of metal oxides using O_2, see, for example, (a) Son, K.-A.; Mao, A. Y.; Sun, Y.-M.; Kim, B. Y.; Liu, F.; Kamath, A.; White, J. M.; Kwong, D. L.; Roberts, D. A.; Vrtis, R. N. *Appl. Phys. Lett.* **1998**, *72*, 1187. (b) Niimi, H.; Johnson, R. S.; Lucovsky, G.; Massoud, H. Z. *Proc. Electrochem. Soc.* **2000**, *2000-2*, 487. (c) Eichler, J. F.; Just, O.; Rees, W. S., Jr. *J. Mater. Chem.* **2004**, *14*, 3139. (d) Takahashi, K.; Funakubo, H.; Hino, S.; Nakayama, M.; Ohashi, N.; Kiguchi, T.; Tokumitsu, E. *J. Mater. Res.* **2004**, *19*, 584. (e) Ogura, A.; Ito, K.; Ohshita, Y.; Ishikawa, M.; Machida, H. *Thin Solid Films* **2003**, *441*, 161. (f)

Rodriguez-Reyes, J. C. F.; Teplyakov, A. V. *J. Appl. Phys.* **2008**, *104*, 084907/1. (g) Ohshita, Y.; Ogura, A.; Ishikawa, M.; Kada, T.; Machida, H. *Jpn. J. Appl. Phys. 2.* **2003**, *42*, L578. (h) Matero, R.; Ritala, M.; Leskelae, M.; Sajavaara, T.; Jones, A. C.; Roberts, J. L. *Chem. Mater.* **2004**, *16,* 5630. (i) Kan, B.-C.; Boo, J.-H.; Lee, I.; Zaera, F. *J. Phys. Chem. A* **2009**, *113*, 3946. (j) Hausmann, D. M.; de Rouffignac, P.; Smith, A.; Gordon, R.; Monsma, D. *Thin Solid Films* **2003**, *443*, 1. (k) Meiere, S. H.; Peck, J.; Litwin, M. *ECS Trans.* **2006**, *1*, 103. (l) Chen, T.; Cameron, T. M.; Nguyen, S. D.; Stauf, G. T.; Peters, D. W.; Maylott, L.; Li, W.; Xu, C.; Roeder, J. F.; Hendrix, B. C.; Hilgarth, M.; Niinisto, J.; Kukli, K.; Ritala, M.; Leskela, M. *ECS Trans.* **2008**, *16*, 87. (m) Lee, S.; Kim, W.-G.; Rhee, S.-W.; Yong, K. *J. Electrochem. Soc.* **2008**, *155*, H92. (n) Schaeffer, J.; Edwards, N. V.; Liu, R.; Roan, D.; Hradsky, B.; Gregory, R.; Kulik, J.; Duda, E.; Contreras, L.; Christiansen, J.; Zollner, S.; Tobin, P.; Nguyen, B.-Y.; Nieh, R.; Ramon, M.; Rao, R.; Hegde, R.; Rai, R.; Baker, J.; Voight, S. *J. Electrochem. Soc.* **2003**, *150*, F67. (o) Woods, J. B.; Beach, D. B.; Nygren, C. L.; Xue, Z.-L. *Chem. Vap. Deposition* **2005**, *11*, 289. (p) Lehn, J.-S.; Javed, S.; Hoffman, D. M. *Chem. Vap. Deposition* **2006**, *12*, 280. (q) Chiu, H.-T.; Wang, C.-N.; Chuang, S.-H.; *Chem. Vap. Deposition* **2000**, *6*, 223. (r) Wiedmann, M. K.; Heeg, M. J.; Winter, C. H. *Inorg. Chem.* **2009**, *48*, 5382.

9. For CVD of metal oxides using water, see, for example, (a) Dezelah, C. L., IV; Niinisto, J.; Kukli, K.; Munnik, F.; Lu, J.; Ritala, M.; Leskela, M.; Niinisto, L. *Chem. Vap. Deposition* **2008**, *14*, 358. (b) Dezelah, C. L., IV; El-Kadri, O. M.;

Szilagyi, I. M.; Campbell, J. M.; Arstila, K.; Niinistoe, L.; Winter, C. H. *J. Am. Chem. Soc.* **2006**, *128*, 9638. (c) Majumder, P.; Jursich, G.; Takoudis, C. *J. Appl. Phys.* **2009**, *105*, 104106/1. (d) Consiglio, S.; Clark, R. D.; Nakamura, G.; Wajda, C. S.; Leusink, G. J. *J. Vacuum Sci. Technol., A* **2012**, *30*, 01A119/1. (e) Tao, Q.; Kueltzo, A.; Singh, M.; Jursich, G.; Takoudis, C. G. *J. Electrochem. Soc.* **2011**, *158*, G27. (f) Shi, X.; Tielens, H.; Takeoka, S.; Nakabayashi, T.; Nyns, L.; Adelmann, C.; Delabie, A.; Schram, T.; Ragnarsson, L.; Schaekers, M.; Date, L.; Schreutelkamp, R.; Van Elshocht, S. *J. Electrochem. Soc.* **2011**, *158*, H69.

10. See, e.g., Bradley, D. C.; Thomas, I. M. *Proc. Chem. Soc.* **1959**, 225.
11. (a) Wang, R.; Zhang, X.; Chen, S.-J.; Yu, X.; Wang, C.; Beach, D. B.; Wu, Y.; Xue, Z. *J. Am. Chem. Soc.* **2005**, *127*, 5204. (b) Chen, S.; Zhang, X.; Yu, X.; Qiu, H.; Yap, G. P. A.; Guzei, I. A.; Lin, Z.; Wu, Y.; Xue, Z. *J. Am. Chem. Soc.* **2007**, *129*, 14408. (c) Chen, S.-J.; Zhang, X.-H.; Lin, Z.; Wu, Y.-D.; Xue, Z.-L. *Sci*. China Chem. **2009**, *52*, 1723. (d) Chen, S.-J.; Yap, G. P. A.; Xue, Z.-L. *Sci*. China Chem. **2009**, *52*, 1583. (e) Chen, S.-J.; Zhang, J.; Yu, X.; Bu, X.; Chen, X.; Xue, Z. *Inorg. Chem.* **2010**, *49*, 4017. (f) Chen, T.-N.; Zhang, X.-H.; Wang, C.-S.; Chen, S.-J.; Wu, Z.-Z.; Li, L.-T.; Sorasaenee, K. R.; Diminnie, J. B.; Pan, H.-J.; Guzei, I. A.; Rheingold, A. L.; Wu, Y.-D.; Xue, Z.-L. *Organometallics* **2005**, *24*, 1214. (g) Qiu, H.; Chen, S.-J.; Wang, C.-S.; Wu, Y.-D.; Guzei, I. A.; Chen, X.-T.; Xue, Z.-L. *Inorg. Chem.* **2009**, *48*, 3073. (h) Yu, X.; Chen, X.-T.; Xue, Z.-L. *Organometallics* **2009**, *28*, 6642. (i) Chen, S.-J.; Xue, Z.-L. *Organometallics* **2010**, *29*, 5579. (j) Wu, Z.; Cai, H.; Yu, X.-H.;

Blanton, J. R.; Diminnie, J. B.; Pan, H.-J. ; Xue, Z.-L. *Organometallics* **2002**, *21*, 3973.

12. For the studies of amidinate complexes as catalysts, see, for example, (a) Edelmann, F. T. *Adv. Organom. Chem.* **2008**, *57*, 183. (b) Collins, S. *Coord. Chem. Rev.* **2011**, *255*, 118. (c) Kissounko, D. A.; Zabalov, M. V.; Brusova, G. P.; Lemenovskii, D. A. *Russ. Chem. Rev.* **2006**, *75*, 351. (c)
13. Fontaine, P. P.; Yonke, B. L.; Zavalij, P. Y.; Sita, L. R. *J. Am. Chem. Soc.* **2010**, *132*, 12273.
14. Tiong, P. J.; Nova, A.; Clot, E.; Moundtford, P. *Chem. Commun.* **2001**, *47*, 3147.
15. For the studies of amidinate complexes as CVD/ALD precursors, see, for example, (a) Krisyuk, V.; Aloui, L.; Prud'homme, N.; Sysoev, S.; Senocq, F.; Samelor, D.; Vahlas, C. *Electrochem. Solid-State Lett.* **2011**, *14*, D26. (b) Seetula, J.; Kalliorinne, K.; Koskikallio, J. *J. Photochem. Photobiol., A.: Chem.* **1988**, *43*, 31. (c) Thiede, T. B.; Krasnopolski, M.; Milanov, A. P.; Arcos, T.; Ney, A.; Becker, H.-W; Rogalla, D.; Winter, J.; Devi, A.; Fischer, R. A. *Chem. Mater.* **2011**, *23*, 1430. (d) Eleter, M.; Hubert-Pfalzgraf, L., G.; Daniele, S.; Pilet, G.; Tinant, B. *Polyhedron* **2010**, 29, 2522. (e) Li, Z.; Gordon, R. G.; Pallem, V.; Li, H.; Shenai, D. V. *Chem. Mater.* **2010**, *22*, 3060. (f) Xu, K.; Milanov, A. P.; Winter, M.; Barreca, D.; Gasparotto, A.; Becker, H.-W.; Devi, A. *Eur. J. Inorg. Chem.* **2010**, 1679. (g) Eleter, M.; Daniele, S.; Brizé, V.; Dubourdieu, C.; Lachaud, C.; Blasco, N.; Pinchart, A. *ECS Trans.* **2009**, *25*, 151. (h) Gleizes, A. N.; Krisyuk, V. V.; Aloui, L.; Turgambaeva, A. E.;

Sarapata, B.; Prud'homme, N.; Senocq, F.; Samélor, D.; Zielinska-Lipiec, A.; Dumestre, F.; Vahlas, C. *ECS Trans.* **2009**, *25*, 181. (i) Pallem, V.R.; Dussarrat, C., U.S. Pat. Appl. Publ., 2011, US 20110250354 A1 20111013. (j) Turgambaeva, A.; Prud'homme, N.; Krisyuk, V.; Vahlas, C. *J. Nanosci. Nanotechnol.* **2011**, *11*, 8198. (k) Shenai-Khatkhate, D. V.; Manzik, S. J.; Wang, Q. M., U.S. Pat. Appl. Publ., 2009, US 20090017208 A1 20090115. (l) Li, Z.; Lee, D. K.; Coulter, M.; Rodriguez, L. N. J.; Gordon, R. G. *Dalton Trans.* **2008**, 2592. (m) Li, X.-G.; Li, Z.; Li, H.; Gordon, R. G. *Eur. J. Inorg. Chem.* **2007**, 1135. (n) Li, Z.; Barry, S. T.; Gordon, R. G. *Inorg. Chem.* **2005**, *44*, 1728.

16. Sun, J.; Chen, S.-J.; Duan, Y.; Li, Y.; Chen, X.; Xue, Z. *Organometallics* **2009**, *28*, 3088.
17. Chen, S.-J.; Dougan, B. A.; Chen, X.-T.; Xue, Z.-L. *Organometallics* **2012**, *31*, 3443.
18. (a) Forsberg, J. H.; Spaziano, V. T.; Balasubramanian, T. M.; Liu, G. K.; Kinsley, S. A.; Duckworth, C. A.; Poteruca, J. J.; Brown, P. S.; Miller, J. L. *J. Org. Chem.* **1987**, *52*, 1017. (b) Xu, F.; Sun, J.; Shen, Q. *Tetrahedron Letters* **2002**, *43*, 1867. (c) Tada, K.-I.; Inaba, K.; Furukawa, T.; Yamakawa, T.; Oshima, N. PCT Int. Appl., 2007, WO 2007015436 A1 20070208. The patent is in Japanese with an English abstract.
19. Bailar, J. C. *J. Inorg. Nucl. Chem.* **1958**, *8*, 165.
20. Dimitrov, V. S.; Ladd, J. A. *Magn. Reson. Chem.* **1985**, *23*, 529.
21. It should be noted that this experiment used a 400 MHz NMR spectrometer.

The coalesence and static spectra temperatures are dependant on the magnetic field. Thus NMR spectra at other frequencies would show slightly different temperatures of coalescence.

22. Sandstrom, J. *Dynamic NMR Spectroscopy*; Academic Press: London, 1982.
23. Macomber, R. S. *A Complete Introduction to Modern NMR Spectroscopy*; Wiley: New York, 1998; pp. 158-160.
24. The rate constants here are the chemical rate constants, and they differ from the observed magnetization transfer rate constants by a factor of 2.
25. Green, M. L. H.; Wong, L. L.; Sella, A. *Organometallics* **1992**, *11*, 2660.
26. The systematic uncertainties δk_{sys} were estimated based on the subjective judgment of the sensitivities of the NMR integration to the changes in concentrations. The total uncertainties δk were calculated from $\delta k = (\delta k_{ran}^2 + \delta k_{sys}^2)^{1/2}$ (δk_{ran}: random uncertainty).
27. Taylor, J. *An Introduction to Error Analysis*; University Science Books: Milley Valley, CA, 1982; Chapter 4.
28. Sharma, B., Ph. D. dissertation, The University of Tennessee, Knoxville, 2013.
29. Diamond, G. M.; Jordan, R. F.; Petersen, J. L. *Organometallics* **1996***, 15,* 4030.
30. Morse, P. M.; Spencer, M. D.; Wilson, S. R.; Girolami, G. S. *Organometallics* **1994**, *13*, 1646.

Part 3

Reactions of Zirconium Amidinate Amide Complexes with Dioxygen, Water or Hydrogen Peroxide

Abstract

The reactions of Zr amidinate amide complexes $Zr[MeC(N^iPr)_2]_2(NR_2)_2$ (R = Me, **10**; Et, **12**) with either O_2 or water have been studied. Two major products for both reactions of **10** or **12** with O_2 or H_2O are dimer $\{(\mu\text{-}O)Zr[MeC(N^iPr)_2]_2\}_2$ (**14**) and its insoluble polymer $\{(\mu\text{-}O)Zr[MeC(N^iPr)_2]_2\}_n$ (**17**). **14** was characterized by ^1H and $^{13}C\{^1H\}$ NMR spectroscopies and MS. $\{(\mu\text{-}O)Zr[MeC(N^iPr)_2]_2\}_n$ (**17**) was characterized by elemental analysis, solid-state ^{13}C NMR and IR spectroscopies, thermal gravimetric analysis (TGA), and stability tests. An unusual Zr peroxo trimer, $\{(\mu\text{-}\eta^2\text{:}\eta^2\text{-}O_2)Zr[MeC(N^iPr)_2]_2\}_3$ (**20**), has been obtained from the reaction of **10** with O_2 and its crystal structure has been determined. **20** has also been prepared from the reaction of $Zr[MeC(N^iPr)_2]_2Cl_2$ (**8**) with Na_2O_2. Attempts to make **20** by the reaction of H_2O_2 with $Zr[MeC(N^iPr)_2]_2(NMe_2)_2$ (**10**) instead gave **14** and **17**. $\{(\mu\text{-}\eta^2\text{:}\eta^2\text{-}O_2)Zr[MeC(N^iPr)_2]_2\}_3$ (**20**) reacts with $Zr[MeC(N^iPr)_2]_2(NMe_2)_2$ (**10**) to give the zirconium oxo products, dimer $\{(\mu\text{-}O)Zr[MeC(N^iPr)_2]_2\}_2$ (**14**), its polymer $\{(\mu\text{-}O)Zr[MeC(N^iPr)_2]_2\}_n$ (**17**), $HNMe_2$, and $CH_2(NMe_2)_2$ (**19**).

3.1. Introduction

Early transition metal complexes are often sensitive to O_2 and water, and these complexes are thus usually handled under an inert atmosphere.[1-6] Many early transition metal complexes contain no valence *d* electrons (d^0)[1-5] and their reactivities toward O_2 and water are different from complexes with valence *d* electrons (d^n).[6] The reactions with O_2 and water have been used to make microelectronic metal oxide (MO_n) materials through chemical vapor deposition (CVD) and atomic layer deposition (ALD) processes.[7-9] The metal oxides, as gate insulating materials, make transistors thinner and microelectronic devices faster while batteries last longer. Metal oxide thin films have been prepared using d^0 amide[8a-o,9b,e,f] and imide[8q,r] complexes as precursors through CVD/ALD processes. Even though the CVD/ALD reactions have been successfully used to make metal oxides, the mechanism of the reactions is not well understood. This is in part because O_2 is a diradical, and many of its reactions are radical in nature.

Our group has studied the reactions of O_2 with homoleptic early transition metal amide complexes. $Ti(NMe_2)_4$ as a CVD precursor reacts with O_2 to form a TiO_2 thin film.[8o] The reactions of $M(NMe_2)_4$ (M = Zr, Hf) with O_2 afford unusual oxo aminoxides $M_3(NMe_2)_6(\mu\text{-}NMe_2)_3(\mu_3\text{-}O)(\mu_3\text{-}ONMe_2)$ and Me_2NNMe_2.[10a] Reactions of $M(NR_2)_5$ (M = Nb, Ta; R = Me, Et) toward O_2 were also studied.[10b,e] The isolated products are shown in Scheme 3.1. DFT studies of the reactions between $Ta(NMe_2)_5$ and O_2 are presented in Scheme 3.2.[10b] One key step in this reaction is the insertion of O_2 into a M-N bond.

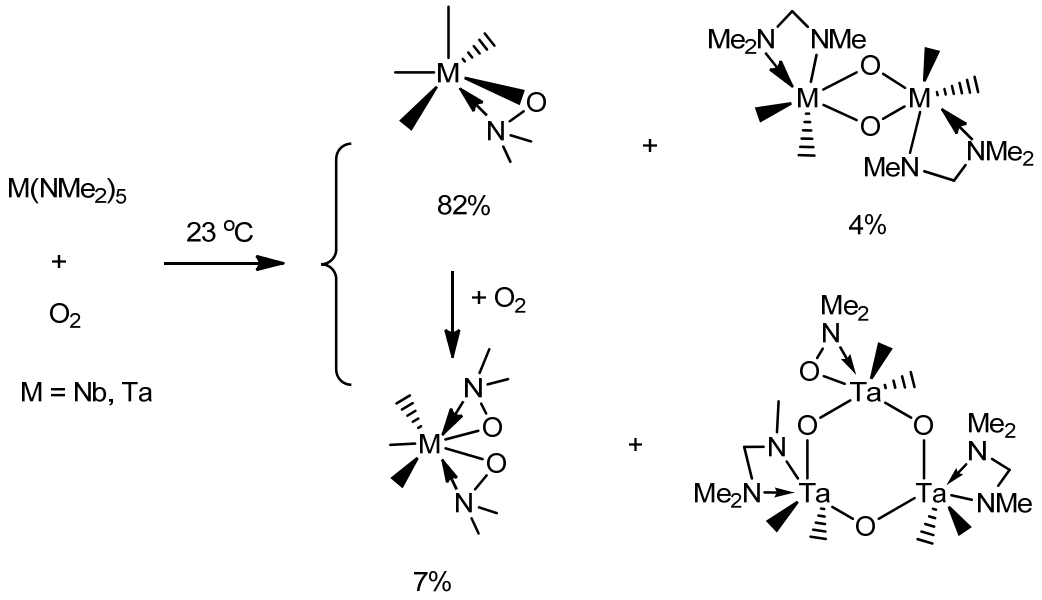

Scheme 3.1. Reactions of $M(NMe_2)_5$ (M = Nb, Ta) with O_2.[10b,e]

The homoleptic amide complexes $M(NR_2)_n$[8a-o,9b,e,f] are too sensitive towards air to handle. Ancillary ligands such as amidinates have thus been used to make precursor compounds more stable.[12] The amidinate ligand is bidentate and donates four electrons to the metal center. In Part 2, our syntheses of Zr amidinate amides, $Zr[MeC(N^iPr)_2]_2(NR_2)_2$ (R = Me, **10**; Et, **12**), are reported. We have studied the reactions of **10** with O_2, H_2O, or H_2O_2, and **12** with H_2O or O_2. These reactions give oxo dimer $\{(\mu\text{-}O)Zr[MeC(N^iPr)_2]_2\}_2$ (**14**) and its polymer $\{(\mu\text{-}O)Zr[MeC(N^iPr)_2]_2\}_n$ (**17**). In addition to $HNMe_2$, $CH_2(NMe_2)_2$ (**19**) is a volatile product in the reactions of **10** with O_2 or H_2O_2. A peroxo product $\{(\mu\text{-}\eta^2\text{:}\eta^2\text{-}O_2)Zr[MeC(N^iPr)_2]_2\}_3$ (**20**) has been obtained from the reaction of **10** with O_2. Our studies are reported here.

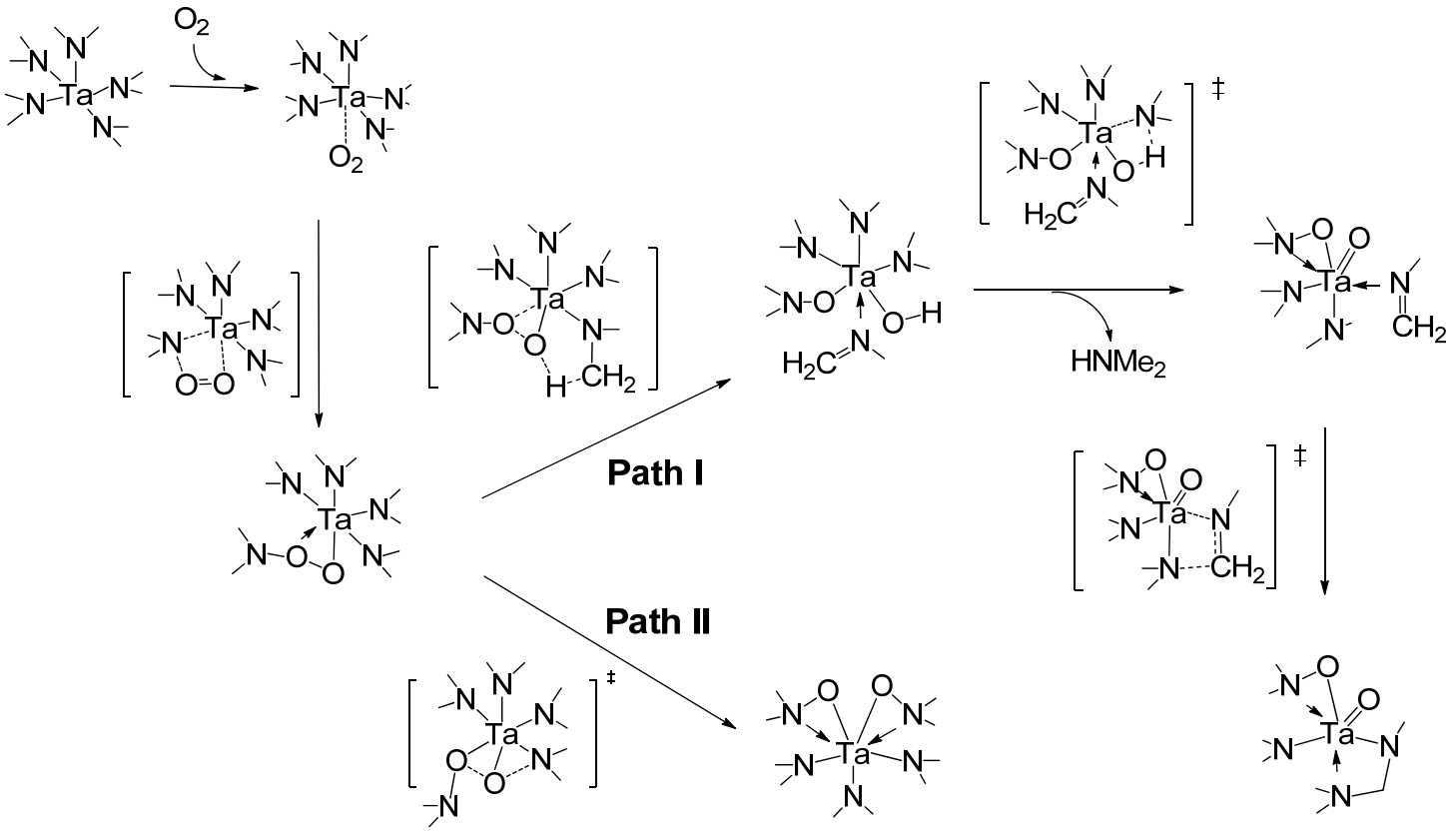

Scheme 3.2. Pathways in the reaction of $Ta(NMe_2)_5$ with O_2 based on DFT studies.[10]

3.2. Results and Discussion

3.2.1. Reaction of $Zr[MeC(N^iPr)_2]_2(NMe_2)_2$ (10) with O_2

The Zr amidinate amide complex **10** reacts slowly with 1 atm of O_2 at 70 °C in benzene-d_6 (Scheme 3.3). ^{1}H NMR monitoring showed that it took ca. 12 days to complete the reaction. Throughout the process, the peaks of **10** gradually decreased and a new set of peaks appeared that are consistent with an oxo-bridged dimer **14** along with a precipitant that is insoluble. Two organic byproducts; $HNMe_2$ and $CH_2(NMe)_2$ (**19**) were also observed in ^{1}H and $^{13}C\{^1H\}$ NMR spectra and GC-MS. The *soluble*, Zr-containing product was identified to be the dimer $\{(\mu\text{-}O)Zr[MeC(N^iPr)_2]_2\}_2$ (**14**). The insoluble product was characterized as a polymer $\{(\mu\text{-}O)Zr[MeC(N^iPr)_2]_2\}_n$ (**17**) of the monomer $(O=)[ZrMeC(N^iPr)_2]_2$ (**13**) and is discussed in Section 3.2.6. The structure of **14** is based on its ^{1}H and $^{13}C\{^1H\}$ NMR and MS spectra. As the reaction progressed, more precipitate formed while the peaks of the oxo-dimer **14** stayed about the same intensity.

When a solution of **10** in pentane was exposed to air at -35 °C, crystals of the peroxo $\{(\mu\text{-}\eta^2\text{:}\eta^2\text{-}O_2)Zr[MeC(N^iPr)_2]_2\}_3$ (**20**) were obtained as a solid mixture with **14**, **17**, and unreacted **10**. Its crystal structure and properties are discussed in Section 3.2.4.

The ^{1}H NMR spectrum of **14** in benzene-d_6 (Figure 3.1) shows two doublets at 1.02 and 1.25 ppm for the CH*Me*$_2$ methyl groups. A singlet at 1.34 ppm is assigned to the methyl group on the amidinate ligand (^{i}PrN)(*Me*)C(N^{i}Pr). Two multiplets for the C*H*Me$_2$ atom are assigned at 3.47 and 4.26 ppm. In the

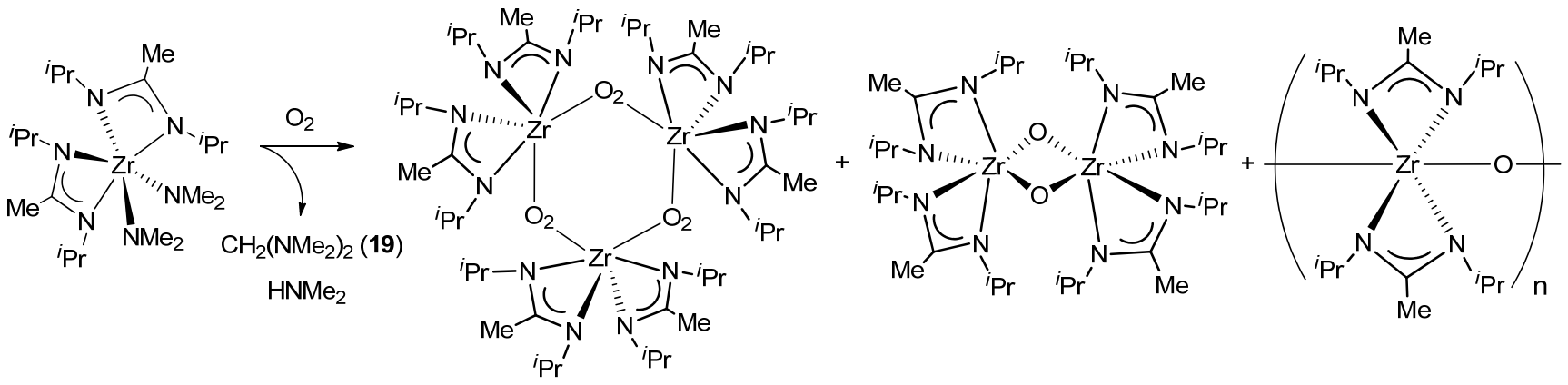

Scheme 3.3. Reaction of **10** with O_2.

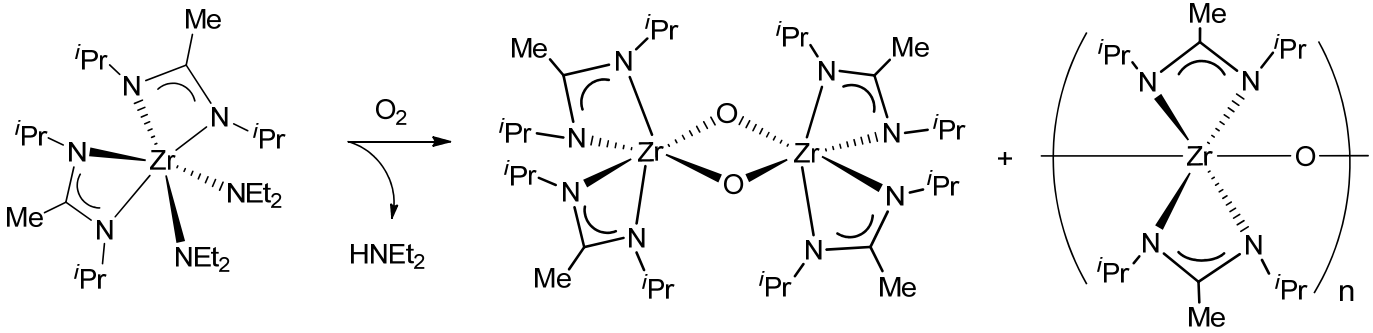

Scheme 3.4. Reaction of **12** with O_2.

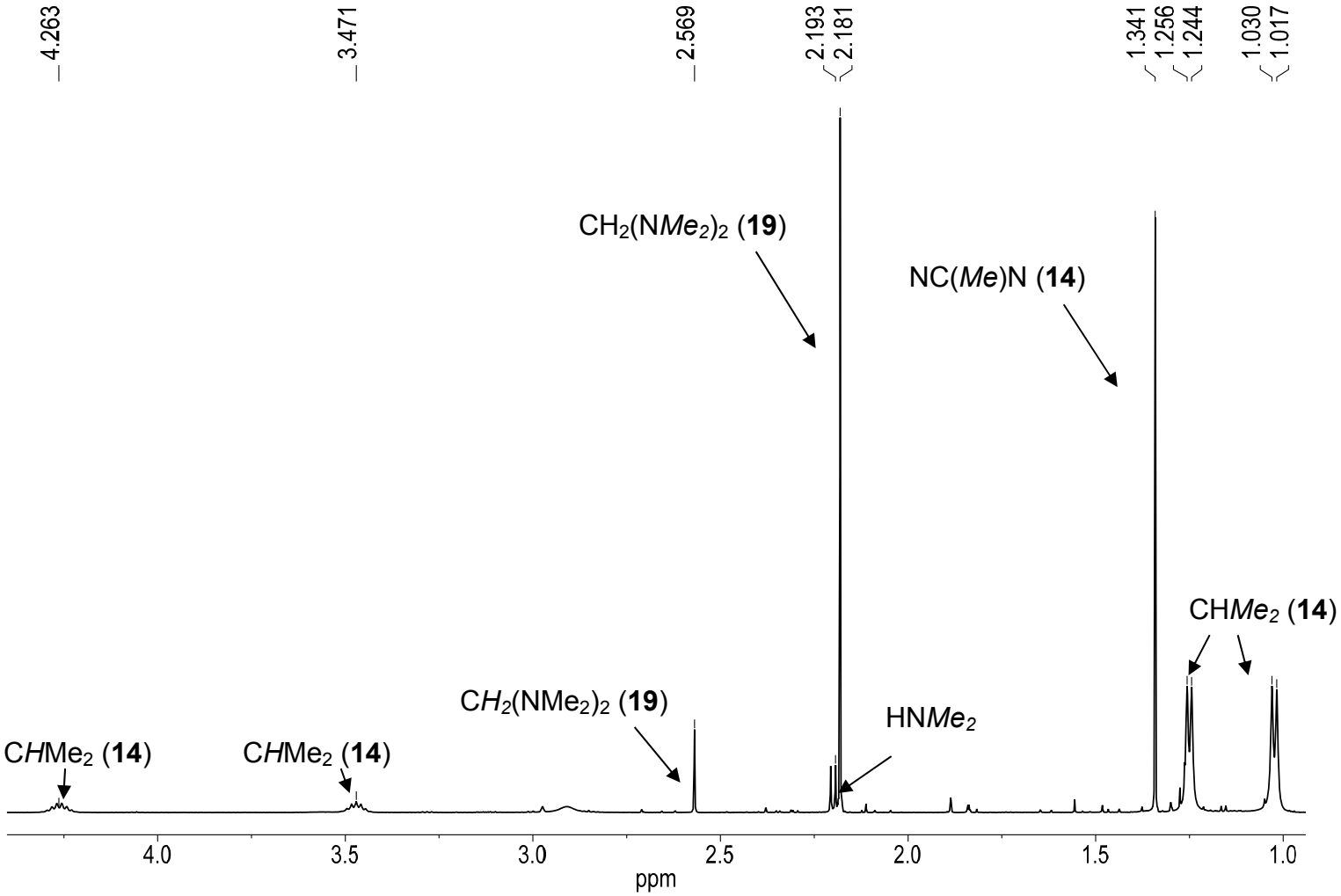

Figure 3.1. ^{1}H NMR spectrum of the product mixture from the reaction of **10** with O_2 in benzene-d_6.

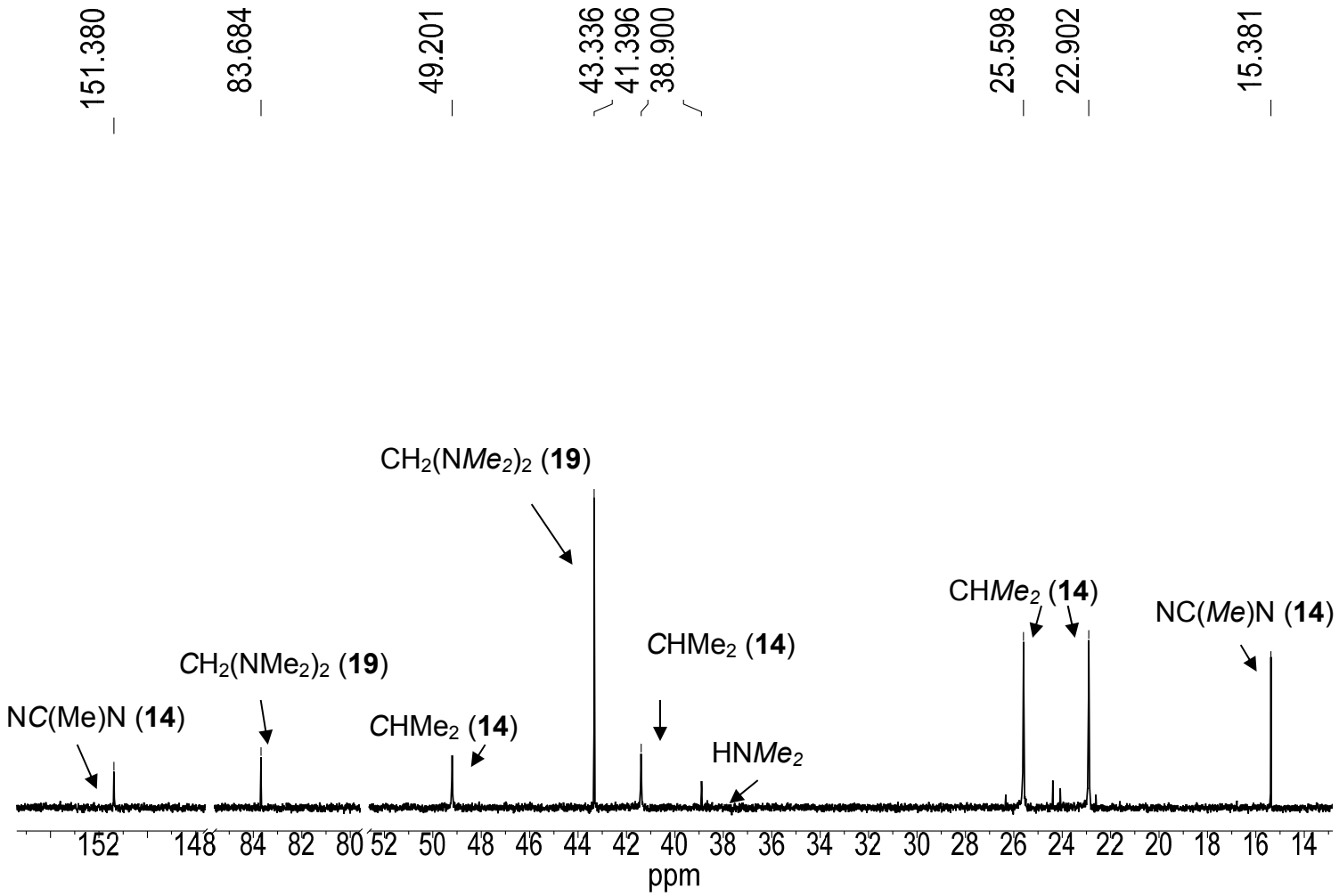

Figure 3.2. $^{13}C\{^{1}H\}$ NMR spectrum of the product mixture from the reaction of **10** with O_2 in benzene-d_6.

^{13}C NMR spectrum of **14** in benzene-d_6 (Figure 3.2) two peaks appear at 22.90 and 25.60 ppm which are assigned for the CH*Me*$_2$ methyl groups, and their *C*H atoms at 41.40 and 49.20 ppm. The quaternary carbon atom peak appeared at 151.38 ppm. These observations suggest that the amide ligands are replaced with an oxygen moiety to give the oxo-dimer **14** in Scheme 3.3. After the reaction was completed, attempts to crystallize the soluble oxo-dimer **14** were unsuccessful, as it formed the insoluble polymer $\{(\mu\text{-O})[Zr[MeC(N^iPr)_2]_2\}_n$ (**17**) over time and precipitated from the solution. The polymer **17**, however, does not dissolve in benzene-d_6, DMF, Et_2O, hexanes, methanol, pentane, THF, or toluene-d_8.

It should be noted that the NMR spectra of the oxo-dimer **14** also support the structures of the oxo monomer **13**, trimer **15**, tetramer **16**, or the polymer **17**. The following observations and analysis support the oxo dimer **14**: (1) **14** was also observed in the reaction between **10** and H_2O (Section 3.2.3); (2) **14** was observed in MS in the reaction of **10** with H_2O in air; (3) Reactions between $Zr[MeC(N^iPr)_2]_2(NEt_2)_2$ (**12**) and O_2 or H_2O, discussed in Sections 3.2.2 and 3.2.3, respectively, also give **14**; (4) Elemental analysis of the polymer **17** is consistent with the composition that this species is an oligomer of **13**.

Although the monomer $(O=)Zr[MeC(N^iPr)_2]_2$ (**13**) was also observed in MS as discussed later in Section 3.2.5, it is unlikely the observed product in NMR because it is penta-coordinated and perhaps less stable than the hexa-coordinated oxo dimer **14**. We cannot rule out the observed species is the oxo trimer **15** (Scheme 3.5), which is also hexa-coordinated. But it is unlikely to be

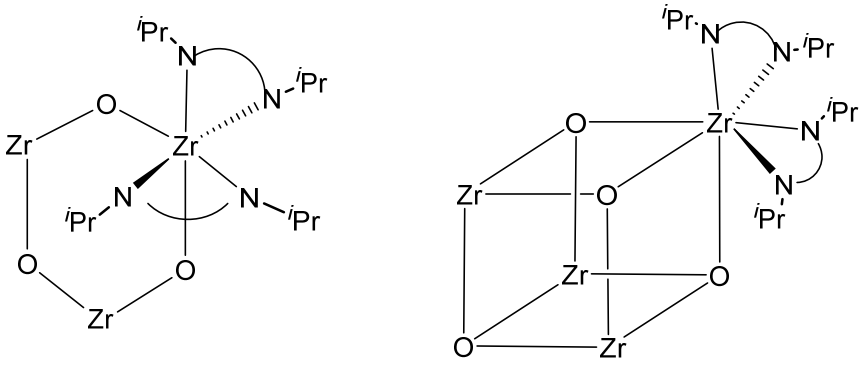

15 **16**

Scheme 3.5. Hexa-coordinated trimer **15** and hepta-coordinated tetramer **16**.

the hepta-coordinated tetramer **16** as Zr centers are perhaps too crowded.

The identification of $HNMe_2$ and $CH_2(NMe_2)_2$ (**19**) as byproducts in the reaction of **10** with O_2 suggests this reaction is radical.[13] Several papers have reported that, once $\bullet NMe_2$ radicals are formed, their reactions lead to the formation of $HNMe_2$ and $CH_2(NMe_2)_2$ (**19**) involving intermediates such as $CH_3\bullet$, CH_2=NH, H•, CH_3N=CH_2, and $(CH_3)_2N$-$CH_2\bullet$.[13a,b] This helps explain the formation of the major products, **14** and **17**, in the reaction of **10** with O_2 (Scheme 3.3) giving $HNMe_2$ and **19**. We earlier reported that the reactions of $M(NMe_2)_4$ (M = Zr, Hf) with O_2 gives aminoxides $M_3(NMe_2)_6(\mu\text{-}NMe_2)_3(\mu_3\text{-}O)(\mu_3\text{-}ONMe_2)$ and Me_2NNMe_2 (Scheme 3.6) which probably goes through a radical process.[10a] DFT calculations using models suggest that a mechanism involving $\bullet NMe_2$ radicals from homoleptic cleavage of newly formed ZrO-NMe_2 bonds from insertion of an O atom into a Zr-NMe_2 bond.[10a] It is surprising that the fate of the NMe_2 ligands is different in the reactions of $M(NMe_2)_4$ (M = Zr, Hf) and **10** with O_2.

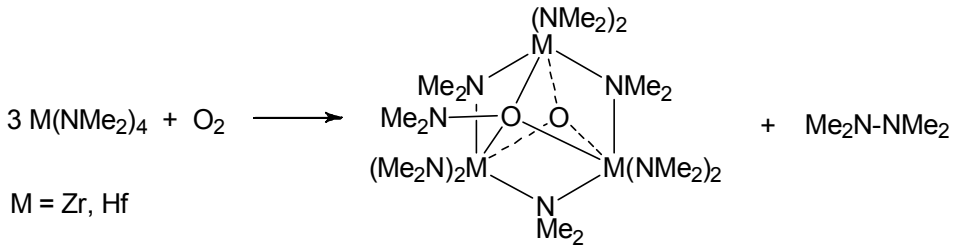

Scheme 3.6. Reactions of Zr and Hf amides with O_2.[10a]

3.2.2. Reaction of Zr[MeC(N^{i}Pr)$_2$]$_2$(NEt$_2$)$_2$ (12) with O_2

Since the reaction of dimethylamide amidinate Zr[MeC(N^{i}Pr)$_2$]$_2$(NMe$_2$)$_2$ (**10**) with O_2 gives several products, including the oxo dimer {(μ-O)Zr[MeC(N^{i}Pr)$_2$]$_2$}$_2$ (**14**) and polymer {(μ-O)Zr[MeC(N^{i}Pr)$_2$]$_2$}$_n$ (**17**) that contain no amide ligands. One method to support the identity of **14** and **17** was to study the reaction of diethylamide amidinate **12** with O_2 and see if it also forms **14** and **17**. Indeed the reaction yielded the soluble oxo-dimer **14** product and the insoluble solid **17**, as shown in Scheme 3.4. ^{1}H and ^{13}C{^{1}H} NMR spectra are given in Figures 3.3 and 3.4, respectively. The only organic product was HNEt$_2$ which was confirmed by ^{1}H and ^{13}C{^{1}H} NMR spectra and GC-MS. It should also be noted that this reaction was completed more quickly than its methyl analog **10**. The reaction of **12** with O_2 requires heating at 70 °C for 7 days. The reaction of **10** with O_2 at 70 °C, in comparison, took ca. 12 days to complete.

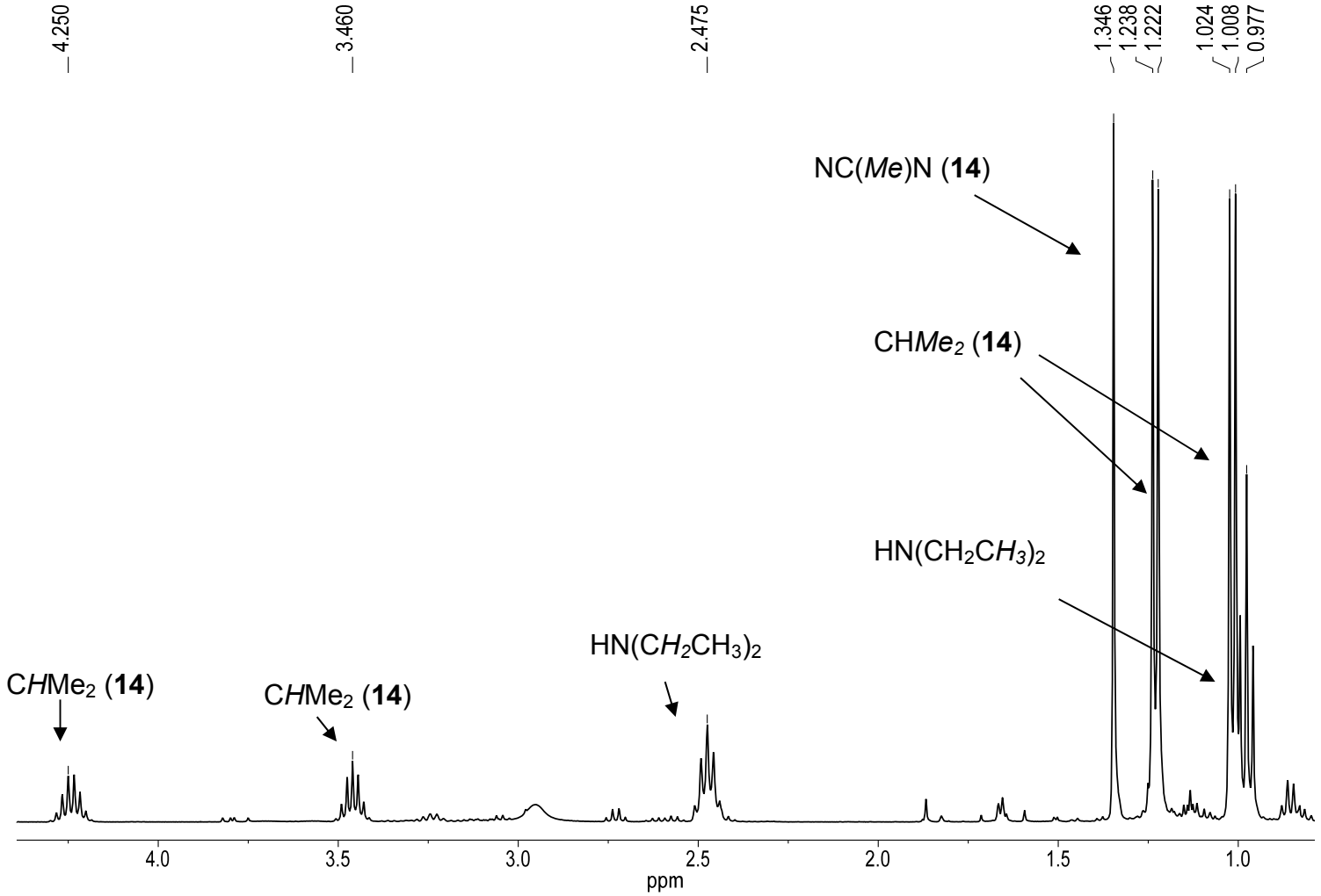

Figure 3.3. ^{1}H NMR spectrum of the product mixture from the reaction of **12** with O_2 in benzene-d_6.

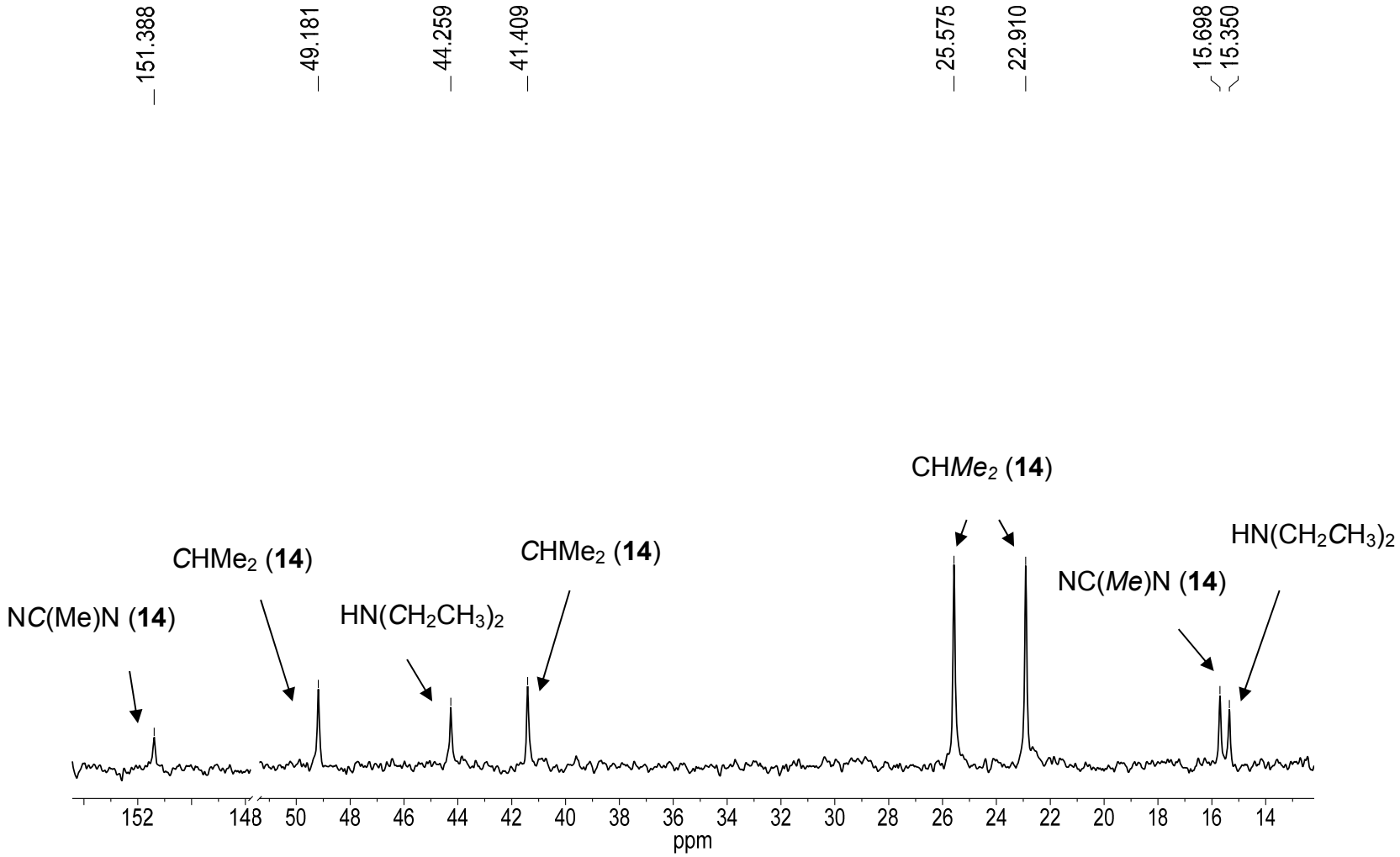

Figure 3.4. $^{13}C\{^{1}H\}$ NMR spectrum of the product mixture from the reaction of **12** with O_2 in benzene-d_6.

3.2.3. Reactions of $Zr[MeC(N^iPr)_2]_2(NR_2)_2$ (R = Me, 10; Et, 12) with H_2O

The reactions were monitored by ^1H and $^{13}C\{^1H\}$ NMR spectroscopies. Addition of 1 equiv of H_2O in THF to **12** in benzene–d_6 was found to give soluble products $HNEt_2$ and the dimer $\{(\mu\text{-}O)Zr[MeC(N^iPr)_2]_2\}_2$ (**14**, Scheme 3.7). The reaction was much faster than that of **10** or **12** with O_2, and was completed in a few minutes. The product mixture turned cloudy, presumably as the result of the precipitation of the polymer $\{(\mu\text{-}O)Zr[MeC(N^iPr)_2]_2\}_n$ (**17**). The NMR chemical shifts of **14** (Figures 3.5 and 3.6, only the chemical shifts of **14** are labeled) are identical to those from the reactions of O_2 with $Zr[MeC(N^iPr)_2]_2(NR_2)_2$ (R = Me, **10**; Et, **12**) (Figures 3.1-3.4). The amount of the solid was too small to be isolated. These observations point to the reaction in Scheme 3.7. Since the reactions here with H_2O unlikely give peroxo products, the observations of **14** and **17** in the reactions in Scheme 3.7 support the assignments of **14** and **17** as the dimeric and polymeric oxo products, ruling out that they are peroxo species.

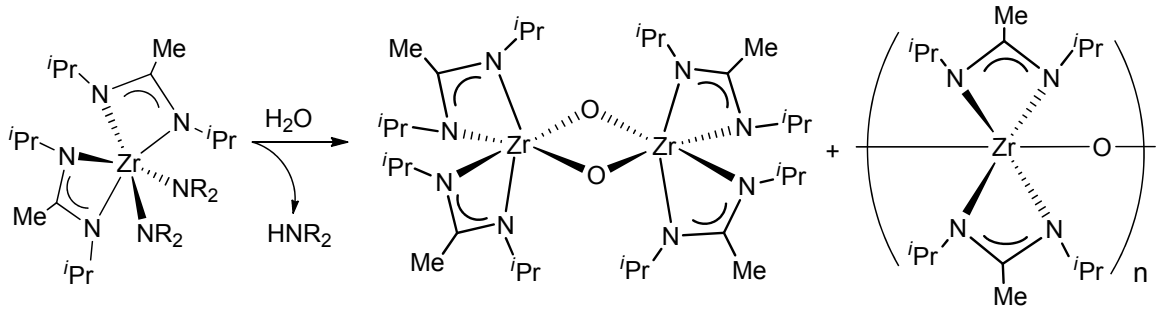

R = Me, **10**; Et, **12** **14** **17**

Scheme 3.7. Reaction of $Zr[MeC(N^iPr)_2]_2(NR_2)_2$ (R = Me, **10**; Et, **12**) with H_2O.

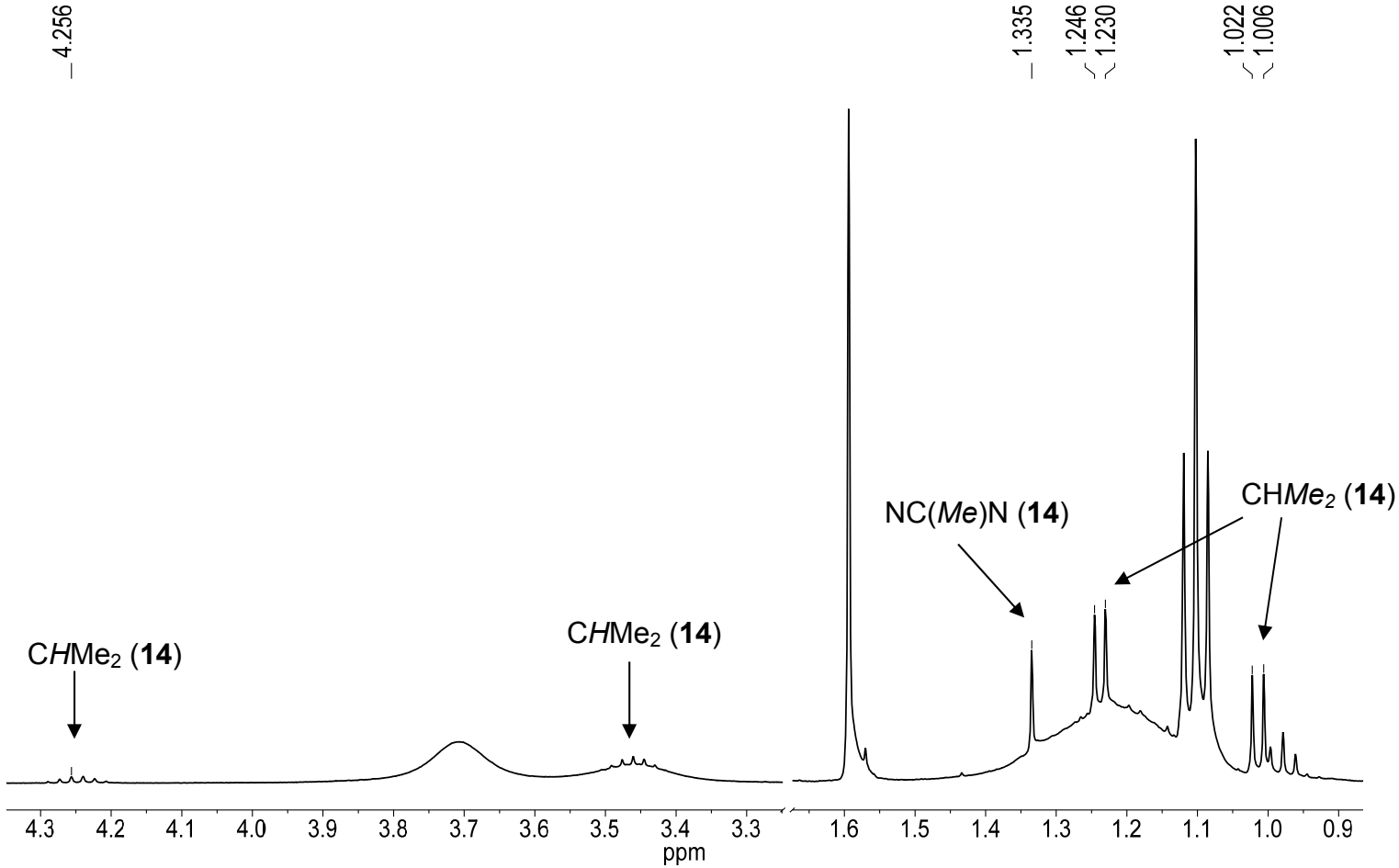

Figure 3.5. ^{1}H NMR spectrum of the product mixture from the reaction of **12** with H_2O in benzene-d_6. Unlabeled peaks are those of **12**.

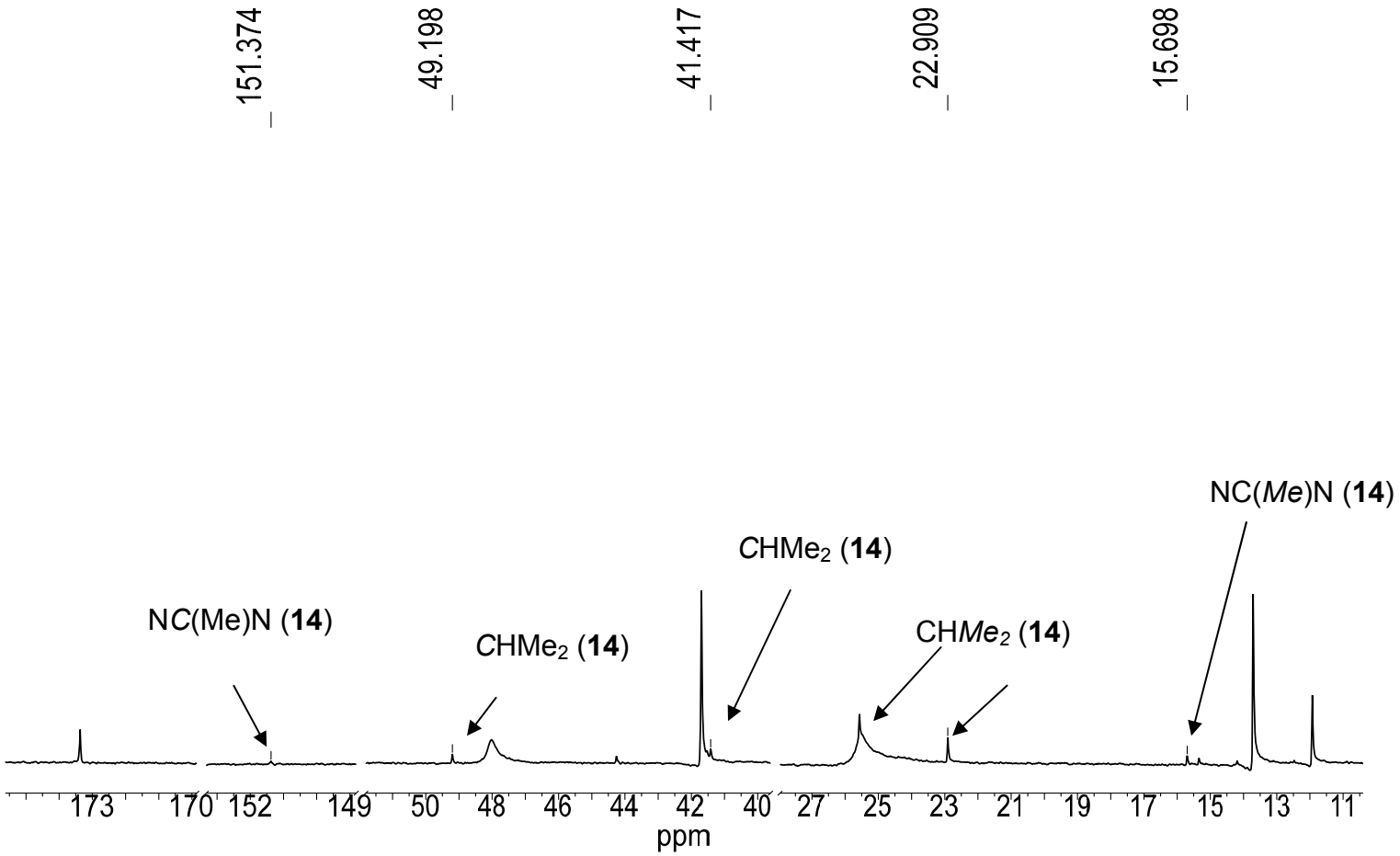

Figure 3.6. $^{13}C\{^1H\}$ NMR spectrum of the product mixture from the reaction of **12** with H_2O in benzene-d_6. Unlabeled peaks are those of **12**.

Bernasek and Schwartz reported earlier that the reactions of $Zr(O^tBu)_4$ with surface OH groups are faster than those of its alkyl analog $Zr(CH_2{}^tBu)_4$.[14] Lone pair electrons on the O^tBu ligands assist the H^+ migration from the OH groups to the alkoxide ligand, removing the latter as the alcohol HO^tBu. The amide ligands NMe_2 in $Zr[MeC(N^iPr)_2]_2(NR_2)_2$ (R = Me, **10**; Et, **12**) contain lone pair electrons as well and they may assist the H^+ migration and removal of the amide ligands (Scheme 3.8).

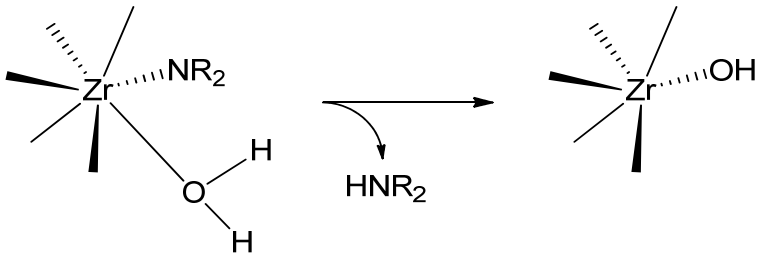

Scheme 3.8. H^+ transfer assisted by lone pair electrons on amide ligands.

3.2.4. Formation and X-ray Crystal Structure of $\{(\mu\text{-}\eta^2\text{:}\eta^2\text{-}O_2)Zr[MeC(N^iPr)_2]_2\}_3$ (20)

Crystals of $\{(\mu\text{-}\eta^2\text{:}\eta^2\text{-}O_2)Zr[MeC(N^iPr)_2]_2\}_3$ (**20**) were obtained as a solid mixture with $Zr[MeC(N^iPr)_2]_2(NMe_2)_2$ (**10**), $\{(\mu\text{-}O)Zr[MeC(N^iPr)_2]_2\}_2$ (**14**) and $\{(\mu\text{-}O)Zr[MeC(N^iPr)_2]_2\}_n$ (**17**), after a solution of **10** in pentane at -30 °C was exposed to air over a period of weeks. Given that air contains 21% O_2, peroxo **20** is likely the product of the reaction between **10** and O_2 at -30 °C (Scheme 3.3). The low

temperature of -30 °C may have helped the isolation of the crystals of **20**, as we have found that **20** reacts with **10** in solution at room temperature. The reaction between **20** and **10** is discussed below.

$\{(\mu\text{-}\eta^2\text{:}\eta^2\text{-}O_2)Zr[MeC(N^iPr)_2]_2\}_3$ (**20**) is significant as, to our knowledge, such a Zr peroxo complex, yielded from molecular oxygen and not supported by a redox-active ligand, has not been reported. In addition, characterization of **20** helps understand the pathways in CVD/ALD of metal oxide materials. Peroxo Zr complexes are rare.[2,15,16] Abu-Omar and coworkers recently reported the preparation and structure of the bisperoxo complex **22** (Scheme 3.9) containing two redox-active diimine ligands.[2] The redox-active diimine ligands each donate 2e to O_2 to give the peroxo ligands. In the peroxo complex **20**, there is no redox-active ligand to support the complex (Scheme 3.3). In the formation of **20**, the anionic amide ligands NMe_2 in **10** are apparently oxidized to radicals $\bullet NMe_2$. Several studies have demonstrated that, once $\bullet NMe_2$ radicals are formed, their reactions lead to the formation of $HNMe_2$ and $CH_2(NMe_2)_2$ (**19**) involving

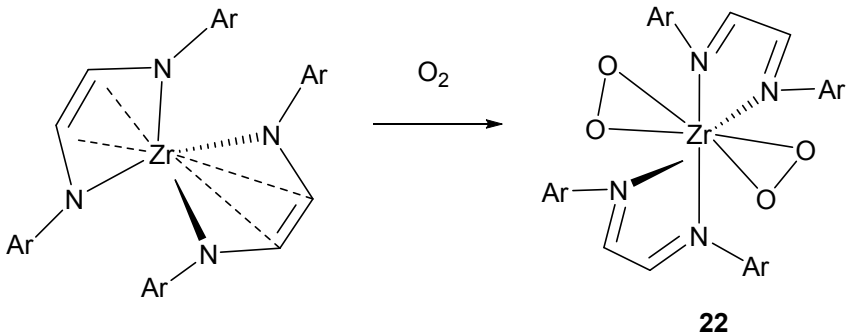

22

Scheme 3.9. Synthesis of a Zr peroxo complex **22** with two redox-active ligands.[2]

intermediates such as CH_3•, CH_2=NH, H•, CH_3N=CH_2, and $(CH_3)_2N$-CH_2•.[13a,b] Such a pathway may operate in the current reaction of **10** with O_2, giving $CH_2(NMe_2)_2$ (**19**) and $HNMe_2$.

Kortz and coworkers have reported a family of dimeric, peroxo-containing heteropolytungstates $[M_2(O_2)_2(XW_{11}O_{39})_2]^{12-}$ (M = Zr, X = Si, **23**; Ge, **24**; M = Hf, X = Si) through the reactions reacting $ZrCl_4$/$HfCl_4$ with $[XW_{11}O_{39}]^{8-}$, followed by treatment with H_2O_2.[15] The exchanges of the oxo O^{2-} ligands with peroxide (O_2^{2-}) lead to the peroxo ligands in the products. Leung and coworkers found that the reaction of $Zr(O^tBu)_4$ with phosphinic amine $^iPr_2P(=O)$-NH-$P(=O)^iPr_2$ in THF yielded the di-μ-peroxo complex $\{Zr[N(^iPr_2PO)_2]_2\}_2(\mu\text{-}\eta^2\text{:}\eta^2\text{-}O_2)_2$ (**25**, Chart 3.1), although the authors do not know how the complex is formed and what led to the peroxo ligands.[16]

The crystal structure of $\{(\mu\text{-}\eta^2\text{:}\eta^2\text{-}O_2)Zr[MeC(N^iPr)_2]_2\}_3$ (**20**) is given in Figure 3.7 and its crystal data are given in Tables 3.1-3.5. The Zr atoms are linked by the peroxo ligands that bind to the metals in the η^2:η^2 mode. The three

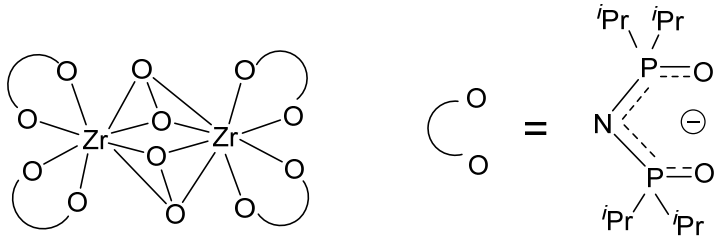

25

Chart 3.1. Structure of $\{Zr[N(^iPr_2PO)_2]_2\}_2(\mu\text{-}\eta^2\text{:}\eta^2\text{-}O_2)_2$ (**25**).[16]

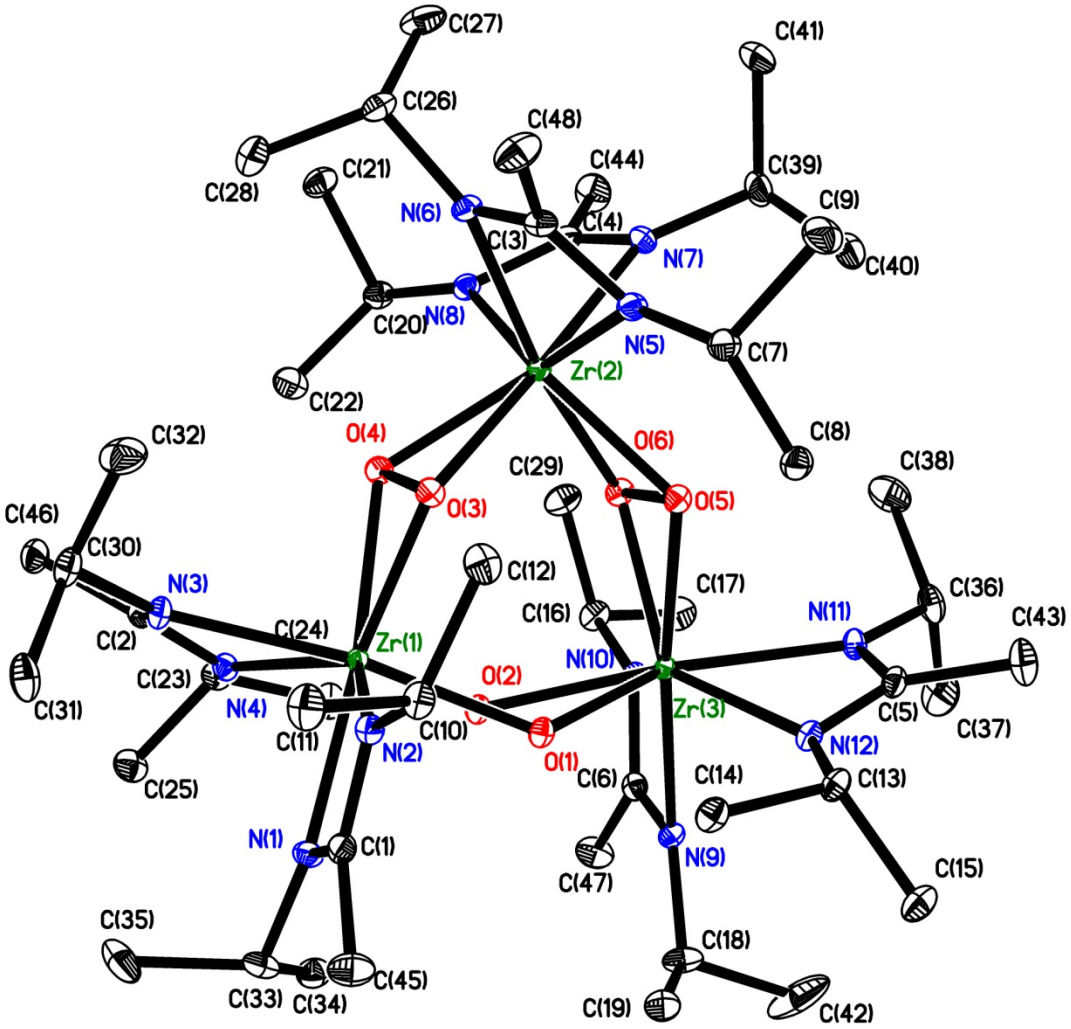

Figure 3.7. ORTEP view of **20**.

Table 3.1. Crystal data and structure refinement for **20**

Empirical formula	C48 H102 N12 O6 Zr3	
Formula weight	1217.08	
Temperature	100(2) K	
Wavelength	0.71073 Å	
Crystal system	Monoclinic	
Space group	*P* 21/c	
Unit cell dimensions	*a* = 23.4504(4) Å	α = 90°
	b = 13.3481(2) Å	β = 103.2850(10)°
	c = 20.7646(3) Å	γ = 90°
Volume	6325.76(17) Å^3	
Z	4	
Density (calculated)	1.278 Mg/m^3	
Absorption coefficient	0.535 mm^{-1}	
F(000)	2568	
Crystal size	0.10 x 0.05 x 0.02 mm^3	
θ range for data collection	0.89 to 29.59°	
Index ranges	$-32 \leq h \leq 32$, $-18 \leq k \leq 18$, $-28 \leq l \leq 28$	
Reflections collected	87696	
Independent reflections	17768 [*R*(int) = 0.0304]	
Completeness to θ = 29.59°	99.8%	
Absorption correction	Semi-empirical from equivalents	

Table 3.1. Continued

Max. and min. transmission	0.9894 and 0.9485
Refinement method	Full-matrix least-squares on F^2
Data / restraints / parameters	17768 / 0 / 652
Goodness-of-fit on F^2	1.054
Final R indices [$I > 2\,\sigma(I)$]	$R1$ = 0.0259, w$R2$ = 0.0628
R indices (all data)	$R1$ = 0.0355, w$R2$ = 0.0660
Largest diff. peak and hole	0.485 and -0.355 e.Å^{-3}

Table 3.2. Atomic coordinates (x 10^4) and equivalent isotropic displacement parameters (Å^2 x 10^3) for **20**. *U*(eq) is defined as one third of the trace of the orthogonalized U^{ij} tensor.

	x	*y*	*z*	*U*(eq)
O(1)	1729(1)	-577(1)	2239(1)	15(1)
O(2)	1671(1)	44(1)	1615(1)	14(1)
O(3)	2442(1)	1137(1)	3008(1)	15(1)
O(4)	2438(1)	1713(1)	2378(1)	16(1)
O(6)	2983(1)	-57(1)	1811(1)	16(1)
O(5)	3051(1)	-573(1)	2474(1)	16(1)
Zr(1)	1583(1)	1025(1)	2387(1)	11(1)
Zr(3)	2323(1)	-1165(1)	1703(1)	11(1)
Zr(2)	3255(1)	967(1)	2657(1)	12(1)
N(4)	1216(1)	2105(1)	1528(1)	15(1)
N(6)	3693(1)	2029(1)	3461(1)	17(1)
N(9)	1618(1)	-1920(1)	932(1)	15(1)
N(7)	4126(1)	839(1)	2379(1)	18(1)
N(2)	1337(1)	500(1)	3344(1)	16(1)
N(1)	668(1)	534(1)	2393(1)	17(1)
N(11)	2919(1)	-2469(1)	1660(1)	17(1)
N(10)	2244(1)	-900(1)	598(1)	16(1)

Table 3.2. Continued

	x	*y*	*z*	*U*(eq)
N(8)	3507(1)	2016(1)	1889(1)	16(1)
N(3)	1300(1)	2587(1)	2568(1)	17(1)
N(5)	3645(1)	422(1)	3725(1)	17(1)
N(12)	2368(1)	-2511(1)	2397(1)	16(1)
C(4)	3993(1)	1497(1)	1889(1)	19(1)
C(6)	1742(1)	-1406(1)	435(1)	17(1)
C(2)	1231(1)	2873(1)	1942(1)	16(1)
C(3)	3751(1)	1357(1)	3944(1)	18(1)
C(1)	798(1)	243(1)	3021(1)	17(1)
C(5)	2819(1)	-2908(1)	2198(1)	18(1)
C(8)	3377(1)	-1342(1)	3823(1)	22(1)
C(9)	4272(1)	-662(1)	4590(1)	29(1)
C(7)	3652(1)	-411(1)	4191(1)	20(1)
C(11)	1299(1)	813(1)	4519(1)	26(1)
C(10)	1566(1)	199(1)	4036(1)	19(1)
C(12)	2228(1)	299(1)	4227(1)	24(1)
C(13)	2206(1)	-2877(1)	3001(1)	18(1)
C(15)	1922(1)	-3922(1)	2899(1)	25(1)
C(14)	1791(1)	-2145(1)	3222(1)	20(1)

Table 3.2. Continued

	x	*y*	*z*	*U*(eq)
C(17)	2699(1)	-902(1)	-370(1)	28(1)
C(16)	2437(1)	-273(1)	107(1)	20(1)
C(19)	866(1)	-2582(1)	1462(1)	27(1)
C(18)	1095(1)	-2551(1)	839(1)	25(1)
C(20)	3283(1)	2757(1)	1368(1)	19(1)
C(21)	3645(1)	3729(1)	1465(1)	25(1)
C(22)	2645(1)	3005(1)	1341(1)	26(1)
C(25)	505(1)	2573(1)	483(1)	26(1)
C(24)	1318(1)	1360(1)	476(1)	24(1)
C(23)	1140(1)	2282(1)	812(1)	18(1)
C(26)	3897(1)	3056(1)	3580(1)	21(1)
C(28)	3409(1)	3788(1)	3310(1)	35(1)
C(27)	4425(1)	3225(2)	3280(1)	33(1)
C(29)	2883(1)	502(1)	442(1)	26(1)
C(31)	753(1)	3002(1)	3394(1)	28(1)
C(30)	1275(1)	3276(1)	3108(1)	24(1)
C(32)	1848(1)	3235(2)	3634(1)	36(1)
C(34)	127(1)	117(1)	1276(1)	23(1)
C(33)	83(1)	446(1)	1965(1)	22(1)

Table 3.2. Continued

	x	*y*	*z*	*U*(eq)
C(35)	-237(1)	1452(2)	1939(1)	36(1)
C(36)	3328(1)	-2886(1)	1293(1)	25(1)
C(38)	3740(1)	-2081(2)	1152(1)	36(1)
C(37)	2981(1)	-3379(2)	661(1)	37(1)
C(41)	5176(1)	742(2)	2873(2)	71(1)
C(40)	4545(1)	-774(1)	2808(1)	28(1)
C(39)	4645(1)	200(1)	2472(1)	28(1)
C(42)	1228(1)	-3600(2)	642(1)	67(1)
C(43)	3200(1)	-3741(1)	2555(1)	30(1)
C(44)	4345(1)	1604(2)	1367(1)	31(1)
C(46)	1217(1)	3963(1)	1738(1)	24(1)
C(45)	370(1)	-343(1)	3322(1)	29(1)
C(47)	1327(1)	-1372(1)	-244(1)	27(1)
C(48)	3895(1)	1654(1)	4670(1)	30(1)

Table 3.3. Bond lengths (Å) in **20**

O(1)-O(2)	1.5172(13)	O(1)-Zr(3)	2.1239(10)
O(1)-Zr(1)	2.1992(10)	O(2)-Zr(1)	2.1162(10)
O(2)-Zr(3)	2.2014(10)	O(3)-O(4)	1.5147(13)
O(3)-Zr(1)	2.1320(10)	O(3)-Zr(2)	2.2038(10)
O(4)-Zr(2)	2.1179(10)	O(4)-Zr(1)	2.2082(10)
O(6)-O(5)	1.5150(13)	O(6)-Zr(3)	2.1148(10)
O(6)-Zr(2)	2.2007(10)	O(5)-Zr(2)	2.1242(10)
O(5)-Zr(3)	2.2026(10)	Zr(1)-N(3)	2.2450(12)
Zr(1)-N(1)	2.2462(12)	Zr(1)-N(4)	2.3003(12)
Zr(1)-N(2)	2.3021(11)	Zr(3)-N(11)	2.2468(12)
Zr(3)-N(9)	2.2574(12)	Zr(3)-N(10)	2.2860(11)
Zr(3)-N(12)	2.2910(12)	Zr(2)-N(6)	2.2508(12)
Zr(2)-N(7)	2.2536(12)	Zr(2)-N(8)	2.2986(12)
Zr(2)-N(5)	2.3141(12)	N(4)-C(2)	1.3341(19)
N(4)-C(23)	1.4748(17)	N(6)-C(3)	1.3291(19)
N(6)-C(26)	1.4551(19)	N(9)-C(6)	1.3278(18)
N(9)-C(18)	1.4630(19)	N(7)-C(4)	1.325(2)
N(7)-C(39)	1.4622(19)	N(2)-C(1)	1.3331(18)
N(2)-C(10)	1.4700(18)	N(1)-C(1)	1.3272(18)
N(1)-C(33)	1.4591(18)	N(11)-C(5)	1.3288(19)
N(11)-C(36)	1.4657(18)	N(10)-C(6)	1.3327(19)

Table 3.3. Continued

N(10)-C(16)	1.4681(18)	N(8)-C(4)	1.3348(19)
N(8)-C(20)	1.4710(19)	N(3)-C(2)	1.3294(18)
N(3)-C(30)	1.4612(19)	N(5)-C(3)	1.332(2)
N(5)-C(7)	1.4714(19)	N(12)-C(5)	1.3317(19)
N(12)-C(13)	1.4736(18)	C(4)-C(44)	1.514(2)
C(6)-C(47)	1.517(2)	C(2)-C(46)	1.512(2)
C(3)-C(48)	1.520(2)	C(1)-C(45)	1.515(2)
C(5)-C(43)	1.511(2)	C(8)-C(7)	1.523(2)
C(9)-C(7)	1.537(2)	C(11)-C(10)	1.535(2)
C(10)-C(12)	1.518(2)	C(13)-C(14)	1.522(2)
C(13)-C(15)	1.539(2)	C(17)-C(16)	1.531(2)
C(16)-C(29)	1.521(2)	C(19)-C(18)	1.511(2)
C(18)-C(42)	1.510(3)	C(20)-C(22)	1.521(2)
C(20)-C(21)	1.538(2)	C(25)-C(23)	1.538(2)
C(24)-C(23)	1.521(2)	C(26)-C(28)	1.512(2)
C(26)-C(27)	1.525(2)	C(31)-C(30)	1.522(2)
C(30)-C(32)	1.524(2)	C(34)-C(33)	1.523(2)
C(33)-C(35)	1.533(3)	C(36)-C(38)	1.518(3)
C(36)-C(37)	1.525(2)	C(41)-C(39)	1.513(3)
C(40)-C(39)	1.518(2)		

Symmetry transformations used to generate equivalent atoms:

Table 3.4. Bond angles (°) in **20**

O(2)-O(1)-Zr(3)	72.23(5)	O(2)-O(1)-Zr(1)	66.51(5)
Zr(3)-O(1)-Zr(1)	125.06(5)	O(1)-O(2)-Zr(1)	72.38(5)
O(1)-O(2)-Zr(3)	66.75(5)	Zr(1)-O(2)-Zr(3)	125.34(4)
O(4)-O(3)-Zr(1)	72.30(5)	O(4)-O(3)-Zr(2)	66.47(5)
Zr(1)-O(3)-Zr(2)	124.13(4)	O(3)-O(4)-Zr(2)	72.56(5)
O(3)-O(4)-Zr(1)	66.90(5)	Zr(2)-O(4)-Zr(1)	124.61(5)
O(5)-O(6)-Zr(3)	72.60(5)	O(5)-O(6)-Zr(2)	66.80(5)
Zr(3)-O(6)-Zr(2)	126.15(4)	O(6)-O(5)-Zr(2)	72.23(6)
O(6)-O(5)-Zr(3)	66.38(5)	Zr(2)-O(5)-Zr(3)	125.57(5)
O(2)-Zr(1)-O(3)	104.96(4)	O(2)-Zr(1)-O(1)	41.11(3)
O(3)-Zr(1)-O(1)	89.84(4)	O(2)-Zr(1)-O(4)	90.24(4)
O(3)-Zr(1)-O(4)	40.80(4)	O(1)-Zr(1)-O(4)	103.45(4)
O(2)-Zr(1)-N(3)	141.79(4)	O(3)-Zr(1)-N(3)	96.20(4)
O(1)-Zr(1)-N(3)	171.08(4)	O(4)-Zr(1)-N(3)	85.38(4)
O(2)-Zr(1)-N(1)	94.76(4)	O(3)-Zr(1)-N(1)	141.96(4)
O(1)-Zr(1)-N(1)	84.02(4)	O(4)-Zr(1)-N(1)	172.43(4)
N(3)-Zr(1)-N(1)	87.19(5)	O(2)-Zr(1)-N(4)	83.39(4)
O(3)-Zr(1)-N(4)	123.91(4)	O(1)-Zr(1)-N(4)	122.90(4)
O(4)-Zr(1)-N(4)	84.94(4)	N(3)-Zr(1)-N(4)	58.43(4)
N(1)-Zr(1)-N(4)	89.99(4)	O(2)-Zr(1)-N(2)	123.54(4)
O(3)-Zr(1)-N(2)	83.59(4)	O(1)-Zr(1)-N(2)	84.39(4)

Table 3.4. Continued

O(4)-Zr(1)-N(2)	122.78(4)	N(3)-Zr(1)-N(2)	89.74(4)
N(1)-Zr(1)-N(2)	58.48(4)	N(4)-Zr(1)-N(2)	137.46(4)
O(6)-Zr(3)-O(1)	103.76(4)	O(6)-Zr(3)-O(2)	88.45(4)
O(1)-Zr(3)-O(2)	41.02(3)	O(6)-Zr(3)-O(5)	41.02(4)
O(1)-Zr(3)-O(5)	88.77(4)	O(2)-Zr(3)-O(5)	101.78(4)
O(6)-Zr(3)-N(11)	95.72(4)	O(1)-Zr(3)-N(11)	142.74(4)
O(2)-Zr(3)-N(11)	172.37(4)	O(5)-Zr(3)-N(11)	85.50(4)
O(6)-Zr(3)-N(9)	141.90(4)	O(1)-Zr(3)-N(9)	94.25(4)
O(2)-Zr(3)-N(9)	83.53(4)	O(5)-Zr(3)-N(9)	174.42(4)
N(11)-Zr(3)-N(9)	89.27(4)	O(6)-Zr(3)-N(10)	83.51(4)
O(1)-Zr(3)-N(10)	123.85(4)	O(2)-Zr(3)-N(10)	84.79(4)
O(5)-Zr(3)-N(10)	123.01(4)	N(11)-Zr(3)-N(10)	89.33(4)
N(9)-Zr(3)-N(10)	58.74(4)	O(6)-Zr(3)-N(12)	123.71(4)
O(1)-Zr(3)-N(12)	84.25(4)	O(2)-Zr(3)-N(12)	123.83(4)
O(5)-Zr(3)-N(12)	84.70(4)	N(11)-Zr(3)-N(12)	58.58(4)
N(9)-Zr(3)-N(12)	90.92(4)	N(10)-Zr(3)-N(12)	137.31(4)
O(4)-Zr(2)-O(5)	104.74(4)	O(4)-Zr(2)-O(6)	89.79(4)
O(5)-Zr(2)-O(6)	40.96(4)	O(4)-Zr(2)-O(3)	40.97(3)
O(5)-Zr(2)-O(3)	89.03(4)	O(6)-Zr(2)-O(3)	102.37(4)
O(4)-Zr(2)-N(6)	97.83(4)	O(5)-Zr(2)-N(6)	141.93(4)

Table 3.4. Continued

O(6)-Zr(2)-N(6)	169.21(4)	O(3)-Zr(2)-N(6)	88.36(4)
O(4)-Zr(2)-N(7)	141.47(4)	O(5)-Zr(2)-N(7)	93.46(4)
O(6)-Zr(2)-N(7)	82.07(4)	O(3)-Zr(2)-N(7)	175.31(4)
N(6)-Zr(2)-N(7)	87.22(4)	O(4)-Zr(2)-N(8)	83.40(4)
O(5)-Zr(2)-N(8)	123.29(4)	O(6)-Zr(2)-N(8)	84.18(4)
O(3)-Zr(2)-N(8)	123.13(4)	N(6)-Zr(2)-N(8)	89.10(4)
N(7)-Zr(2)-N(8)	58.40(4)	O(4)-Zr(2)-N(5)	122.92(4)
O(5)-Zr(2)-N(5)	83.69(4)	O(6)-Zr(2)-N(5)	123.23(4)
O(3)-Zr(2)-N(5)	84.10(4)	N(6)-Zr(2)-N(5)	58.27(4)
N(7)-Zr(2)-N(5)	92.22(4)	N(8)-Zr(2)-N(5)	138.40(4)
C(2)-N(4)-C(23)	120.35(12)	C(2)-N(4)-Zr(1)	91.86(8)
C(23)-N(4)-Zr(1)	144.99(10)	C(3)-N(6)-C(26)	122.30(12)
C(3)-N(6)-Zr(2)	94.91(9)	C(26)-N(6)-Zr(2)	142.78(10)
C(6)-N(9)-C(18)	121.47(12)	C(6)-N(9)-Zr(3)	93.69(9)
C(18)-N(9)-Zr(3)	143.71(9)	C(4)-N(7)-C(39)	121.99(13)
C(4)-N(7)-Zr(2)	94.53(9)	C(39)-N(7)-Zr(2)	141.87(10)
C(1)-N(2)-C(10)	120.80(12)	C(1)-N(2)-Zr(1)	92.35(8)
C(10)-N(2)-Zr(1)	145.09(9)	C(1)-N(1)-C(33)	123.09(12)
C(1)-N(1)-Zr(1)	95.02(9)	C(33)-N(1)-Zr(1)	141.87(10)
C(5)-N(11)-C(36)	122.22(13)	C(5)-N(11)-Zr(3)	94.38(9)
C(36)-N(11)-Zr(3)	143.36(10)	C(6)-N(10)-C(16)	120.52(12)

Table 3.4. Continued

C(6)-N(10)-Zr(3)	92.28(8)	C(16)-N(10)-Zr(3)	144.90(10)
C(4)-N(8)-C(20)	120.62(12)	C(4)-N(8)-Zr(2)	92.25(9)
C(20)-N(8)-Zr(2)	144.58(9)	C(2)-N(3)-C(30)	123.49(13)
C(2)-N(3)-Zr(1)	94.44(9)	C(30)-N(3)-Zr(1)	141.11(10)
C(3)-N(5)-C(7)	120.66(12)	C(3)-N(5)-Zr(2)	91.99(9)
C(7)-N(5)-Zr(2)	144.07(9)	C(5)-N(12)-C(13)	120.73(12)
C(5)-N(12)-Zr(3)	92.33(9)	C(13)-N(12)-Zr(3)	144.32(10)
N(7)-C(4)-N(8)	113.24(13)	N(7)-C(4)-C(44)	122.81(14)
N(8)-C(4)-C(44)	123.88(14)	N(9)-C(6)-N(10)	113.78(12)
N(9)-C(6)-C(47)	122.00(13)	N(10)-C(6)-C(47)	124.15(13)
N(3)-C(2)-N(4)	112.84(13)	N(3)-C(2)-C(46)	122.71(14)
N(4)-C(2)-C(46)	124.30(13)	N(6)-C(3)-N(5)	113.29(13)
N(6)-C(3)-C(48)	122.25(14)	N(5)-C(3)-C(48)	124.39(14)
N(1)-C(1)-N(2)	113.30(12)	N(1)-C(1)-C(45)	122.16(13)
N(2)-C(1)-C(45)	124.52(13)	N(11)-C(5)-N(12)	113.14(13)
N(11)-C(5)-C(43)	122.53(13)	N(12)-C(5)-C(43)	124.27(14)
N(5)-C(7)-C(8)	110.32(12)	N(5)-C(7)-C(9)	112.61(12)
C(8)-C(7)-C(9)	109.35(14)	N(2)-C(10)-C(12)	110.61(12)
N(2)-C(10)-C(11)	112.43(12)	C(12)-C(10)-C(11)	109.18(13)
N(12)-C(13)-C(14)	110.50(12)	N(12)-C(13)-C(15)	111.83(12)
C(14)-C(13)-C(15)	109.78(13)	N(10)-C(16)-C(29)	111.04(12)

Table 3.4. Continued

N(10)-C(16)-C(17)	111.79(13)	C(29)-C(16)-C(17)	109.48(13)
N(9)-C(18)-C(42)	110.48(15)	N(9)-C(18)-C(19)	110.76(13)
C(42)-C(18)-C(19)	110.07(16)	N(8)-C(20)-C(22)	110.73(12)
N(8)-C(20)-C(21)	112.27(12)	C(22)-C(20)-C(21)	109.21(14)
N(4)-C(23)-C(24)	110.54(12)	N(4)-C(23)-C(25)	111.71(12)
C(24)-C(23)-C(25)	109.94(13)	N(6)-C(26)-C(28)	110.73(13)
N(6)-C(26)-C(27)	109.61(13)	C(28)-C(26)-C(27)	111.70(15)
N(3)-C(30)-C(31)	109.02(13)	N(3)-C(30)-C(32)	110.05(13)
C(31)-C(30)-C(32)	111.58(14)	N(1)-C(33)-C(34)	109.70(12)
N(1)-C(33)-C(35)	109.60(14)	C(34)-C(33)-C(35)	110.95(14)
N(11)-C(36)-C(38)	110.70(14)	N(11)-C(36)-C(37)	109.07(13)
C(38)-C(36)-C(37)	112.16(14)	N(7)-C(39)-C(41)	110.42(16)
N(7)-C(39)-C(40)	110.35(13)	C(41)-C(39)-C(40)	110.56(17)

Symmetry transformations used to generate equivalent atoms:

Table 3.5. Anisotropic displacement parameters ($Å^2$ x 10^3) for **20**. The anisotropic displacement factor exponent takes the form: $-2\pi[h^2a^{*2}U^{11} + \ldots + 2ha^*b^*U^{12}]$

	U^{11}	U^{22}	U^{33}	U^{23}	U^{13}	U^{12}
O(1)	19(1)	13(1)	13(1)	4(1)	5(1)	1(1)
O(2)	19(1)	14(1)	12(1)	3(1)	4(1)	2(1)
O(3)	16(1)	17(1)	13(1)	3(1)	5(1)	0(1)
O(4)	16(1)	16(1)	16(1)	4(1)	6(1)	0(1)
O(6)	19(1)	16(1)	12(1)	2(1)	4(1)	-1(1)
O(5)	18(1)	16(1)	13(1)	2(1)	3(1)	0(1)
Zr(1)	11(1)	10(1)	12(1)	0(1)	3(1)	1(1)
Zr(3)	13(1)	10(1)	11(1)	-1(1)	3(1)	0(1)
Zr(2)	10(1)	12(1)	12(1)	-1(1)	2(1)	-1(1)
N(4)	15(1)	15(1)	15(1)	3(1)	3(1)	2(1)
N(6)	18(1)	15(1)	17(1)	-2(1)	2(1)	-3(1)
N(9)	17(1)	14(1)	15(1)	-3(1)	3(1)	-2(1)
N(7)	13(1)	19(1)	24(1)	-1(1)	6(1)	1(1)
N(2)	17(1)	16(1)	15(1)	0(1)	5(1)	1(1)
N(1)	13(1)	19(1)	19(1)	1(1)	4(1)	-1(1)
N(11)	19(1)	15(1)	18(1)	-2(1)	6(1)	4(1)
N(10)	20(1)	16(1)	12(1)	0(1)	5(1)	-1(1)

Table 3.5. Continued

	U^{11}	U^{22}	U^{33}	U^{23}	U^{13}	U^{12}
N(8)	17(1)	15(1)	18(1)	1(1)	6(1)	-2(1)
N(3)	21(1)	13(1)	19(1)	-1(1)	7(1)	3(1)
N(5)	16(1)	16(1)	16(1)	2(1)	1(1)	-2(1)
N(12)	21(1)	13(1)	15(1)	0(1)	5(1)	0(1)
C(4)	18(1)	19(1)	22(1)	-4(1)	8(1)	-5(1)
C(6)	19(1)	17(1)	14(1)	-3(1)	3(1)	2(1)
C(2)	11(1)	15(1)	24(1)	2(1)	5(1)	2(1)
C(3)	16(1)	20(1)	17(1)	-2(1)	2(1)	-3(1)
C(1)	18(1)	15(1)	21(1)	0(1)	10(1)	0(1)
C(5)	22(1)	13(1)	18(1)	-2(1)	2(1)	2(1)
C(8)	23(1)	18(1)	23(1)	4(1)	2(1)	-1(1)
C(9)	24(1)	31(1)	26(1)	9(1)	-4(1)	-1(1)
C(7)	20(1)	19(1)	19(1)	4(1)	2(1)	-1(1)
C(11)	34(1)	27(1)	19(1)	-1(1)	11(1)	5(1)
C(10)	24(1)	18(1)	16(1)	1(1)	7(1)	2(1)
C(12)	26(1)	28(1)	17(1)	2(1)	3(1)	4(1)
C(13)	25(1)	13(1)	16(1)	2(1)	5(1)	-1(1)
C(15)	34(1)	17(1)	25(1)	3(1)	6(1)	-5(1)
C(14)	26(1)	18(1)	19(1)	1(1)	9(1)	-1(1)

Table 3.5. Continued

	U^{11}	U^{22}	U^{33}	U^{23}	U^{13}	U^{12}
C(17)	34(1)	32(1)	19(1)	-4(1)	12(1)	-3(1)
C(16)	26(1)	21(1)	14(1)	0(1)	7(1)	-2(1)
C(19)	24(1)	26(1)	32(1)	2(1)	10(1)	-3(1)
C(18)	24(1)	31(1)	20(1)	-2(1)	2(1)	-12(1)
C(20)	21(1)	19(1)	18(1)	3(1)	5(1)	-3(1)
C(21)	29(1)	20(1)	29(1)	3(1)	8(1)	-7(1)
C(22)	22(1)	27(1)	29(1)	13(1)	3(1)	-1(1)
C(25)	22(1)	29(1)	23(1)	9(1)	0(1)	2(1)
C(24)	31(1)	26(1)	14(1)	2(1)	5(1)	3(1)
C(23)	18(1)	20(1)	16(1)	6(1)	2(1)	0(1)
C(26)	25(1)	16(1)	20(1)	-2(1)	3(1)	-6(1)
C(28)	37(1)	18(1)	48(1)	0(1)	5(1)	2(1)
C(27)	31(1)	31(1)	40(1)	-7(1)	11(1)	-17(1)
C(29)	34(1)	25(1)	21(1)	2(1)	11(1)	-8(1)
C(31)	34(1)	28(1)	27(1)	-1(1)	14(1)	13(1)
C(30)	31(1)	15(1)	26(1)	-3(1)	10(1)	4(1)
C(32)	34(1)	41(1)	34(1)	-18(1)	8(1)	-10(1)
C(34)	22(1)	23(1)	23(1)	1(1)	1(1)	-3(1)
C(33)	13(1)	29(1)	23(1)	3(1)	2(1)	-4(1)

Table 3.5. Continued

	U^{11}	U^{22}	U^{33}	U^{23}	U^{13}	U^{12}
C(35)	20(1)	51(1)	33(1)	-9(1)	0(1)	12(1)
C(36)	26(1)	28(1)	24(1)	0(1)	10(1)	12(1)
C(38)	25(1)	50(1)	36(1)	-2(1)	14(1)	1(1)
C(37)	49(1)	33(1)	33(1)	-12(1)	19(1)	4(1)
C(41)	17(1)	31(1)	151(3)	8(2)	-13(1)	-1(1)
C(40)	21(1)	26(1)	37(1)	3(1)	7(1)	5(1)
C(39)	18(1)	24(1)	45(1)	5(1)	13(1)	6(1)
C(42)	98(2)	39(1)	86(2)	-40(1)	66(2)	-41(1)
C(43)	36(1)	28(1)	28(1)	9(1)	10(1)	15(1)
C(44)	30(1)	33(1)	37(1)	2(1)	22(1)	1(1)
C(46)	25(1)	16(1)	31(1)	5(1)	7(1)	3(1)
C(45)	26(1)	35(1)	27(1)	3(1)	10(1)	-9(1)
C(47)	24(1)	38(1)	15(1)	1(1)	0(1)	-2(1)
C(48)	44(1)	26(1)	18(1)	-3(1)	4(1)	-10(1)

O-O bond lengths of 1.5147(13)-1.5172(13) Å in **20** are similar to 1.504(4)-1.512(4) Å in **22** stabilized by redox-active ligands,[2] and those in $[M_2(O_2)_2(XW_{11}O_{39})_2]^{12-}$ [X = Si, **23**, 1.491(11) Å; Ge, **24**, 1.529(13) Å],[15] but are longer than 1.394(4) and 1.401(4) Å in **25**.[16] The Zr-O bond lengths of 2.1148(10)-2.2038(10) Å in **20** are longer than 2.027(3)-2.038(3) Å in **22**,[2] but are similar to 2.145(3)−2.177(3) Å in **25**.[16]

MS characterization of $\{(\mu\text{-}\eta^2\text{:}\eta^2\text{-}O_2)Zr[MeC(N^iPr)_2]_2\}_3$ (**20**) gave a spectrum consistent with the dimeric peroxo complex $\{(\mu\text{-}O_2)Zr[MeC(N^iPr)_2]_2\}_2$ (**21**) with an *m*/z = 809.26 [**21**+H^+]. The MS spectrum is given in Figure 3.8 along with the predicted spectrum. Zr is an element with five stable isotopes (^{90}Zr, ^{91}Zr, ^{92}Zr, ^{94}Zr, ^{96}Zr), as shown in Table 2.1. Mass spectra of Zr compounds containing, e.g., one and two Zr atoms thus each show unique isotopic patterns. The identification of **21** is based on the isotopic pattern. The observation of **21** indicates that, during the MS process, the trimeric peroxo **20** is likely converted to the dimeric peroxo **21**.

We have found that **20** reacts with **10** to give the oxo dimer $\{(\mu\text{-}O)Zr[MeC(N^iPr)_2]_2\}_2$ (**14**), polymer **17**, $HNMe_2$ and $CH_2(NMe_2)_2$ (**19**). When the crystals of **20**, which were mixed with solids of unreacted $Zr[MeC(N^iPr)_2]_2(NMe_2)_2$ (**10**), were dissolved with benzene-d_6 at 23 °C, only **10**, oxo dimer **14**, solid of **17,** $HNMe_2$ and $CH_2(NMe_2)_2$ (**19**) were observed. **20** was also prepared from the reaction of **8** with Na_2O_2. The reaction was carried out in THF at 50 °C for 24 h, and **8** was found to have fully reacted. After volatiles were removed, extraction with pentane give the peroxo **20** and it was characterized by ^1H and $^{13}C\{^1H\}$ NMR

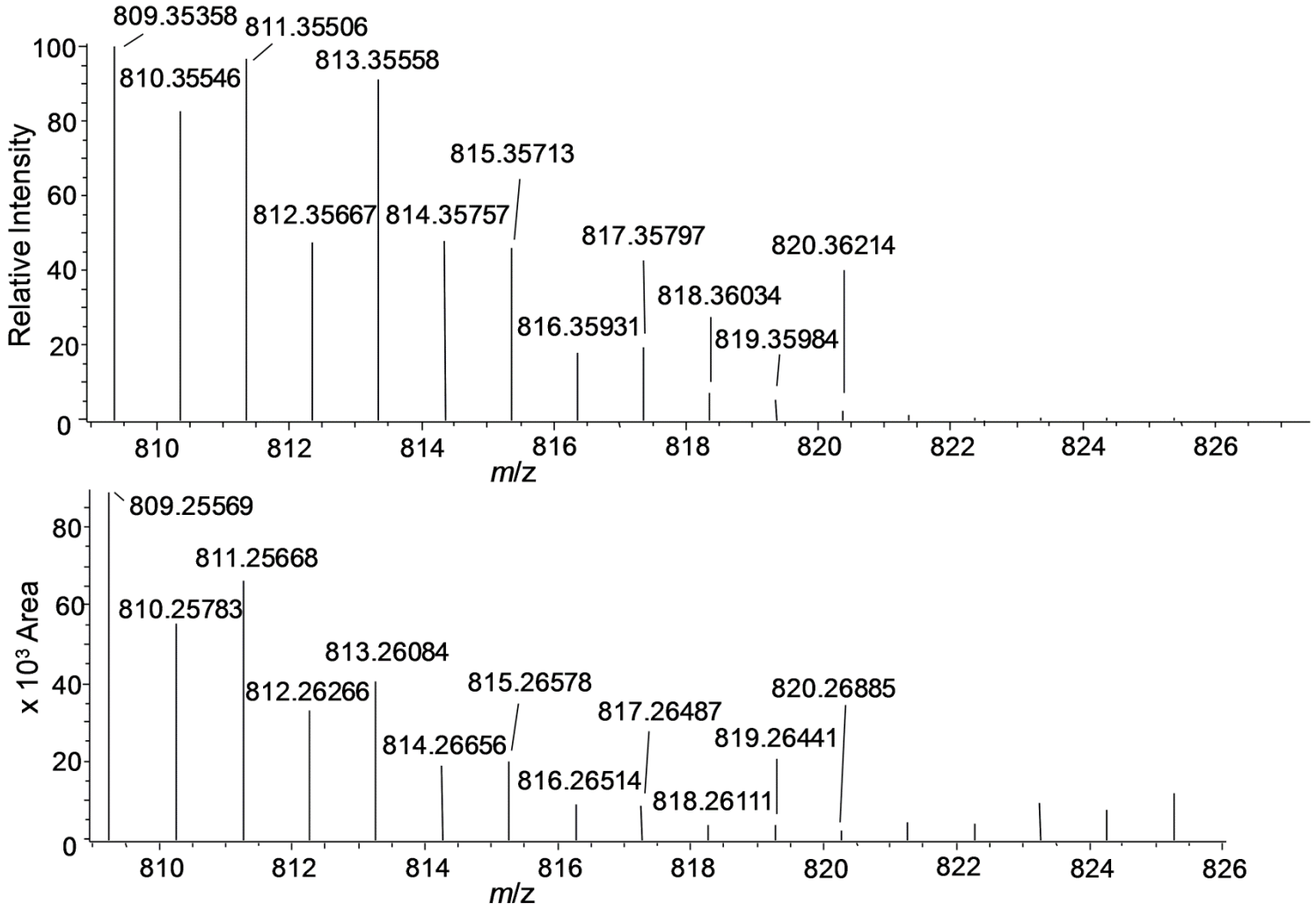

Figure 3.8. (Top) Calculated and (Bottom) Observed MS of [**21**+H^+].

spectroscopy. The solid residue after the pentane extraction was then extracted with H_2O, and the residue was found to contain 87% of 2 equiv of Cl^- ions, as a test using $AgNO_3$ showed. This observation, indicating that both chloride ligands in **8** have been replaced by O_2^{2-}, is consistent with the formation of **20**. When **10** was added to a solution of peroxo **20** prepared from **8** and Na_2O_2, the oxo dimer $\{(\mu\text{-O})Zr[MeC(N^iPr)_2]_2\}_2$ (**14**), polymer **17**, $HNMe_2$ and $CH_2(NMe_2)_2$ (**19**) were observed (Scheme 3.10). This reactivity is consistent with that of the crystals of **20** prepared from the reaction of **10** with O_2 at -35 °C. In a control experiment, Na_2O_2 was added to a solution of **10** and heated at 55 °C for 48 h and no reaction occurred.

We then prepared high purity H_2O_2 by evacuating 20 mL of 30% aqueous H_2O_2 solution at 23 °C until the volume of the solution was ca. 2 mL. Since boiling points of H_2O_2 and water are 150.2 and 100 °C, respectively, water was expected to be preferentially removed during the process. Such an approach has been used to obtain high purity H_2O_2 and D_2O_2.[17] One equiv of the high purity H_2O_2 was added to a THF solution of **10**. Again, oxo dimer **14** was observed, along with unreacted **10** and an insoluble solid presumably to be **17**.

Reaction of the high purity H_2O_2 with solid **10** was also studied. Liquid H_2O_2 was added directly on powders of **10**. This was an attempt to minimize the contact of the product, peroxo **20**, with the unreacted **10** by not using a solvent. As soon as the liquid H_2O_2 was added via syringe to the powders of **10**, a spark with smoke occurred. This observation suggests that **20** is very reactive in the presence of **10** (Scheme 3.10).

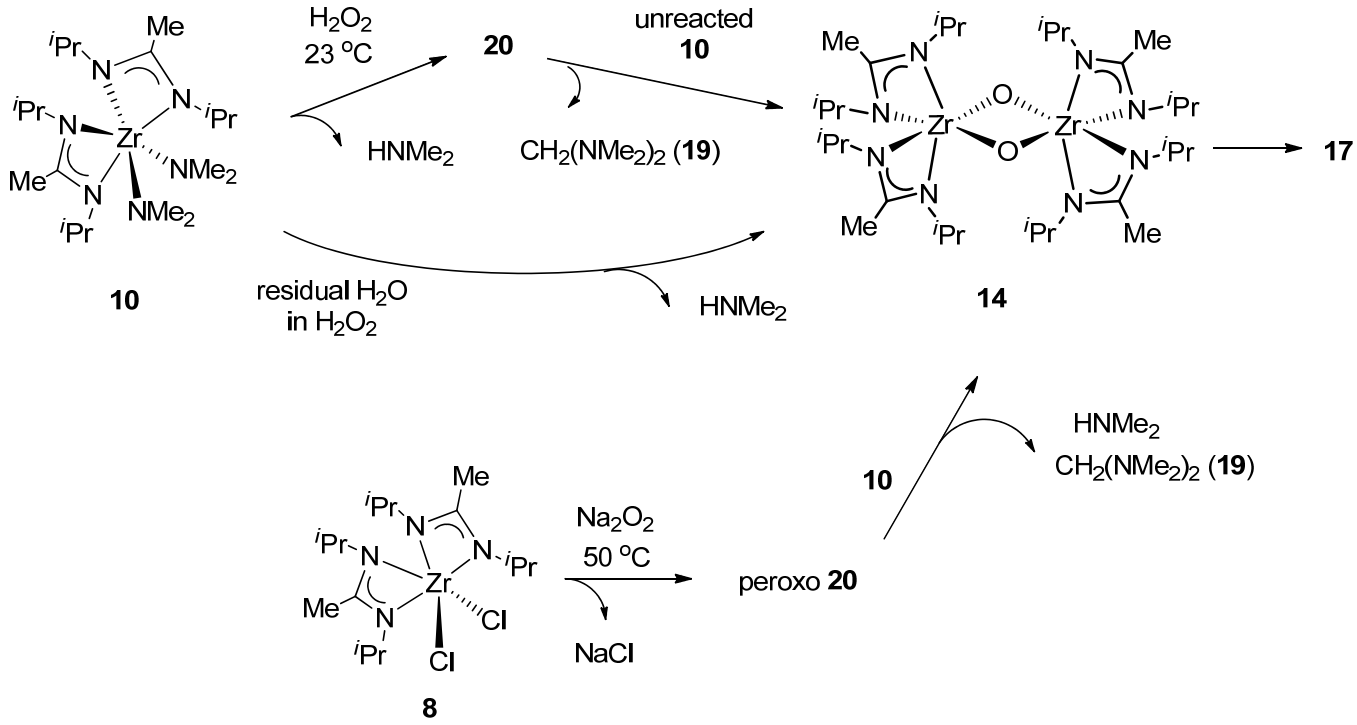

Scheme 3.10. Preparation of **20**. Trace water in high purity H_2O_2 may also lead to the formation of **14**.

3.2.5. Mass Spectrometric Studies of the Reactions between $Zr[MeC(N^iPr)_2]_2(NR_2)_2$ (R = Me, 10; Et, 12) and H_2O in Air

Loading samples for use in mass spectrometers usually requires the sample to be exposed to air. For air-sensitive compounds this may pose a problem, unless the mass spectrometers are equipped with an inert gas apparatus.

Since the reactions of $Zr[MeC(N^iPr)_2]_2(NR_2)_2$ (R = Me, **10**; Et, **12**) with O_2 or water have been studied, it is of interest to see what products would be detected in MS from the reactions. In MS, there is a brief exposure time for the sample to enter into the gas phase. The exposure to O_2 was not of concern because it takes days for **10** or **12** to react with O_2. Since Zr has five stable isotopes (^{90}Zr, ^{91}Zr, ^{92}Zr, ^{94}Zr, and ^{96}Zr; Table 2.1), and thus a unique isotopic pattern. It is easy to determine whether a compound has one Zr atom or two Zr atoms because their MS patterns are different.

Solid powders of **10** or **12** were kept in a sealed vial under nitrogen until the MS analysis by a JEOL AccuTOF™ DART (Direct Analysis in Real Time) mass spectrometer was heated to 200 °C. The powders were collected on the sealed end of a capillary tube and added quickly to the heated stream of He gas in air. Compounds **10** or **12** reacted with H_2O in air and the volatile products $[M+H^+]$ (species+H^+) were then analyzed by MS.

Since the reactions of both **10** and **12** with water give the same products, it was not surprising that the same products are observed in MS. The MS analyzer detected three zirconium and oxygen containing products: oxo

monomer **13**, oxo dimer **14**, and a dihydroxyl complex **18** as shown in Scheme 3.11. The calculated mass for [**13**+H^+] is 389.18579 *m*/z, and the cation was observed at 389.18249 *m*/z. The calculated and observed isotopic patterns for [**13**+H^+] are given in Figure 3.9. One possible pathway for the formation of **13** is dehydration of **18** (Scheme 3.11). The calculated mass for [**18**+H^+] is 407.19635 *m*/z, and the cation was observed at 407.19077 *m*/z. The calculated and observed isotopic patterns for [**18**+H^+] are shown in Figure 3.10. The calculated mass for [**14**+H^+] is 777.36375 *m*/z, and the cation was observed at 777.37085 *m*/z. The calculated and observed isotopic patterns for [**14**+H^+], a two Zr atoms complex, are shown in Figure 3.11.

3.2.6. Characterization and Stability of $\{(\mu\text{-O})Zr[MeC(N^iPr)_2]_2\}_n$ (17)

17 does not dissolve in benzene-d_6, DMF, Et_2O, hexanes, methanol, pentane, THF, or toluene-d_8. The characterization of **17** was based on elemental analysis, IR, and solid-state ^{13}C NMR. IR spectrum of **17** in a KBr pellet (Figure 3.12) revealed a peak at 1641 cm^{-1}, and this peak was assigned to the C=N stretch, as the stretching frequencies of C=N are in the range of 1690-1640 cm^{-1}.[18] Solid Solid-state ^{13}C NMR spectrum of **17** (Figure 3.13) shows peaks at 14.19 ppm for NC(*Me*)N, 23.27 ppm for -CH*Me*$_2$, 46.34 ppm for -*C*HMe_2, and 152.35 ppm for N*C*(Me)N. Raman spectroscopy was used in an attempt to characterize the Zr-O bonds but due to florescence of the sample no signals was observed in the Raman spectrum. Also, a powder X-ray study of the sample did not give a diffraction pattern, probably due to the lack of crystallinity of **17**. Mass

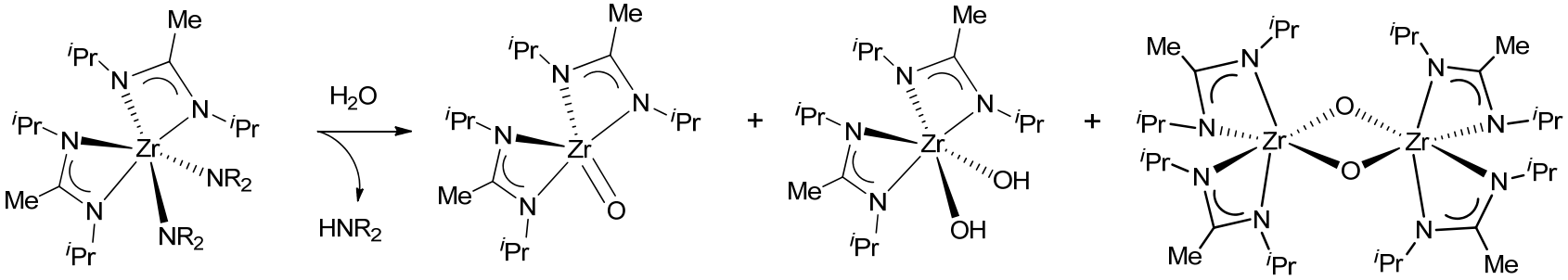

R = Me, **10**; Et, **12** **13** **18** **14**

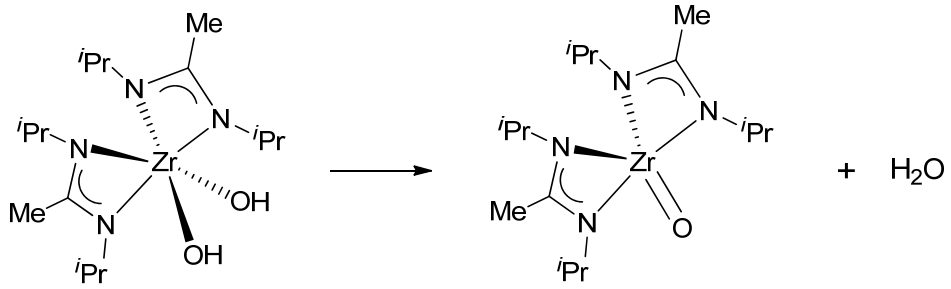

18 **13**

Scheme 3.11. Observed species by mass spectroscopy in the reactions of $Zr[MeC(N^iPr)_2]_2(NR_2)_2$ (R = Me, **10**; Et, **12**) with water in air.

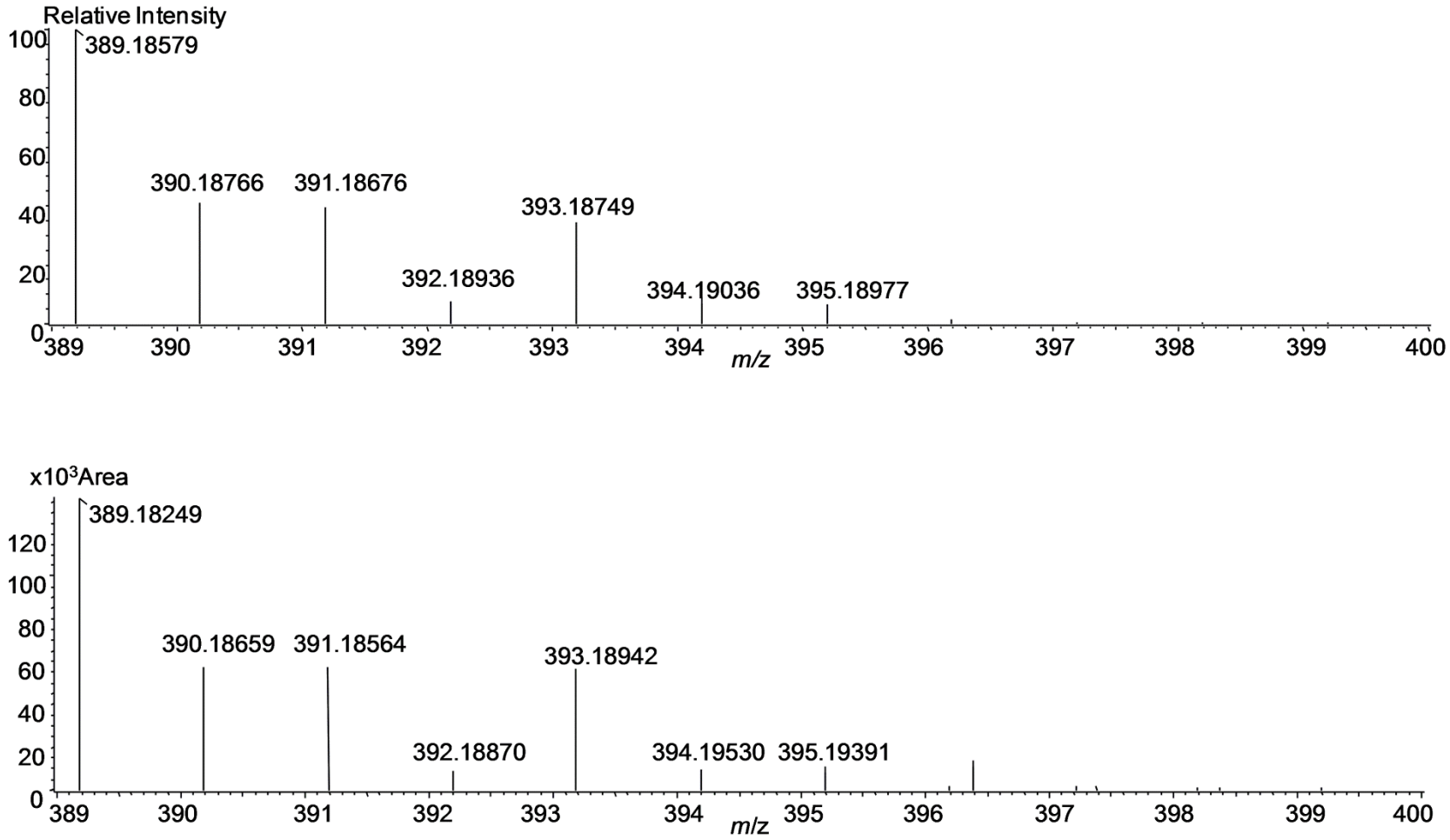

Figure 3.9. (Top) Calculated and (Bottom) Observed MS for [**13**+H^+].

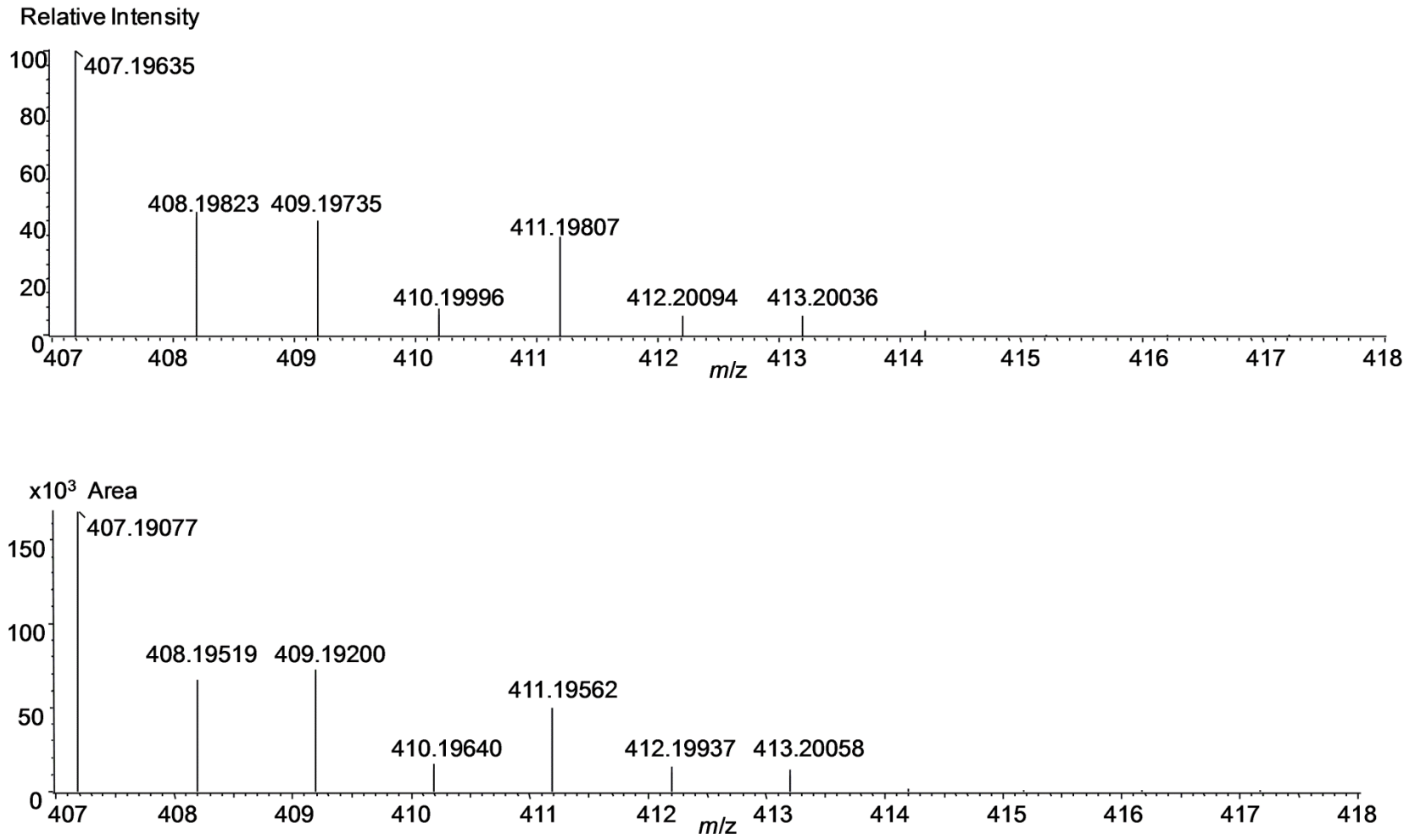

Figure 3.10. (Top) Calculated and (Bottom) Observed MS for [**18**+H^+].

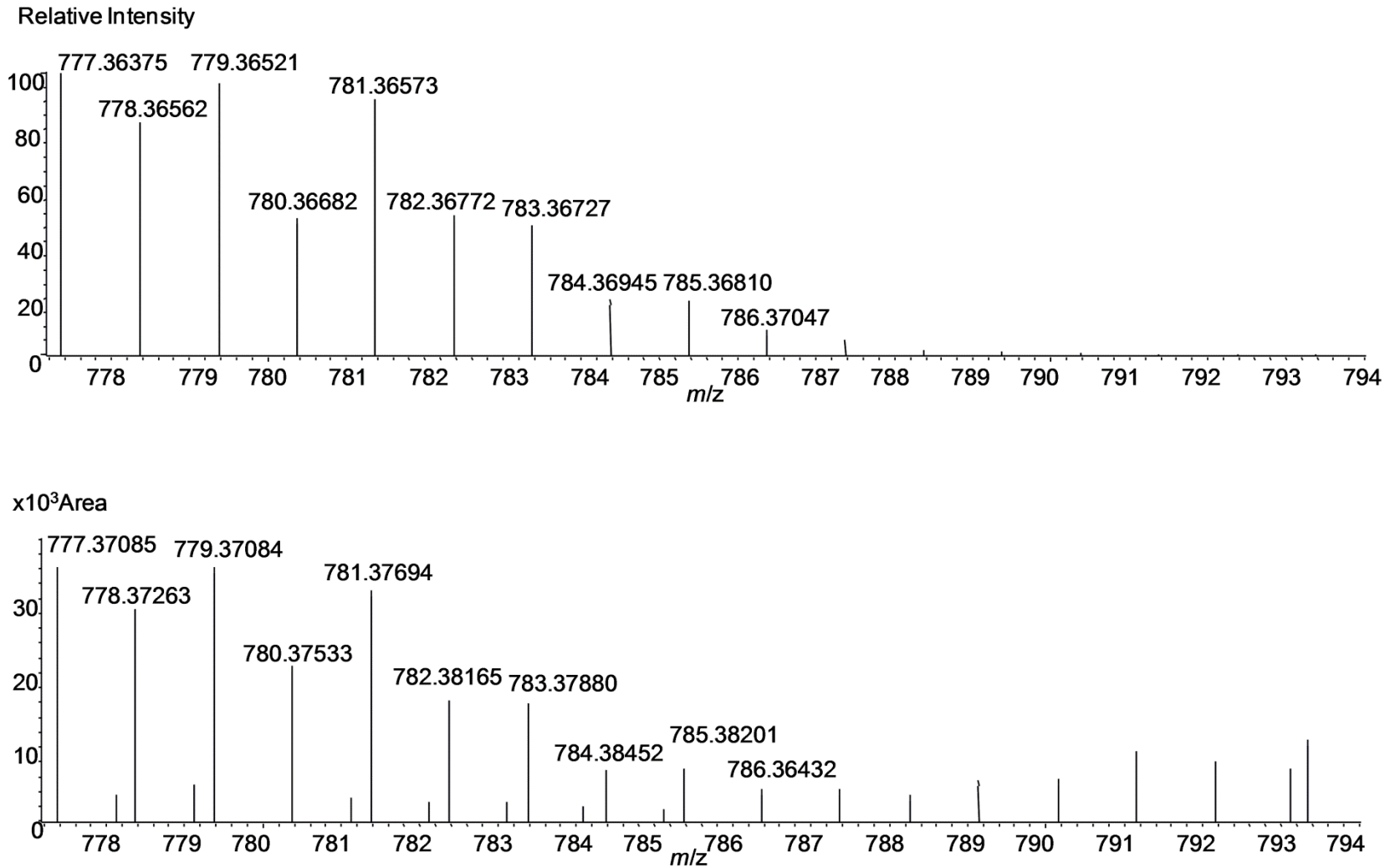

Figure 3.11. (Top) Calculated and (Bottom) Observed MS for [**14**+H^+].

spectroscopy was also used in several attempts to characterize **17** using different ionizing sources: direct analysis in real time (DART, at 200 °C, 300 °C and 400 °C), electrospray ionization (ESI) and matrix-assisted laser desorption ionization time-of-flight (MALDI). However, no Zr isotopic patterns were observed in the MS spectra.

Three tests were performed to determine the stability of the polymer product. The first test was to add a solvent that could donate a proton and possibly protonate the amidinate ligand. Methonal was chosen as the solvent, and it was added to **17** in benzene-d_6 and monitored by ^{1}H NMR. Spectra were collected at 5 min and then 12, 24 and 96 h. There was no change in the ^{1}H NMR spectra. We also did not observe the amidine ^{i}PrN(H)C(Me)=N^{i}Pr (**7**), the protonated ligand.

A thermal gravametric analysis (TGA) was performed to see if the amidinate ligand could be removed. At 900 °C, the removal of one amidinate ligand was observed by a percent loss of 36.21 (Figure 3.14). Since it requires such a high temperature to remove one amidinate ligand, the polymer **17** is considered very stable.

A third test was performed testing the stability of **17** was to make an IR pellet of **17** and KBr and expose it to air. IR spectra were recorded before exposure and 2 and 16 h after exposure to air. Little change in the C=N stretching frequency was observed.

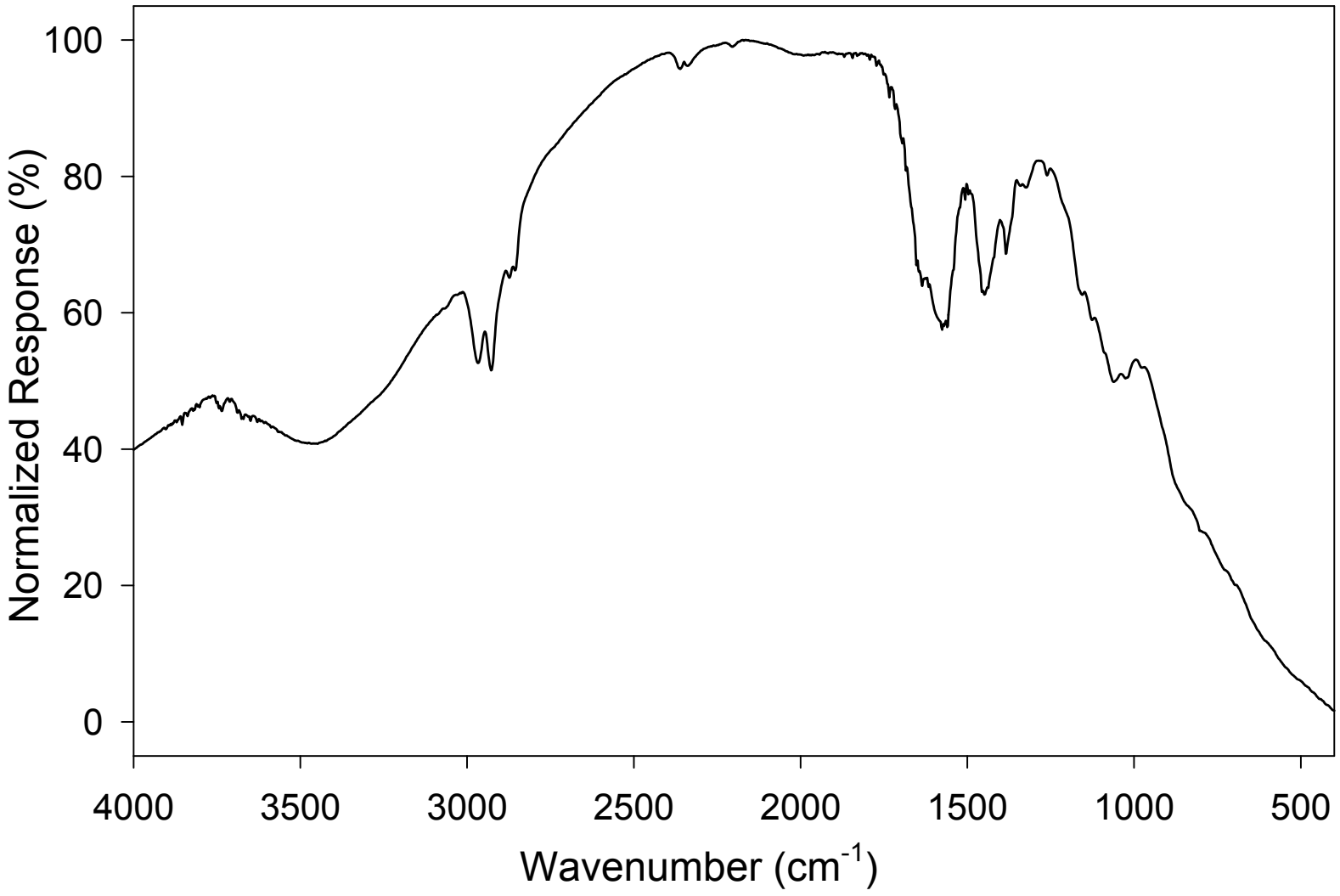

Figure 3.12. IR spectrum of **17** in KBr.

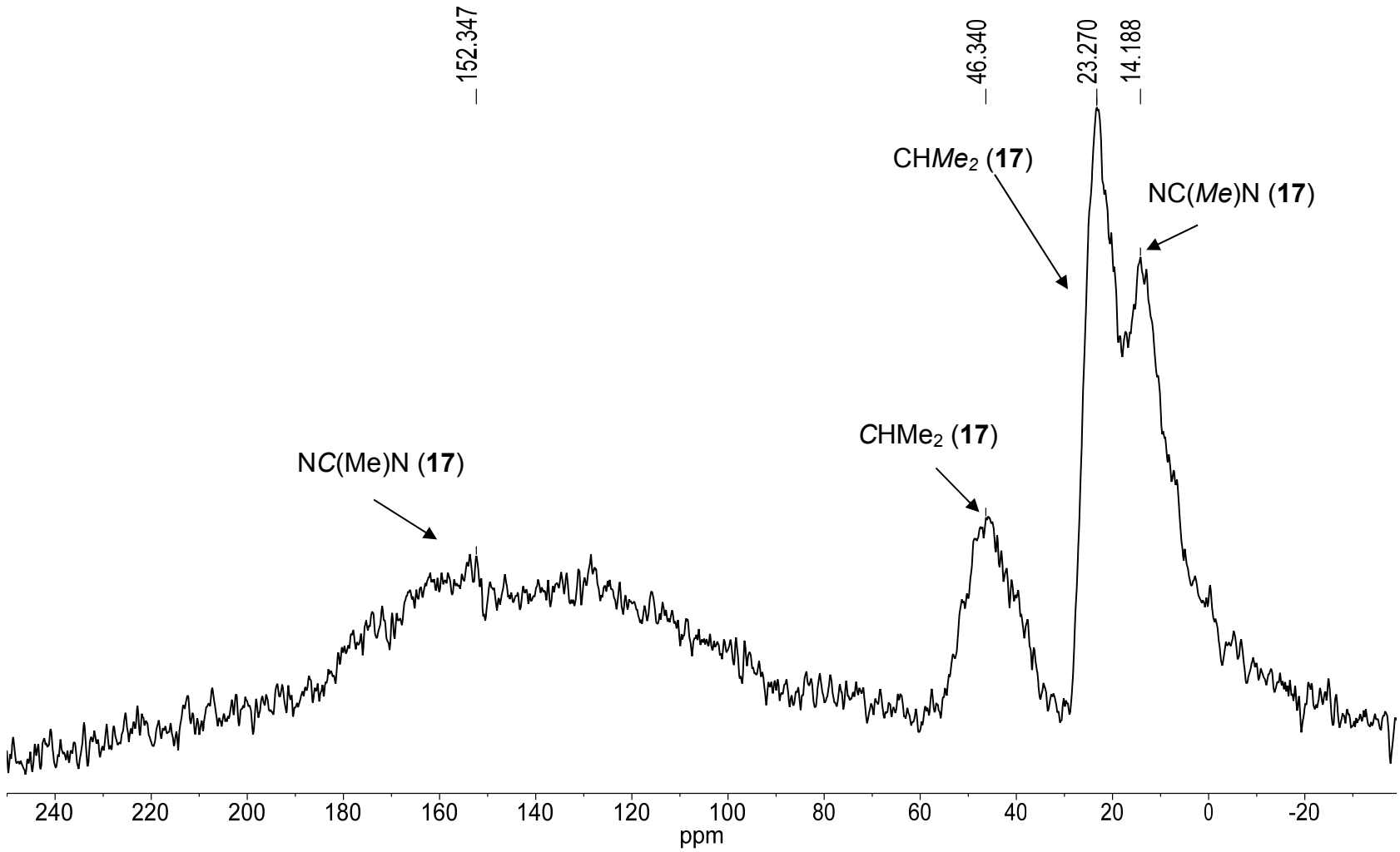

Figure 3.13. Solid-state ^{13}C NMR spectrum of **17**.

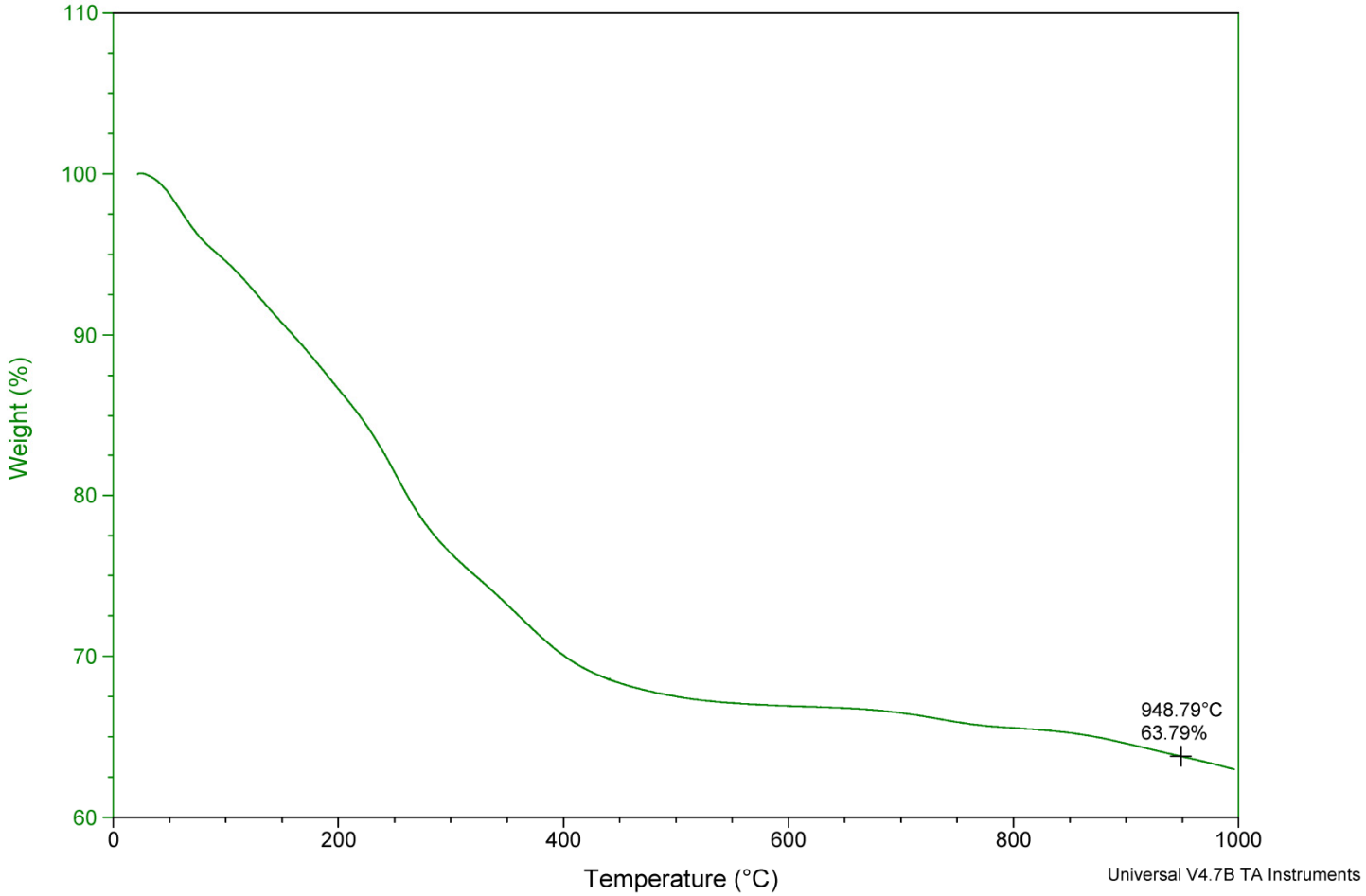

Figure 3.14. TGA spectrum of **17**.

3.2.7. Reaction with 12 and O_2 with AIBN

Since the reaction between **12** and O_2 (Scheme 3.4) is slow, a radical initiator was used to increase the rate of the reaction. The initiator we chose was azobisisobutyronitrile (AIBN), it decomposes under heating into two radicals and N_2, as shown in Scheme 3.12. These radicals are expected to speed up the reaction between **12** and O_2. In a Young's tube, AIBN was added to a solution of **12** in benzene-d_6 in a 1:1 molar ratio. O_2 at 1 atm was then added by the procedure described in Section 3.2.1. The reaction was completed in 2 days at 72 °C. In comparison, without AIBN, the reaction between **12** and O_2 took 7 days to complete. The observations support that the reaction between **12** and O_2 is radical in nature.

3.3. Concluding Remarks

In this part, studies of the reactions between Zr amidinate amides $Zr[MeC(N^iPr)_2]_2(NR_2)_2$ (R = Me, **10**; Et, **12**) and O_2 or water are reported. Interestingly, these reactions with O_2 or water yielded the same oxo-bridging

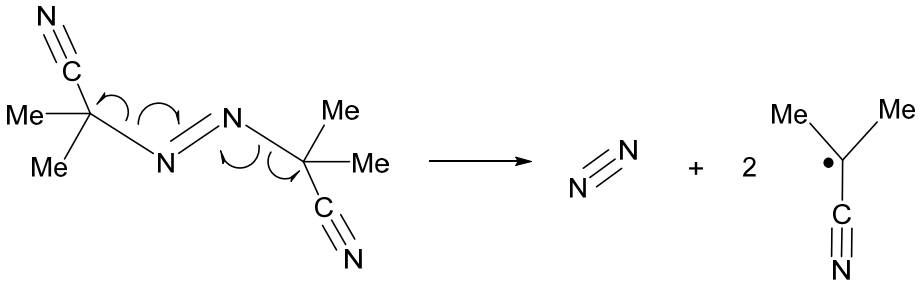

Scheme 3.12. Thermal decomposition of AIBN.

compounds **14** and **17**. The reactions with H_2O are much faster than those with O_2. Detailed MS studies were also conducted for the characterization of products obtained from the reactions with water in air. An unusual Zr peroxo trimer, $\{(\mu\text{-}\eta^2\text{:}\eta^2\text{-}O_2)Zr[MeC(N^iPr)_2]_2\}_3$ (**20**), has been obtained from the reaction of **10** with O_2 and its crystal structure has been determined. $\{(\mu\text{-}\eta^2\text{:}\eta^2\text{-}O_2)Zr[MeC(N^iPr)_2]_2\}_3$ (**20**) reacts with $Zr[MeC(N^iPr)_2]_2(NMe_2)_2$ (**10**) to give the oxo dimer $\{(\mu\text{-}O)Zr[MeC(N^iPr)_2]_2\}_2$ (**14**) and its polymer $\{(\mu\text{-}O)Zr[MeC(N^iPr)_2]_2\}_n$ (**17**). **20** was also prepared from the reaction of $Zr[MeC(N^iPr)_2]_2Cl_2$ (**8**) with Na_2O_2. A quantitative Cl^- test using $AgNO_3$ indicated that both chloride ligands in **8** were replaced in the reaction.

3.4. Experimental Section

All manipulations were carried out under a dry nitrogen atmosphere with the use of either a glovebox or standard Schlenk techniques. All glassware was flamed dried under vacuum. Solvents were purified by distillation from a potassium benzophenone ketyl. NMR solvents were dried and stored over 5 Å molecular sieves. O_2 (Airgas) was purified by passing it through a P_2O_5 column. Deionized H_2O was degassed and stored in a Schlenk flask. The high purity H_2O_2 was prepared, using an approach similar to those in the literature,[17] by evacuating 20 mL of an aqueous H_2O_2 solution (Fischer Scientific, 30% reagent grade) at 23 °C until the volume of the solution was ca. 2 mL. Na_2O_2 (Fischer Scientific, 99%) was ground with a mortar and pestle before use. $AgNO_3$ (J. T. Baker, 99.7%) was used as received. ^1H and $^{13}C\{^1H\}$ NMR spectra were

recorded on an AMX-400 FT or Varian VNMRS-500 spectrometer. Solid-state NMR spectrum was recorded on a Solid-State Varian INOVA 400 MHz spectrometer and referenced to adamantine. Elemental analyses were conducted by Complete Analysis Laboritories, Inc., Parsippany, NJ. Mass spectra were recorded on a JEOL AccuTOF™ DART Mass Spectrometer. To record IR spectra, solid samples were grounded with KBr, which had been dried at 100 °C and under vacuum, and then pressed into pellets. IR spectra were recorded on a Varian 4100 Excalibur. Thermal gravametreic analysis was recorded on a Q-50 TGA.

Caution: Extreme care should be taken in using sodium peroxide and hydrogen peroxide in the reactions. A shield should be used for protection.

3.4.1. Reaction of $Zr[MeC(N^iPr)_2]_2(NMe_2)_2$ (10) with O_2

NMR-scale Reactions. In a Young's tube, **10** (28.9 mg, 0.0626 mmol) was dissolved in benezene-d_6. The headspace volume in the Young's tube was 2.6 mL. The solution was frozen in liquid nitrogen and nitrogen gas was removed in vacuo. O_2 (0.5 atm; 0.0626 mmol) was then added. Several ^1H NMR spectra were taken and after 3 weeks, the disappearance of **10** and the appearance of soluble species **14**, $HNMe_2$, $CH_2(NMe_2)_2$ (**19**) and an insoluble solid **17** had occurred.

In a separate test, O_2 (1 atm; 0.0396 mmol) was added to **10** (18.3 mg, 0.0396 mmol) in benzene-d_6. Volume of the headspace in the Young's tube was 2.1 mL. The Young's tube was heated at 70 °C. After about ca. 12 days, the

reaction was quenched in ice water and the ^{1}H NMR spectrum showed the disappearance of **10** and appearance of new peaks which corresponds to a oxo-bridged dimer **14**. ^{1}H NMR also revealed two byproducts: $HNMe_2$ (0.125 mg, 6.99% yield based on NMR) and $CH_2(NMe_2)_2$ (**19**, 1.09 mg, 26.9% yield based on NMR). The byproducts, $HNMe_2$ and **19** were confirmed with GC-MS. A light yellow precipitate formed which was identified to be the polymeric product **17** (9 mg, 58.4% yield).

Reaction Conducted in a Schlenk Flask. In another experiment, O_2 (1 atm, 2.014 mmol) was added to **10** (0.465 g, 1.007 mmol) in toluene in a Schlenk flask. The headspace of the flask was 20.0 mL. The solution was heated at 80 °C for ca. 5 days. A pale yellow solid had precipitated from the solution. Volatiles were removed in vacuo and pentane was added. The solution was filtered and concentrated in attempts to grow crystals. Over time, a light yellow/white solid would precipitate out. An attempt to grow crystals of **14** in Et_2O, hexanes and toluene was also made. The characterization of the precipitate **17** is discussed in Section 3.4.3.

^{1}H NMR (benzene-d_6, 400.17 MHz, 23 °C): δ 4.26 (m, 2H, C*H*Me_2), 3.47 (m, 2H, C*H*Me_2), 1.34 (s, 6H, NC(*Me*)N), 1.25 (d, 12H, CH*Me*$_2$) 1.02 (d, 12H, CH*Me*$_2$); ^{13}C{^{1}H} NMR (benzene-d_6, 100.63 MHz, 23 °C): δ 151.38 (N*C*(Me)N), 49.20 (*C*HMe_2), 41.40 (*C*HMe_2), 25.60 (CH*Me*$_2$), 22.90 (CH*Me*$_2$), 15.38 (NC(*Me*)N). ^{1}H and ^{13}C{^{1}H} NMR assignments were confirmed by HSQC spectra.

3.4.2. Reaction of $Zr[MeC(N^iPr)_2]_2(NEt_2)_2$ (12) with O_2

NMR-scale Reaction. In a Young's tube, **12** (16.5 mg, 0.0319 mmol) was dissolved in benzene-d_6. Volume of headspace in the Young's tube was 2.3 mL. Before adding O_2, the solution was frozen in liquid nitrogen and nitrogen gas was removed in vacuo. O_2 (1 atm, 0.0319 mmol) was then added. The solution was then heated at 70 °C for 7 days. ^{1}H NMR revealed the oxo-bridged dimer **14** and $HNEt_2$ had formed. Based on NMR the yield of $HNEt_2$ was 14.1% (2 mg). $HNEt_2$ was confirmed by GC-MS. A light yellow precipitate was identified as $\{(\mu\text{-}O)Zr[MeC(N^iPr)_2]_2\}_n$ (**17**) (7.8 mg, 62.8% yield). The NMR chemical shifts were the same for the reaction of the methyl amide analog **10** with O_2 to produce the oxo-bridged dimer **14**.

Reaction Conducted in a Schlenk Flask. In a large scale experiment, O_2 (1 atm, 1.06 mmol) was added to **12** (0.549 g, 1.06 mmol) in toluene in a Schlenk flask. The volume of the headspace of the Schlenk flask was 53.6 mL. The solution was heated at 80 °C for 4 days. A pale yellow solid **17** had precipitated. Volatiles were removed in vacuo and pentane was added. The solution was filtered and concentrated in an attempt to grow crystals. Over time a cloudy solution would form and it was believed the polymer **17** had formed. Characterization of the precipitate **17** is discussed in Section 3.4.3.

3.4.3. Characterization of $\{(\mu\text{-}O)Zr[MeC(N^iPr)_2]_2\}_n$ (17)

It is presumed that the polymer $\{(\mu\text{-}O)Zr[MeC(N^iPr)_2]_2\}_n$ (**17**) is the same for the reactions of **10** and **12** with O_2. For the characterization here, the polymer

17 was prepared from the reaction of **12** with O_2. The solid-state ^{13}C NMR spectrum of **17** (Figure 3.13) shows peaks at 14.19 ppm for NC(*Me*)N, 23.27 ppm for -CH*Me*$_2$, 46.34 ppm for -*C*HMe$_2$, and 152.35 ppm for N*C*(Me)N. The IR spectrum shows a C=N peak at 1641 cm^{-1}. A TGA experiment was performed under N_2, the sample was heated from room temperature to 1000 °C at a rate of 10 °C per minute. There was a 36.21% loss which accounted for one amidinate ligand to be removed and **17** is considered to be a stable compound at room temperature. Anal. Calcd: C, 49.31; H, 8.79; N, 14.38. Found: C, 49.24; H, 8.71; N, 14.29.

3.4.4. Reaction of Zr[MeC(N^{i}Pr)$_2$]$_2$Cl$_2$ (8) with Na_2O_2

Zr[MeC(N^{i}Pr)$_2$]$_2$Cl$_2$ (**8**) (321 mg, 0.722 mmol) in THF (10 mL) was added to Na_2O_2 (71.5 mg, 0.917 mmol) in THF (10 mL). The solution was heated at 50 °C for 24 h. A condenser was attached and connected to a bubbler to ensure no pressure buildup. Volatiles were then removed in vacuo. Extraction of the remaining solid by pentane, followed by removing volatiles in vacuo, gave peroxo **20** (40 mg, 0.033 mmol, 14% yield). ^1H NMR (benzene-d_6, 400.17 MHz, 23 °C): δ 3.58 (br, 4H, C*H*Me$_2$), 1.41 (s, 6H, NC(*Me*)N), 1.14 (d, 24H, CH*Me*$_2$); $^{13}C\{^1H\}$ NMR (benzene-d_6, 100.63 MHz, 23 °C): δ 178.25 (N*C*(Me)N), 48.62 (*C*HMe$_2$), 24.51 (CH*Me*$_2$), 10.53 (NC(*Me*)N). The NMR spectra of the pentane extract showed that **8** had fully reacted.

The solid residue from the pentane extraction was then extracted with H_2O (34 mL), and the mixture was filtered. The solution was added $AgNO_3$ (245 mg,

1.44 mmol). AgCl precipitated and the mixture was centrifuged to collect AgCl. The solid was dried at 65 °C overnight and then under vacuum (<0.01 mmHg) for over 1 h to give AgCl (179.4 mg, 1.252 mmol, 87% yield).

Then **10** was added to this NMR solution at 23 °C. The peaks of **20** disappeared, and peaks of **14**, $HNMe_2$ and $CH_2(NMe_2)_2$ (**19**) were observed. A solid, presumably to be the polymer **17**, precipitated from the solution.

3.4.5. Reaction of $Zr[MeC(N^iPr)_2]_2(NMe_2)_2$ (10) with H_2O_2

NMR-scale Reaction. In a Young's tube, **10** (13.6 mg, 0.0294 mmol) was dissolved in benzene-d_6. H_2O_2 (0.7 μL, 0.0297 mmol) was then added. The ^1H and $^{13}C\{^1H\}$ NMR revealed the oxo-bridged dimer **14** and $CH_2(NMe_2)_2$ (**19**). A precipitate formed and was presumed to be $\{(\mu\text{-}O)Zr[MeC(N^iPr)_2]_2\}_n$ (**17**). The NMR chemical shifts were the same for the reaction of the methyl amide analog **10** with O_2 to produce the oxo-bridged dimer **14**.

Reaction Conducted in a Schlenk Flask. In a large scale experiment, H_2O_2 (26.5 mg, 0.780 mmol) in THF (20 mL) at 0 °C was added to **10** (3.567 g, 0.772 mmol) in THF (15 mL) and cooled to -50 °C. It was allowed to stir overnight and volatiles were removed in vacuo. The ^1H NMR revealed the oxo-bridged dimer **14**. A precipitate formed and was presumed to be $\{(\mu\text{-}O)Zr[MeC(N^iPr)_2]_2\}_n$ (**17**).

*Reactions of Solid **10** with H_2O_2.* High purity H_2O_2 (0.4 μL) was added directly on powders of $Zr[MeC(N^iPr)_2]_2(NMe_2)_2$ (**10**, 17.1 mg, 0.0370 mmol) in a glovebox. As soon as the liquid H_2O_2 was added via syringe to the powders of **10**, a spark with smoke occurred.

3.4.6. Reaction of 12 with O_2 in the Presence of the Radical Initiator Azobisisobutyronitrile (AIBN)

In a Young's tube, AIBN (13.6 mg, 0.0828 mmol) was added to a benzene-d_6 solution of **12** (45.0 mg, 0.0869 mmol). The solution was frozen with liquid nitrogen and O_2 (1 atm; 0.0869 mmol) was added. (Volume of the headspace in the Young's tube was 2.1 mL.) The Young's tube was heated at 72 °C. After 2 days, the reaction was completed. ^{1}H NMR spectrum showed the oxo-dimer **14** had formed.

3.4.7. Determination of the Crystal Structure of 20

The X-ray crystal structure of **20** was determined on a Bruker AXS Smart 1000 X-ray diffractometer equipped with a CCD area detector and a graphite-monochromated Mo source ($K\alpha$ radiation, 0.71073 Å) and fitted with an upgraded Nicolet LT-2 low temperature device. A suitable crystal was coated with paratone oil (Exxon) and mounted on a fiber loop under a stream of nitrogen at 100(2) K. The structure was solved by direct methods. All non-hydrogen atoms were anistropically refined. Empirical absorption correction was performed with SADABS.[19a] Global refinements for the unit cells and data reductions were performed under the Saint program (Version 6.02). All calculations were performed using SHELXTL (Version 5.1) proprietary software package.[19b]

References

1. (a) Tilley, T. D. *Organometallics* **1985**, *4*, 1452. (b) Blackburn, T. F.; Labinger, J. A.; Schwartz, J. *Tetrahedron Lett.* **1975**, *16*, 3041. (c) Labinger, J. A.; Hart, D. W.; Seibert, W. E.; Schwartz, J. *J. Am. Chem. Soc.* **1975**, *97*, 3851. (d) Lubben, T. V.; Wolczanski, P. T. *J. Am. Chem. Soc.* **1987**, *109*, 424. (e) Lubben, T. V.; Wolczanski, P. T. *J. Am. Chem. Soc.* **1985**, *107*, 701. (f) Wang, R.; Folting, K.; Huffman, J. C.; Chamberlain, L. R.; Rothwell, I. P. *Inorg. Chim. Acta* **1986**, *120*, 81. (g) Gibson, V. C.; Redshaw, C.; Walker, G. L. P.; Howard, J. A. K.; Hoy, V. J.; Cole, J. M.; Kuzmina, L. G.; De Silva, D. S. *J. Chem. Soc., Dalton Trans.* **1999**, 161. (h) Schaverien, C. J.; Orpen, A. G. *Inorg. Chem.* **1991**, *30*, 4968. (i) Liu, X.; Cui, D. *Dalton Trans.* **2008**, 3747. (j) Van Asselt, A.; Santarsiero, B. D.; Bercaw, J. E. *J. Am. Chem. Soc.* **1986**, *108*, 8291. (k) Brindley, P. B.; Hodgson, J. C. *J. Organomet. Chem.* **1974**, *65*, 57. (l) Kim, S. J.; Choi, D. W.; Lee, Y. J.; Chae, B. H.; Ko, J. J.; Kang, S. O. *Organometallics* **2004**, *23*, 559. (m) Morris, A. M.; Pierpont, C. G.; Finke, R. G. *Inorg. Chem.* **2009**, *48*, 3496. (n) Adam, W.; Putterlik, J.; Schuhmann, R. M.; Sundermeyer, J. *Organometallics* **1996**, *15*, 4586. (o) Vetter, W. M.; Sen, A. *Organometallics* **1991**, *10*, 244. (p) Van Asselt, A.; Trimmer, M. S.; Henling, L. M.; Bercaw, J. E. *J. Am. Chem. Soc.* **1988**, *110*, 8254. (q) Boro, B. J.; Lansing, R.; Goldberg, K. I.; Kemp, R. A. *Inorg. Chem. Comm.* **2011**, *14*, 531.
2. Stanciu, C.; Jones, M. E.; Fanwick, P. E.; Abu-Omar, M. M. *J. Am. Chem. Soc.* **2007**, *129*, 12400.

3. Lu, F.; Zarkesh, R. A.; Heyduk, A. F. *Eur. J. Inorg. Chem.* **2012**, 467.

4. Chisholm, M. H.; Hammond, C. E.; Huffman, J. C. *J. Chem. Soc., Chem. Commun.* **1987**, 1423.

5. Brindley, P. B.; Hodgson, J. C. *J. Organomet. Chem.* **1974**, *65*, 57.

6. For studies of the reactions between O_2 and late transition metal complexes, see, for example, (a) Campbell, A. N.; Stahl, S. S. *Acc. Chem. Res.* **2012**, *45*, 851. (b) Theopold, K. H.; Reinaud, O. M.; Blanchard, S.; Leelasubeharoen, S.; Hess, A.; Thyagarajan, S. *ACS Symp. Ser.* **2002**, *823*, 75. (c) Que, L.; Tolman, W. B. *Nature* **2008**, *455*, 333. (d) Himes, R. A.; Karlin, K. D. *Curr. Top. Chem. Biol.* **2009**, *13*, 119. (e) Shook, R. L.; Borovik, A. S. *Chem. Comm.* **2008**, 6095. (f) Sheldon, R. A. in *Biomimetic Oxidations Catalyzed by Transition Metal Complexes*, Meunier, B. ed., Imperial College Press, 2000, pp. 613-662. (g) *Metal-Dioxygen Complexes: A Perspective.* Special Issue, *Chem. Rev.* **1994**, *94*, Issue 3, 567-856. (h) Monillas, W. H.; Yap, G. P. A.; MacAdams, L. A.; Theopold, K. H. *J. Am. Chem. Soc.* **2007**, *129*, 8090. (i) McQuilken, A. C.; Jiang, Y.; Siegler, M. A.; Goldberg, D. P. *J. Am. Chem. Soc.* **2012**, *134*, 8758. (j) Prokop, K. A.; Goldberg, D. P. *J. Am. Chem. Soc.* **2012**, *134*, 8014. (k) Scheuermann, M. L.; Fekl, U.; Kaminsky, W.; Goldberg, K. I. *Organometallics* **2010**, *29*, 4749. (l) Boisvert, L.; Denney, M. C.; Kloek Hanson, S.; Goldberg, K. I. *J. Am. Chem. Soc.* **2009**, *131*, 15802. (m) Khusnutdinova, J. R.; Rath, N. P.; Mirica, L. M. *J. Am. Chem. Soc.* **2012**, *134*, 2414. (n) Nguyen, K. T.; Rath, S. P.; Latos-Grazynski, L.; Olmstead, M. M.; Balch, A. L. *J. Am. Chem. Soc.* **2004**, *126*, 6210. (o) Maury, J.; Feray, L.;

Bazin, S.; Clement, J.-L.; Marque, S. R. A.; Siri, D.; Bertrand, M. P. *Chem. Eur. J.* **2011**, *17*, 1586. (p) Lewinski, J.; Koscielski, M.; Suwala, K.; Justyniak, I. *Angew. Chem. Int. Ed.* **2009**, *48*, 7017. (q) Mukherjee, D.; Ellern, A.; Sadow, A. D. *J. Am. Chem. Soc.* **2012**, *134*, 13018. (r) Jana, S.; Berger, R. J. F.; Fröhlich, R.; Pape, T.; Mitzel, N. W. *Inorg. Chem.* **2007**, *46*, 4293. (s) Lee, C.-M.; Chuo, C.-H.; Chen, C.-H.; Hu, C.-C.; Chiang, M.-H.; Tseng, Y.-J.; Hu, C.-H.; Lee, G.-H. *Angew. Chem. Int. Ed.* **2012**, *51*, 5427. (t) Kelley, M. R.; Rohde, J.-U. *Chem. Comm.* **2012**, *48*, 2876. (u) Brown, S. N.; Mayer, J. M. *Inorg. Chem.* **1992**, *31*, 4091. (v) Parkin, G.; Bercaw, J. E. *J. Am. Chem. Soc.* **1989**, *111*, 391.

7. (a) Robertson, J. *Rep. Prog. Phys.* **2006**, *69*, 327. (b) Jones, A. C.; Aspinall, H. C.; Chalker, P. R.; Potter, R. J.; Kukli, K.; Rahtu, A.; Ritala, M.; Leskelae, M. *J. Mater. Chem.* **2004**, *14*, 3101. (c) Arghavani, R.; Miner, G.; Agustin, M. *Semicond. Internal.* **2007**, *30*, 32-34, 36, 38.

8. For CVD of metal oxides using O_2, see, for example, (a) Son, K.-A.; Mao, A. Y.; Sun, Y.-M.; Kim, B. Y.; Liu, F.; Kamath, A.; White, J. M.; Kwong, D. L.; Roberts, D. A.; Vrtis, R. N. *Appl. Phys. Lett.* **1998**, *72*, 1187. (b) Niimi, H.; Johnson, R. S.; Lucovsky, G.; Massoud, H. Z. *Proc. Electrochem. Soc.* **2000**, *2000-2*, 487. (c) Eichler, J. F.; Just, O.; Rees, W. S., Jr. *J. Mater. Chem.* **2004**, *14*, 3139. (d) Takahashi, K.; Funakubo, H.; Hino, S.; Nakayama, M.; Ohashi, N.; Kiguchi, T.; Tokumitsu, E. *J. Mater. Res.* **2004**, *19*, 584. (e) Ogura, A.; Ito, K.; Ohshita, Y.; Ishikawa, M.; Machida, H. *Thin Solid Films* **2003**, *441*, 161. (f) Rodriguez-Reyes, J. C. F.; Teplyakov, A. V. *J. Appl. Phys.*

2008, *104*, 084907/1. (g) Ohshita, Y.; Ogura, A.; Ishikawa, M.; Kada, T.; Machida, H. *Jpn. J. Appl. Phys. 2.* **2003**, *42*, L578. (h) Matero, R.; Ritala, M.; Leskelae, M.; Sajavaara, T.; Jones, A. C.; Roberts, J. L. *Chem. Mater.* **2004**, *16,* 5630. (i) Kan, B.-C.; Boo, J.-H.; Lee, I.; Zaera, F. *J. Phys. Chem. A* **2009**, *113*, 3946. (j) Hausmann, D. M.; de Rouffignac, P.; Smith, A.; Gordon, R.; Monsma, D. *Thin Solid Films* **2003**, *443*, 1. (k) Meiere, S. H.; Peck, J.; Litwin, M. *ECS Trans.* **2006**, *1*, 103. (l) Chen, T.; Cameron, T. M.; Nguyen, S. D.; Stauf, G. T.; Peters, D. W.; Maylott, L.; Li, W.; Xu, C.; Roeder, J. F.; Hendrix, B. C.; Hilgarth, M.; Niinisto, J.; Kukli, K.; Ritala, M.; Leskela, M. *ECS Trans.* **2008**, *16*, 87. (m) Lee, S.; Kim, W.-G.; Rhee, S.-W.; Yong, K. *J. Electrochem. Soc.* **2008**, *155*, H92. (n) Schaeffer, J.; Edwards, N. V.; Liu, R.; Roan, D.; Hradsky, B.; Gregory, R.; Kulik, J.; Duda, E.; Contreras, L.; Christiansen, J.; Zollner, S.; Tobin, P.; Nguyen, B.-Y.; Nieh, R.; Ramon, M.; Rao, R.; Hegde, R.; Rai, R.; Baker, J.; Voight, S. *J. Electrochem. Soc.* **2003**, *150*, F67. (o) Woods, J. B.; Beach, D. B.; Nygren, C. L.; Xue, Z.-L. *Chem. Vap. Deposition* **2005**, *11*, 289. (p) Lehn, J.-S.; Javed, S.; Hoffman, D. M. *Chem. Vap. Deposition* **2006**, *12*, 280. (q) Chiu, H.-T.; Wang, C.-N.; Chuang, S.-H.; *Chem. Vap. Deposition* **2000**, *6*, 223. (r) Wiedmann, M. K.; Heeg, M. J.; Winter, C. H. *Inorg. Chem.* **2009**, *48*, 5382.

9. For CVD of metal oxides using water, see, for example, (a) Dezelah, C. L., IV; Niinisto, J.; Kukli, K.; Munnik, F.; Lu, J.; Ritala, M.; Leskela, M.; Niinisto, L. *Chem. Vap. Deposition* **2008**, *14*, 358. (b) Dezelah, C. L., IV; El-Kadri, O. M.; Szilagyi, I. M.; Campbell, J. M.; Arstila, K.; Niinistoe, L.; Winter, C. H. *J. Am.*

Chem. Soc. **2006**, *128*, 9638. (c) Majumder, P.; Jursich, G.; Takoudis, C. *J. Appl. Phys.* **2009**, *105*, 104106/1. (d) Consiglio, S.; Clark, R. D.; Nakamura, G.; Wajda, C. S.; Leusink, G. J. *J. Vacuum Sci. Technol., A* **2012**, *30*, 01A119/1. (e) Tao, Q.; Kueltzo, A.; Singh, M.; Jursich, G.; Takoudis, C. G. *J. Electrochem. Soc.* **2011**, *158*, G27. (f) Shi, X.; Tielens, H.; Takeoka, S.; Nakabayashi, T.; Nyns, L.; Adelmann, C.; Delabie, A.; Schram, T.; Ragnarsson, L.; Schaekers, M.; Date, L.; Schreutelkamp, R.; Van Elshocht, S. *J. Electrochem. Soc.* **2011**, *158*, H69.

10. (a) Wang, R.; Zhang, X.; Chen, S.; Yu, X.; Wang, C.; Beach, D. B.; Wu, Y.; Xue, Z. *J. Am. Chem. Soc.* **2005**, *127*, 5204. (b) Chen, S.; Zhang, X.; Yu, X.; Qiu, H.; Yap, G. P. A.; Guzei, I. A.; Lin, Z.; Wu, Y.; Xue, Z. *J. Am. Chem. Soc.* **2007**, *129*, 14408. (c) Chen, S.-J.; Zhang, X.-H.; Lin, Z.; Wu, Y.-D.; Xue, Z.-L. *Sci*. China Chem. **2009**, *52*, 1723. (d) Chen, S.-J.; Yap, G. P. A.; Xue, Z.-L. *Sci*. China Chem. **2009**, 52, 1583. (e) Chen, S.; Zhang, J.; Yu, X.; Bu, X.; Chen, X.; Xue, Z. *Inorg. Chem.* **2010**, *49*, 4017. (f) Chen, T.-N.; Zhang, X.-H.; Wang, C.-S.; Chen, S.-J.; Wu, Z.-Z.; Li, L.-T.; Sorasaenee, K. R.; Diminnie, J. B.; Pan, H.-J.; Guzei, I. A.; Rheingold, A. L.; Wu, Y.-D.; Xue, Z.-L. *Organometallics* **2005**, *24*, 1214. (g) Qiu, H.; Chen, S.-J.; Wang, C.-S.; Wu, Y.-D.; Guzei, I. A.; Chen, X.-T.; Xue, Z.-L. *Inorg. Chem.* **2009**, *48*, 3073. (h) Yu, X.; Chen, X.-T.; Xue, Z.-L. *Organometallics* **2009**, *28*, 6642. (i) Chen, S.-J.; Xue, Z.-L. *Organometallics* **2010**, *29*, 5579. (j) Wu, Z.; Cai, H.; Yu, X.-H.; Blanton, J. R.; Diminnie, J. B.; Pan, H.-J.; Xue, Z.-L. *Organometallics* **2002**, *21*, 3973.

11. (a) Miller, J. B.; Schwartz, J.; Bernasek, S. L. *J. Am. Chem. Soc.* **1984**, *115*, 8239. (b) Feinstein-Jaffe, I.; Gibson, D.; Lippard, S. J.; Schrock, R. R.; Spool, A. *J. Am. Chem. Soc.* **1984**, *106*, 6305. (c) Schoettel, G.; Kress, J.; Fischer, J.; Osborn, J. A. *J. Chem. Soc. Chem. Comm*. **1988**, 914. (d) Legzdins P.; Phillips, E. C.; Rettig, S. J.; Sanchez, L.; Trotter, J.; Yee, V. C. *Organometallics* **1988**, *7*, 1877. (e) Gamble, A. S.; Boncella, J. M., *Organometallics* **1993**, *12*, 2814. (f) Guzyr, O. I.; Prust, J.; Roesky, H. W.; Lehmann, C.; Teichert, M.; Cimpoesu, F. *Organometallics* **2000**, *19*, 1549. (g) Yoon, M.; Tyler, D. R. *Chem. Comm.* **1997**, 639. (h) Chen, S.-J.; Abbott, J. K. C.; Steren, C. A.; Xue, Z.-L. *J. Clust. Sci.* **2010**, *21*, 325. (i) Chen, S.-J.; Cai, H.; Xue, Z.-L. *Organometallics* **2009**, *28*, 167.

12. For the studies of amidinate complexes as CVD/ALD precursors, see, for example, (a) Krisyuk, V.; Aloui, L.; Prud'homme, N.; Sysoev, S.; Senocq, F.; Samelor, D.; Vahlas, C. *Electrochem. Solid-State Lett.* **2011**, 14, D26. (b) Seetula, J.; Kalliorinne, K.; Koskikallio, J. *J. Photochem. Photobiol., A.: Chem.* **1988**, *43*, 31. (c) Thiede, T. B.; Krasnopolski, M.; Milanov, A. P.; Arcos, T.; Ney, A.; Becker, H.-W; Rogalla, D.; Winter, J.; Devi, A.; Fischer, R. A. *Chem. Mater.* **2011**, 23, 1430. (d) Eleter, M.; Hubert-Pfalzgraf, L. G.; Daniele, S.; Pilet, G.; Tinant, B. *Polyhedron* **2010**, 29, 2522. (e) Li, Z.; Gordon, R. G.; Pallem, V.; Li, H.; Shenai, D. V. *Chem. Mater.* **2010**, 22, 3060. (f) Xu, K.; Milanov, A. P.; Winter, M.; Barreca, D.; Gasparotto, A.; Becker, H.-W.; Devi, A. *Eur. J. Inorg. Chem.* **2010**, 1679. (g) Eleter, M.; Daniele, S.; Brizé, V.; Dubourdieu, C.; Lachaud, C.; Blasco, N.; Pinchart, A. *ECS Trans.* **2009**, 25,

151. (h) Gleizes, A. N.; Krisyuk, V. V.; Aloui, L.; Turgambaeva, A. E.; Sarapata, B.; Prud'homme, N.; Senocq, F.; Samélor, D.; Zielinska-Lipiec, A.; Dumestre, F.; Vahlas, C. *ECS Trans.* **2009**, 25, 181. (i) Pallem, V.R.; Dussarrat, C., U.S. Pat. Appl. Publ., 2011, US 20110250354 A1 20111013. (j) Turgambaeva, A.; Prud'homme, N.; Krisyuk, V.; Vahlas, C. *J. Nanosci. Nanotechnol.* **2011**, *11*, 8198. (k) Shenai-Khatkhate, D. V.; Manzik, S. J.; Wang, Q. M., U.S. Pat. Appl. Publ., 2009, US 20090017208 A1 20090115. (l) Li, Z.; Lee, D. K.; Coulter, M.; Rodriguez, L. N. J.; Gordon, R. G. *Dalton Trans.* **2008**, 2592. (m) Li, X.-G.; Li, Z.; Li, H.; Gordon, R. G. *Eur. J. Inorg. Chem.* **2007**, 1135. (n) Li, Z.; Barry, S. T.; Gordon, R. G. *Inorg. Chem.* **2005**, *44*, 1728.

13. (a) Seetula, J.; Kalliorinne, K.; Koskikallio, J. *J. Photochem. Photobiol., A.: Chem.* **1988**, *43*, 31. (b) Hancock, K. G.; Dickinson, D. A. *J. Org. Chem.* **1975**, *40*, 969. (c) Zhang, X.-H.; Chen, S.-J.; Cai, H.; Im, H.-J.; Chen, T.; Yu, X.; Chen, X.; Lin, Z.; Wu, Y.-D.; Xue, Z.-L. *Organometallics* **2008**, *27*, 1338.
14. Miller, J. B.; Bernasek, S. L.; Schwartz, J. *J. Am. Chem. Soc.* **1995**, *117*, 4037.
15. Mal, S. S.; Nsouli, N. H.; Carraro, M.; Sartorel, A.; Scorrano, G.; Oelrich, H.; Walder, L.; Bonchio, M.; Kortz, U. *Inorg. Chem.* **2010**, *49*, 7.
16. Wang, G.-C.; Sung, H. H. Y.; Williams, I. D.; Leung, W.-H. *Inorg. Chem.* **2012**, *51*, 3640.
17. (a) Gericke, K. H.; Gölzenleuchter, H.; Comes, F. J. *J. Chem. Phys.* **1988**, *89*, 345. (b) Lee, J.; Chasteen, N. De.; Zhao, G.; Papaefthymiou, G. C.; Gorun, S.

M. *J. Am. Chem. Soc.* **2002**, *124*, 3042.

18. http://www.chemistry.ccsu.edu/glagovich/teaching/316/ir/table.html. Accessed on 05/18/2013.

19. (a) Sheldrick, G. M. SADABS, *A Program for Empirical Absorption Correction of Area Detector Data*; University of Göttingen, Göttingen, Germany, 1996. (b) Sheldrick, G. M. SHELXL-97, *A Program for the Refinement of Crystal Structures*, University of Göttingen, Göttingen, Germany, 1997.

Part 4

Syntheses and Characterization of Group 5 Amidinate Amide Complexes

Abstract

M[MeC(N^{i}Pr)$_2$](NMe$_2$)$_4$ (M = Nb, **26**; Ta, **27**) have been prepared by the aminolysis of M(NMe$_2$)$_5$ (M = Nb, Ta) with ^{i}PrN(H)C(Me)=N^{i}Pr (**7**). Compounds **26** and **27** have been characterized by ^{1}H and ^{13}C{^{1}H} NMR spectroscopies and elemental analyses. CCl_4 reacts with **27** and replaces an amide ligand with a chloride to form Ta[MeC(N^{i}Pr)$_2$](NMe$_2$)$_3$Cl (**28**). Compound **28** has also been prepared through the aminolysis of Ta(NMe$_2$)$_4$Cl with **7**. **28** has been characterized by ^{1}H, ^{13}C{^{1}H} , and 2-D NMR spectroscopies and MS.

4.1. Introduction

Early transition metal complexes with nitrogen-containing ligands are currently studied as precursors to metal oxide thin films through their reactions with O_2, H_2O or O_3 in chemical vapor deposition (CVD) and atomic layer deposition (ALD) processes.[1,2] These complexes often contain metals with no valence *d* electrons (d^0).[3] Their reactions with O_2[3,4] are different from those of late transition metal complexes containing *d* electrons (d^n).[5]

Homoleptic Group 5 amides $M(NR_2)_n$ (M = Nb, Ta) have been used as CVD precursors.[1a,6] As the earlier work of our group shows, these amide complexes such as $M(NMe_2)_n$ (M = Nb, Ta) are very sensitive to O_2[3b,3e] and H_2O.[7] For example, $M(NMe_2)_5$ reacts with O_2 at -25 to 23 °C, yielding several products (Scheme 4.1).[3b,3e] Exposure of $M(NMe_2)_n$ (M = Nb, Ta) to H_2O at -40 °C and then at 23 °C yields metal cage complexes $[(Me_2N)_3MO]_4$ (Scheme 4.2).[7] Bidentate ligands such as amidinate, β-diketiminate, and guanidinate (Figure 4.1) have been introduced as ancillary ligands in order to make complexes more stable or less reactive towards an O-source.

In the current work, two Group 5 amidinate amide complexes $M[MeC(N^iPr)_2](NMe_2)_4$ (M = Nb, **26**; Ta, **27**) have been prepared through aminolysis. They are good candidates as precursors for making metal oxide thin films. Since reactions with O_2 often occur through a radical process, CCl_4, a radical trap, has been tested to see if it could be used in trapping an intermediate. However, CCl_4 reacts with **27**, undergoing a Cl^--NMe_2^- exchange to yield $Ta[MeC(N^iPr)_2](NMe_2)_3Cl$ (**28**). Our studies are reported here.

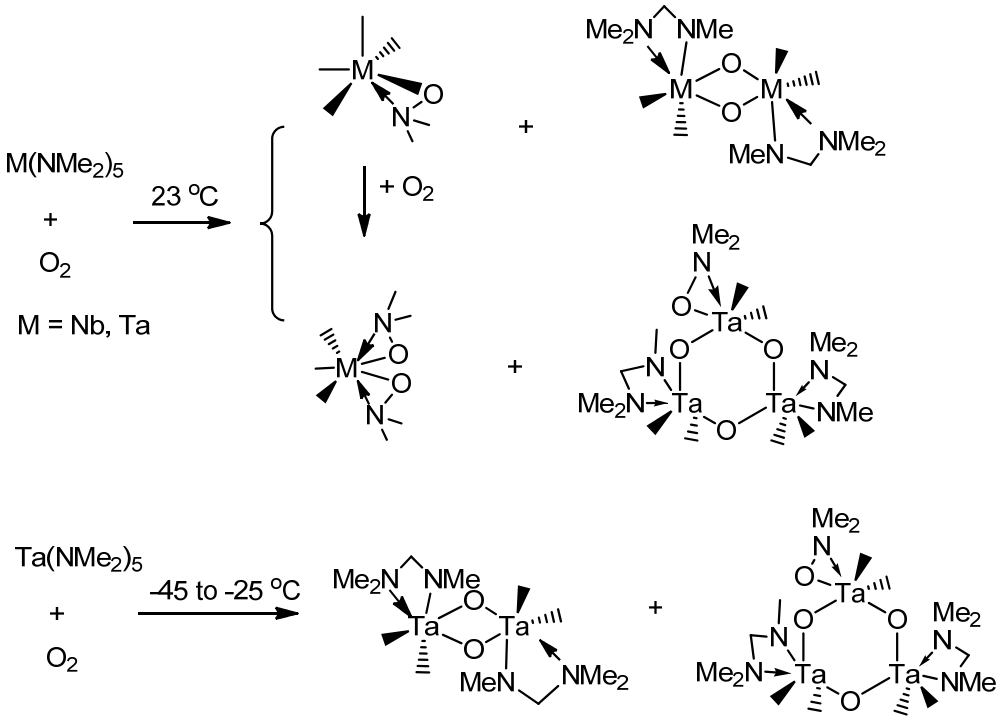

Scheme 4.1. Reactions of $M(NMe_2)_5$ (M = Nb, Ta) with O_2.[3b,3e]

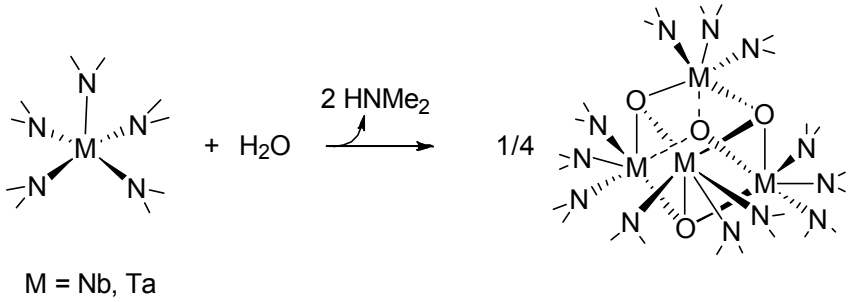

Scheme 4.2. Reactions of $M(NMe_2)_5$ (M = Nb, Ta) with H_2O.[7]

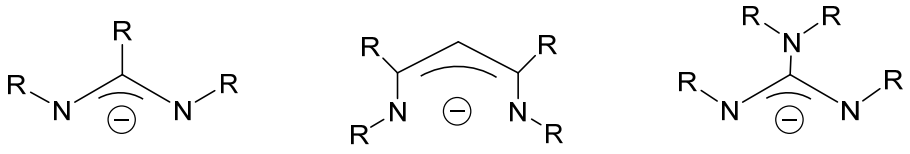

Figure 4.1. Bidentate nitrogen donor ancillary ligands.

4.2. Results and Discussion

4.2.1. Synthesis of Nb[MeC(N^{i}Pr)$_2$](NMe$_2$)$_4$ (26)

Nb[MeC(N^{i}Pr)$_2$](NMe$_2$)$_4$ (**26**) was prepared by reacting 1 equiv of ^{i}PrN(H)C(Me)=N^{i}Pr (**7**) with Nb(NMe$_2$)$_5$ (Scheme 4.3). Volatiles were removed in vacuo and pentane was added in order to grow crystals of **26**. Crystals of **26** in 78.5% yield were washed at -30 °C with pentane and showed they were analytically pure. Crystals of **26** here and those from recrystallization from toluene were not of X-ray quality.

The ^{1}H NMR spectrum of **26** in benzene-d_6 (Figure 4.2) showed a doublet at 1.18 ppm. Three singlets were observed, one for NC(*Me*)N and two for the amide groups at 1.60, 3.25 and 3.36 ppm, respectively. A multiplet was observed at 3.64 ppm for the C*H*Me$_2$ groups. The ^{13}C{^{1}H} NMR spectrum (Figure 4.3), peaks at 12.64 and 169.04 ppm were assigned to -C(*Me*) and -*C*(Me)- groups on the amidinate, respectively. The CH*Me$_2$* groups were observed at 25.34 ppm. The *C*H carbon atoms of the *C*HMe$_2$ groups appear at 48.56 ppm. The peaks at 49.37 and 49.90 ppm account for the N*Me$_2$* groups.

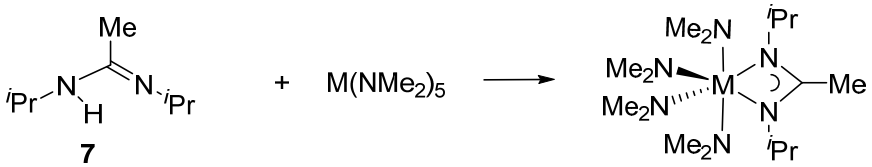

M = Nb, **26**; Ta, **27**

Scheme 4.3. Preparation of **26** and **27**.

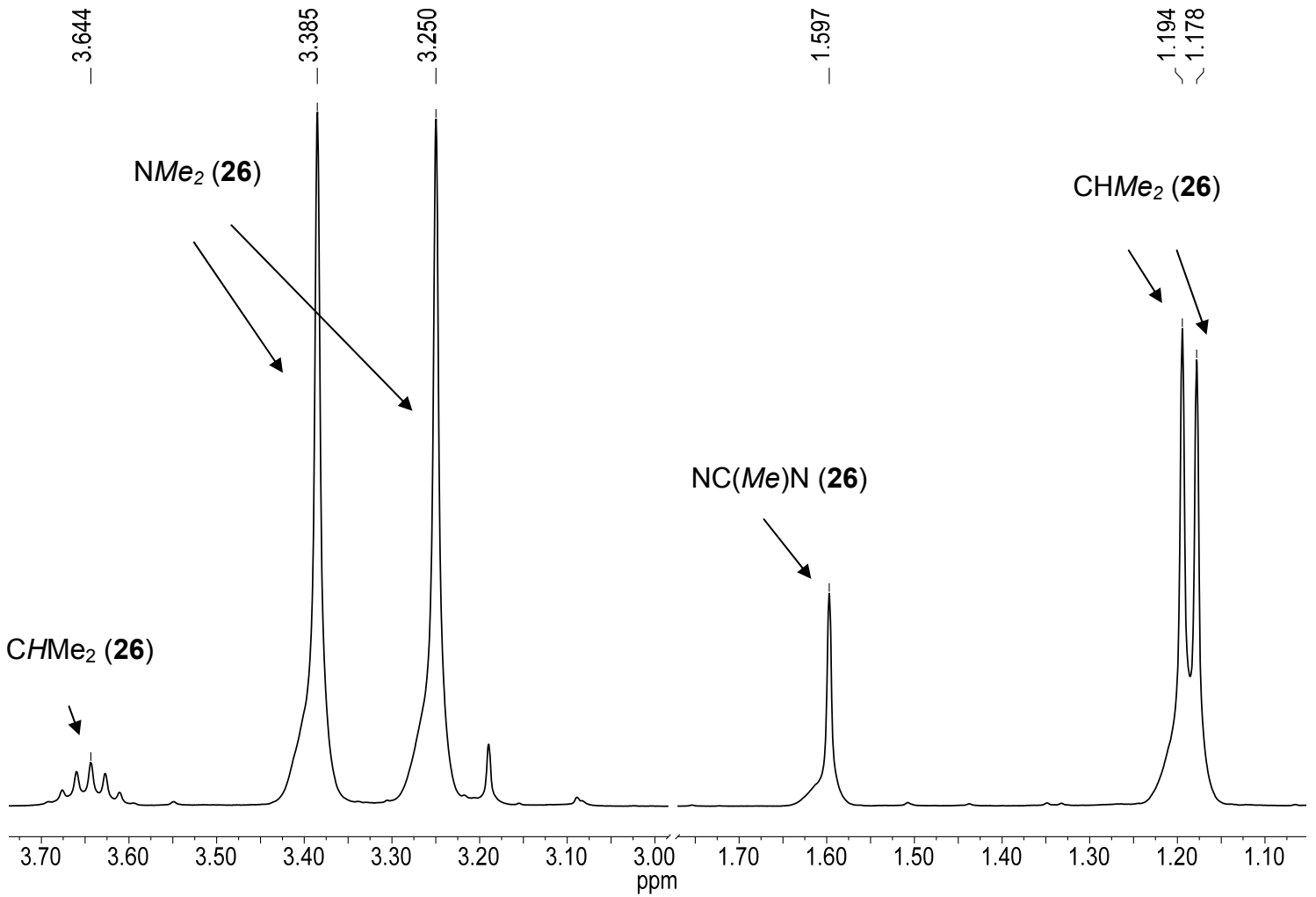

Figure 4.2. ^{1}H NMR spectrum of **26** in benzene-d_6.

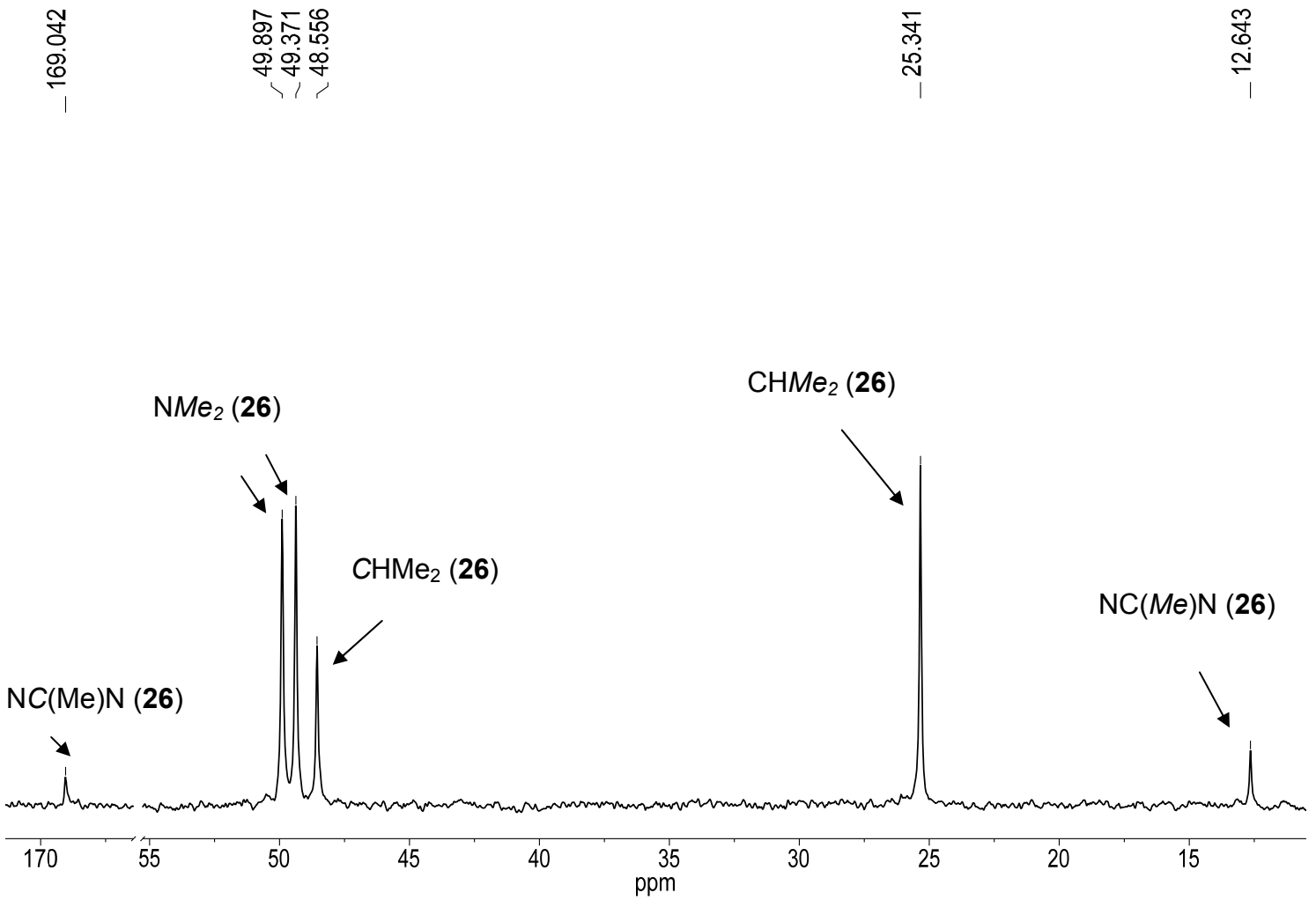

Figure 4.3. $^{13}C\{^{1}H\}$ NMR spectrum of **26** in benezene-d_6.

4.2.2. Synthesis of Ta[MeC(N^{i}Pr)$_2$](NMe$_2$)$_4$ (27)

Ta[MeC(N^{i}Pr)$_2$](NMe$_2$)$_4$ (**27**) was prepared by reacting 1 equiv of **7** with Ta(NMe$_2$)$_5$ (Scheme 4.3). Volatiles were removed in vacuo and pentane was added in order to grow crystals of **27**. Crystals of **27** were washed at -30 °C with pentane and gave analytically pure **27** in 86.0% yield. Crystals of **27** here and those from recrystallization in toluene were not of X-ray quality.

The ^{1}H NMR spectrum of **27** in benzene-d_6 (Figure 4.4) showed a doublet at 1.18 ppm. Three singlets were observed, one for NC(*Me*)N and two for the amide groups at 1.52, 3.41 and 3.52 ppm, respectively. A multiplet was observed at 3.72 ppm for the C*H*Me$_2$ groups. The ^{13}C{^{1}H} NMR spectrum (Figure 4.5), peaks at 13.97 and 169.40 ppm were assigned to -C(*Me*) and -*C*(Me)- groups on the amidinate, respectively. The peak at 25.05 ppm accounts for the CH*Me$_2$* groups. The *C*H carbon atoms of the *C*HMe$_2$ groups appear at 48.07 ppm. The peaks at 47.94 and 48.49 ppm account for the N*Me$_2$* groups.

4.2.3. Synthesis and Discussion of Ta[MeC(N^{i}Pr)$_2$](NMe$_2$)$_3$Cl (28)

O_2 is a diradical and the reaction of **10** with O_2 goes through a radical process. It is of interest to see if the reaction of Ta[MeC(N^{i}Pr)$_2$](NMe$_2$)$_4$ (**27**) and O_2 also goes through a pathway involving radical intermediates.

$BrCCl_3$ and CCl_4 have both been used extensively for radical trapping.[8] For example, the cyclopropyl radical is known to be a rapidly inverting σ radical of high reactivity. Experiments have been performed using radical trapping to determine the extent substituted cyclopropyl radicals are capable of maintaining

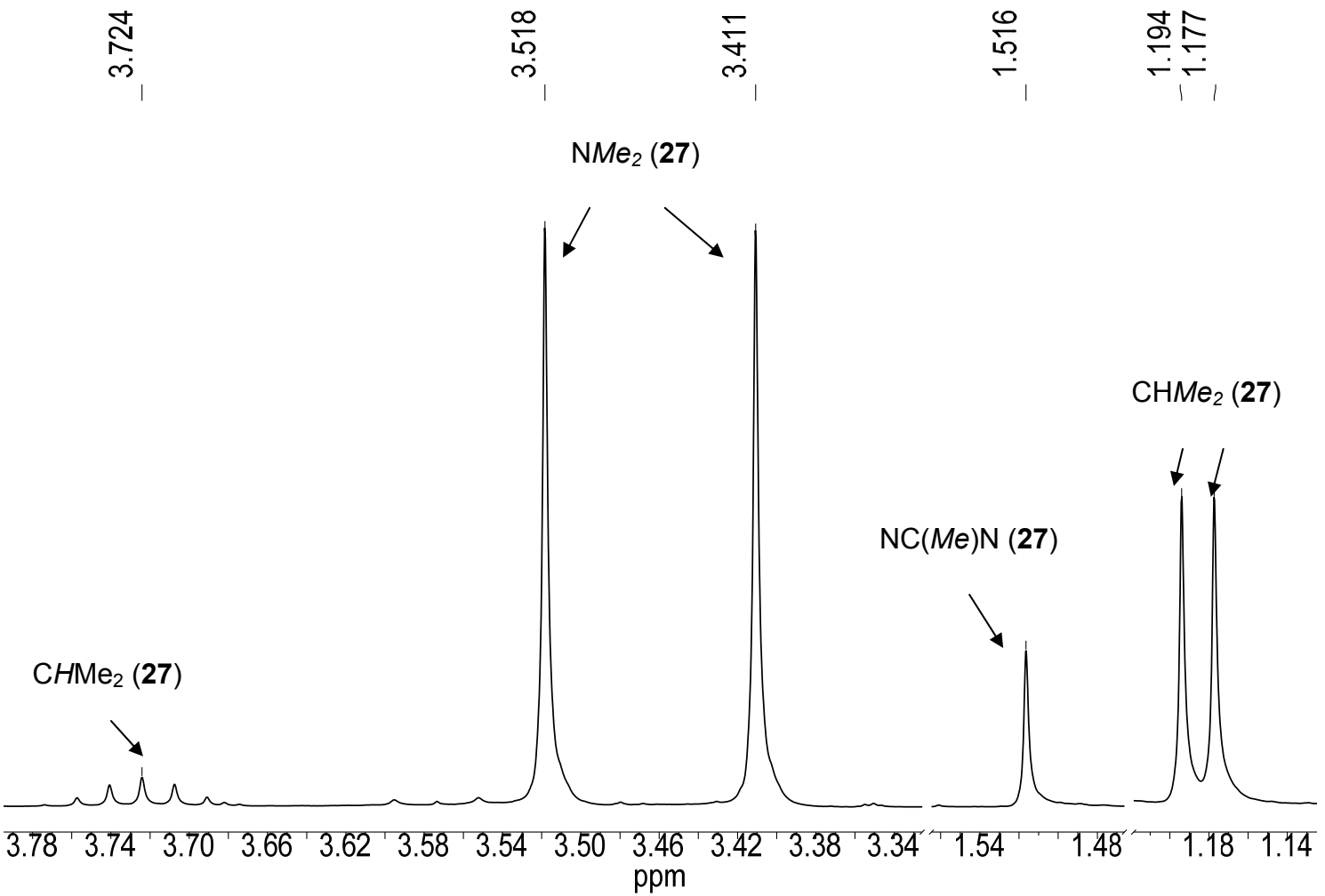

Figure 4.4. ^{1}H NMR spectrum of **27** in benzene-d_6.

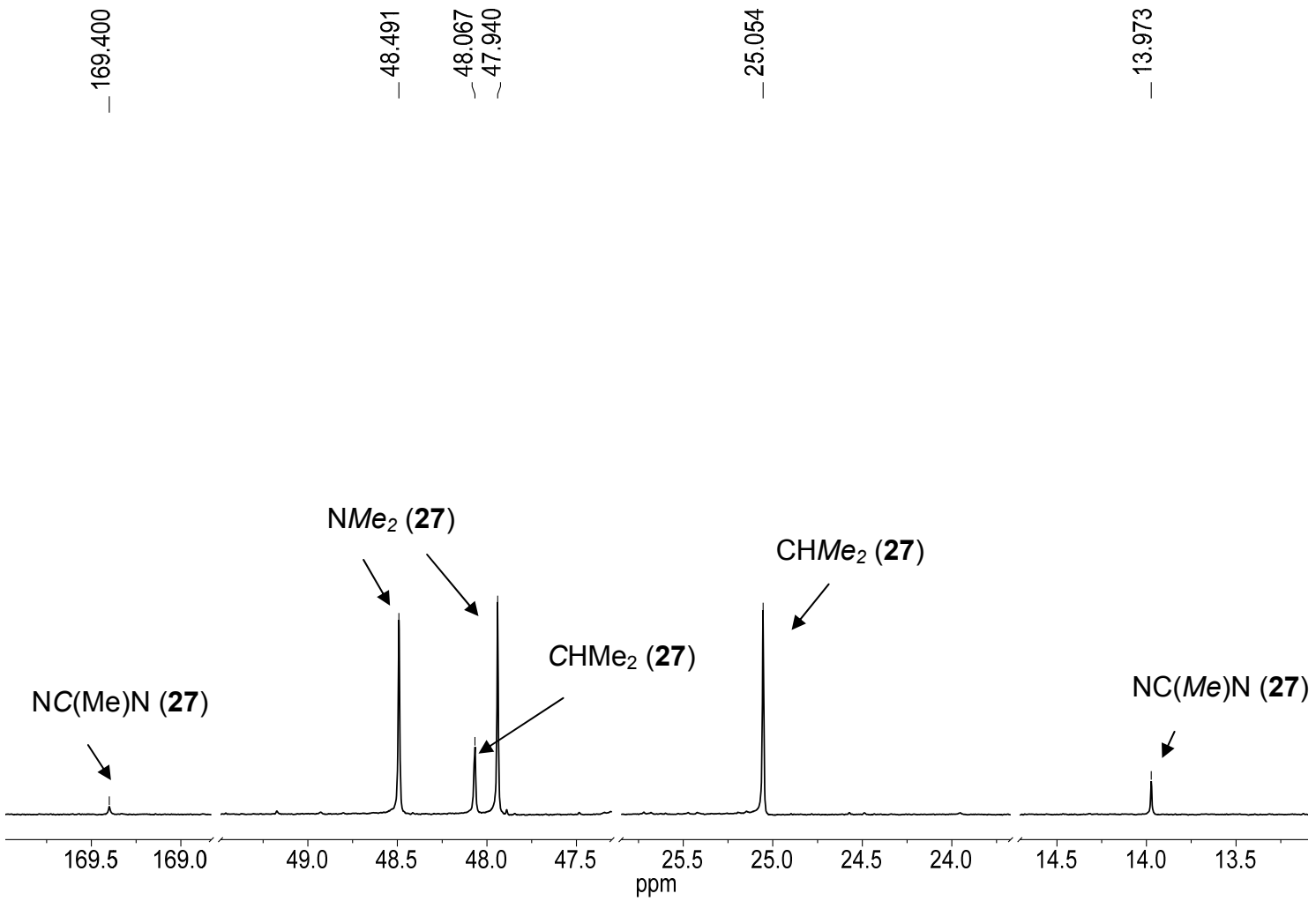

Figure 4.5. $^{13}C\{^{1}H\}$ NMR spectrum of **27** in benzene-d_6.

their original configuration.[8a] CCl_4 was chosen as a trap for the cyclopropyl radical (Scheme 4.4).

$$c\text{-}C_3H_5\bullet + CCl_4 \rightarrow c\text{-}C_3H_5Cl + \bullet CCl_3$$

Scheme 4.4. CCl_4 as a radical trap.

If CCl_4 is used as a radical trap for the reaction of Ta[MeC(N^{i}Pr)$_2$](NMe$_2$)$_4$ (**27**) with O_2, it should not react with **27** itself. We have tested to see if CCl_4 reacts with **27**. In a Young's tube, **27** in benzene-d_6 was added CCl_4 and heated at 65 °C for 4 h. ^{1}H NMR spectrum showed that CCl_4 did react with **27** (Scheme 4.5) and an amide and chloride exchange occurred to form Ta[MeC(N^{i}Pr)$_2$](NMe$_2$)$_3$Cl (**28**). To confirm **28**, it was prepared by reacting 1 equiv of **7** with Ta(NMe)$_4$Cl[8,9] in 85.1% yield (Scheme 4.5).

The ^{1}H NMR spectrum of **28** in benzene-d_6 (Figure 4.6) showed two doublets at 1.16 and 1.29 ppm. Three singlets were observed. One for NC(*Me*)N and two for the amide groups at 1.48, 3.43 and 3.70 ppm, respectively. A multiplet was observed at 3.80 ppm for the C*H*Me$_2$ groups.

The ^{13}C{^{1}H} NMR spectrum (Figure 4.7), peaks at 13.31 and 172.14 ppm were assigned to -C(*Me*) and -*C*(Me)- groups on the amidinate, respectively. Two peaks at 24.12 and 24.26 ppm account for the CH*Me$_2$* groups. The *C*H carbon

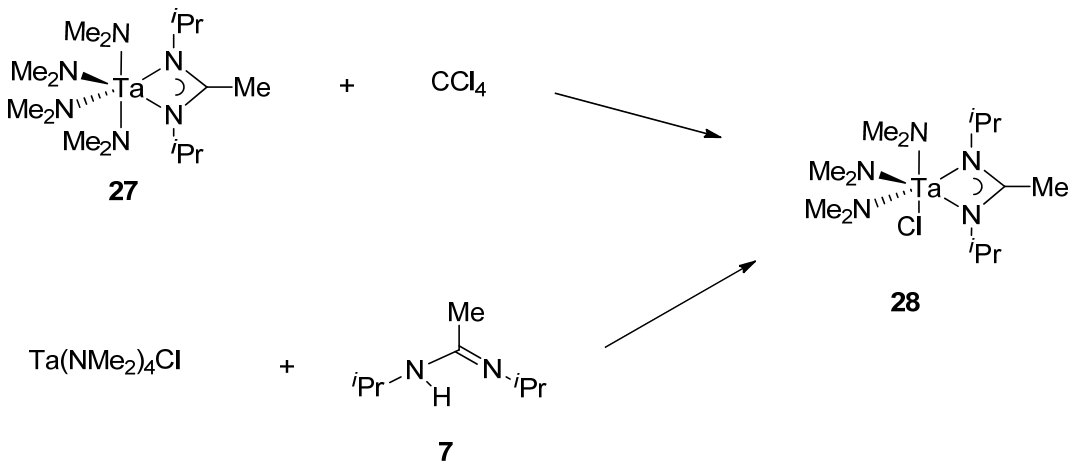

Scheme 4.5. Two methods to prepare **28**.

atoms of the *C*HMe$_2$ groups appear at 48.94 ppm. The peaks at 48.70 and 48.36 ppm account for the N*Me$_2$*.

Compound **28** was also characterized by mass spectrometry with an *m*/z = 445.15 for [**28**-NMe$_2^+$]. Tantalum has one stable isotope (^{181}Ta; Table 4.1) and chlorine has two isotopes (^{35}Cl, ^{37}Cl; Table 4.1). Thus MS of **28** is expected to show a unique pattern. Solid powders of **28** were placed in a heated (400 °C) He stream by the sealed end of a capillary tube. The MS spectrum is given in Figure 4.8 along with the predicted spectrum. The MS spectrum confirmed the identity of **28**.

Table 4.1. Stable isotopes of tantalum and chlorine

Isotope	Accurate Mass	% Natural Abundance
^{181}Ta	180.947992(3)	99.988(2)
^{35}Cl	34.968852721(69)	75.78(4)
^{37}Cl	36.96590262(11)	24.22(4)

4.3. Concluding Remarks

Two Group 5 amidinate amide complexes, **26** and **27**, have been prepared and characterized. The radical trap, CCl_4, did react with **27** and replaced one amide ligand with a chloride to form **28**. **28** has also been prepared by reacting $Ta(NMe_2)_4Cl$ with **7**. It has been characterized through NMR spectroscopies and MS.

4.4. Experimental Section

All manipulations were carried out under a dry nitrogen atmosphere with the use of either a glovebox or standard Schlenk techniques. All glassware was flamed dried under vacuum. $LiNMe_2$ was purchased from Acros and used without further purification. Solvents were purified by distillation from a potassium benzophenone ketyl. NMR solvents were dried and stored over 5 Å molecular sieves. $NbCl_5$ and $TaCl_5$ were purchased from Strem and were used without

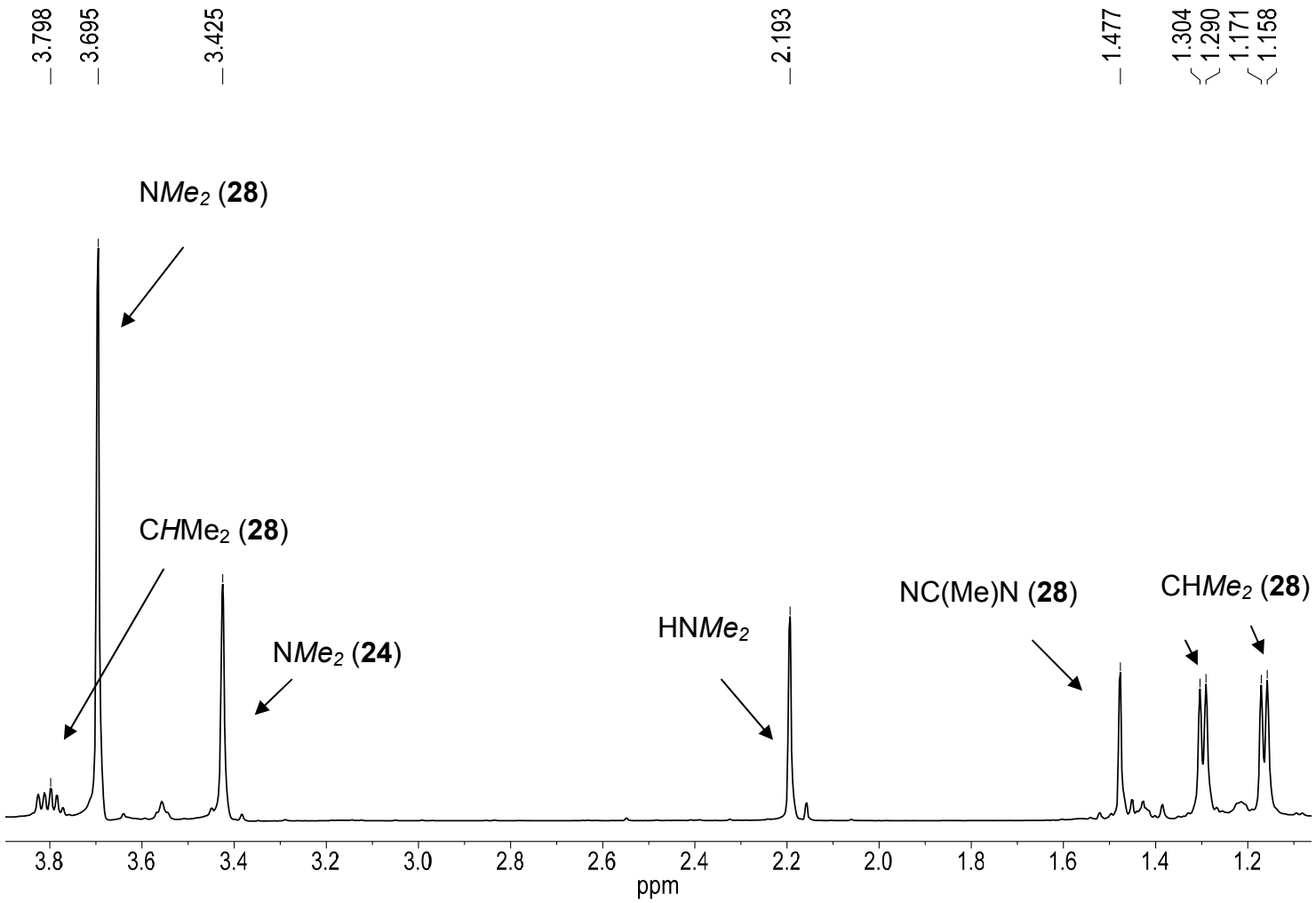

Figure 4.6. ^{1}H NMR spectrum of reaction mixture of **7** and $Ta(NMe_2)_4Cl$ giving **28** in benzene-d_6.

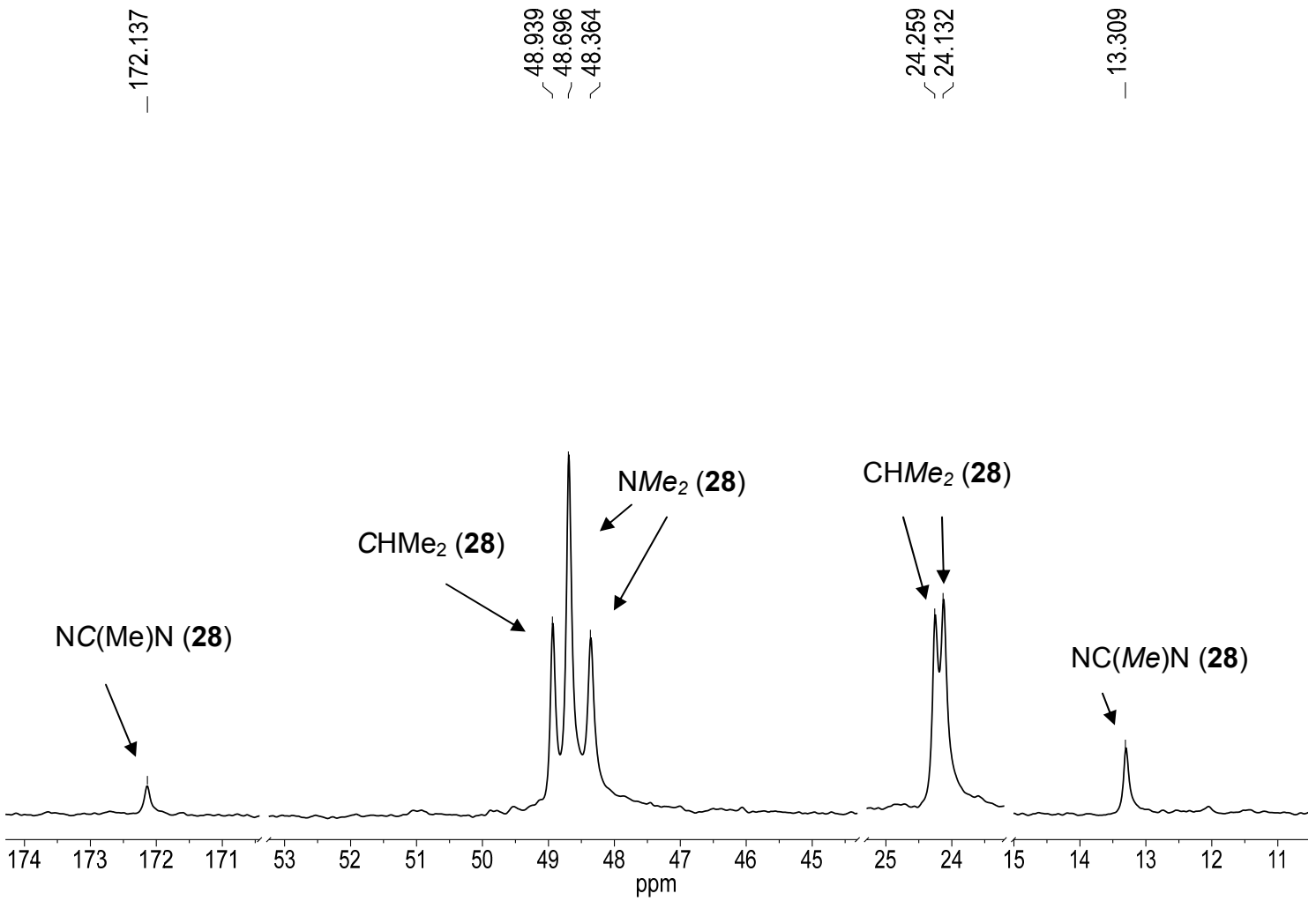

Figure 4.7. $^{13}C\{^{1}H\}$ NMR spectrum of **28** in benzene-d_6.

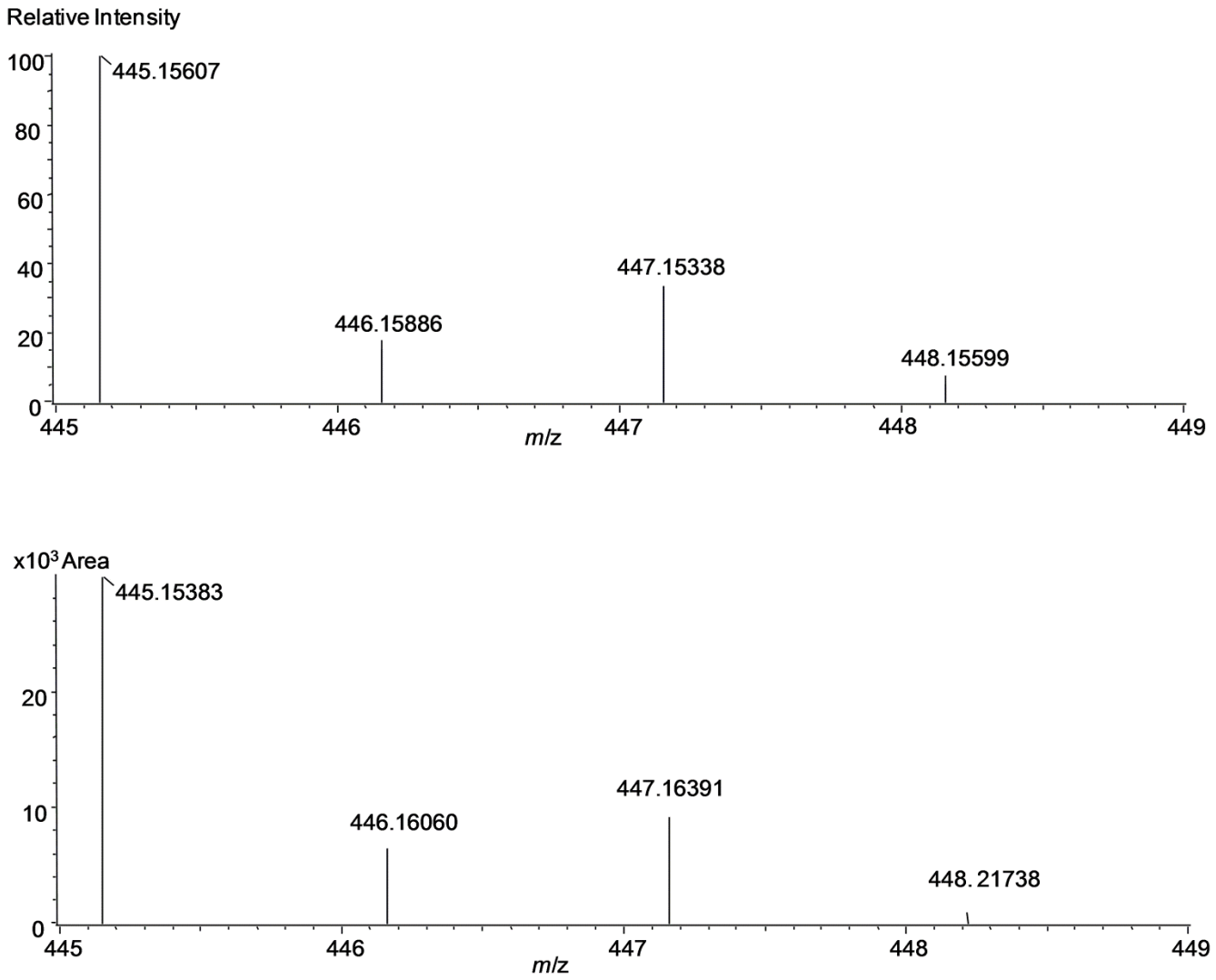

Figure 4.8. (Top) Calculated and (Bottom) Observed MS of [**28**-NMe_2^+].

further purification. $M(NMe_2)_5$ (M = Nb, Ta)[10,11] and $Ta(NMe)_4Cl$[8,9] were prepared by the literature methods. **7** was made according to Section 2.4.3. CCl_4 was dried over activated molecular sieves and stored under nitrogen. ^1H and $^{13}C\{^1H\}$ NMR spectra were recorded on a AMX-400 FT or Varian VNMRS-500 spectrometer. Elemental analyses were conducted by Complete Analysis Laboritories, Inc., Parsippany, NJ. Mass spectra were recorded on a JEOL AccuTOF™ DART Mass Spectrometer.

4.4.1. Synthesis of Nb[MeC(N^{i}Pr)$_2$](NMe$_2$)$_4$ (26)

$Nb(NMe_2)_5$ (2.882 g, 9.20 mmol) was dissolved in pentane (50 mL) and cooled to -30 °C. Compound **7** (1.345 g, 9.46 mmol) was dissolved in pentane (50 mL) and added dropwise to the pentane solution of $Nb(NMe_2)_5$. The solution was stirred for 12 h and volatiles removed in vacuo affording a red solid (2.964 g, 7.22 mmol, 78.51% yield). ^1H NMR (benzene-d_6, 400.17 MHz, 23 °C): δ 3.64 (m, 2H, C*H*Me$_2$), 3.39 (s, 12H, N*Me$_2$*), 3.26 (s, 12H, N*Me$_2$*), 1.58 (s, 3H, NC(*Me*)N), 1.19 (d, 12H, CH*Me$_2$*); ^{13}C NMR (benzene-d_6, 100.63 MHz, 23 °C): δ 169.06 (N*C(*Me)N), 49.93 (N*Me$_2$*), 49.36 (N*Me$_2$*), 48.53 (*C*HMe$_2$), 25.33 (CH*Me$_2$*), 12.58 (NC(*Me*)N). ^1H and ^{13}C assignments were confirmed by DEPT, HMQC and Nosey experiments. Anal. Calcd: C, 46.82; H, 10.07; N, 20.48. Found: C, 46.75; H, 9.98; N, 20.45.

4.4.2. Synthesis of Ta[MeC(N^{i}Pr$_2$)](NMe$_2$)$_4$ (27)

$Ta(NMe_2)_5$ (1.147 g, 2.86 mmol) was dissolved in pentane (50 mL) and cooled to -30 °C. Compound **7** (0.410 g, 2.88 mmol) was dissolved in pentane (50 mL) and added dropwise to the pentane solution of $Ta(NMe_2)_5$. The solution was stirred for 12 h and volatiles removed in vacuo affording a yellow solid (1.225 g, 2.46 mmol, 86.00% yield). ^{1}H NMR (benzene-d_6, 400.17 MHz, 23 °C): δ 3.72 (m, 2H, C*H*Me$_2$), 3.52 (s, 12H, N*Me$_2$*), 3.41 (s, 12H, N*Me$_2$*), 1.51 (s, 3H, NC(*Me*)N), 1.18 (d, 12H, CH*Me$_2$*); ^{13}C NMR (benzene-d_6, 100.63 MHz, 23 °C): δ 169.42 (N*C(*Me)N), 48.49 (N*Me$_2$*), 48.06 (*C*HMe$_2$), 47.94 (N*Me$_2$*), 25.05 (CH*Me$_2$*), 13.96 (NC(*Me*)N). ^{1}H and ^{13}C assignments were confirmed by DEPT and HSQC experiments. Anal. Calcd: C, 38.55; H, 8.29; N, 16.86. Found: C, 38.47; H, 8.24; N, 16.74.

4.4.3. Synthesis of Ta[MeC(N^{i}Pr)$_2$](NMe$_2$)$_3$Cl (28)

Method 1. This reaction was conducted in a J. Young's tube and reagents were mixed in a glovebox. $Ta(NMe)_4Cl$ (23.2 mg, 0.0591 mmol) was dissolved in benzene-d_6 (1 mL). Compound **7** (8.6 mg, 0.061 mmol) was added to a vial and dissolved in benzene-d_6 (1 mL) and added dropwise via pipette to the solution of $Ta(NMe_2)_4Cl$. The solution was allowed to be mixed and volatiles removed in vacuo affording a yellow solid (24.6 mg, 0.0502 mmol, 85.1% yield).

Method 2. Ta[MeC(N^{i}Pr)$_2$](NMe$_2$)$_4$ (**27**) was dissolved in benzene-d_6 and added to a J. Young's tube. Excess CCl_4 was added and the NMR tube was placed in an oil bath at 65 °C and heated for 4 h. The volatiles were then

removed in vacuo, and benzene-d_6 was added to obtain NMR spectra. ^{1}H NMR (benzene-d_6, 400.17 MHz, 23 °C): δ 3.78 (m, 2H, C*H*Me$_2$), 3.68 (s, 12H, N*Me$_2$*), 3.41 (s, 6H, N*Me$_2$*), 1.46 (s, 6H, NC(*Me*)N), 1.29 (d, 12H, CH*Me$_2$*), 1.16 (d, 12H, CH*Me$_2$*); ^{13}C NMR (benzene-d_6, 100.62 MHz, 23 °C): δ 172.14 (N*C(*Me)N), 48.94 (*C*HMe$_2$), 48.70 (N*Me$_2$*) 48.36 (N*Me$_2$*), 24.26 (CH*Me$_2$*), 24.13 (NC(*Me*)N). ^{1}H and ^{13}C assignments were confirmed by COSY, DEPT and HSQC experiments. DART-MS: Calc'd for [**28**-NMe$_2^+$], *m*/z = 445.15607; Obs'd, 445.15383.

References

1. For CVD of metal oxides using O_2, see, for example, (a) Son, K.-A.; Mao, A. Y.; Sun, Y.-M.; Kim, B. Y.; Liu, F.; Kamath, A.; White, J. M.; Kwong, D. L.; Roberts, D. A.; Vrtis, R. N. *Appl. Phys. Lett.* **1998**, *72*, 1187. (b) Niimi, H.; Johnson, R. S.; Lucovsky, G.; Massoud, H. Z. *Proc. Electrochem. Soc.* **2000**, *2000-2*, 487. (c) Eichler, J. F.; Just, O.; Rees, W. S., Jr. *J. Mater. Chem.* **2004**, *14*, 3139. (d) Takahashi, K.; Funakubo, H.; Hino, S.; Nakayama, M.; Ohashi, N.; Kiguchi, T.; Tokumitsu, E. *J. Mater. Res.* **2004**, *19*, 584. (e) Ogura, A.; Ito, K.; Ohshita, Y.; Ishikawa, M.; Machida, H. *Thin Solid Films* **2003**, *441*, 161. (f) Rodriguez-Reyes, J. C. F.; Teplyakov, A. V. *J. Appl. Phys.* **2008**, *104*, 084907/1. (g) Ohshita, Y.; Ogura, A.; Ishikawa, M.; Kada, T.; Machida, H. *Jpn. J. Appl. Phys. 2.* **2003**, *42*, L578. (h) Matero, R.; Ritala, M.; Leskelae, M.; Sajavaara, T.; Jones, A. C.; Roberts, J. L. *Chem. Mater.* **2004**, *16,* 5630. (i) Kan, B.-C.; Boo, J.-H.; Lee, I.; Zaera, F. *J. Phys. Chem. A* **2009**, *113*, 3946. (j) Hausmann, D. M.; de Rouffignac, P.; Smith, A.; Gordon, R.; Monsma, D. *Thin Solid Films* **2003**, *443*, 1. (k) Meiere, S. H.; Peck, J.; Litwin, M. *ECS Trans.* **2006**, *1*, 103. (l) Chen, T.; Cameron, T. M.; Nguyen, S. D.; Stauf, G. T.; Peters, D. W.; Maylott, L.; Li, W.; Xu, C.; Roeder, J. F.; Hendrix, B. C.; Hilgarth, M.; Niinisto, J.; Kukli, K.; Ritala, M.; Leskela, M. *ECS Trans.* **2008**, *16*, 87. (m) Lee, S.; Kim, W.-G.; Rhee, S.-W.; Yong, K. *J. Electrochem. Soc.* **2008**, *155*, H92. (n) Schaeffer, J.; Edwards, N. V.; Liu, R.; Roan, D.; Hradsky, B.; Gregory, R.; Kulik, J.; Duda, E.; Contreras, L.; Christiansen, J.; Zollner, S.; Tobin, P.; Nguyen, B.-Y.; Nieh, R.; Ramon, M.;

Rao, R.; Hegde, R.; Rai, R.; Baker, J.; Voight, S. *J. Electrochem. Soc.* **2003**, *150*, F67. (o) Woods, J. B.; Beach, D. B.; Nygren, C. L.; Xue, Z.-L. *Chem. Vap. Deposition* **2005**, *11*, 289. (p) Lehn, J.-S.; Javed, S.; Hoffman, D. M. *Chem. Vap. Deposition* **2006**, *12*, 280. (q) Chiu, H.-T.; Wang, C.-N.; Chuang, S.-H.; *Chem. Vap. Deposition* **2000**, *6*, 223. (r) Wiedmann, M. K.; Heeg, M. J.; Winter, C. H. *Inorg. Chem.* **2009**, *48*, 5382.

2. For CVD of metal oxides using water, see, for example, (a) Dezelah, C. L., IV; Niinisto, J.; Kukli, K.; Munnik, F.; Lu, J.; Ritala, M.; Leskela, M.; Niinisto, L. *Chem. Vap. Deposition* **2008**, *14*, 358. (b) Dezelah, C. L., IV; El-Kadri, O. M.; Szilagyi, I. M.; Campbell, J. M.; Arstila, K.; Niinistoe, L.; Winter, C. H. *J. Am. Chem. Soc.* **2006**, *128*, 9638. (c) Majumder, P.; Jursich, G.; Takoudis, C. *J. Appl. Phys.* **2009**, *105*, 104106/1. (d) Consiglio, S.; Clark, R. D.; Nakamura, G.; Wajda, C. S.; Leusink, G. J. *J. Vacuum Sci. Technol., A* **2012**, *30*, 01A119/1. (e) Tao, Q.; Kueltzo, A.; Singh, M.; Jursich, G.; Takoudis, C. G. *J. Electrochem. Soc.* **2011**, *158*, G27. (f) Shi, X.; Tielens, H.; Takeoka, S.; Nakabayashi, T.; Nyns, L.; Adelmann, C.; Delabie, A.; Schram, T.; Ragnarsson, L.; Schaekers, M.; Date, L.; Schreutelkamp, R.; Van Elshocht, S. *J. Electrochem. Soc.* **2011**, *158*, H69.

3. (a) Wang, R.; Zhang, X.; Chen, S.-J.; Yu, X.; Wang, C.; Beach, D. B.; Wu, Y.; Xue, Z. *J. Am. Chem. Soc.* **2005**, *127*, 5204. (b) Chen, S.; Zhang, X.; Yu, X.; Qiu, H.; Yap, G. P. A.; Guzei, I. A.; Lin, Z.; Wu, Y.; Xue, Z. *J. Am. Chem. Soc.* **2007**, *129*, 14408. (c) Chen, S.-J.; Zhang, X.-H.; Lin, Z.; Wu, Y.-D.; Xue, Z.-L. *Sci. China Chem.* **2009,** *52*, 1723. (d) Chen, S.-J.; Yap, G. P. A.; Xue, Z.-L.

Sci. China Chem. **2009**, *52*, 1583. (e) Chen, S.-J.; Zhang, J.; Yu, X.; Bu, X.; Chen, X.; Xue, Z. *Inorg. Chem.* **2010**, *49*, 4017. (f) Chen, T.-N.; Zhang, X.-H.; Wang, C.-S.; Chen, S.-J.; Wu, Z.-Z.; Li, L.-T.; Sorasaenee, K. R.; Diminnie, J. B.; Pan, H.-J.; Guzei, I. A.; Rheingold, A. L.; Wu, Y.-D.; Xue, Z.-L. *Organometallics* **2005**, *24*, 1214. (g) Qiu, H.; Chen, S.-J.; Wang, C.-S.; Wu, Y.-D.; Guzei, I. A.; Chen, X.-T.; Xue, Z.-L. *Inorg. Chem.* **2009**, *48*, 3073. (h) Yu, X.; Chen, X.-T.; Xue, Z.-L. *Organometallics* **2009**, *28*, 6642. (i) Chen, S.-J.; Xue, Z.-L. *Organometallics* **2010**, *29*, 5579. (j) Wu, Z.; Cai, H.; Yu, X.-H.; Blanton, J. R.; Diminnie, J. B.; Pan, H.-J. ; Xue, Z.-L. *Organometallics* **2002**, *21*, 3973.

4. (a) Tilley, T. D. *Organometallics* **1985**, *4*, 1452. (b) Blackburn, T. F.; Labinger, J. A.; Schwartz, J. *Tetrahedron Lett.* **1975**, *16*, 3041. (c) Labinger, J. A.; Hart, D. W.; Seibert, W. E.; Schwartz, J. *J. Am. Chem. Soc.* **1975**, *97*, 3851. (d) Lubben, T. V.; Wolczanski, P. T. *J. Am. Chem. Soc.* **1987**, *109*, 424. (e) Lubben, T. V.; Wolczanski, P. T. *J. Am. Chem. Soc.* **1985**, *107*, 701. (f) Wang, R.; Folting, K.; Huffman, J. C.; Chamberlain, L. R.; Rothwell, I. P. *Inorg. Chim. Acta* **1986**, *120*, 81. (g) Gibson, V. C.; Redshaw, C.; Walker, G. L. P.; Howard, J. A. K.; Hoy, V. J.; Cole, J. M.; Kuzmina, L. G.; De Silva, D. S. *J. Chem. Soc., Dalton Trans.* **1999**, 161. (h) Schaverien, C. J.; Orpen, A. G. *Inorg. Chem.* **1991**, *30*, 4968. (i) Liu, X.; Cui, D. *Dalton Trans.* **2008**, 3747. (j) Van Asselt, A.; Santarsiero, B. D.; Bercaw, J. E. *J. Am. Chem. Soc.* **1986**, *108*, 8291. (k) Brindley, P. B.; Hodgson, J. C. *J. Organomet. Chem.* **1974**, *65*, 57. (l) Kim, S. J.; Choi, D. W.; Lee, Y. J.; Chae, B. H.; Ko, J. J.; Kang, S. O.

Organometallics **2004**, *23*, 559. (m) Morris, A. M.; Pierpont, C. G.; Finke, R. G. *Inorg. Chem.* **2009**, *48*, 3496. (n) Adam, W.; Putterlik, J.; Schuhmann, R. M.; Sundermeyer, J. *Organometallics* **1996**, *15*, 4586. (o) Vetter, W. M.; Sen, A. *Organometallics* **1991**, *10*, 244. (r) Van Asselt, A.; Trimmer, M. S.; Henling, L. M.; Bercaw, J. E. *J. Am. Chem. Soc.* **1988**, *110*, 8254. (p) Boro, B. J.; Lansing, R.; Goldberg, K. I.; Kemp, R. A. *Inorg. Chem. Comm.* **2011**, *14*, 531. (q) Stanciu, C.; Jones, M. E.; Fanwick, P. E.; Abu-Omar, M. M. *J. Am. Chem. Soc.* **2007**, *129*, 12400. (r) Lu, F.; Zarkesh, R. A.; Heyduk, A. F. *Eur. J. Inorg. Chem.* **2012**, 467. (s) Chisholm, M. H.; Hammond, C. E.; Huffman, J. C. *J. Chem. Soc., Chem. Commun.* **1987**, 1423. (t) Brindley, P. B.; Hodgson, J. C. *J. Organomet. Chem.* **1974**, *65*, 57.

5. For studies of the reactions between O_2 and late transition metal complexes, see, for example, (a) Campbell, A. N.; Stahl, S. S. *Acc. Chem. Res.* **2012**, *45*, 851. (b) Theopold, K. H.; Reinaud, O. M.; Blanchard, S.; Leelasubeharoen, S.; Hess, A.; Thyagarajan, S. *ACS Symp. Ser.* **2002**, *823*, 75. (c) Que, L.; Tolman, W. B. *Nature* **2008**, *455*, 333. (d) Himes, R. A.; Karlin, K. D. *Curr. Top. Chem. Biol.* **2009**, *13*, 119. (e) Shook, R. L.; Borovik, A. S. *Chem. Comm.* **2008**, 6095. (f) Sheldon, R. A. in *Biomimetic Oxidations Catalyzed by Transition Metal Complexes*, Meunier, B. ed., Imperial College Press, 2000, pp. 613-662. (g) *Metal-Dioxygen Complexes: A Perspective.* Special Issue, *Chem. Rev.* **1994**, *94*, Issue 3, 567-856. (h) Monillas, W. H.; Yap, G. P. A.; MacAdams, L. A.; Theopold, K. H. *J. Am. Chem. Soc.* **2007**, *129*, 8090. (i) McQuilken, A. C.; Jiang, Y.; Siegler, M. A.; Goldberg, D. P. *J. Am. Chem.*

Soc. **2012**, *134*, 8758. (j) Prokop, K. A.; Goldberg, D. P. *J. Am. Chem. Soc.* **2012**, *134*, 8014. (k) Scheuermann, M. L.; Fekl, U.; Kaminsky, W.; Goldberg, K. I. *Organometallics* **2010**, *29*, 4749. (l) Boisvert, L.; Denney, M. C.; Kloek Hanson, S.; Goldberg, K. I. *J. Am. Chem. Soc.* **2009**, *131*, 15802. (m) Khusnutdinova, J. R.; Rath, N. P.; Mirica, L. M. *J. Am. Chem. Soc.* **2012**, *134*, 2414. (n) Nguyen, K. T.; Rath, S. P.; Latos-Grazynski, L.; Olmstead, M. M.; Balch, A. L. *J. Am. Chem. Soc.* **2004**, *126*, 6210. (o) Maury, J.; Feray, L.; Bazin, S.; Clement, J.-L.; Marque, S. R. A.; Siri, D.; Bertrand, M. P. *Chem. Eur. J.* **2011**, *17*, 1586. (p) Lewinski, J.; Koscielski, M.; Suwala, K.; Justyniak, I. *Angew. Chem. Int. Ed.* **2009**, *48*, 7017. (q) Mukherjee, D.; Ellern, A.; Sadow, A. D. *J. Am. Chem. Soc.* **2012**, *134*, 13018. (r) Jana, S.; Berger, R. J. F.; Fröhlich, R.; Pape, T.; Mitzel, N. W. *Inorg. Chem.* **2007**, *46*, 4293. (s) Lee, C.-M.; Chuo, C.-H.; Chen, C.-H.; Hu, C.-C.; Chiang, M.-H.; Tseng, Y.-J.; Hu, C.-H.; Lee, G.-H. *Angew. Chem. Int. Ed.* **2012**, *51*, 5427. (t) Kelley, M. R.; Rohde, J.-U. *Chem. Comm.* **2012**, *48*, 2876. (u) Brown, S. N.; Mayer, J. M. *Inorg. Chem.* **1992**, *31*, 4091. (v) Parkin, G.; Bercaw, J. E. *J. Am. Chem. Soc.* **1989**, *111*, 391.

6. (a) Breme, F.; Guther, V.; Van Osten, K-U. EP 897997, 1998. (b) Senzaki, Y.; Roberts, D. A.; Norman, J. A. T. EP 1067595, 2001. (c) Bott, S. G.; Hoffman, D. M.; Rangarajan, S. P. *Inorg. Chem.* **1995**, *34*, 4305. (d) Fix, R.; Gordon, R. G.; Hoffman, D. M. *Chem. Mater.* **1993**, *5*, 614. (e) Lehn, J-S. M.; Heide, P. van der.; Wang, Y.; Suha, S.; Hoffman, D. M. *J. Mater. Chem.* **2004**, *14*, 3239. (f) Dezelah, C. L.; Wiedmann, M. K.; Mizohata, K.; Baird, R. J.; Niinisto,

L.; Winter, C. H. *J. Am. Chem. Soc.* **2007**, *129*, 12370. (g) Baunemann, A.; Lemberger, M.; Bauer, A. J.; Parala, H.; Fischer, R. A. *Chem. Vap. Deposition* **2007**, *13*, 77. (h) Gonohe, N.; Toyoda, S.; Ushikawa, H.; Kondo, T.; Nakamura, K. PCT Int. Appl. WO 2006093259, 2006. (i) Brown, G. M.; Maya, L. *J. Am. Ceram. Soc.* **1988**, *71*, 78.

7. Chen, S.-J.; Abbott, J. K. C.; Steren, C. A.; Xue, Z.-L. *J. Clust. Sci.* **2010**, *21*, 325.
8. Chisholm, M. H.; Tan, L.-S.; Huffman, J. C. *J. Am. Chem. Soc.* **1982**, *104,* 4879.
9. Chen, S.-J.; Cai, H.; Xue, Z.-L. *Organometallics* **2009**, *28*, 167.
10. Bradley, D. C.; Thomas, I. M. *Can. J. Chem.* **1962**, 449.
11. Bradley, D. C.; Thomas, I. M. *Can. J. Chem.* **1962**, 1355.

Part 5

Studies of the Reaction between $W(OMe)_3Cl_3$ and $Zn(CH_2{}^tBu)_2$

Abstract

Reaction between $W(OMe)_3Cl_3$ (**29**) and $Zn(CH_2{}^tBu)_2$ gives the previously reported alkylidyne complex $W(CH_2{}^tBu)_3(\equiv C{}^tBu)$ (**30**). The study, using the alkyl zinc reagent which is a weaker nucleophilic reagent than $LiCH_2{}^tBu$ and $Mg(CH_2{}^tBu)_2$, is an attempt to identify the intermediate(s) in the formation of $W(CH_2{}^tBu)_3(\equiv C{}^tBu)$ (**30**). The reaction between $W(OMe)_3Cl_3$ and $Zn(CH_2{}^tBu)_2$ also yields a side product $W(OMe)_2Cl(CH_2{}^tBu)_3$ (**21**) which has been characterized by ^1H, $^{13}C\{^1H\}$, HSQC, DEPT, and 1-D NOESY NMR spectroscopies.

5.1. Introduction

In 1973, E. O. Fischer reported the first d^n carbyne complex.[1] A carbyne complex contains at least one M≡C triple bond. Two types of carbyne complexes have since been reported: low-oxidation-state transition metal complexes (Fischer-type) and high-oxidation-state transition metal complexes (Schrock-type).[2] The Schrock-type carbyne complexes are also called alkylidynes. After the discovery of alkylidyne chemistry, the complexes have been actively studied. One approach to alkylidyne complexes is metathesis reactions between acetylenes and compounds with M≡M bonds.[3] Another widely used approach to alkylidyne complexes is reactions between RCH_2MgCl [R = CMe_3 (^{t}Bu), $SiMe_3$] and WCl_6 or $W(OMe)_3Cl_3$.[4,5] One typical reaction to give an alkylidyne complex is shown in Figure 5.1.[5] The use of more soluble $W(OMe)_3Cl_3$ increases the yield of the product **30**. One fundamental question that has not been answered is when the W≡C triple bond forms in the reactions to give, e.g., **30**.[3,4b] Attempts have been made in the past to identify the intermediates in the formation of **30**.[3,4b]

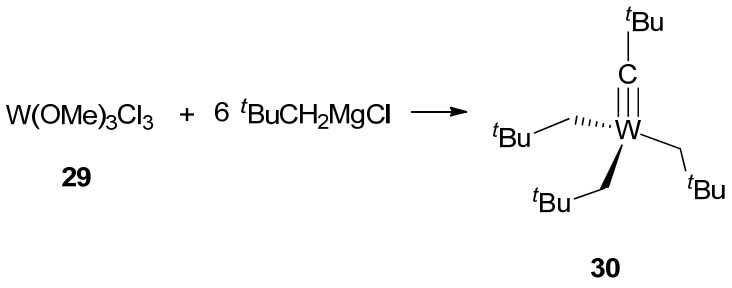

Scheme 5.1. Formation of an alkylidyne complex.

Schrock-type carbene (also known as alkylidene) complexes are another class of complexes with metal-carbon unsaturated bonds.[2] A carbene is a metal complex with at least one M=C double bond. Alkylidene compounds contain d^0 metal atoms at their high oxidation states. The first such compound is $(^t\text{BuCH}_2)_3\text{Ta}{=}\text{CH}^t\text{Bu}$ prepared by Schrock.[6] It was prepared by the reactions shown in Scheme 5.2. The reaction of $TaCl_5$ with $Zn(CH_2{}^t\text{Bu})_2$ gives $(^t\text{BuCH}_2)_3TaCl_2$, which then reacts with 2 equiv of $^t\text{BuCH}_2\text{Li}$ to give $(^t\text{BuCH}_2)_3\text{Ta}{=}\text{CH}^t\text{Bu}$ (Scheme 5.2).[6b]

$$TaCl_5 + Zn(CH_2{}^t\text{Bu})_2 \longrightarrow Ta(CH_2{}^t\text{Bu})_3Cl_2$$

$$Ta(CH_2{}^t\text{Bu})_3Cl_2 + LiCH_2{}^t\text{Bu} \longrightarrow Ta(=CH^t\text{Bu})(CH_2{}^t\text{Bu})_3$$

Scheme 5.2. Preparation of $(^t\text{BuCH}_2)_3\text{Ta}{=}\text{CH}^t\text{Bu}$.

The mechanistic pathway involves the initial formation of $Ta(CH_2{}^t\text{Bu})_5$, which was observed at 233 K and is short lived before it converts to $(^t\text{BuCH}_2)_3\text{Ta}{=}\text{CH}^t\text{Bu}$, as our group reported.[7] We have also used the reaction of $(^t\text{BuCD}_2)_3TaCl_2$ with $^t\text{BuCD}_2\text{Li}$ to probe the pathway in the formation of the M=C bond in the alkylidene complex.[8] In this design, only the methyl resonances would be observed in the ^{1}H NMR spectrum, reducing peak overlap. In addition,

by replacing the hydrogen atoms with deuterium atoms, the intermediate $Ta(CD_2{}^tBu)_5$ has a much longer life to be characterized and follow the kinetics of α-D abstraction to give the $Ta{=}CD{}^tBu$ bond in $({}^tBuCD_2)_3Ta{=}CD{}^tBu$. The kinetic isotope effect of the α-H/D in $Ta(CH_2{}^tBu)_5/Ta(CD_2{}^tBu)_5$ was measured.[8]

In the current work, a similar approach was used by reacting $Zn(CH_2{}^tBu)_2$ with two d^0 W(VI) complexes, WCl_6 and $W(OMe)_3Cl_3$ (**29**). The zinc alkyl reagent was selected because it is not as strong of an alkylating reagent as its lithium alkyl or magnesium alkyl analogs which have been used in making tungsten alkylidyne compounds.[4,5] The reaction between WCl_6 and $Zn(CH_2{}^tBu)_2$ at both 23 °C and -30 °C, which would be similar to the first step in Scheme 5.2, did not proceed as cleanly as the Ta analog $TaCl_5$. Since WCl_6 is not soluble in Et_2O, it was decided to use more soluble $W(OMe)_3Cl_3$ (**29**) in order to have a homogenous reaction between **29** and $Zn(CH_2{}^tBu)_2$. However, when $W(OMe)_3Cl_3$ (**29**) reacts with $Zn(CH_2{}^tBu)_2$, the products are the alkylidyne $W(CH_2{}^tBu)_3(\equiv C{}^tBu)$ (**30**) and another species identified to be $W(OMe)_2Cl(CH_2{}^tBu)_3$ (**31**). No reaction was observed between $W(OMe)_2Cl(CH_2{}^tBu)_3$ (**31**) and additional $Zn(CH_2{}^tBu)_2$. Thus $Zn(CH_2{}^tBu)_2$ is still too strong an alkylating reagent for $W(OMe)_3Cl_3$ (**29**), and **31** is apparently not an intermediate to **30** in the reaction between **26** and $Zn(CH_2{}^tBu)_2$ to give **30**. The reaction of **29** with $Zn(CH_2{}^tBu)_2$ is shown here to be another method to form **30**.

5.2. Results and Discussion

The reaction of $W(OMe)_3Cl_3$ (**29**) with $Zn(CH_2{}^tBu)_2$ (Scheme 5.3) at 23 °C in benzene-d_6 was quick. ^1H and $^{13}C\{^1H\}$ NMR spectra (Figures 5.1 and 5.2) showed the formation of the alkylidyne **30**,[5] neopentane CMe_4 and **31** which was characterized below.

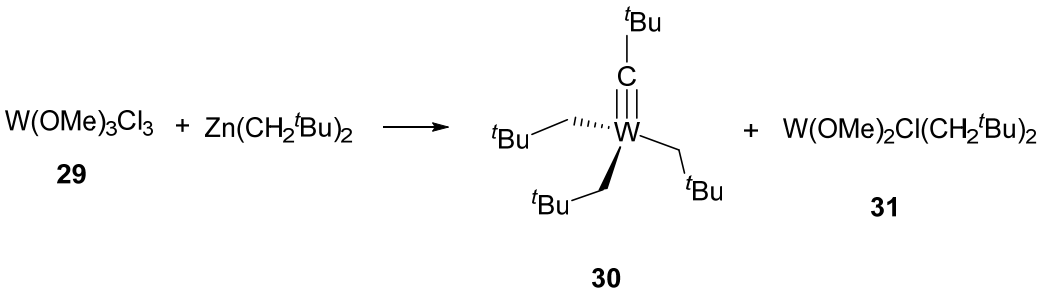

Scheme 5.3. Formation of **30** and **31**.

After removing the volatiles under vacuo, benzene-d_6 was added and the solution was filtered through Celite. **30** was no longer observed in ^1H and $^{13}C\{^1H\}$ NMR spectra, suggesting it may have been removed under evacuation or reacted with H_2O or surface –OH groups on Celite.

The set of peaks corresponding to $W(OMe)_2Cl(CH_2{}^tBu)_3$ (**31**) remained in the filtrate. Characteristics of this species by ^1H, $^{13}C\{^1H\}$, HSQC, DEPT, HMBC, 1-D and 2-D NOESY NMR spectroscopies are consistent with **31**. The ^1H NMR of **31** in benzene-d_6 (Figure 5.3) shows three singlets at 4.01, 2.32, and 0.94 ppm

which were assigned to the O*Me* groups, C*H*$_2$CMe$_3$, and CH$_2$C*Me*$_3$ groups, respectively. The observation of the ^{1}H NMR peaks in this range suggests that this species is unlikely to be a d^1 W(V) species as such d^1 species are paramagnetic and their NMR peaks are usually shifted outside the range in Figure 5.3. ^{1}H peak integrations indicate there are two OMe and three neopentyl ligands in this species. Other NMR spectroscopies below show that these ligands are all on the same molecules. The formula W(OMe)$_2$Cl(CH$_2$^{t}Bu)$_3$ (**31**) is consistent with the observations.

In the ^{13}C{^{1}H} NMR spectrum of **31** in benzene-d_6 (Figure 5.4), the O*Me* methyl groups were observed at 66.89 ppm. The *C*H$_2$CMe$_3$ carbon atom was observed at 88.97 ppm. The CH$_2$C*Me*$_3$ methyl groups were assigned to the peak at 35.58 ppm. The CH$_2$*C*Me$_3$ carbon was observed at 38.29 ppm. The DEPT (Figure 5.5) experiment determined that the peak at 88.97 ppm was a methylene carbon. Heteronuclear multiple-bond correlation (HMBC, Figure 5.6) spectroscopy was used to determine the CH$_2$*C*Me$_3$ atoms. The protons on the methylene carbon coupled to the carbon atoms. Thus the peak at 38.29 ppm is assigned to the CH$_2$*C*Me$_3$ atoms. 1-D and 2-D NOESY (Figures 5.7 and 5.8) experiments were conducted in order to relate through space the OMe ligand and CH$_2$CMe$_3$ ligand. The NOESY spectra show that the two ligands are on the same W atom, thus the same molecule.

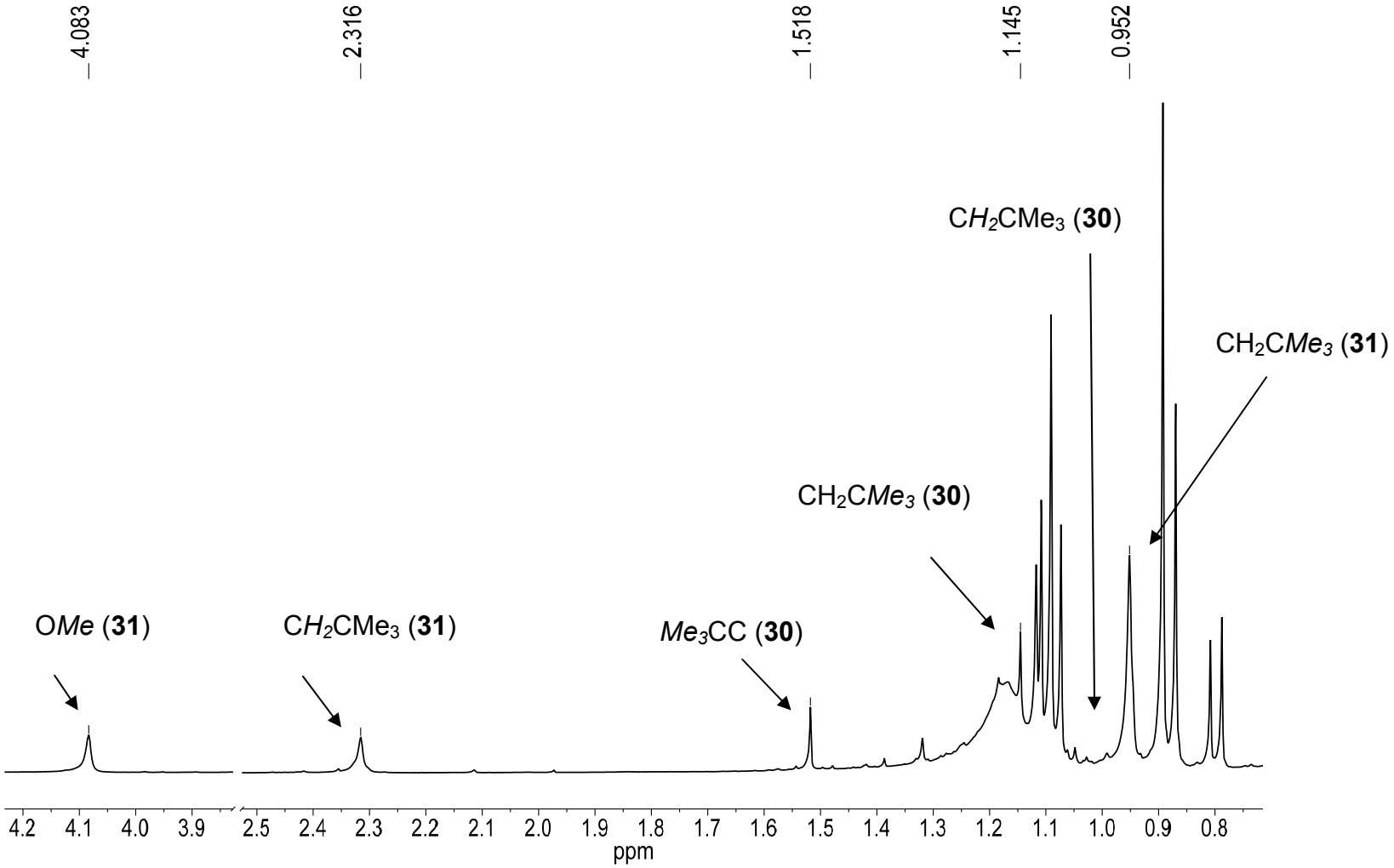

Figure 5.1. ^{1}H NMR spectrum of product mixture of **30** and **31** in benezene-d_6.

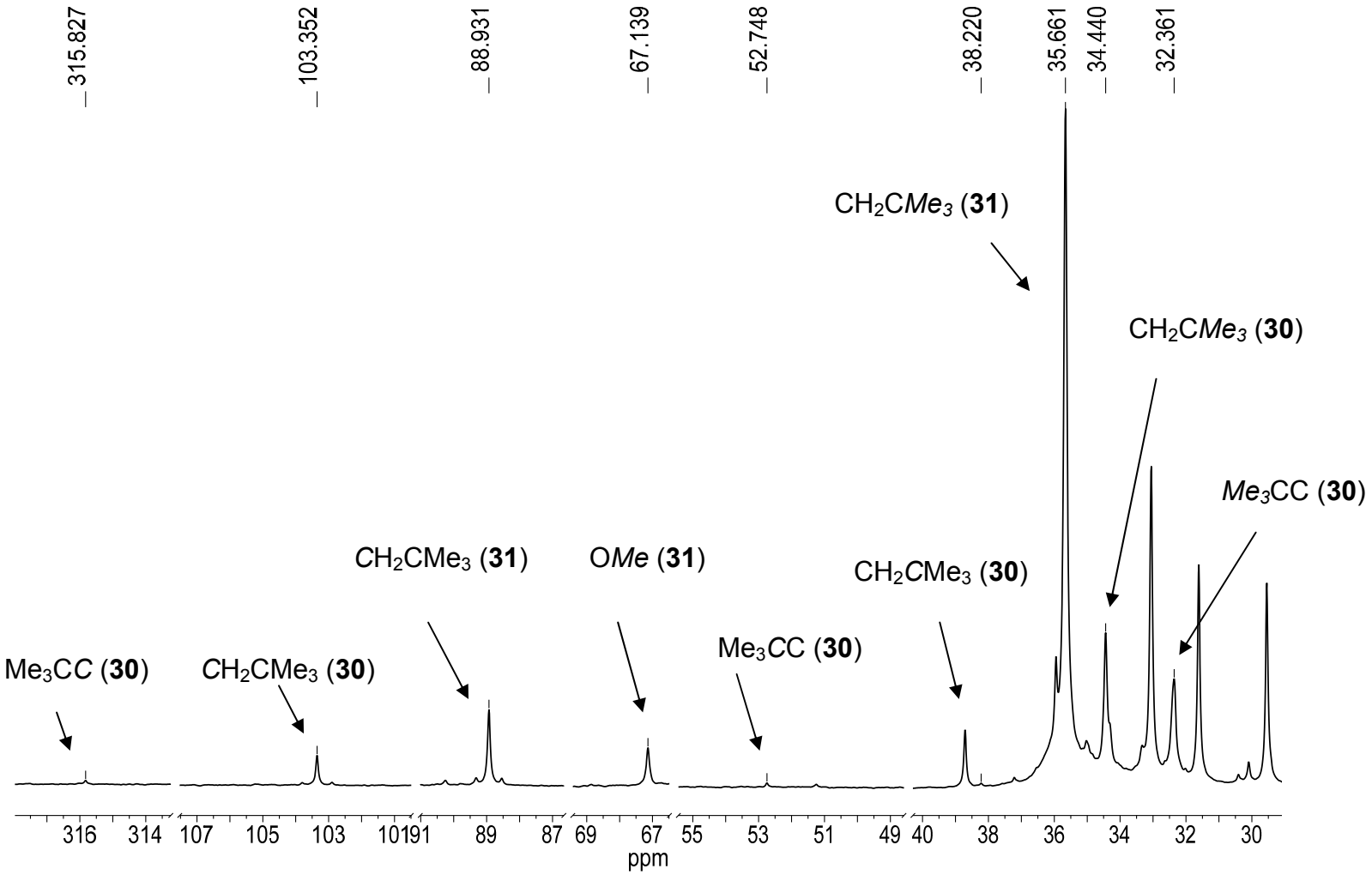

Figure 5.2. $^{13}C\{^{1}H\}$ NMR spectrum of product mixture of **30** and **31** in benezene-d_6.

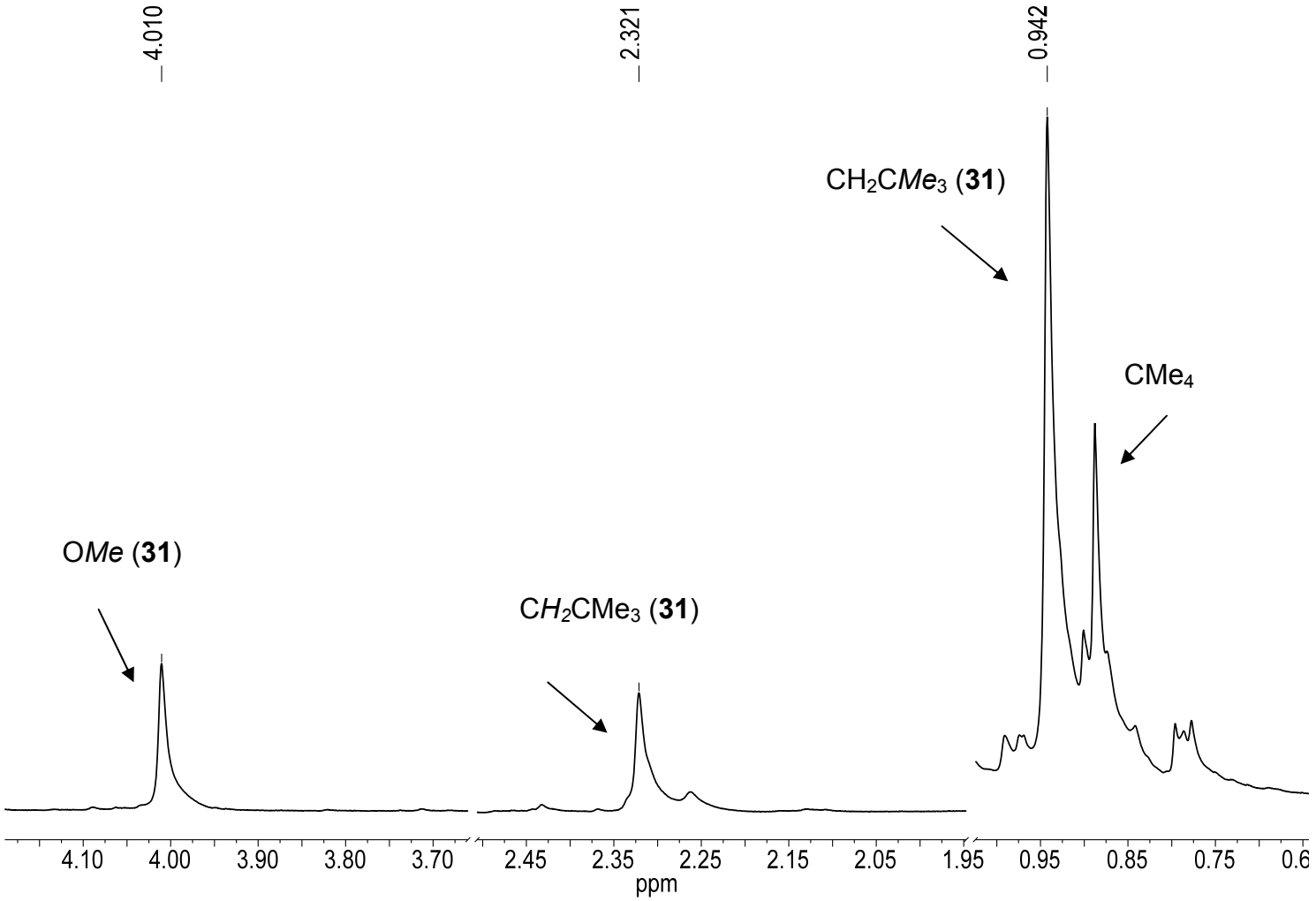

Figure 5.3. ^{1}H NMR spectrum of **31** in benzene-d_6.

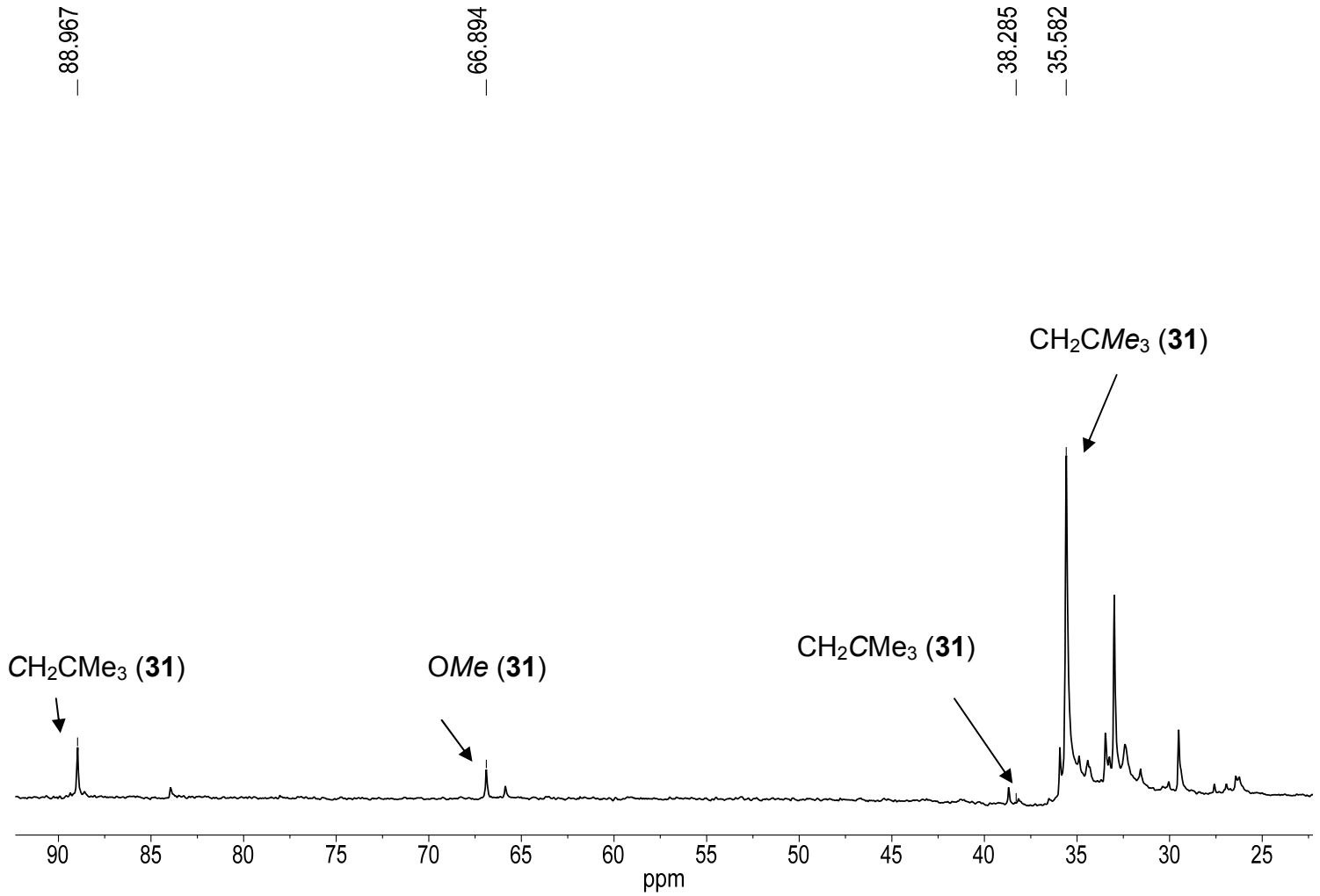

Figure 5.4. $^{13}C\{^{1}H\}$ NMR spectrum of **31** in benzene-d_6.

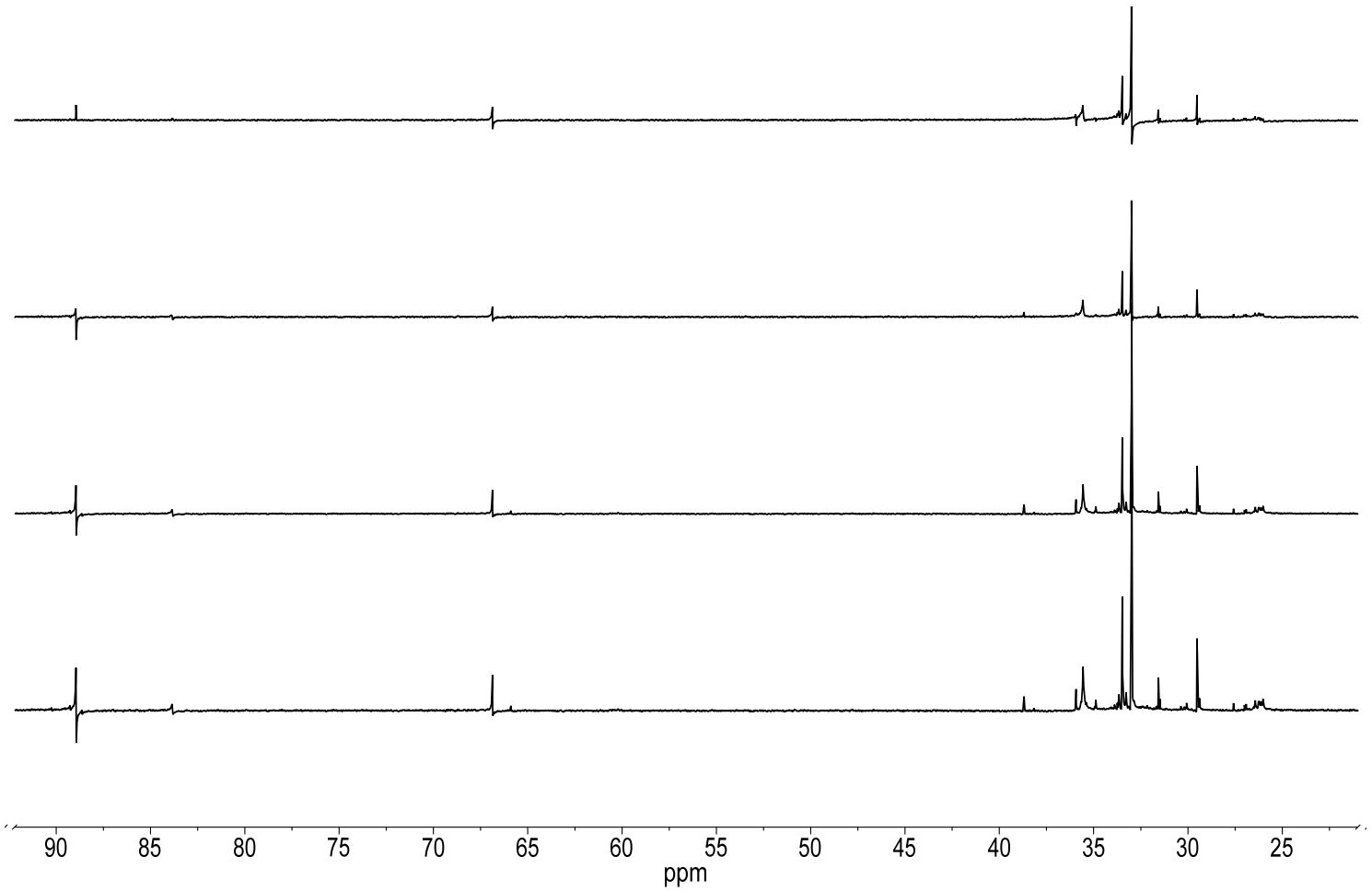

Figure 5.5. DEPT spectra of **31** in benzene-d_6.

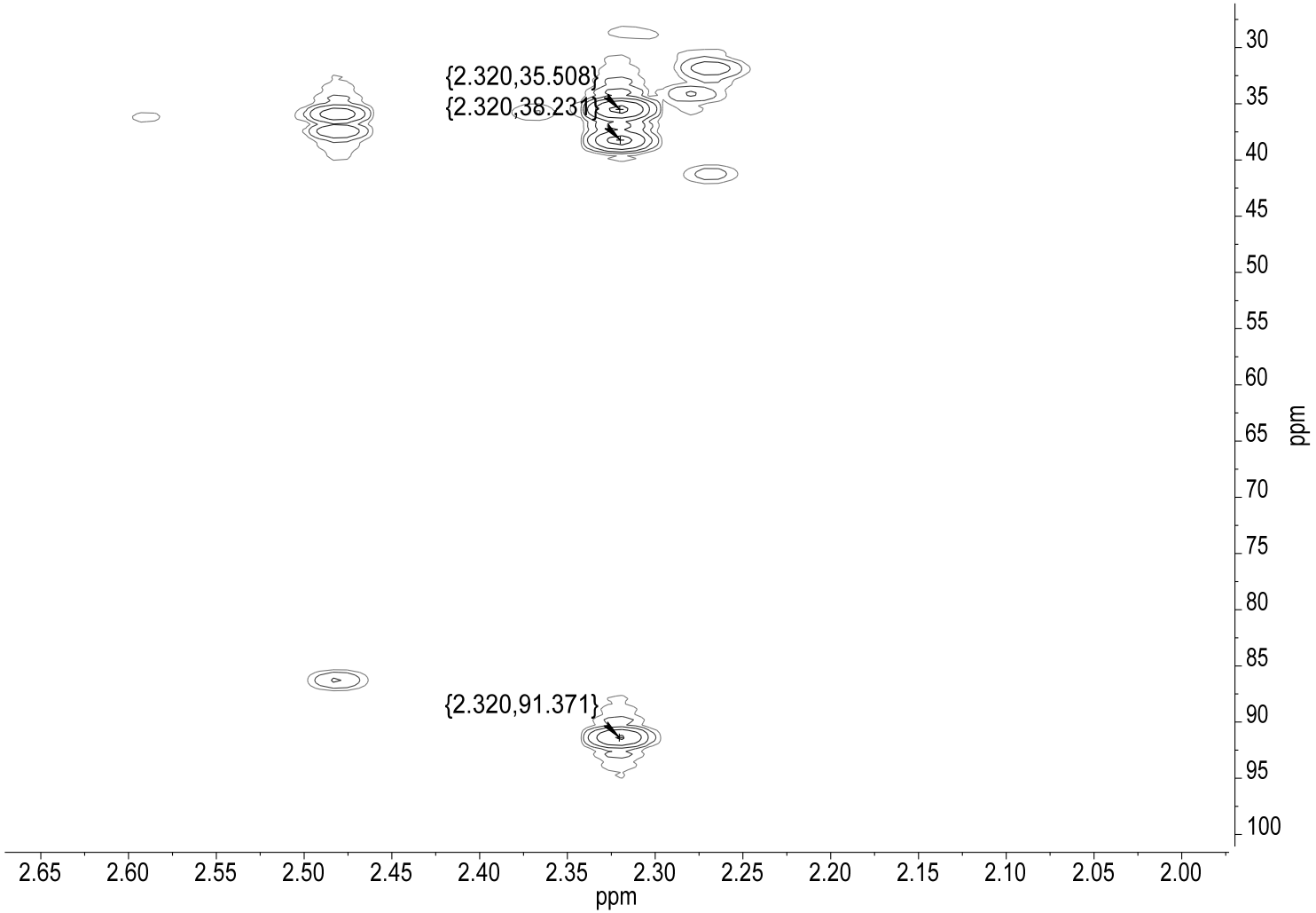

Figure 5.6. HMBC spectrum of **31** in benzene-d_6.

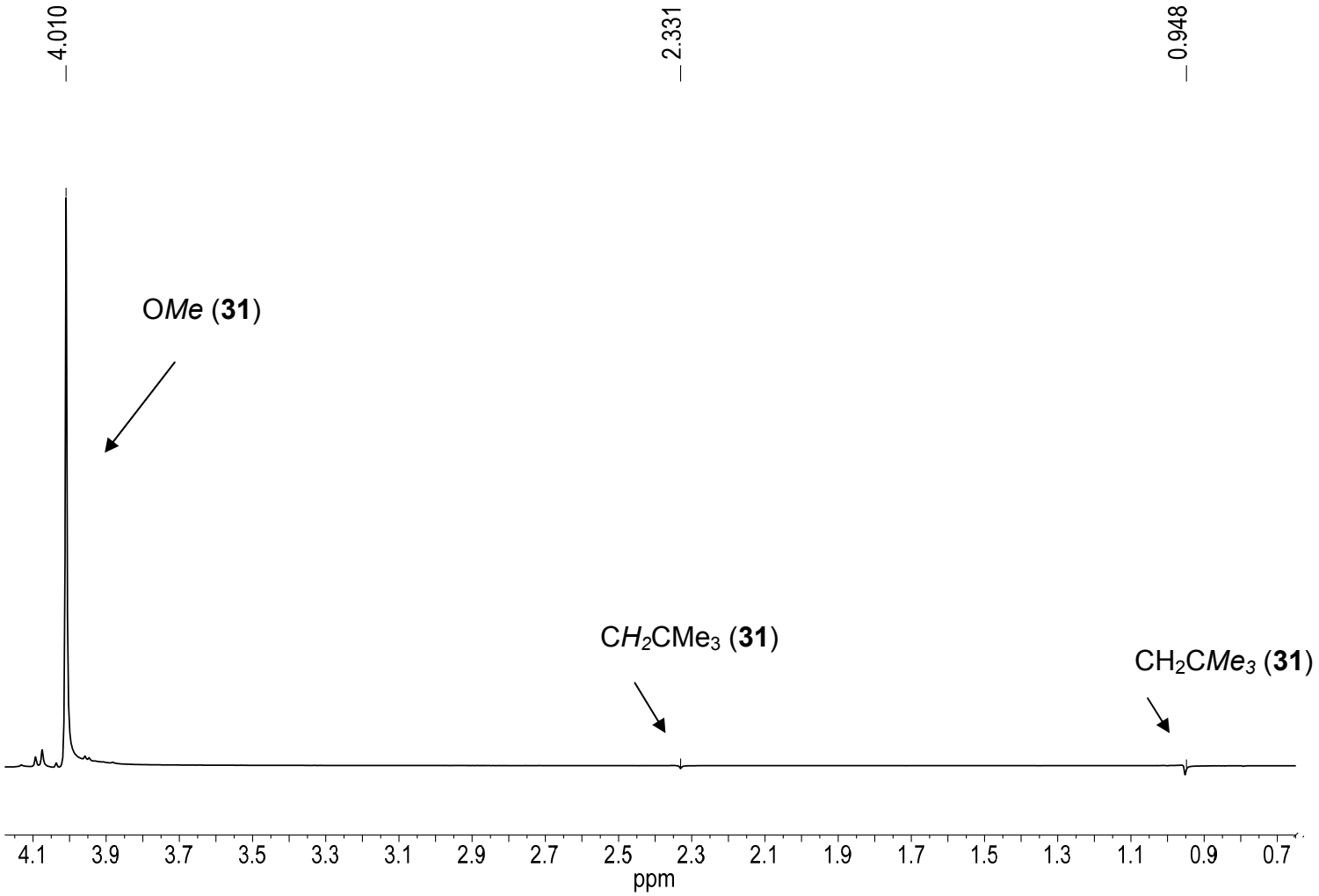

Figure 5.7. 1-D NOESY of **31**.

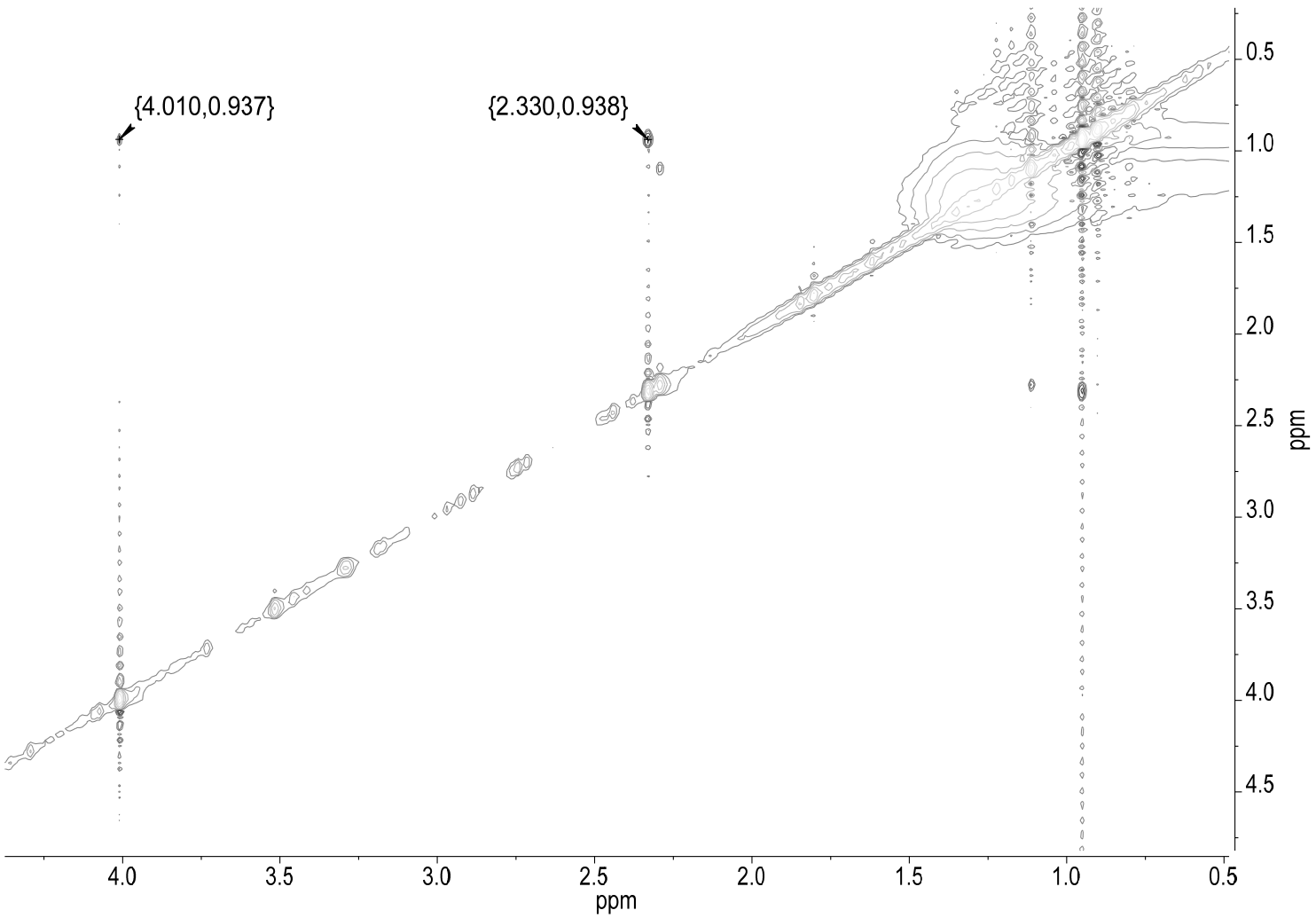

Figure 5.8. 2-D NOESY spectrum of **31**.

It was of interest to see if **31** was an intermediate to **30**. An additional drop of $Zn(CH_2{}^tBu)_2$ was added to the NMR solution of **31** in benzene-d_6 at room temperature. $Zn(CH_2{}^tBu)_2$ and **31** was observed in ^1H NMR and the formation of **30** was not observed. Since **31** is apparently not an intermediate in the formation of **27**, it was not studied further.

5.3. Concluding Remarks

We have shown another way to make $W(CH_2{}^tBu)_3(\equiv C{}^tBu)$ (**30**). In the hopes of capturing an intermediate in the formation of $W(CH_2{}^tBu)_3(\equiv C{}^tBu)$ (**30**) we were able to observe a side product $W(OMe)_2Cl(CH_2{}^tBu)_3$ (**31**). Compound **31** was characterized by ^1H, $^{13}C\{^1H\}$, HSQC, DEPT, HMBC, 1-D NOESY, and 2-D NMR spectroscopies.

5.4. Experimental Section

All manipulations were carried out under a dry nitrogen atmosphere with the use of either a glovebox or standard Schlenk techniques. Solvents were purified by distillation from a potassium benzophenone ketyl. NMR solvents were dried and stored over 5 Å molecular sieves. WCl_6 was purchased from Strem and sublimed before use. $ZnCl_2$ was purchased from Acros and dried with thionyl chloride before use. Me_3SiOMe was purchased from Aldrich and used without further purification. $W(OMe)_3Cl_3$[5] and $Zn(CH_2{}^tBu)_2$[6b] were prepare according to literature. Celite was heated to 200 °C under vacuum. ^1H and $^{13}C\{^1H\}$ NMR spectra were recorded on a AMX-400 FT or Varian VNMRS-500 spectrometer.

5.4.1. Reaction between WCl_6 and $Zn(CH_2{}^tBu)_2$ at 23 °C and -30 °C

NMR-scale Reaction at 23 °C. In a Young's tube, freshly sublimed WCl_6 (41.2 mg, 0.104 mmol) was added to benzene-d_6 (0.5 mL). $Zn(CH_2{}^tBu_3)_2$ (64.8 mg, 0.312 mmol) was then added. According to the ^1H NMR spectrum of the solution, a reaction occurred but the NMR was messy with a lot of peaks. At room temperature, the reaction between WCl_6 and $Zn(CH_2{}^tBu)_2$ may be too fast and several side reactions may occur, giving a messy NMR spectrum.

Reaction Conducted in a Schlenk Flask at -30 °C. In an attempt to better control the reaction between WCl_6 and $Zn(CH_2{}^tBu)_2$, it was carried out in a Schlenk flask at -30 °C. WCl_6 (56.0 mg, 0.146 mmol) in Et_2O (10 mL) was cooled to -30 °C. $Zn(CH_2{}^tBu)_2$ (86.2 mg, 0.415 mmol) in Et_2O (10 mL) cooled to -30 °C was slowly added to the solution of WCl_6. The solution was allowed to stir overnight. After filtration, volatiles were removed in vacuo and the residue was dissolved in benzene-d_6. ^1H NMR spectrum again showed several peaks. Pentane was added to the reaction flask in order to grow crystals. Over time a solid would precipitate from the solution. The solid was, however, not soluble in benzene-d_6.

5.4.2. Reaction of $W(OMe)_3Cl_3$ (29) with $Zn(CH_2{}^tBu)_2$

In a J. Young's tube, **29** (69.0 mg, 0.180 mmol) was dissolved in benzene-d_6. $Zn(CH_2{}^tBu)_2$ (120 mg, 0.576 mmol) was added to a vial in the glovebox and dissolved in benzene-d_6 (1 mL) and added dropwise to the J. Young's tube. The

reaction was quick. NMR spectroscopic characterization showed that the solution is a mixture of **30** and **31** in a 43% : 57% molar ratio. CMe_4 was also observed.

Volatiles were then removed in vacuo. Benzene-d_6 was added and the solution was filtered through a short Celite column (ca. 1 cm in length in a 5.75" disposable Pasteur pipet; Glass wool was used at the bottom of the Celite column). At this point, $W(CH_2{}^tBu)_3(\equiv C{}^tBu)$ (**30**) was not observed anymore, and only $W(OMe)_2Cl(CH_2{}^tBu)_3$ (**31**) was observed. ^1H NMR of **31** (benzene-d_6, 400.17 MHz, 23 °C): δ 4.01 (s, 6H, O*Me*), 2.32 (s, 6H, C*H*$_2$CMe$_3$), 0.94 (s, 9H, CH$_2$C*Me*$_3$); $^{13}C\{^1H\}$ NMR (benzene-d_6, 100.64 MHz, 23 °C): δ 88.97 (*C*H$_2$CMe$_3$), 66.89 (O*Me*), 38.29 (CH$_2$*C*Me$_3$), 35.58 (CH$_2$C*Me*$_3$). ^1H and $^{13}C\{^1H\}$ NMR assignments were confirmed by HSQC, HMBC and DEPT experiments.

References

1. Fischer, E. O.; Kreis, G.; Kreiter, C. G.; Müller, J.; Huttner, G.; Lorenz, H. *Angew Chem. Int. Ed. Engl.* **1973**, *12*, 564.
2. Crabtree, R. H. *The Organometallic Chemistry of the Transition Metals*, 2009, Ch. 11, p. 296.
3. Listemann, M. L.; Schrock, R. R. *Organometallics* **1985**, *4*, 74.
4. (a) Clark, D. N.; Schrock, R. R. *J. Am. Chem. Soc.* **1978**, *100*, 6774. (b) Schrock, R. R.; Clark, D. N.; Sancho, J.; Wengrovius, J. H.; Rocklage, S. M.; Pedersen, S. F. *Organometallics* **1982**, *1*, 1645.
5. Schrock, R. R.; Sancho, J.; Pederson, S. F. *Inorg. Synth.* **1989**, *26*, 45.
6. (a) Schrock, R. R. *J. Am. Chem. Soc.* **1974**, *96*, 6796. (b) Schrock, R. R.; Fellmann, J. D. *J. Am. Chem. Soc.* **1978**, *100*, 3359.
7. Li, L.-T.; Hung, M.-L.; Xue, Z.-L. *J. Am. Chem. Soc.* **1995**, *117*, 12746.
8. Abbott, J. K. C.; Li, L.; Xue, Z.-L. *J. Am. Chem. Soc.* **2009**, *131*, 8246.

Part 6

Conclusion and Future Studies

This dissertation focused on the following three chemistries: (a) Syntheses of Groups 4 and 5 amidinate amides; (b) Reactions of Zr amidinate amides with O_2, H_2O or H_2O_2; (c) A new route to $W(CH_2{}^tBu)_3(\equiv C{}^tBu)$ (**30**). $Zr[MeC(N{}^iPr)_2]_2(NMe_2)_2$ (**10**) has been made by three different routes and the best method to make **10** is through the aminolysis of $Zr(NMe_2)_4$ (**1**) with amidine **7**. After optimizing the reaction conditions, the aminolysis of several Group 4 and 5 amide complexes was used to make their respective amidinate amide complexes. $Zr[MeC(N{}^iPr)_2]_2(NR_2)_2$ (R = Me, **10**; Et, **12**) were first prepared in order to study their reactions with O_2. The reactions between **10** and H_2O or H_2O_2 were then carried out in order to confirm the results from the reactions with O_2. A radical trap, CCl_4, was found to react with $Ta[MeC(N{}^iPr)_2](NMe_2)_4$ (**27**). An amide-chloride exchange occurred and the formation of $Ta[MeC(N{}^iPr)_2](NMe_2)_3Cl$ (**28**) was observed. We have also found a new path to $W(CH_2{}^tBu)_3(\equiv C{}^tBu)$ (**30**).

In Part 2, syntheses and characterization of zirconium amidinate amides were presented. $Zr[MeC(N{}^iPr)_2]_2(NMe_2)_2$ (**10**) was prepared by three different ways: two salt metathesis routes and an aminolysis route. The aminolysis route gives the highest yield and was chosen throughout this dissertation. $Zr[MeC(N{}^iPr)_2]_2(NR_2)_2$ (R = Me, **10**; Et, **12**) has been characterized via ^1H and $^{13}C\{^1H\}$ NMR spectroscopies as well as elemental analyses. In making **10** and **12**, their monoamidinate complexes $Zr[MeC(N{}^iPr)_2](NR_2)_3$ (R = Me, **9**; Et, **11**) were observed and characterized by ^1H and $^{13}C\{^1H\}$ NMR spectroscopies. Compound **12** revealed an interesting dynamic NMR behavior. Variable-temperature NMR spectroscopy was used to study the Bailar twist process. The

activation parameters determined are $\Delta H^{\ddagger}$ = 10.9(1.1) kcal mol^{-1}, $\Delta S^{\ddagger}$ = -11(4) eu and $\Delta G^{\ddagger}_{303\,K}$ = 14(2) kcal mol^{-1}.

In Part 3, the reaction between Zr[MeC(N^{i}Pr)$_2$]$_2$(NMe$_2$)$_2$ (**10**) and O_2 was extensively studied in part because several products were observed. One product was a Zr peroxo complex {(μ-η^2:η^2-O_2)Zr[MeC(N^{i}Pr)$_2$]$_2$}$_3$ (**20**) and its crystal structure was determined. **20** was also prepared from the reaction of Zr[MeC(N^{i}Pr)$_2$]$_2$Cl$_2$ (**8**) with Na_2O_2. Two other Zr containing products from the reaction of **10** with O_2 were identified: oxo-dimer {(μ-O)Zr[MeC(N^{i}Pr)$_2$]$_2$}$_2$ (**14**) and polymer {(μ-O)Zr[MeC(N^{i}Pr)$_2$]$_2$}$_n$ (**17**). They have been confirmed by the following studies: (a) Reaction of **12** with O_2; (b) Reactions of Zr[MeC(N^{i}Pr)$_2$]$_2$(NR$_2$)$_2$ (R = Me, **10**; Et, **12**) with H_2O; (c) MS analysis of the reactions between Zr[MeC(N^{i}Pr)$_2$]$_2$(NR$_2$)$_2$ (R = Me, **10**; Et, **12**) with H_2O; (d) Reaction of **10** with H_2O_2; (e) NMR spectroscopies and elemental analysis.

In Part 4, two Group 5 amidinate amides M[MeC(N^{i}Pr)$_2$](NMe$_2$)$_4$ (M = Nb, **26**; Ta, **27**) have been prepared through aminolysis. They have been characterized by NMR spectroscopies and elemental analyses. The reaction between **27** and CCl_4 was also studied in order to see if CCl_4 could be used as a radical trap in the reaction of **27** with O_2. It was determined that CCl_4 cannot be used because it reacts with **27** forming Ta[MeC(N^{i}Pr)$_2$](NMe$_2$)$_3$Cl (**28**). Compound **28** was prepared by an alternate route.

In Part 5, the reaction between W(OMe)$_3$Cl$_3$ (**29**) and Zn(CH$_2$^{t}Bu)$_2$ was studied and the tungsten alkylidyne complex W(CH$_2$^{t}Bu)$_3$(≡C^{t}Bu) (**30**) was observed along with another product W(OMe)$_2$Cl(CH$_2$^{t}Bu)$_3$ (**31**). The work here

thus could not provide an answer to the fundamental question - when the W≡C triple bond forms in the reactions to give **30**. The alkylating reagent $Zn(CH_2{}^tBu)_2$ is still too strong, yielding **30** directly. It was also found that **31** is not an intermediate to **30**.

Future work will focus on the reactions of O_2 with Zr monoamidinate amide complexes (**9** and **11**) and Group 5 amidinate amide complexes (**26** and **27**). Theoretical studies will help understand the mechanistic pathways of **10** and O_2. A milder reagent than $Zn(CH_2{}^tBu)_2$ may be used to probe the formation of **30**, revealing the intermediates in the formation of the W≡C triple bond in **30**. Tetraneopentyltin $Sn(CH_2{}^tBu)_4$ has been reported,[1] and it may also be employed to react with $W(OMe)_3Cl_3$ (**29**), probing the pathway in the formation of the W≡C triple bond. $TlCH_2{}^tBu$ and $AgCH_2{}^tBu$ have not been reported.[2,3] If they are prepared in the future, they are probably good reagents to remove chloride ligands in $W(OMe)_3Cl_3$ (**29**) as TlCl and AgCl, respectively, perhaps making it easier to obtain the intermediates in the formation of $W(CH_2{}^tBu)_3(\equiv C{}^tBu)$ (**30**).

References

1. Mitchell, T. N.; Fabisch, B. *J. Organomet. Chem.* **1984**, *269*, 249.
2. Searches of *Chemical Abstracts* (*SciFinder*) on August 20, 2013 using "neopentyl thallium," "C5 H11 Tl," or "Chemical Structure" showed that only Tl(III) compounds such as $X_2TlCH_2{}^tBu$ and $XTl(CH_2{}^tBu)_2$ (X = Cl, Br) had been reported. See, e.g., (a) Johnson, M. D. *J. Chem. Soc. D: Chem. Commun.* **1970**, 1037. (b) Brady, F.; Henrick, K.; Matthews, R. W.; Gillies, D. G. *J. Organomet. Chem.* **1980**, *193*, 21.
3. Searches of *Chemical Abstracts* (*SciFinder*) on August 20, 2013 using "neopentyl silver," "C5 H11 Ag," or "Chemical Structure" showed that $AgCH_2{}^tBu$ had not been reported.

Vita

Adam C. Lamb was born on August 16, 1984 in Asheboro, NC to Barbara and Eddie Lamb. He has an older brother Corey, who is married to Lorie and has two kids Keirstan and Braeden. The adolescence education of Adam was through the Randolph County School Systems in which he graduated in the top ten from Eastern Randolph High School (2003). The following fall he attended Wingate University (Wingate, NC). He graduated in May 2007 with a B.S. in chemistry and a minor in mathematics. He is a member of Kappa Alpha Order and at Wingate he held several positions within the Order. He conducted undergraduate research under Dr. Deborah Sunderland and was advised by Dr. Christopher Dahm. In August 2007, he enrolled at the University of Tennessee.